Agradecimientos

Al Ministerio de Ciencia, Innovación y Universidades, por otorgarme un contrato del programa FPU y por la financiación que ha permitido la realización de esta Tesis Doctoral.

A mis directores de tesis, la Dra. María Jesús Delgado y el Dr. Andrew Gates, por haber hecho posible esta tesis, por vuestra ayuda y apoyo. A la Dra. María Jesús Delgado, por el tiempo que hemos compartido y por haberme ofrecido tu experiencia y amplio conocimiento. Al Dr. Andrew Gates, por haberme acogido en tu laboratorio para realizar las estancias, por tu hospitalidad y sabios consejos.

Al Dr. Eulogio Bedmar y a la Dra. Socorro Mesa, por haber estado siempre dispuestos a resolver cualquier duda y por las ideas aportadas durante la realización de esta tesis.

A mis compañeros de laboratorio, por vuestro apoyo y disposición a ayudarme en todo lo que he necesitado.

A mi hermano, Miguel Ángel, la luz que más brilla en el cielo, la luz que me guía y me acompaña cada día. Gracias por todo lo que me enseñaste, por todo lo que aprendí de ti, por cuidarme y por mostrarme lo mejor de ti. Te llevo conmigo.

A mis padres, Miguel Ángel y Mercedes, por vuestro cariño y amor incondicional, por vuestro apoyo, por darme motivos para seguir adelante en los momentos más duros y difíciles. Por vuestro ejemplo de superación y lucha incansable. Por todo lo que hacéis por mí.

A Miguel, por tu ayuda, por tus ánimos, por tu confianza, por tu paciencia. Por estar siempre ahí. Gracias por todo.

UNIVERSIDAD DE GRANADA

PROGRAMA DE DOCTORADO DE BIOLOGÍA FUNDAMENTAL Y DE SISTEMAS

TESIS DOCTORAL

Exploring the role of the haemoglobin from *Bradyrhizobium diazoefficiens* in nitric oxide detoxification during free-living and endosymbiotic lifestyles

Departamento de Microbiología del Suelo y Sistemas Simbióticos
Estación Experimental del Zaidín, CSIC-Granada

Ana Salas Huertas

Granada, 2020

UNIVERSIDAD DE GRANADA

PROGRAMA DE DOCTORADO DE BIOLOGÍA FUNDAMENTAL Y DE SISTEMAS

Departamento de Microbiología del Suelo y Sistemas Simbióticos
Estación Experimental del Zaidín, CSIC-Granada

Exploring the role of the haemoglobin from *Bradyrhizobium diazoefficiens* in nitric oxide detoxification during free-living and endosymbiotic lifestyles

Memoria de Tesis Doctoral presentada por la licenciada en Ciencias Ambientales Ana Salas Huertas para aspirar al Grado de Doctora

Fdo. Ana Salas Huertas

VºBº Los Directores

Fdo. María J. Delgado Igeño
Doctora en Biología
Investigadora Científica del CSIC

Fdo. Andrew J. Gates
Doctor en Química
Associate Professor of Bacterial Bioenergetics de la UEA

Granada, 2020

Editor: Universidad de Granada. Tesis Doctorales
Autor: Ana Salas Huertas
ISBN: 978-84-1306-497-0
URI: http://hdl.handle.net/10481/62283

This Doctoral Thesis has been carried out in the Nitrogen Metabolism Group from Department of Soil Microbiology and Symbiotic Systems from Estación Experimental del Zaidín (Consejo Superior de Investigaciones Científicas, CSIC), Granada, Spain.

Part of the results obtained during this Doctoral Thesis have been published in a scientific journal:

> **The Hemoglobin Bjgb from *Bradyrhizobium diazoefficiens* Controls NO Homeostasis in Soybean Nodules to Protect Symbiotic Nitrogen Fixation. Salas, A.**, Tortosa, G., Hidalgo-García, A., Delgado, A., Bedmar, E.J., Richardson, D.J., Gates, A.J., and Delgado M.J. (2020). *Front. Microbiol.* 10, 2915. doi: 10.3389/fmicb.2019.02915. (Impact Factor: 4.259, Q1, Microbiology).

The results obtained during this Doctoral Thesis have been presented in the following national and international meetings and congresses:

> **Greenhouse gas emissions by legume root nodules. Salas**, **A.**, Tortosa, G., Hidalgo-García, A., Pacheco, P.J., Mesa, S., Bedmar, E.J., Richardson, D.J., Gates, A.J., and Delgado, M.J. 21st ICNF International congress on nitrogen fixation. Wuhan, China. 10-15 October 2019. Oral communication.
>
> **Reduction of nitric oxide levels in soybean nodules by deletion of the *Bradyrhizobium diazoefficiens* Hemoglobin, Bjgb, improves nitrogen fixation tolerance to flooding**. **Salas, A.**, Tortosa, G., Hidalgo-García, A., Delgado, A., Bedmar, E.J., Richardson, D.J., Gates, A.J., and Delgado, M.J. XVII National meeting of the Spanish society of nitrogen fixation and VI Portuguese-Spanish congress on nitrogen fixation. Madrid, Spain. 10-12 July 2019. Oral communication.
>
> **Nitric oxide metabolism in plant associated endosymbiotic bacteria**. **Salas, A.**, Edwards, M.J., Cabrera, J.J., Bedmar, E.J., Richardson, D.J., Gates, A.J., and Delgado, M.J. 7th Plant nitric oxide international meeting. Nice, France. 24-26 October 2018. Invited talk.
>
> **Biochemical characterisation of Bjgb-Flp, a two-component system from *B. diazoefficiens* for nitric oxide detoxification**. **Salas, A.**, Edwards, M.J., Cabrera, J.J., Bedmar, E.J., Richardson, D.J., Delgado, M.J., and Gates, A.J. 23rd European nitrogen cycle meeting. Alicante, Spain. 18-21 September 2018. Oral communication.

Purificación y caracterización bioquímica del sistema Bjgb-Flp de *Bradyrhizobium diazoefficiens* implicado en la destoxificación de óxido nítrico. **Salas, A.**, Cabrera, J.J., Bedmar, E.J., Richardson, D.J., Delgado, M.J., and Gates, A.J. III Conferences/I National congress of researchers in training: encouraging interdisciplinarity. Granada, Spain. 20-22 June 2018. Oral communication.

Producción de óxido nítrico y óxido nitroso por bacterias endosimbióticas de leguminosas. Delgado, M.J., Torres, M.J., Cabrera, J.J., **Salas, A.**, Hidalgo-García, A., Jiménez-Leiva, A., Tortosa, G., Mesa, S., and Bedmar, E.J. XIV National meeting of nitrogen metabolism. Segovia, Spain. 16-18 May 2018. Plenary talk.

Biochemical characterization of the two-component nitric oxide detoxification system Bjgb-Flp from *Bradyrhizobium diazoefficiens*. **Salas, A.**, Cabrera, J.J., Bedmar, E.J., Richardson, D.J., Delgado, M.J., and Gates, A.J. 22nd European nitrogen cycle meeting. Córdoba, Spain. 24-26 September 2017. Oral communication.

Involvement of the *Bradyrhizobium diazoefficiens* assimilatory nitrate reductase (NasC) and NO detoxifying haemoglobin (Bjgb) in the response of soybean nodules to flooding. **Salas, A.**, Hidalgo, A., Tortosa, G., Bedmar, E.J., Richardson, D.J., Gates, A., and Delgado, M.J. 20th ICNF International congress on nitrogen fixation. Granada, Spain. 3-7 September 2017. Poster communication.

Involvement of the *Bradyrhizobium diazoefficiens* nitrate assimilation/nitric oxide detoxification integrated system in the response of soybean nodules to flooding. **Salas, A.**, Hidalgo, A., Tortosa, G., Bedmar, E.J., Gates, A.J., and Delgado, M.J. 6th Plant nitric oxide international meeting. Granada, Spain. 14-16 September 2016. Poster communication.

A coordinated pathway for nitrate assimilation and nitric oxide metabolism in plant-associated endosymbiotic bacteria. Delgado, M.J., **Salas, A.**, Cabrera, J.J., Torres, M.J., Hidalgo, A., Tortosa, G., Mesa, S., Bedmar, E.J., Girard, L., Richardson, D.J., and Gates, A.J. 21st European nitrogen cycle annual meeting. Norwich, United Kingdom. 5-7 September 2016. Invited talk.

Purification and biochemical characterization of the two-component nitric oxide detoxification system Bjgb-Flp from *Bradyrhizobium diazoefficiens*. Salas, A., Edwards, M.J., Cabrera, J.J., Bedmar, E.J., Richardson, D.J., Delgado, M.J., and Gates, A.J. 21st European nitrogen cycle annual meeting. Norwich, United Kingdom. 5-7 September 2016. Poster communication.

Nitrate assimilation and nitric oxide metabolism in *Bradyrhizobium japonicum*. Salas, A., Cabrera, J.J., Mesa, S., Bedmar, E.J., Richardson, D.J., Gates, A.J., and Delgado, M.J. XIII National meeting of nitrogen metabolism. Villanueva de la Serena (Badajoz), Spain. 4-6 February 2016. Oral communication.

Nitric oxide and nitrous oxide metabolism in the *Glycine max-Bradyrhizobium japonicum* symbiosis. Cabrera, J.J., **Salas, A.**, Torres, M.J., Bedmar, E.J., Richardson, D.J., Gates, A.J., and Delgado, M.J. 23rd North American conference on symbiotic nitrogen fixation. Ixtapa, México. 6-10 December 2015. Invited talk.

Nitrate assimilation and nitric oxide detoxification *in Bradyrhizobium japonicum*. Salas, A., Cabrera, J.J., López, M.F., Torres, M.J., López-García, S.L., Mesa, S., Bedmar, E.J., Richardson, D.J., Gates, A.J., and Delgado, M.J. XV National meeting of the Spanish society of nitrogen fixation and IV Portuguese-Spanish congress on nitrogen fixation. León, Spain. 16-18 June 2015. Poster communication.

Co-regulation of nitrate assimilation and nitric oxide metabolism in *Bradyrhizobium japonicum*. Salas, A., Cabrera, J.J., López, M.F., Torres, M.J., López-García, S.L., Bedmar, E.J., Richardson, D.J., Gates, A.J., and Delgado, M.J. Meeting of bacterial electron transfer processes and their regulation. Vimeiro, Portugal. 15-18 March 2015. Oral communication.

La doctoranda / *The doctoral candidate* **Ana Salas Huertas** y los directores de la tesis / *and the thesis supervisors*: **María Jesús Delgado Igeño** y **Andrew James Gates**

Garantizamos, al firmar esta Tesis Doctoral, que el trabajo ha sido realizado por la doctoranda bajo la dirección de los directores de la tesis y hasta donde nuestro conocimiento alcanza, en la realización del trabajo, se han respetado los derechos de otros autores a ser citados, cuando se han utilizado sus resultados o publicaciones.

/

Guarantee, by signing this Doctoral Thesis, that the work has been done by the doctoral candidate under the direction of the thesis supervisors and, as far as our knowledge reaches, in the performance of the work, the rights of other authors to be cited (when their results or publications have been used) have been respected.

Lugar y fecha / *Place and date*:

Granada, a 20 de enero de 2020

Directores de la Tesis / *Thesis supervisors;* Doctoranda / *Doctoral candidate*:

Firma / *Signed*

María Jesús Delgado Igeño

Firma / *Signed*

Ana Salas Huertas

Andrew James Gates

ÍNDICE

1

RESUMEN/SUMMARY

1. RESUMEN

El óxido nítrico (NO) es un gas diatómico, formado por un átomo de oxígeno (O) y otro de nitrógeno (N), con un electrón desapareado que lo convierte en un radical (Bartberger et al., 2002). El NO puede reaccionar con diferentes especies de oxígeno para formar las especies reactivas de nitrógeno (RNS) (Earnshaw y Greenwood, 1997). El NO está presente en todos los organismos vivos, donde puede actuar de forma diferente dependiendo de su concentración. A bajas concentraciones (niveles nmolares) el NO actúa como molécula señal, mientras que a concentraciones más altas (niveles µmolares) posee un efecto tóxico (Toledo y Augusto, 2012). En bacterias existen múltiples fuentes de NO, siendo la desnitrificación y la reducción desasimilativa de nitrato a amonio (DNRA) las principales fuentes respiratorias de NO (revisado en Torres et al., 2016). Además, debido al efecto tóxico del NO, las bacterias presentan diferentes sistemas y enzimas para su eliminación. Entre estos sistemas se encuentran las hemoglobinas, que son las proteínas mejor estudiadas y más importantes para la destoxificación aeróbica de NO en bacterias. En procariotas se han identificado tres tipos de hemoglobinas: flavohemoglobinas (fHbs), hemoglobinas de dominio único (sdHbs) y hemoglobinas truncadas (tHbs) (revisado en Poole, 2005; Stern y Zhu, 2014; Gell, 2018).

Bradyrhizobium diazoefficiens es una α-proteobacteria, Gram-negativa, perteneciente al orden *Rhizobiales*. Esta bacteria es capaz de crecer en condiciones limitantes de O_2, empleando el nitrato (NO_3^-) como única fuente de N para asimilarlo y/o para respirarlo, actuando como aceptor final de electrones. En esta bacteria, la respiración de NO_3^- constituye la primera etapa del proceso de desnitrificación. Además, *B. diazoefficiens* es un diazótrofo que establece asociaciones simbióticas con plantas de soja (*Glycine max*). Esta asociación simbiótica tiene lugar en los nódulos, que son unas estructuras especializadas de la raíz de la planta. En los nódulos, las formas diferenciadas del rizobio, los bacteroides, son los responsables de fijar el N_2 atmosférico mediante la actuación de la enzima nitrogenasa. *B. diazoefficiens*, además de fijar N_2 en simbiosis, también es capaz de llevar a cabo el proceso de desnitrificación, tanto en vida libre como en los nódulos de soja. En esta bacteria las reacciones de desnitrificación son catalizadas por las enzimas nitrato reductasa

periplásmica (Nap), nitrito reductasa (NirK), óxido nítrico reductasa (Nor) y óxido nitroso reductasa (Nos), que reducen el NO_3^- hasta N_2 mediante la formación de NO y óxido nitroso (N_2O) como intermediarios gaseosos. Estas enzimas están codificadas por los genes *napEDABC* (Delgado et al., 2003), *nirK* (Velasco et al., 2001), *norCBQD* (Mesa et al., 2002) y *nosRZDYFLX* (Velasco et al., 2004), respectivamente (revisado en Bedmar et al., 2005, 2013).

Estudios previos, realizados en el Grupo del Metabolismo del Nitrógeno del Departamento de Microbiología del Suelo y Sistemas Simbióticos de la Estación Experimental del Zaidín (Granada), demostraron que la hipoxia y el NO_3^- inducen la formación de NO en nódulos de soja, siendo la desnitrificación en los bacteroides el principal proceso implicado en su formación. En este contexto, es preciso la existencia en el nódulo de mecanismos de destoxificación de NO, ya que se ha demostrado que el NO inhibe la actividad nitrogenasa, así como la expresión del gen *nifH*, responsable de su síntesis. En este sentido, se ha propuesto a la enzima desnitrificante Nor como la principal proteína implicada en la eliminación de NO en los nódulos de soja (Sánchez et al., 2010).

Además de desnitrificar, *B. diazoeficciens* es capaz de asimilar NO_3^- en vida libre mediante la expresión de un sistema coordinado de asimilación de NO_3^- y destoxificación de NO, codificado por el operón *narK-bjgb-flp-nasC*. Este operón es responsable de la síntesis de un transportador de NO_3^-/NO_2^- (NarK), una hemoglobina (Bjgb), una flavoproteína dependiente de NAD(P)H (Flp) y una nitrato reductasa asimilativa (NasC). Cerca de estos genes se encuentra otro operón que incluye genes que codifican para una nitrito reductasa asimilativa (NirA) y un sistema regulador de respuesta a NO_3^-/NO_2^- (NasST). Estudios previos han demostrado que Bjgb es una hemoglobina de dominio único implicada en la destoxificación de NO en células cultivadas en vida libre (Cabrera et al., 2016).

En esta Tesis Doctoral, se ha demostrado el papel *in vitro* de la hemoglobina Bjgb y la flavoproteína Flp de *B. diazoefficiens* en el metabolismo del NO. Con este objetivo, se han clonado los genes *bjgb* y *flp* de *B. diazoefficiens* en plásmidos de expresión para, posteriormente, sobre-expresar y purificar las proteínas Bjgb y Flp. Una vez purificadas dichas proteínas, se ha realizado un estudio *in vitro* de las mismas

mediante espectroscopía UV-Vis. Se ha confirmado la capacidad de la flavoproteína Flp de recibir electrones del NADH y de reducir a la hemoglobina de dominio único Bjgb. Una vez reducida la Bjgb, el grupo hemo de esta proteína es capaz de unir NO. Con estos resultados se ha demostrado la capacidad de Bjgb de unir NO *in vitro*, lo cual confirmaría el papel de esta proteína de destoxificar NO *in vivo*.

Además, se ha estudiado el papel de la lisina-52 de la Bjgb de *B. diazoefficiens*. Para ello, se ha realizado una mutación puntual mediante QuickChange de esta lisina por una alanina (K52A Bjgb). El análisis de la función *in vivo* de esta proteína mutada se ha llevado a cabo mediante la complementación de la mutante *bjgb* de *B. diazoefficiens* con dos plásmidos, uno que sobre-expresa la proteína nativa Bjgb y otro que sobre-expresa la proteína mutante K52A Bjgb. El análisis de la expresión de Nor mediante el uso de una fusión transcripcional *norC-lacZ*, la detección de la proteína NorC y la medición de la capacidad de producción de N_2O, el producto de Nor, demostró que la lisina-52 tiene un papel crítico en la expresión de Nor y, por consiguiente, en la homeostasis del NO *in vivo*.

En esta Tesis Doctoral, también se ha abordado el estudio de la implicación de la Bjgb de *B. diazoefficiens* en la interacción simbiótica con plantas de soja y en la homeostasis de NO en los nódulos. Mediante la técnica de la dilución isotópica del ^{15}N y análisis de la actividad y expresión de la enzima nitrogenasa, se ha demostrado que las plantas de soja inoculadas con la cepa mutante en la hemoglobina tienen mayor tolerancia al encharcamiento que aquellas plantas inoculadas con la cepa parental. Este efecto beneficioso se debe a la reducción de la acumulación de NO en los nódulos producidos por plantas de soja inoculadas con la cepa mutante en la hemoglobina y sometidas a encharcamiento, en comparación con los nódulos encharcados de la cepa parental. Esta disminución en la acumulación de NO podría ser debida a la inducción de la expresión y actividad de la enzima Nor, la cual es la principal proteína implicada en la eliminación de NO en los nódulos de soja.

Por último, se ha estudiado la implicación en simbiosis del proceso de asimilación de NO_3^-. Para ello, se han utilizado las mutantes en los genes *nasC* y *nirA*, responsables de la síntesis de la nitrato reductasa y nitrito reductasa asimilativa, respectivamente. Mediante el análisis de la actividad nitrogenasa y contenido en

leghemoglobina (Lb) de los nódulos de soja, se ha demostrado que la inoculación de las plantas de soja con una cepa mutante *nirA* confiere protección de la fijación biológica de nitrógeno (BNF) frente al encharcamiento, en comparación con aquellas plantas inoculadas con la cepa parental. Sin embargo, en las plantas inoculadas con la cepa mutante *nasC* y sometidas a encharcamiento no se observaron diferencias significativas en la BNF en comparación con aquellas plantas inoculadas con la cepa parental. Estos resultados, junto con el análisis de la actividad nitrato reductasa (NR) en bacteroides, sugieren que la nitrato reductasa asimilativa (NasC) no tiene un papel relevante en la reducción de NO_3^- en los bacteroides, siendo la nitrato reductasa periplásmica (NapA) la principal enzima implicada. Con el objeto de profundizar en el posible papel de la asimilación de NO_3^- por los bacteroides en nódulos de soja, se ha utilizado una cepa de *B. diazoeficciens* mutante en el gen *nifH*, responsable de la síntesis de la Fe-proteína del complejo nitrogenasa. El análisis de la expresión del gen *narK*, el primer gen del operón que codifica para las enzimas implicadas en la asimilación de NO_3^-, demostró una significativa inducción de su expresión en nódulos de una cepa mutante *nifH* en relación con los niveles de expresión observados en los nódulos producidos por la cepa parental. Estos resultados se confirmaron mediante la detección de un incremento en el contenido en amonio (NH_4^+) de los nódulos de la cepa mutante *nifH* aislados de plantas cultivadas con NO_3^-, en comparación con los cosechados de plantas crecidas en ausencia de NO_3^-, donde no se detectó producción de NH_4^+ en los bacteroides. Por tanto, estos resultados sugieren que la asimilación de NO_3^- por los bacteroides podría tener una función relevante en nódulos de soja en aquellos casos en los que la fijación del N_2 se ve afectada y, por consiguiente, la producción de NH_4^+ en los bacteroides se reduce significativamente.

Los resultados obtenidos durante esta Tesis Doctoral han contribuido a incrementar el conocimiento sobre la función *in vivo* e *in vitro* de la proteína Bjgb de *B. diazoefficiens* en la destoxificación de NO, tanto en vida libre como en asociación simbiótica con plantas de soja. Además, se ha establecido el posible papel de las proteínas NasC y NirA de *B. diazoefficiens* en la simbiosis con plantas de soja.

SUMMARY

Nitric oxide (NO) is a diatomic gas, formed by an oxygen (O) and nitrogen (N) atom, with an unpaired electron, which turns it into a radical (Bartberger et al., 2002). This molecule may react with different oxygen species to form reactive nitrogen species (RNS) (Earnshaw and Greenwood, 1997). NO is present in all living organisms where it has different roles depending on its concentration. At low concentrations (nmolar levels) NO acts as a signalling molecule, while at higher concentrations (µmolar levels) it has a toxic effect (Toledo and Augusto, 2012). In bacteria, there are many sources of NO, being denitrification and dissimilatory reduction of nitrate to ammonium (DNRA) the main respiratory sources of NO (reviewed by Torres et al., 2016). Due to the toxic effect of NO, bacteria possess several systems and enzymes to remove it. Among these systems, the best studied and most important proteins for NO detoxification are the haemoglobins. In prokaryotes, three types of haemoglobins have been identified: flavohaemoglobins (fHbs), single domain haemoglobins (sdHbs) and truncated haemoglobins (tHbs) (reviewed by Poole, 2005; Stern and Zhu, 2014; Gell, 2018).

Bradyrhizobium diazoefficiens is a Gram-negative α-proteobacterium, belonging to the *Rhizobiales* order, that establishes symbiotic associations with soybean plants (*Glycine max*). This symbiotic association takes places inside the nodules, which are specialized structures in the roots. In the nodules, the differentiated forms of rhizobium, the bacteroids, are responsible for fixing atmospheric nitrogen (N_2) by the action of the nitrogenase enzyme. *B. diazoeficciens* is also able to grow under O_2 limiting conditions using nitrate (NO_3^-) as the only N source, by assimilating it and using it as final electron acceptor through NO_3^- respiration, that constitutes the first step of the denitrification pathway. In addition to fix N_2 in symbiosis, *B. diazoefficiens* is also capable of performing denitrification process inside soybean nodules. In this bacterium, denitrification reactions are catalyzed by the periplasmic nitrate reductase (Nap), nitrite reductase (NirK), nitric oxide reductase (Nor) and nitrous oxide reductase (Nos), enzymes which reduce NO_3^- to N_2 through the formation of NO and nitrous oxide (N_2O) as gaseous intermediates. These enzymes are encoded by the *napEDABC* (Delgado et al., 2003), *nirK* (Velasco et al., 2001), *norCBQD* (Mesa et al., 2002) and

nosRZDYFLX (Velasco et al., 2004) genes, respectively (reviewed by Bedmar et al., 2005, 2013).

Previous studies carried out in the Nitrogen Metabolism Group from Department of Soil Microbiology and Symbiotic Systems (Estación Experimental del Zaidín, CSIC), showed that hypoxia and NO_3^- induce NO synthesis in soybean nodules, being denitrification in bacteroids the major process involved in its formation. In this context, the presence of NO detoxification mechanisms in the nodules is necessary, since it has been evidenced that NO inhibits nitrogenase activity, as well as expression of *nifH* gene, responsible for nitrogenase synthesis. The denitrifying enzyme Nor has been proposed as the principal protein implicated in NO removal in soybean nodules (Sánchez et al., 2010).

In addition to denitrify, *B. diazoefficiens* is also able to assimilate NO_3^- in free living conditions through the expression of a coordinated system for NO_3^- assimilation and NO detoxification, which is encoded by the *narK-bjgb-flp-nasC* operon. This operon is responsible for the synthesis of a NO_3^-/NO_2^- (NarK) transporter, a haemoglobin (Bjgb), a NAD(P)H dependent flavoprotein (Flp) and an assimilatory nitrate reductase (NasC). Close to those genes, there is another gene cluster that includes genes coding for an assimilatory nitrite reductase (NirA) and a NO_3^-/NO_2^- response regulatory system (NasST). Earlier studies have revealed that Bjgb is a single domain haemoglobin involved in NO detoxification in cells grown under free-living conditions (Cabrera et al., 2016).

In this Doctoral Thesis, the role *in vitro* of *B. diazoefficiens* Bjgb and Flp in NO detoxification has been demonstrated. To achieve this goal, *bjgb* and *flp* genes from *B. diazoefficiens* have been cloned into expression plasmids to subsequently over-express and purify Bjgb and Flp proteins. UV-Vis spectroscopy analyses of purified Bjgb and Flp showed the ability of Flp to reduce Bjgb. Once Bjgb is reduced, the haem group of this protein is capable to bind NO. These results have proved the ability of Bjgb to bind NO *in vitro*, confirming the role of this protein to detoxify NO *in vivo*.

The function of the lysine-52 of Bjgb has also been investigated by carrying out a site directed mutation of this lysine by an alanine (K52A Bjgb). The role *in vivo* of this K52A Bjgb protein mutant has been investigated by complementing a *B. diazoefficiens*

bjgb mutant with two plasmids, one that over-expresses the native Bjgb protein and another that over-expresses the K52A Bjgb mutant protein. The analysis of Nor expression by using a *norC-lacZ* transcriptional fusion, detection of NorC protein and measurement of the capacity of N_2O production, the product of Nor, demonstrated that the lysine-52 haem-iron ligand from Bjgb has a critical role on *nor* expression and, consequently, on NO homeostasis *in vivo*.

In this Doctoral Thesis, the involvement of Bjgb from *B. diazoefficiens* in the symbiotic interaction with soybean plants and in NO homeostasis in the nodules has also been investigated. By using the isotopic ^{15}N dilution technique and analyzing expression of nitrogenase, we have demonstrated that soybean plants inoculated with the *bjgb* mutant strain had greater tolerance to flooding than those plants inoculated with the parental strain. This beneficial effect is probably due to the reduction of NO accumulation in nodules produced by the *bjgb* mutant in response to flooding, as compared to parental flooded nodules. The decrease in NO accumulation could be due to the induction of expression and activity of Nor, which is the main protein involved in NO removal in soybean nodules.

Finally, the involvement of NO_3^- assimilation in the *B. diazoefficiens-Glycine max* symbiosis has also been investigated in this Doctoral Thesis. To achieve this goal, *B. diazoeficciens* mutants defective in *nasC* and *nirA* genes, encoding the assimilatory nitrate and nitrite reductases, respectively, have been used to inoculate soybean plants. By analyzing nitrogenase activity and leghaemoglobin content (Lb) of the nodules, we found that inoculation with the *nirA* mutant confers protection of biological nitrogen fixation (BNF) to flooding, compared to those plants inoculated with parental strain. However, no differences in BNF were observed in plants inoculated with the *nasC* mutant and subjected to flooding compared to those plants inoculated with the parental strain. These results, together with the analysis of nitrate reductase activity (NR) in the bacteroids, suggest that the assimilatory nitrate reductase, NasC, has not a relevant role in NO_3^- reduction in bacteroids, being the periplasmic nitrate reductase (NapA) the main enzyme involved. In order to go deeper in the study of the possible role of NO_3^- assimilation by the bacteroids in soybean nodules, a *B. diazoefficiens* mutant in the *nifH* gene, responsible for the synthesis of

the Fe-protein of the nitrogenase complex, has been used. Interestingly, expression of *narK* gene, the first gene of the operon that codes for the enzymes implicated in NO_3^- assimilation, was significantly induced in nodules from the *nifH* mutant. We also analyzed NH_4^+ production capacity by the bacteroids. As expected, *nifH* bacteroids from plants grown in the absence of NO_3^-, were unable to produce NH_4^+ due to the lack of nitrogenase activity. However, when plants were grown with NO_3^-, bacteroids from the *nifH* mutant were able to produce NH_4^+. These results suggest that NO_3^- assimilation by bacteroids might have a relevant role in those nodules where nitrogenase is impaired.

The results obtained during this Doctoral Thesis have contributed to increase the knowledge about the function *in vivo* and *in vitro* of Bjgb from *B. diazoefficiens* in NO detoxification, both in free living conditions and in symbiotic association with soybean plants. In addition, the putative role of *B. diazoefficiens* nitrate assimilation in soybean nodules has also been established.

2

INTRODUCTION

2. INTRODUCTION

2.1. Introduction to the nitric oxide (NO) molecule

Nitric oxide (NO), or nitrogen monoxide, is a diatomic gas, composed of an oxygen (O) atom and a nitrogen (N) atom, leaving a single unpaired electron on the molecule which makes it a radical chemically represented as NO·. Its chemical composition gives it unusual and unintuitive properties because, despite being radical, NO is not especially susceptible to oxidation or reduction. However, it can react with several oxygen species, such as superoxide anion ($O_2{\cdot}^-$) and molecular oxygen (O_2), to form the so-called reactive nitrogen species (RNS), such as peroxynitrite ($ONOO^-$), nitrogen dioxide radical ($NO_2{\cdot}$), dinitrogen trioxide (N_2O_3), nitrosonium cation (NO^+), or nitroxyl anion (NO^-) (reviewed by Bartberger et al., 2002; Hughes, 2008; Möller et al., 2019) (Figure 2.1.).

NO is slightly soluble in water and more soluble in organic solvents, consequently, it is able to diffuse through the hydrophilic parts of the cell, such as the cytoplasm, and it can also move freely through the lipid phase and diffuse to neighboring cells. Being a reactive free radical, it has a relatively short half-life (on the order of a few seconds), therefore, its effects are mostly limited to the cell in which it is produced, or to the nearest neighboring cells. NO is present in all living organisms where it can play different functions, for example, physiological molecular signalling, or pathological. At low concentrations (nmolar levels) NO acts as signalling molecule, while at higher concentrations (µmolar levels) it acts as a pathological or cytotoxic agent (Toledo and Augusto, 2012). Especially in the presence of reactive oxygen species (ROS), NO produces toxic nitrogen oxides, and can also damage enzymes that result in the inhibition of bacterial growth (reviewed by Stern and Zhu, 2014). In biological systems, NO can induce formation of other reactive species, such as hydroxyl and carbonate radicals (OH·and $CO_3{\cdot}^-$, respectively) (Figure 2.1.). Some of these species are powerful oxidants that can directly oxidize and damage DNA. For example, a high concentration of NO causes cytosine deamination and drives the mutation of cytosine (C) to thymine (T) (Wink et al., 1991), and peroxynitrite can directly oxidize guanosine residues transforming them to 8-oxo-2'-deoxyguanosine that causes DNA strand

breaks (Salgo et al., 1995; Burney et al., 1999). In addition to the formation of powerful oxidants, RNS cause formation of stable modifications in macromolecules, such as dinitrosyl iron complexes (DNICs), S-nitrosylation of Cys residues to form S-nitrosothiols (SNOs), and tyrosine nitration (NO_2-Tyr) (Figure 2.1.). These modifications alter protein structure and function and, consequently, also gene regulation and cell physiology (reviewed by Stern and Zhu, 2014).

NO reacts readily with transition metals, such as iron (Fe), reacting with both haem and non-heam Fe, including Fe-sulfur (Fe-S) cofactors, and has greater affinity for ferrous compared with ferric forms. NO binds to Fe in a similar way as O_2 does, because both molecules have an unpaired electron capable of forming a covalent bond coordinated with the *d*- orbital of the Fe atom. The capacity for binding both NO and O_2 makes Fe paradoxically a key element for sensitivity, for example blocking respiratory chains, but also promoting tolerance to NO given the capacity of haemoglobins to detoxify NO (reviewed by Gell, 2018).

At the level of proteins however, the most important modification produced by NO is S-nitrosylation, which modifies all main classes of proteins and provides a fundamental redox-based cellular signalling mechanism. A large number of bacterial proteins are affected by the formation of SNO groups when they are exposed to NO (Rhee et al., 2005; Brandes et al., 2007; Seth et al., 2012, 2018). These include transcription factors, such as *Escherichia coli* OxyR that induces expression of a specialized regulons during anaerobic respiration (Seth et al., 2012). The mechanism by which NO induces the formation of SNO groups is unclear since NO does not react directly with thiol groups under physiological conditions (reviewed by Stern and Zhu, 2014). In contrast to other posttranslational protein modifications, S-nitrosylation is generally considered to be non-enzymatic, involving multiple chemical routes. However, it has been recently reported that protein S-nitrosylation by NO in *E. coli* is essentially enzymatic, involving a multitude of enzymatic mechanisms (Seth et al., 2018).

Another protein modification induced by NO is NO_2-Tyr formation. Similarly to S-nitrosylation, NO does not react directly with tyrosines but it can indirectly through the formation of peroxynitrite (Souza et al., 2008). Tyrosine nitration has less capacity

for enzymatic inhibition than S-nitrosylations and, additionally, requires the presence of ROS (Figure 2.1.). The current knowledge on the biochemistry of peroxynitrite and tyrosine nitration has been recently reviewed by Bartesaghi and Radi (2018).

In addition to reacts in biological systems, NO plays an important role in atmospheric chemistry and influences the production of ground-level ozone and acid rain (Pilegaard, 2013).

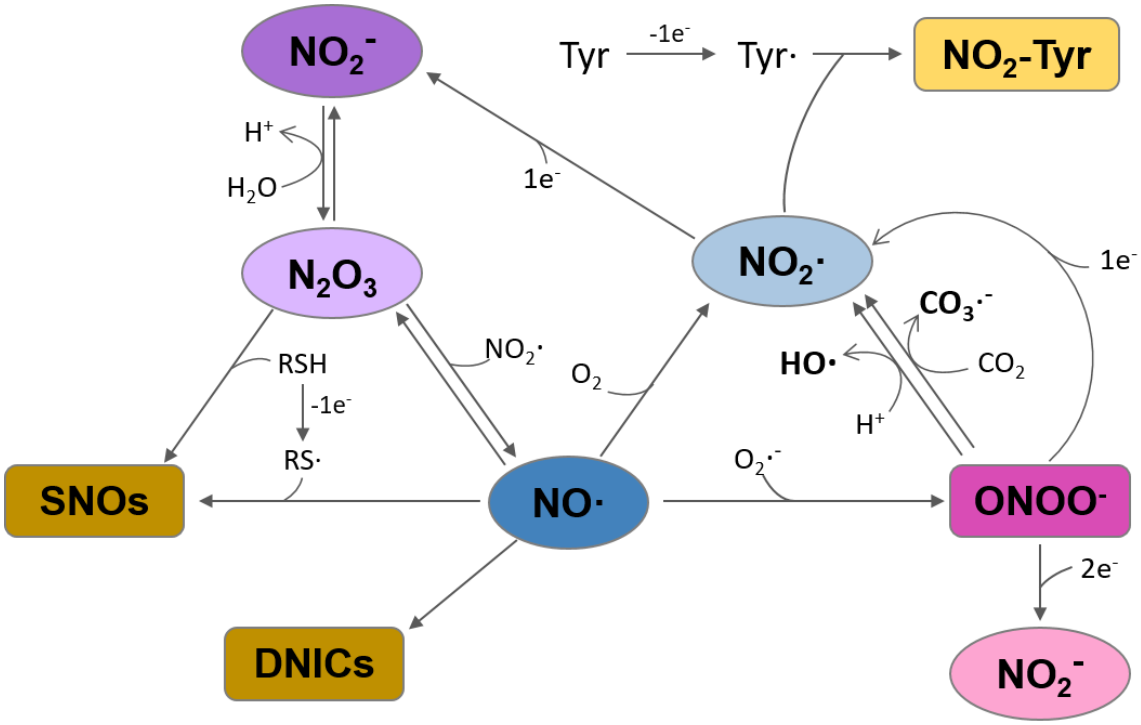

Figure 2.1. Nitric oxide (NO·) reactions and its biological targets. Adapted from Möller et al. (2019).

2.2. NO metabolism in bacteria

2.2.1. NO production

In bacteria, NO can be generated by multiple mechanisms, which are detailed below.

2.2.1.1. Respiratory sources

Among the many processes involved in bacterial NO synthesis that have been described, denitrification and the dissimilatory nitrate reduction to ammonium (DNRA) are currently considered the main respiratory sources of NO (reviewed by Torres et al., 2016). NO is a key intermediate of the denitrification process by which nitrate (NO_3^-) is

reduced to molecular nitrogen (N_2) for respiratory purposes (Zumft, 1997). DNRA consists of the respiratory reduction of NO_3^- to nitrite (NO_2^-) and, finally, to ammonium (NH_4^+), whereby NO is produced either chemically and/or enzymatically from NO_2^- (reviewed by Simon and Klotz, 2013).

2.2.1.1.1. Denitrification

Denitrification is defined as the respiratory reduction of NO_3^- or NO_2^- anions to generate ATP. These substrates are widely distributed in aquatic and terrestrial ecosystems. The complete denitrification process consists of four enzymatic steps. First, NO_3^- is reduced to NO_2^-, which is subsequently reduced to NO, nitrous oxide (N_2O) and, finally, N_2. Each nitrogen oxyanion and nitrogen oxide acts individually as a final electron acceptor associated to a respiratory chain, that functions under O_2 limiting conditions and allows the survival and replication of the microorganism during its anaerobic life-style (Zumft, 1997).

$$2NO_3^- \xrightarrow{4e^-} 2NO_2^- \xrightarrow{2e^-} 2NO \xrightarrow{2e^-} N_2O \xrightarrow{2e^-} N_2$$

Denitrification is widely distributed in Bacteria and appears to be dominant within Proteobacteria (Shapleigh, 2006). In addition, there is evidence that some fungi (Takaya, 2002; Prendergast-Miller et al., 2011; reviewed by Shoun and Fushinobu, 2017) and archaea (Treusch et al., 2005) can also denitrify, and some nitrifying organisms also have genes involved in denitrification (Cébron and Garnier, 2005). Most studies on denitrification have focused on Gram-negative bacteria that inhabit terrestrial niches. The α-proteobacteria *Paracoccus denitrificans* and the γ-proteobacteria *Pseudomonas stutzeri* and *Pseudomonas aeruginosa* are considered model organisms in the study of denitrification (reviewed by Zumft, 1997; van Spanning et al., 2007; Kraft et al., 2011; Richardson, 2011; Torres et al., 2016). The denitrification reactions are catalyzed by the periplasmic nitrate reductase (Nap) or membrane-associated nitrate reductase (Nar), nitrite reductases (NirK or NirS), nitric oxide reductases (cNor, qNor or Cu_ANor) and nitrous oxide reductase (Nos). These reductases consist of multisubunit metalloprotein complexes coupled to electron transport chains. Many components of these complexes require membrane transport

and insertion, complex assembly and cofactor incorporation. All these processes are mediated by fine-tuned stable and transient protein-protein interactions. Recently, an interactomic approach was used to determine the exact protein-protein interactions involved in the assembly of the denitrification apparatus of *P. aeruginosa* (reviewed by Borrero-de Acuña et al., 2017).

Most denitrifiers have three different types of nitrate reductases (NR) that catalyze the reduction of NO_3^- to NO_2^- and belong to the family of molybdopterin oxidoreductases. There are: (i) the cytosolic assimilatory NR (Nas), the respiratory membrane-bound NR (Nar) and the periplasmic NR (Nap) (for reviews see Potter et al., 2001; González et al., 2006; Richardson et al., 2007; Richardson, 2011; Simon and Klotz, 2013; Torres et al., 2016; González et al., 2017). Depending on the species, Nap can be used for anaerobic NO_3^- respiration or as an electron sink to maintain redox homeostasis by dissipating excess reducing power. This occurs in *P. denitrificans* that expresses Nap in addition to Nar. In this bacterium, Nap serves to dissipate the excess reduction equivalents formed during aerobic growth. The Nap enzyme is a heterodimer comprising the catalytic subunit NapA (90 kDa), that contains a *bis* molybdopterin guanine dinucleotide (Mo[MGD]$_2$) cofactor and a [4Fe-4S] center, and NapB (15 kDa), that contains 2 haem *c* groups and receives the electrons from the membrane-bound NapC (25 kDa), which binds 4 haem *c* groups (Figure 2.2.). NapC is a quinol-oxidase that receives the electrons from the ubiquinone pool. The *napEFDABC* genes encode the structural proteins (NapAB), as well as proteins necessary for the synthesis, maturation and enzymatic activity of Nap. In most Nap proteins, the transfer of electrons from the quinones pool to the NapAB complex requires NapC. However, in *E. coli* and *Wolinella succinogenes* a second quinol oxidase has been identified, NapGH, which is encoded in the operon *napFDAGHBC* and *napAGHBFLD*, respectively, in which NapH would act as a quinol dehydrogenase bound to the membrane, and NapG is a periplasmic protein that contains Fe-S centers and transfers the electrons to NapB.

Similarly to Nap, Nar is also a molybdoenzyme and respiratory NO_3^- reductase but with different biochemical properties to Nap. Nar is a larger trimeric enzyme complex (NarGHI) associated with the membrane and has been widely studied in *E. coli*. The NarG subunit (140 kDa) is oriented towards the cytoplasm and contains

Mo[MGD]$_2$ and a [4Fe-4S] cluster. NarH (60 kDa) contains one [3Fe-4S] and also three [4Fe-4S] clusters. NarG and NarH are located in the cytoplasm and associate with NarI (25 kDa), an integral membrane dihaem cytochrome *b* quinol oxidase (Figure 2.2.). Nar proteins are encoded by the *narGHJI* operon. Whereas *narGHI* encodes the structural subunits, *narJ* codes for a cognate chaperone required for the proper maturation and membrane insertion of Nar. Recent studies have shown in *P. denitrificans* that NarJ serves not only as chaperone of Nar, but also of the assimilatory nitrate reductase (NasC) (Pinchbeck et al., 2019). NarGHI is encoded by the *narK1K2GHIJ* genes. The *narK1K2* genes encode a functional fused transmembrane transporter that belongs to the facilitator superfamily (MFS) of proteins. NarK1 is a NO_3^-/H^+ symporter and NarK2 is a NO_3^-/NO_2^- antiporter (Goddard et al., 2008). Recently, it has been demonstrated by complementation assays in *P. denitrificans* that the NarK1-like domain of a NarK1-NarK2 fused protein functions primarily as a NO_3^- transporter, while the NarK2-like domain is more specialized in NO_3^-/NO_2^- antiport (Goddard et al., 2017).

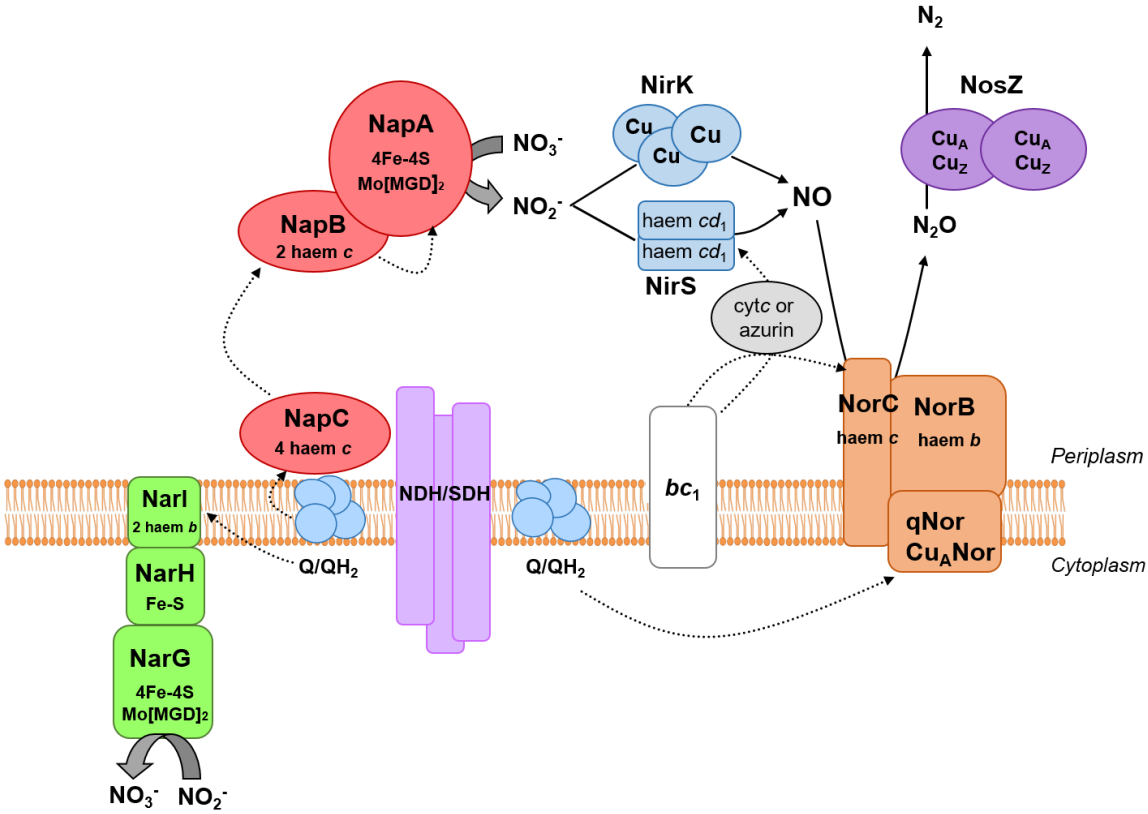

Figure 2.2. Schematic representation of denitrification enzymes. The membrane-bound (NarGHI), and periplasmic (NapABC) nitrate reductases, nitrite reductases (NirK and NirS), nitric oxide reductases (cNor, qNor and Cu_ANor) and nitrous oxide reductase (NosZ) are shown. Adapted from Torres et al. (2016).

2.2.1.1.1.1. Nitrite reductases NirK and NirS

NO production during denitrification occurs in the second stage of the route and is catalyzed by respiratory nitrite reductases, of which two types have been described: NirS (cd_1 type) and NirK (Cu-type) (reviewed by Rinaldo et al., 2008; van Spanning, 2011). These enzymes catalyze the reduction of NO_2^- to NO in the periplasmic space and receive electrons from cytochromes *c* or from the blue copper protein, pseudoazurin, via the cytochrome bc_1 complex (Figure 2.2.). Most denitrifiers have only NirK or NirS, however, it has recently been shown that *Bacillus nitroreducens* sp. nov (Jang et al., 2018) and *Bradyrhizobium oligotrophicum* (Sánchez and Minamisawa, 2018) possess genes of both nitrite reductases.

NirS is a homodimer with a small haem *c* domain and a larger haem d_1 domain for each monomer. The electrons are transferred from the electron donor via haem *c* to haem d_1, where NO_2^- is bound and reduced to NO (Rinaldo et al., 2008). The genes involved in NirS synthesis have been broadly characterized in *P. aeruginosa* (*nirSMCFDLGHJEN*), *P. denitrificans* (*nirXISECFDLGHJN*) and *P. stutzeri* (*nirSTBMCFDLGH* and *nirJEN*). The gene *nirS* encodes the functional subunit of the NirS dimer, and all other genes are needed for the haem d_1 cofactor synthesis, assembly and insertion to the active centre. The biosynthesis of haem d_1 cofactor has been the subject of numerous investigations (reviewed by Bali et al., 2014; Rinaldo et al., 2017).

NirK enzymes are homotrimers that contain three type 1 Cu (T1Cu) centres and three type 2 Cu (T2Cu) centres. NO_2^- binds to T2Cu, replacing an exogenous ligand (water or chloride ion), and here it is reduced to NO by electronic transfer from the T1Cu site. The structural properties of NirK have been recently reviewed by Horrel and colleagues (2017) and Nojiri (2017). Most of the two-domain NirKs are named as classes I and II depending on the colour of their (T1Cu) centre, class I is blue and class II is green. Three-domain NirKs (Class III) have been recently identified and comprises an extra T1Cu. This is the case of *Thermus scotoductus* SA-01 NirK, a homotrimer with subunits of 451 residues. The N-terminal region possesses a T2Cu and a T1CuN, while the C-terminus contains an extra T1CuC bound within a cupredoxin motif (Opperman et al., 2019).

In contrast to the complex organization of genes that encode NirS protein, NirK is encoded by a single gene, *nirK*. Sometimes, next to *nirK* there is another gene, *nirV*, responsible for the NirV protein synthesis, which is related to the desulforases and may be necessary for the insertion of Cu to the catalytic centre (reviewed by van Spanning, 2011).

The next step of denitrification is the NO reduction to N_2O by the Nor enzyme on the outer face of the cytoplasmic membrane (reviewed by Zumft, 2005; de Vries and Pouvreau, 2007; Richardson, 2011; Tosha and Shiro, 2017). Depending on the electron donor, the Nor enzymes are categorised into three different groups, cNor, qNor and Cu_ANor, which receive electrons from *c* type cytochromes and/or quinones (Figure 2.2.) (a detailed description of Nors is showed in Chapter 2.2.2.2.).

In the last stage of denitrification, N_2O produced by Nor is reduced with two electrons to N_2, catalyzed by the soluble enzyme nitrous oxide reductase (NosZ). NosZ (120-160 kDa) is a Cu-containing enzyme with two Cu centers: CuA center (a binuclear copper center) and CuZ center (tetranuclear copper sulfide center) (Figure 2.2.). CuA functions as the electron transferring center to CuZ, that is the catalytic center. There are two different forms of CuZ center: a CuZ * (4Cu1S) inactive form, and CuZ (4Cu2S) active form (for details about the structural and spectroscopic properties see reviews by Eady et al., 2016; Carreira et al., 2017; Pauleta et al., 2017, 2019).

Two different clades of this enzyme, that are differentially distributed by microbial taxa, are known. NosZ clade I, also known as the typical NosZ, is predominantly present in denitrifying organisms, and NosZ clade II or atypical, that curiously can be found in non-denitrifying bacteria, possibly to eliminate N_2O generated by NO detoxification systems (for a review see Hallin et al., 2018; Pauleta et al. 2017, 2019).

The expression, maturation and maintenance of the catalytic subunit of Nos (NosZ) require several auxiliary proteins, all of which are encoded together by a group of six genes (*nosRZDFYL*) in Nos from clade I. This group of genes is associated, in some cases, with *nosX* and *nosC* genes. The *nosDFY* genes encode an ABC-type transporter that is probably involved in the supply of sulfur for the assembly of the CuZ center. Recent genetic and biochemical studies in *P. denitrificans* have shown that NosL is a Cu

(I) binding protein that is required for efficient assembly of the CuZ site (Bennett et al., 2019). NosR and NosX do not participate in the biogenesis of CuZ, but play a role in the reduction of N_2O *in vivo* contributing to the maintenance of the reduced state of the CuZ center (Wunsch and Zumft, 2005). A regulatory role for NosR has also been assigned, since this protein is involved in the transcriptional regulation of *nosZ* in *P. stutzeri* and *P. denitrificans* (Honisch and Zumft, 2003; Sullivan et al., 2013).

The ε-proteobacterium *W. succinogenes* is an example of a clade II NosZ microorganism. The genes *nosZ, -B, -D, -G, -C1, -C2, -H, -F, -Y and -L* are responsible for the synthesis of this enzyme. The presence of *nosB, -G, -H, -C1 and -C2*, as well as the absence of *nosR* and *–X*, are characteristic of this group. The proteins NosG, -C1, -C2 and -H constitute an electron transport pathway from the menaquinol to NosZ. Specifically, NosGH is a menaquinol dehydrogenase complex and NosC1, C2 two cytochromes *c* (Hein et al., 2017).

2.2.1.1.2. Dissimilatory nitrate reduction to ammonium

Dissimilatory nitrate reduction to ammonium (DNRA) consists of the reduction of NO_3^- to NO_2^-, and, finally, to NH_4^+. This process is linked to others, such as formate oxidation, and generates an electrochemical proton gradient across the membrane, which is necessary to phosphorylate ADP to ATP allowing nitrate-ammonifying bacteria to grow thanks to NO_3^- and NO_2^- respiration (reviewed by Kraft et al., 2011; Simon and Klotz, 2013; Torres et al., 2016).

Nitrate-ammonifying organisms and denitrifiers share the NO_3^- to NO_2^- reduction step. To catalyse this reaction, they can use either Nar, Nap or both. In DNRA, next, NO_2^- is reduced to NH_4^+ by the periplasmic NrfA enzyme, which obtains electrons from the quinol/quinone pool through different electronic transport systems depending on the organism (Simon, 2002; Kern and Simon, 2009; Simon and Klotz, 2013). The most relevant examples of nitrate-ammonifying bacteria correspond to γ-, δ- and ε-proteobacteria, including *E. coli*, *Salmonella enterica* serovar Typhimurium, *Shewanella oneidensis*, *Shewanella loihica*, *Anaeromyxobacter dehalogenans*, *Campylobacter jejuni* and *W. succinogenes* and some Bacilli, such as *B. vireti*, *B. azotoformans* or *B. bataviensis* (Heylen and Keltjens, 2012; Mania et al., 2014). With the exception of *S. loihica*, nitrate-ammonifying bacteria normally lack both NirK and

NirS, as well as the classical Nors of denitrifying bacteria. However, DNRA is also a NO source. For example, *Salmonella* species and *E. coli*, which lack NirS or NirK enzymes, they produce NO as a side-product of NO_3^- or NO_2^- metabolism. Studies with *E. coli* mutants suggested that NO_2^--dependent NO formation was a consequence of the 'side' activity of the cytosolic assimilatory nitrite reductase (NirBD), as well as from NrfA, that both catalyse NO_2^- reduction to NH_4^+ (Corker and Poole, 2003; Weiss, 2006) (Figure 2.3.).

NirBD is one of the best studied NAD(P)H-dependent nitrite reductases. In *E. coli* and *S.* Typhimurium, NirBD is not an assimilative nitrite reductase in the strict sense, since it is induced in anaerobiosis when NO_2^- is the only source of N for growth (Cole, 1996; Lin and Stewart, 1998). This enzyme is composed of two different subunits, a large one of 93 kDa (NirB) with a sirohaem group and a [4Fe-4S] group, and a small protein of 12 kDa (NirD) homologous to a ferredoxin with a [2Fe-2S] group (Figure 2.3.). In studies with purified NirB, neither NO nor any other partial reduction product of NO_2^- was detected. Furthermore, the reactions whereby the product of NirB, for example, NH_4^+, can be converted to NO are not known. Therefore, either NO is a previously undetected latent intermediate that leaks from NirB in very small amounts, or perhaps it is the product of a reaction between a cytoplasmic constituent and a NirB-bound intermediate. With the current availability of more sensitive methods of detection, it may be worthwhile to reinvestigate the possibility that traces of NO may be released from purified NirBD (Weiss et al., 2006).

NrfA is located in the periplasm where reduces the NO_2^- produced by Nap to NH_4^+ with six electrons, which are often obtained by formate oxidation. This allows NO_2^- to be used as a final electron acceptor, facilitating anaerobic respiration (reviewed by Clarke et al., 2008; Einsle, 2011; Simon and Klotz, 2013). NrfA was first described in *E. coli*, and it is found in the periplasm of a wide range of γ-, δ- and ε-proteobacteria. In *E. coli*, the *nrfABCDEFG* genes are involved in the synthesis and activity of NrfA. The *nrfA* gene encodes the catalytic subunit NrfA, *nrfB* encodes a small pentahemic electron transporter that allows the electronic flow between the quinol dehydrogenase integrated in the membrane NrfCD and NrfA (Figure 2.3.). The genes *nrfE*, *nrfF* and *nrfG* encode the machinery necessary to couple the haem group of the

NrfA active site with the quinol pool (Clarke et al., 2007). NrfA contains four haem *c* groups where the haem-Fe is coordinated by bis-histidine axial ligation for electronic transport. These differ structurally to the haem of the active centre for the reduction of NO_2^- where the haem is ligated by a single protein residue (lysine or histidine). NO is generated both chemically and enzymatically via NrfA from NO_2^-, although the detailed mechanisms are not very well known. It is thought to occur in multiple stages involving electron transfer from its five haem groups to the substrate, with the formation of NO and NH_2OH as intermediates, unlike denitrifying nitrite reductases (NirK or NirS), which convert NO_2^- directly to NO (Poole, 2005). A combination of electrochemical, structural and spectroscopic studies revealed that NrfA simultaneously binds NO_2^- and electrons at the catalytic haem. As a consequence, the distal His is proposed to play a key role in orienting the NO_2^- molecule for N-O bond breakage (Lockwood et al., 2015).

Another important respiratory process from the N cycle that produces NO is the anaerobic NH_4^+-oxidation (anammox). Anamox bacteria couple NO_2^- reduction to NH_4^+ oxidation with NO and hydrazine as intermediates, and produce N_2 and NO_3^- (Kartal et al., 2013). In the anamox microorganism *Kuenenia stuttgartiensis*, it has been described a novel pathway to make NO from hydroxylamine. This new enzyme is related to octahaem hydroxylamine oxidoreductase, a key protein in aerobic NH_4^+-oxidizing bacteria. By a multiphasic approach including the determination of the crystal structure of the *K. stuttgartiensis* enzyme at 1.8 Å resolution, both in the presence and absence of its substrates, a model for NO formation by the *K. stuttgartiensis* hydroxilamine oxidoreductase has been proposed (Maalcke et al., 2014).

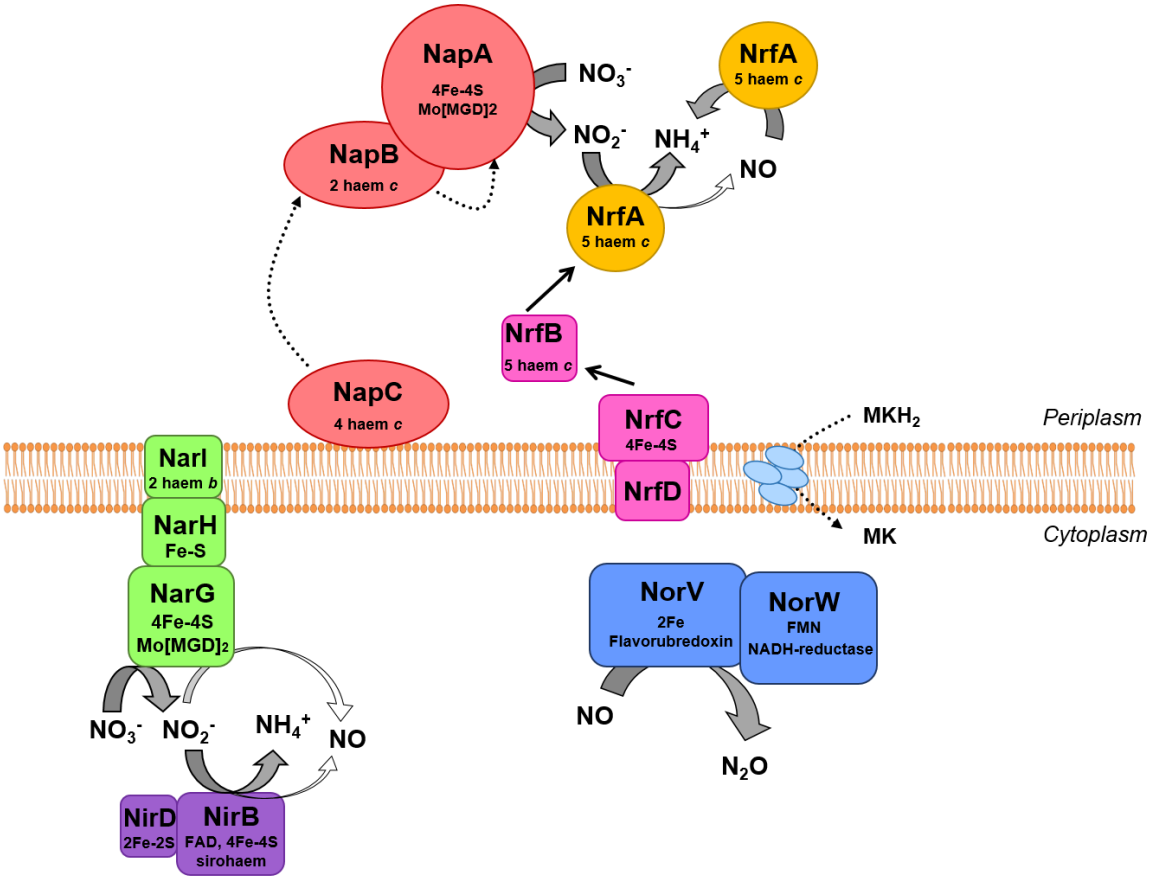

Figure 2.3. Schematic representation of DNRA in *E. coli*. Enzymes involved in NO_3^- reduction (NapABC and NarGHI), NO_2^- reduction (NrfABCD, NirBD), NO production (NrfA/NirBD, NarG) and NO reduction (NorVW) are shown. Adapted from Torres et al. (2016).

2.2.1.2. Non-respiratory sources

For long time, NO formation in prokaryotes has been thought to occur only through denitrification, DNRA, and other related respiratory pathways, such as anaerobic NH_4^+ oxidation (Zumft, 1997; Richardson and Watmough, 1999; Jetten, 2008; Martínez-Espinosa et al., 2011; Maia and Moura, 2014). In these routes, NO is a common and necessary substrate and product, working also as a signal molecule regulating the genes necessary for its own metabolism. However, at present, it is widely recognized that NO is also produced by non-respiratory routes, including oxidative stress cytoprotection in *E. coli*, *Bacillus subtilis*, *Bacillus anthracis* or *Staphylococcus aureus* (Nakano, 2002; Mukhopadhyay et al., 2004; Shatalin et al., 2008; Gusarov et al., 2009), recovery from damage caused by radiation (Patel et al., 2009) or the biosynthesis of

secondary metabolites, such as tryptophan nitration in *Deinococcus radiodurans* (Buddha et al., 2004).

Recently, it has also been demonstrated that ammonia (NH_3)-oxidizing bacteria (AOB) also emit substantial amounts of NO. The currently accepted model for AOB metabolism involves NH_3 oxidation to NO_2^- via a single obligate intermediate, hydroxylamine (NH_2OH). However, recent studies have demonstrated that aerobic NH_3 oxidation occurs via two obligate intermediates: NH_2OH and NO (Caranto and Lancaster, 2017).

2.2.1.2.1. Bacterial nitric oxide synthase

Several prokaryotes, such as *Staphylococcus*, *Geobacillus*, *Bacillus*, *Rhodococcus*, *Streptomyces*, *Deinococcusus* and *Natronomonas*, contain a nitric oxide synthase (bNOS) homologous to the mammalian NOS that catalyzes aerobic NO formation from arginine using cellular redox equivalents (Gusarov et al., 2008). Contrary to the eukaryotic NOS, bNOS normally lacks the reductase domain, with the exception of the bNOS from *Sorangium cellulosum* (Gusarov et al., 2008; Agapie et al., 2009; reviewed by Santolini, 2019). The reductase involved in electron transfer to the oxygenase domain of bNOS is still unknown. The role of bNOS in bacterial physiology has been recently reviewed by Hutfless et al. (2018). The main role of bNOS is to protect cells against oxidative agents (Gusarov and Nudler, 2005; Shatalin et al., 2008) by two different ways: (i) NO produced by bNOSs transiently inhibits the enzymatic reduction of cysteine, preventing this cysteine to be a substrate of the Fenton reaction, in which this cysteine, together with ferric ions and H_2O_2, produce hydroxyl radicals ($OH\cdot$), that react mainly with DNA generating modifications and breaking the DNA strands, (ii) NO produced by bNOS induces the antioxidant catalase, that transforms H_2O_2 in oxygen and H_2O. Consequently, NO production by bNOS is involved in the defense of pathogenic organisms against the immune system oxidative attack, being essential for the virulence of *B. anthracis* (Shatalin et al., 2008), and is also important during the infection of plants by *Streptomyces turgidiscabies* (Johnson et al., 2008). In addition to pathogenic bacteria, bNOS encoding genes are also present in the genome of numerous non-pathogenic soil bacterial species (Gusarov et al., 2008).

NO production by bNOS has also been shown to be involved in antibiotic resistance (Gusarov et al., 2009). Chemical changes of these toxic compounds provoked by NO inactivate them, and, additionally, mitigates the oxidative stress caused by many bacteriocidal antibiotics, such as lactamic, aminoglycosides and quinolones (Kohanski et al., 2007).

It is not known yet that bNOSs could have a similar function to eukaryotic NOSs as growth inhibitors of other bacterial species present in the same medium (reviewed by Stern and Zhu, 2014). Given the important role of bNOS in the resistance of pathogens against antibiotics as well in the immune system activation, the inhibition of this enzyme can constitute an effective antibacterial intervention (Gusarov et al., 2009).

2.2.1.2.2. Molybdoenzymes: a new class of nitric oxide-forming nitrite reductases

For years, NO formation from NO_2^- was assumed to be produced, in addition to the respiratory NiRs (NirK and NirS) from denitrifiers, by NirDB and NrfA from nitrate-ammonifying bacteria. Currently, the largest non-respiratory source of NO_2^--dependent NO is thought to be derived from a new class of NO-forming nitrite reductase molybdoenzymes. Molybdenum (Mo) is essential to most of the living organisms from archaea and bacteria to higher plants and mammals, being part of the active site of enzymes that catalyse important redox reactions of the metabolism of carbon (C), N, and sulphur (S). Presently, more than 50 Mo-containing enzymes are known, many of which have been biochemically and structurally characterised, and several other are foreseen to be “discovered” in the near future based on genomic analyses. Noteworthy, the great majority of the Mo-enzymes are prokaryotic, whereas only a restricted number are found in eukaryotes (for a review see Maia and Moura, 2015; Maia et al., 2017).

As mention above, in prokaryotes, NO_3^- is reduced by both assimilative and disassimilative routes, for which these organisms contain three NR different enzymes distributed in different subcellular locations. First, the membrane-bound respiratory NR (Nar), associated with the generation of proton-motive force (PMF), second the periplasmic NR (Nap), also involved in respiration or as an electron sink to eliminate

the excess of reducing equivalents, and, finally, the assimilative cytoplasmic NR (Nas), involved in NO_3^- assimilation. Nar, Nap and Nas are Mo-enzymes, belonging to the dimethyl sulfoxide reductase (DMSOR) family, which catalyze the reduction of NO_3^- to NO_2^-. In spite of catalyzing the same reaction and having Mo in their active sites coordinated by four sulfur atoms from two pyranopterin cofactor molecules both present as a guanine dinucleotide (Mo $[MGD]_2$), the three NR types display significant differences at the remainder of the Mo coordination sphere. In addition to significant differences present around their active centres, these NRs have different biological roles, subcellular location, different subunits composition and quaternary structure (for a review see Maia and Moura, 2015). While NarGHI is a heterotrimer $(\alpha\beta\gamma)_2$, NapAB is a dimer and Nas constitutes a single subunit, NasC. Similarly to NarGHI and NapAB, NasC contains (Mo $[MGD]_2$), a [4Fe-4S] centre and possibly another [2Fe-2S] centre in the C-terminal region (Gates et al., 2011). Several studies have suggested that the non-respiratory NO generation is due to the NR-catalysed NO_2^- reduction, with the majority of NO being formed by the respiratory membrane-bound Nar and a small contribution (less than 3%) from the periplasmatic Nap (Gilberthorpe and Poole, 2008; Vine et al., 2011; Rowley et al., 2012). Recent works in rhizobia species have proposed the potential contribution of the cytoplasmic assimilative Nas as an NO source (for details see Chapter 2.4.3.). NO formation *in vivo* by NRs could depend on several factors, such as anaerobiosis, NO_3^- deficiency or NO_2^- accumulation (Einsle and Kroneck, 2004; Gilberthorpe and Poole, 2008; Rowley et al., 2012). However, the ability of prokaryotes to produce NO by NRs seems to depend on the organism, and possibly on the role of NO. For example, while NO generation in *E. coli* is estimated to be below 1% of reduced NO_3^- (Calmels et al., 1988; Vine and Cole, 2011; Rowley et al., 2012), in *S.* Typhimurium can reach up to 20% (Rowley et al., 2012).

In addition to prokaryotic NRs, the Mo-enzyme aldehyde oxidoreductase (AOR) can also contribute to the bacterial NO formation. AOR is an xantine oxidase (XO) family member structurally similar to the mammalian XO and AO, but harbouring only two [2Fe-2S] centres (no FAD) and holding a slightly different molybdopterin cofactor. As the mammalian XO and AO enzymes, AOR was recently shown to catalyse NO_2^- reduction to NO (Maia and Moura, 2011). An updated knowledge on the *in vitro* and *in*

vivo role of the Mo-enzymes XO and AO on the NO metabolism in humans has been recently reviewed by Maia and Moura (2018).

2.2.2. NO detoxification

Bacteria use multiple systems to eliminate NO with a large variety of enzymes involved in this process. Most of these systems work by trapping NO directly and transforming it into a less reactive nitrogen oxide molecule, such as NO_3^-, NH_4^+ or N_2O. However, other systems function indirectly at the physiological level, promoting resistance to the toxic effect of NO or repairing the damage caused. The information available on the proteins implicated in NO detoxification in bacteria is detailed below.

2.2.2.1. Haemoglobins

Haemoglobins (Hbs) are Fe-containing proteins distributed across all three domains of life (bacteria, archaea and eukaryotes) that, in addition to be essential for O_2 transport, they are also well-characterized systems for NO detoxification (reviewed recently by Gell et al., 2018). Haemoglobins are the best studied and most important proteins for aerobic NO detoxification in bacteria. In prokaryotes, three types of haemoglobins have been identified: flavohaemoglobins (fHbs), single domain haemoglobins (sdHbs) and truncated haemoglobins (tHbs) (reviewed by Poole, 2005; Stern and Zhu, 2014; Gell, 2018).

All Hbs share a common three-dimensional structure and haem cofactor. They have a conserved core topology, comprising 6-8 α-helices (labelled A-H) (Figure 2.4.). The myoglobin (Mb) from muscle of the sperm and the red blood cell (RBC) Hb from horse erythrocytes were the first Hbs whose structure was determined (Kendrew et al., 1960; Perutz et al., 1960). These studies revealed the globin structural blueprint, and firmly established the enduring paradigm that structure underlies function. Many Hbs structures (>200) are today available in the protein data bank. Among them, position F8 refers to the amino acid residue that is structurally equivalent to the eighth residue in helix F of sperm whale Mb. This haem-coordinating histidine residue (HisF8) is the only residue that is 100% conserved across the whole Hb superfamily (Kapp et al., 1995; Freitas et al., 2004) (Figure 2.4.A.). Residues in non-helical segments are referenced in relation to adjacent helices; thus, CD1 refers to the first residue of the

linker joining α-helices C and D, and HC3 refers to the third residue following helix H, on the carboxyl terminus (Figure 2.4.A.).

Globins can fold in two different structural ways: 3-on-3 and 2-on-2 (reviewed by Gell, 2018). The '3-on-3' structural class consists in the α-helical 'sandwich' composed by the A-G-H and B-E-F helices. The C and D helices are supporting structures and are not always present. The '3-on-3' fold is represented by Mb from muscle of the sperm whale (Figure 2.4.A.). The fHbs and sdHbs present a globin domain with a 3-on-3 α-helical fold similar to Mb (Tinajero-Trejo and Shepherd, 2013) (Figures 2.4.B. and C.). The second structural class is the truncated Hb (trHb) class, also called 2-on-2, 2-over-2, or 2/2 Hbs, based on the arrangement of the B-E and G-H helical pairs (Figure 2.4.D.). In trHbs, the A, C, D, and F helices are much reduced or absent. Whereas some Hbs function as monomers, other Hbs are assembled from multiple globin subunits. Each globin polypeptide binds a single molecule of Fe-protoporphyrin-IX (haem *b*) (Figure 2.4.E.). The haem molecule contains two charged propionate groups that interact with water and/or polar amino acid side chains on the surface of the globin, and the remainder of the haem molecule is largely hydrophobic in nature and binds in the hydrophobic interior of the globin, surrounded by apolar side chains. Each haem has a central Fe atom that is coordinated by four equatorial N ligands, one from each of the four pyrrole rings of the porphyrin (Figure 2.4.E.). Haem is bound to the protein via a coordinate covalent bond from an axial N ligand provided by the imidazole side chain of HisF8, together with multiple non-covalent interactions between the porphyrin and globin. Whilst the Fe of the haem makes a coordinate covalent bond with diatomic gaseous ligands, such as O_2, CO, NO, HNO, NO_2 and H_2S, the globin fold provides the essential environment to achieve reversible and selective ligand binding. The plane of the porphyrin divides the haem pocket into two regions, the Fe-coordinating HisF8 side chain occupies the proximal haem pocket, leaving diatomic ligands bind on the opposite face of the porphyrin, which is the distal haem pocket. Both 3-on-3 Hbs and trHbs (2/2 Hbs) are found in bacteria, archaea and eukaryotes. Sequence phylogeny indicates that 3-on-3 Hbs are divided into two families, and five sub-families which represent functional groupings (reviewed by Gell, 2018). Many members of the plant and metazoan Hb subfamily bind O_2 with moderate

affinity (K_{O2} ~1-20 μM^{-1}) and have roles in O_2 storage or transport. The fHb and sdHb sub-families have high O_2 affinity (K_{O2} = 10-1000 μM^{-1}), they are found only in bacteria, algae, and fungi and are nitric oxide dioxygenase (NOD) enzymes that protect against nitrosative stress by converting toxic NO to NO_3^- (reviewed in Gardner, 2012).

Sequence alignment of several Hbs, including non-symbiotic plant Hbs, fHbs, sdHbs, and trHbs, shows conserved residues, among them, aromatic residues, such as Phe, but also Trp, are common in the haem pocket. Particularly, PheCD1, which makes π-stacking interactions with pyrrole ring C, is the second-most highly conserved globin residue after HisF8 (reviewed in Gell, 2018).

It has been known for long time that NO has extremely high affinity for Hbs (Gibson and Roughton, 1957, 1965). Under physiological conditions, the major Hb/Mb species in mammals are deoxy Hb/MbFe(II) and Hb/Mb(O_2), both of which undergo extremely rapid reaction with NO. Under anaerobic conditions, HbFe(II) and MbFe(II) bind NO reversibly, but with extremely high affinity (K_{NO} ~2×10^{11} M^{-1}). Upon exposure to O_2, the ferrous nitrosyl HbFe(II)(NO) species convert to metHb (Hb^{3+}) and NO_3^- at a rate governed by the slow dissociation of NO from Fe(II) haems (K_{NO} is 10^{-4} to 10^{-5} s^{-1}) (Herold and Rock, 2005). On the other hand, the reaction of NO with O_2-Mb^{2+} or O_2-Hb^{2+} to form Hb^{3+} and NO_3^- is extremely fast (bimolecular rate constant ~1×10^8 $M^{-1}\,s^{-1}$) (Eich et al., 1996). Reaction products of O_2-Mb^{2+} or O_2-Hb^{2+} in excess of NO are exclusively Hb^{3+} and NO_3^- (Figure 2.5., reaction 1). The NO induced oxidation of O_2-Hb^{2+} proceeds by an NO dioxygenation (NOD) mechanism that involves capture of NO in the distal pocket of O_2-Hb^{2+}, where it reacts with bound O_2 to form an Fe(III) cis-peroxynitrite transition state, ONOO-Hb^{3+}, that immediately isomerises to an Hb^{3+}+NO_3^- complex (Yukl et al., 2009) (Figure 2.5., reaction 1). An alternative pathway proceeding by reaction of non-coordinated O_2 in the distal pocket of NO-Hb^{2+}, termed O_2 nitrosylation, has been proposed (Hausladen et al., 1998) (Figure 2.5., reaction 2). However, the NOD mechanism is consistent with kinetics of NO reactions with vertebrate Hb/Mb and bacterial fHbs, and is likely to be a general mechanism for NO reaction with Hb over a wide range of O_2 concentrations *in vivo* (for a review see Gardner, 2005, 2012).

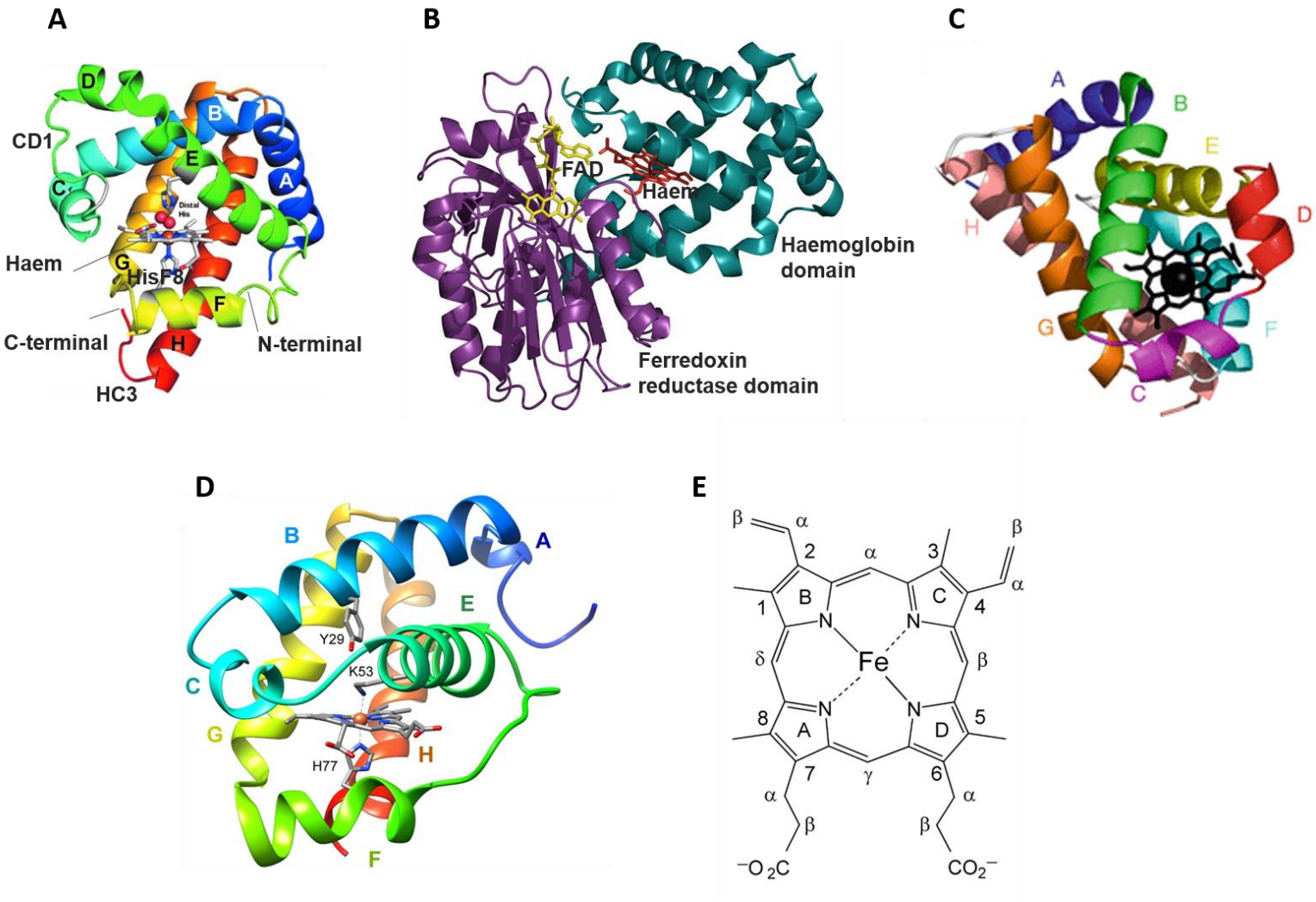

Figure 2.4. Haemoglobin tertiary structures. A. Sperm whale Mb (Richards, 2013). **B.** fHb from *E. coli* (Mowat et al., 2010). **C.** sdHb from *C. jejuni* (Tinajero-Trejo and Shepherd, 2013). **D.** tHb from *Chlamidomonas* (Johnson et al., 2018). **E.** Haem group (Johnson et al., 2018).

2.2.2.1.1. Flavohaemoglobins

The best studied bacterial haemoglobins are fHbs, with *E. coli* Hmp as the main representative (Vasudevan et al., 1991). *Ralstonia eutropha* (formerly *Alcaligenes eutrophus*) fHb was the first X-ray structure determined (Bonamore and Boffi, 2008). They contain three domains: an N-terminal globin domain, a central FAD-binding domain and a C-terminal NADP-binding domain (Figure 2.4.B.). Residues of the haem pocket implicated in NOD activity are highly conserved across fHbs, as are residues surrounding the flavin cofactor that play roles in electron transfer from NADP (Bonamore and Boffi, 2008). fHbs have also been identified in *Salmonella enterica* (McLean et al., 2010), *S.* Typhimurium (Bang et al., 2006), *R. entropha* (Cramm et al., 1994), *S. aureus* (Richardson et al., 2006), *B. subtilis* (Nakano, 2006), and *Saccharomyces cerevisiae* (yeast) (Liu et al., 2000; Lewinska and Bartosz, 2006). By performing gene knockout studies, it has been shown that fHbs protect their host organisms from nitrosative stress. In a number of cases, resistance to nitrosative stress conferred by fHb contributes to pathogen virulence (Bang et al., 2006; Richardson et al., 2006; Svensson et al., 2006).

Regarding the molecular mechanism of fHbs for NO detoxification, two pathways have been proposed depending on the O_2 availability. As mention above, under aerobic conditions, they transform NO into NO_3^- by a NOD activity. Under anaerobic conditions, it has been shown that *E. coli* Hmp is able to reduce NO to N_2O. However, the rates of NO reduction are modest by comparison with better characterised NO reductases in fungi and bacteria (Kim et al., 1999). This led to the conclusion that Hmp does not provide physiologically relevant protection to anaerobic cultures.

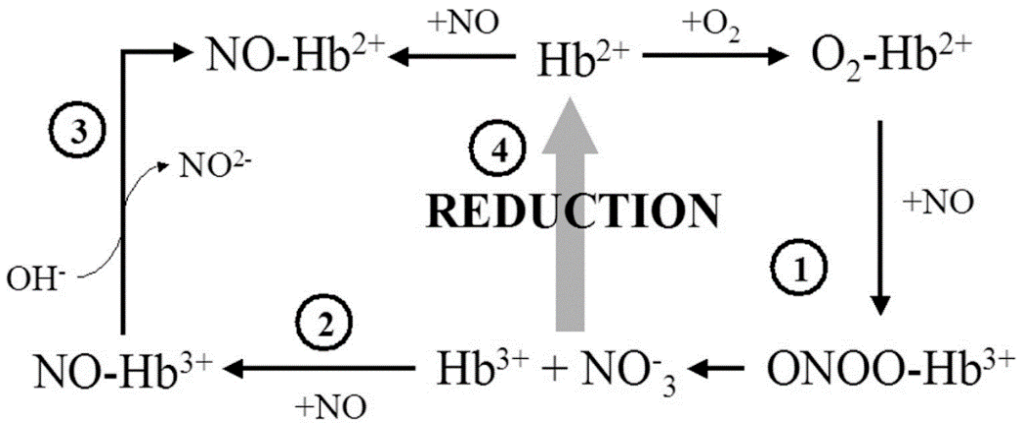

Figure 2.5. NO reactions of haemoglobins. 1. NO dioxygenase activity. **2.** NO binding to the ferric Hbs. **3.** NO-induced haem Fe reduction. **4.** O_2 nitroxylase activity. Smagghe et al. (2008).

2.2.2.1.2. Single domain haemoglobins

sdHbs resemble fHbs but lack the oxidoreductase and FAD domains, containing only one globin domain with one haem *b* group (Figure 2.4.C.). The first haemoglobin of this type to be identified and sequenced was *Vitreoscilla* haemoglobin (Vgb), whose presence increases under microaerobic conditions. The physiological role of Vgb from *Vitreoscilla stercoraria* has not been conclusively demonstrated yet, but an NO detoxification function for this Vgb expressed in a heterologous organism conferred some protection against nitrosative stress (Wu et al., 2003). Vgb fused with a fHb reductase domain has been extensively used in biotechnology applications to protect against nitrosative stress (Kaur et al., 2002). In *C. jejuni*, a NOD function for a sdHb (Cgb) has been demonstrated by gene deletion (Elvers et al., 2004), biochemistry (Lu et al., 2007; Shepherd et al., 2010) and expression analyses (Elvers et al., 2004; Monk et al., 2008). Studies carried out with Cgb have also revealed their importance in NO resistance since a strain deficient in Cgb is hypersensitive to nitrosating agents, such as S-nitrosoglutathione (GSNO) or sodium nitroprusside (SNP), and compounds that release NO, like spermine NONOate. In addition, *cgb* gene expression is induced strongly and specifically by exposure to nitrosative stress (Elvers et al., 2004). Currently, the mechanism of action is not known, since the redox system that recycles ferrous haem has not been identified. The structure of cyanide-bound Cgb was solved by using X-ray crystallography with a resolution of 1.35 Å (Shepherd et al., 2010). Cgb

has structural homology with Vgb from *V. stercoraria* (Tarricone et al., 1997), the N-terminal globin domain of Hmp from *E. coli* (Ilari et al., 2002) and the sperm whale myoglobin (Mb) (Arcovito et al., 2007) (reviewed by Tinajero-Trejo and Shepherd, 2013) (see Figure 2.4.C.). Although evidence that sdHbs function generally as NOD enzymes is emerging, an important piece of the puzzle identifying the reductase for these proteins *in vivo* remains to be solved.

2.2.2.1.3. Truncated haemoglobins

tHbs are widely spread and they are between 20-40 residues shorter than the sdHbs (reviewed by Tinajero-Trejo et al., 2013). Like sdHbs, tHbs lack the flavoreductase domain and they only have the globin domain (Figure 2.4.D.), but they differ from sdHbs since, once translated, they are mannosylated and bound to the cell wall (Arya et al., 2013). By using X-ray crystallography, the structure of dimeric cyanide-bound tHb from *C. jejuni* showed the presence of four α-helices organized in '2-on-2' fold formed by the B-E and G-H helical pairs (Figure 2.4.D.). In this structural class, the A, C, D, and F helices are reduced or missing (Nardini et al., 2006). Although some trHbs supply O_2 in pathogens, others are involved in NO stress tolerance. In *Mycobacterium tuberculosis*, a species in which NO detoxification is a critical component for its virulence (Chan et al., 1992; Yang et al., 2009), the fundamental mechanism to tolerate NO is the truncated haemoglobin HbN (Pathania et al., 2002). In *Mycobacterium bovis*, HbN protects aerobic respiration from NO, and *in vitro* this protein oxidizes NO to NO_3^- (Ouellet et al., 2002). Additionally, HbN heterologous expression experiments in *Mycobacterium smegmatis* and *E. coli* demonstrated the role of these haemoglobins in protecting against NO (Pathania et al., 2002). *C. jejuni* tHb (Ctb) is constitutively expressed under nitrosative stress conditions (Elvers et al., 2004). Nonetheless, Ctb did not protect in the presence of NO or other RNS in *C. jejuni* (Wainwright et al., 2005). The role of Ctb in protection from NO and RNS is not well known, however, it has been demonstrated that it is lower than Cgb (reviewed by Tinajero-Trejo et al., 2013).

In addition to *Mycobacterium* (Ouellet et al., 2002; Arya et al., 2013) and *Campilobacter* species, a role in nitrosative stress response has also been demonstrated genetically for trHbs from *Synechococcus* (Scott et al., 2010), *Chlamydomonas reinhardtii* (Hemschemeier et al., 2013; Johnson et al., 2014), and the

antarcticmarine bacterium *Pseudoalteromonas haloplanktis* (Parrilli et al., 2010). *In vitro* and physiological evidence suggests that the trHb from *C. reinhardtii* converts the NO generated by nitrate reductase (NIT1) into NO_3^- (Rice et al., 2015). The structure of trHb from *C. reinhardtii* resembles other trHbs, but it also exhibits distinct features associated with the coordination of the haem by a proximal histidine (H77) and a distal lysine (K53) (Rice et al., 2015) (Figure 2.4.D.). Site-directed mutagenesis analyses have recently demonstrated that the distal lysine (K53) coordination is related to the ability of *C. reinhardtii* trHb to detoxify NO efficiently (Johnson et al., 2018).

2.2.2.2. Nitric oxide reductases

Under low O_2 conditions, the enzymes with greater relevance in NO detoxification are the denitrifying nitric oxide reductases (Nors). These enzymes have a predominantly physiological role on respiration than in conferring resistance to nitrosative stress, since they are a component of the denitrification pathway. However, in some cases they have a role in resistance to endogenous and exogenous nitrosative stress (Anjum et al., 2002; Wang et al., 2011). Bacterial Nor is a membrane-bound enzyme that catalyzes the reduction of NO to N_2O on the outer site of the cytoplasmic membrane. Currently, three Nor types have been characterized in bacteria: cNor, qNor and Cu_ANor (reviewed by Hendriks et al., 2000; Zumft, 2005; de Vries and Pouvreau, 2007; Richardson, 2011; Tosha and Shiro, 2017). In cNors, the catalytic subunit NorB receives electrons from a cytochrome *c* (NorC subunit), however, the qNor monomers directly react with the quinones (Figure 2.6.).

cNor enzymes have been well characterized in *P. denitrificans*, *P. stutzeri* and *P. aeruginosa* organisms, being cNor from *P. stutzeri* the first to be isolated (Kastrau et al., 1994). The structural subunits, NorCB, are encoded by the *norCB* genes, which are co-transcribed together with the *norD* and *norQ* accessory genes, and, eventually, with the *norE* and *norF* genes (Zumft, 2005). In *Thermales* and *Aquificales* orders the *norC* and *norB* genes are followed by a third gene (*norH*) that encodes a small membrane protein, important for an efficient denitrification (Bricio et al., 2014). The catalytic subunit of cNor enzymes, NorB, belongs to the haem-copper oxidases superfamily (HCOs). NorB has 12 transmembrane helices and contains haem *b* and a binuclear active center (haem b_3 and FeB) (Figure 2.5.A.) (Daskalakis et al., 2015). NorC, is a

membrane-anchored protein that contains haem *c* in a hydrophilic domain and transfers electrons from the bc_1 complex to NorB through cytochromes *c* or pseudoazurins (the structural properties of cNor have been extensively reviewed by Hino et al., 2010; Shiro et al., 2012; Daskalakis et al., 2015; Tosha and Shiro, 2017; Mahinthichaichan et al., 2018). NorD and NorE are membrane-bound proteins involved in the correct assembly of NorCB complex (Butland et al., 2001). Mutation of the *norE* and *norF* genes decreases NO reductase activity in *P. denitrificans* and *Rhodobacter sphaeroides* (de Boer et al., 1996; Hartsock and Shapleigh, 2010). Although these proteins are not essential for Nor activity, they are important under conditions where endogenous Nir activity generates a prolonged exposure to NO (Bergaust et al., 2014). Recently, it has been shown that NorQ and NorD from *P. denitrificans* are implicated in non-haem Fe (Fe_B) insertion cofactor into NorB (Kahle et al., 2018). Crystallography studies of the *P. aeruginosa* cNOR demonstrated that NorB does not have any transmembrane proton channel, unlike proton translocating HCOs, so this enzyme does not act as a proton pump and, therefore, it is not directly involved in energy conservation (Hino et al., 2010; Pisliakov et al., 2012; Shiro et al., 2012).

As discussed previously, qNors obtain electrons from ubiquinol and menaquinol. The qNor structure is similar to the NorB subunit of cNors, differing in an N-terminal extension with homology to the NorC subunit, but without a haem *c* binding motif. Crystallization of the *Geobacillus stearothermophilus* qNor has shown to have an aqueous channel from the cytoplasm that could act to translocate protons (Matsumoto et al., 2012), so it is possible that quinol oxidation coupled to NO reduction by the qNor is electrogenic. This enzyme is also present in Archaea, such as haloarchaea class. The unique *nor* gene found in haloarchaea encodes for a single subunit quinone-dependent respiratory Nor homologous to bacterial qNor (Torregrosa-Crespo et al., 2017). An unusual qNor subgroup, the qCu_ANor, present for example in *B. azotoformans*, contains a NorB subunit in complex with another subunit containing a Cu_A site (typical from HCOs), which makes this enzyme capable of receiving electrons from the membrane-bound cytochrome c_{550} (de Vries and Pouvreau, 2007). However, in the *Bacillus* genus it was shown that qCu_ANor lacks

menaquinone oxidase activity, so a nomenclature change from qCu_ANor to Cu_ANor was suggested (Al-Attar and de Vries, 2015).

In addition to Nors from denitrifiers, it has been recently demonstrated that the anamox bacterium *K. stuttgartiensis* is able to use NO as its terminal electron acceptor, and conserve energy and grow by coupling NO reduction to NH_4^+ oxidation in the absence of NO_2^-. Under these conditions, NO_3^- is not produced and the sole end product is N_2. Using comparative transcriptomics and proteomics, it has been demonstrated that when growing on NO-dependent NH_4^+ oxidation, *K. stuttgartiensis* down regulates the transcription of proteins responsible for NO generation, as well as NO_2^- oxidation (Hu et al., 2019).

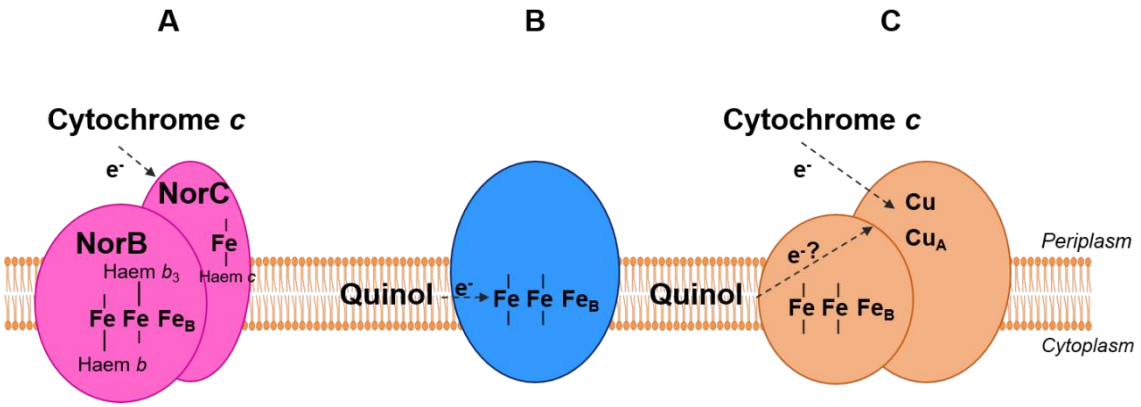

Figure 2.6. Bacterial nitric oxide reductases. A. cNor. **B.** qNor. **C.** Cu_ANor. Adapted from Tosha and Shiro (2017).

2.2.2.3. Flavorubredoxin

In addition to Nors, another NO reductase to be discovered was the flavorubredoxins (Gardner et al., 2002) that receive their name because they are composed by a subunit that contains a FMN group (NorW) and another with a non-haem Fe active centre homologous to that present in the rubredoxins (NorV) (Gomes et al., 2000) (Figure 2.3.). These proteins have an important role in NO detoxification by reducing NO to N_2O. However, they are structurally and mechanistically very different to Nors. In various bacteria, the *norVW* operon encodes the catalytic subunit NorV and a NADH-dependent NorV reductase, the flavoprotein NorW that transfers electrons from NADH

to NorV thanks to its FMN motif (Gardner et al., 2002). The role of NorVW in NO detoxification was first described in *E. coli* which despite lacking the denitrifying Nor enzyme, it still possess NO reductase activity, which is Hmp independent and sensitive to O_2 (Gardner and Gardner, 2002). *E. coli* strains lacking NorVW have a lower survival in macrophages (Baptista et al., 2012). In *S.* Typhimurium it was shown that NorVW has a coordinated role with Hmp and NrfA to resist NO under changing O_2 conditions in the environment (Mills et al., 2008). Moreover, it has been demonstrated in *S.* Typhimurium a coordinated role for NorV and NrfA in NO detoxification in anoxic conditions. It has been proposed that NrfA would metabolize NO before it enters into the cell. In this way, intracellular NO would decrease, and the cytoplasmic NorVW would reduce any NO still present inside the cell (Mills et al., 2008). The involvement of NorVW in the infection process has been suggested. However, this hypothesis has not yet been confirmed *in vivo* indicating that the role of NorVW, compared to Hmp, during pathogenesis is less relevant. Orthologues of the flavorubredoxin NorV are extensively distributed in both aerobic and anaerobic bacteria (reviewed by Cole, 2018).

2.2.2.4. NrfA

Another NO reductase mostly present in enteric bacteria is the periplasmic nitrite reductase, NrfA, which can reduce NO to NH_4^+. As mention in Chapter 2.2.1.1.2., NrfA is a periplasmic cytochrome *c* nitrite reductase that catalyzes NO_2^- reduction to NH_4^+. This process, depending on the circumstances, may result in an indirect decrease of environmental NO by preventing NO_2^- decomposition (Einsle, 2011). NrfA reaction mechanism is thought to occur in multiple stages involving electron transfer from its five haem groups to the substrate, with NO and NH_2OH formation as intermediaries. Additionally, the free NO and NH_2OH can be directly reduced by NrfA to NH_4^+, which gives to this enzyme a protective role against NO. In fact, an *E. coli nrfA* mutant showed a strong growth inhibition in the presence of NO (Poock et al., 2002; Mills et al., 2008), as well as a significant decrease in NO reductase activity (Clarke et al., 2008). In addition to enteric bacteria, a role for NrfA in NO resistance has also been demonstrated in the ε-proteobacteria *C. jejuni* and *W. succinogenes* (Pittman et al., 2007; Kern et al., 2011).

2.2.2.5. Hybrid cluster protein

In *E. coli*, a quadruple mutant lacking both nitrite reductases, NirBD and NrfAB, as well as Hmp and NorV, was more sensitive to nitrosative stress than the parental strain, and it was still moderately resistant to NO. However, this mutant retained the ability to reduce NO (Vine and Cole, 2011). This observation allowed the authors to suggest that enteric bacteria synthesise another NO reductase, the hybrid cluster protein (Hcp) that is present in most bacteria that reduce NO_3^- or NO_2^- anaerobically to NH_4^+, but absent in denitrifying α- or β- proteobacteria. The name "hybrid cluster protein" originated from its unique structure. Although Hcp contains two Fe-S clusters, one of them is neither a conventional [2Fe-2S] nor a [4Fe-4S] cluster, but a hybrid [4Fe-2S-2O] cluster. Like NorV, Hcp is frequently encoded together with an oxidoreductase (Hcr) by the *hcp-hcr* operon, which is expressed only during anaerobic growth. Hcp and Hcr might form a short electron transfer chain where electrons are transfered from NADH via Hcr to Hcp. Several reports have implicated Hcp in protecting anaerobic bacteria against nitrosative stress. Transcriptomic studies have revealed that *hcp* expression is strongly up-regulated in various bacteria under conditions of nitrosative stress (for a review see Cole 2017, 2018). For example, in *Desulfovibrio vulgaris*, a strain lacking *hcp* was hypersensitive to NO, and a deletion of this gene together with *nsrR* and *hmp* in *S*. Typhimurium caused a delay in O_2 and NO consumption (Figueiredo et al., 2013). Wang and colleagues (2016) showed that *E. coli* Hcp is a high affinity NO reductase since an *hcp* mutant showed high sensitivity to NO under anaerobic growth, as well as inactivation of the Fe-S proteins, aconitase and fumarase, due to cytoplasmic NO accumulation. Co-Purified Hcp and Hrc showed NO reduction activity *in vitro*. It has also been demonstrated that deletion of *hcr* resulted in a reversibly inactivation of Hcp by NO, so the primary role proposed for Hcr is to protect Hcp from nitrosylation by NO (Wang et al., 2016). In addition to remove NO, it has also been suggested a specific role of Hcp in NH_2OH detoxification, the intermediate in the reduction by NrfA of NO_2^- and NO to NH_4^+. In fact, purified Hcp from *E. coli* (Wolfe et al., 2002) and *Rhodobacter capsulatus* (Cabello et al., 2004) showed NH_2OH reductase activity, and *hcp* overexpression allowed *R. capsulatus* in *E. coli* to grow with NH_2OH (Cabello et al., 2004). It has been recently reported that endogenous protein S-nitrosylation in *E. coli*

depends principally upon the enzymatic activity of Hcp, employing NO produced by the respiratory nitrate reductase NarGHI (Seth et al., 2018).

2.2.2.6. Other systems to detoxify NO

Although the majority of NO detoxifying proteins that have been described are directly involved in the removal of NO or RNS, there are other important mechanisms involved in NO resistance which do not eliminate NO directly. This is the case of YtfE (or the RIC protein), a protein that acts repairing Fe-S groups of proteins, such as fumarase or aconitase from NO damage. A *ytfE* mutant strain was hypersensitive to NO, and purified YtfE has the ability to restore the functionality of damaged Fe-S groups (Justino et al., 2005, 2007). It has been recently suggested that *E. coli* YtfE is involved in a new pathway where Hcp combines with YtfE. In this pathway, YtfE repairs the nitrosative damage to Fe-S proteins by recycling NO into the cytoplasm. This NO, that accumulates in the cytoplasm in the absence of a functional Hcp, is reduced to N_2O by Hcp (Balasiny et al., 2018) (Figure 2.7.).

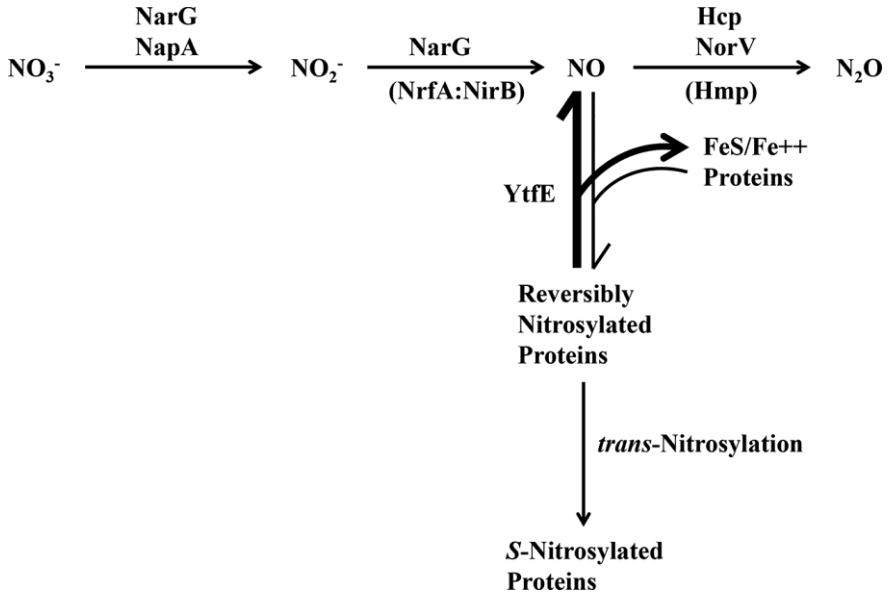

Figure 2.7. Proposed role of YrfE in restoring the functionality of damaged Fe and Fe-S proteins. Balasiny et al. (2018).

In addition to YtfE, two other factors that also seem to repair the damage of the Fe-S groups provoked by NO are DnrN in *Neisseria gonorrhoeae* and ScdA in *S. aureus*.

ScdA is able to complement the deficiencies that are generated when deleting *ytfE* in *E. coli*, which indicates that the repair of Fe-S groups is an important and widely distributed mechanism of NO resistance (Overton et al., 2008).

NnrS is a haem-copper-dependent membrane-bound protein that has been proposed to protect Fe-S cluster enzymes, since they were preferentially inhibited in a strain lacking NnrS due to the formation of Fe-NO complexes. Then, NnrS is particularly important for resistance to nitrosative stress under anaerobic conditions (Stern et al., 2013). The role of NnrS in NO detoxification has recently been demonstrated in *Ensifer meliloti*, both in free life and in symbiotic association with *Medicago truncatula* (Blanquet et al., 2015).

2.3. Rhizobium-Legume symbiosis

2.3.1. Biological nitrogen fixation

N is a key element for all biological organisms because it constitutes 6% of living matter. N is an essential component of proteins, nucleic acids and several cofactors, and it is usually a limiting factor for plant growth and production, even in environments with favourable conditions and enough water to sustain life (reviewed by Martínez-Espinosa et al., 2011).

The earth's N reserve (about 50% of the total N) is in the form of molecular N gas (N_2), constituting 78.03% (v/v) of the total atmosphere. The molecule of N_2 possesses one of the most stable chemical bonds, a triple covalent bond that makes N_2 a very little reactive molecule, practically inert under natural conditions. Its dissociation energy is extremely high (945.41 $KJ \cdot mol^{-1}$), it would be necessary to raise the temperature several thousand degrees to exceed its high reaction energy (Earnshaw and Greenwood, 1997). The main contribution of N to the biosphere from the atmosphere occurs though the biological nitrogen fixation (BNF) process (around 60% of total N). Microorganisms, both eubacteria and archaea, are the living organisms that have been described to perform BNF, they are called diazotrophs. Diazotrophs realize BNF by reducing N_2 to NH_4^+ under free living or in symbiotic association with legumes. Nitrogenase is the enzyme used almost universally to catalyse the reduction of N_2 to NH_4^+, it is able to function under physiological conditions of temperature and

pressure, although in the absence of O_2 (Newton, 2007; Peters et al., 2011). Additionally, the entry of N into the biosphere from the atmosphere may occur by non-biological pathways, such as lightning, volcanoes and other environmental phenomena, which are natural and contribute to maintain the balance of the N cycle. In addition to N_2 fixation, the N cycle is constituted by other pathways with assimilatory or respiratory porposes. Assimilative reactions include N_2 fixation (reviewed by Newton, 2007) and NO_3^- assimilation (reduction of NO_3^- to NH_4^+) (Moreno-Vivián and Flores, 2007) (Figure 2.8.). Both routes produce NH_4^+, which is incorporated into C skeletons in biosynthetic processes for the growth of organisms. NH_4^+ is also incorporated into the N cycle by direct fertilization or by the ammonification process carried out by soil microorganisms, that convert organic N compounds into NH_4^+. This molecule can be oxidized to NO_3^- through the nitrification process, which consists of oxidation from NH_4^+ to NO_2^- and from NO_2^- to NO_3^-. For decades, it was thought that the oxidation of NH_4^+ to NO_3^- was carried out separately by NH_4^+ oxidizing bacteria or archea (BOA and AOA), and by NO_2^- oxidizing bacteria (BON). However, recent studies have demonstrated the existence of complete NH_4^+ to NO_3^- oxidizing bacteria (comammox) in the genus *Nitrospira* (Kits et al., 2017) (Figure 2.8.). Another NH_4^+ oxidation process is the anaerobic oxidation of NH_4^+ (anamox), which produces N_2 by reducing NO_2^- (Strous et al., 1999; Jetten et al., 2009) (Figure 2.8.). Finally, the respiratory pathways from the N cycle occur in O_2 limiting conditions, where nitrogen oxides (NO_X) are used as electron acceptors to produce ATP. One relevant process is denitrification that consists in the reduction of NO_3^- or NO_2^- to N_2 with the formation of intermediate gases, such as NO and N_2O (see section 2.2.1.1.1.; Zumft, 1997) (Figure 2.8.). Another respiratory process is the dissimilatory NO_3^- reduction to NH_4^+ (DNRA), that shares NO_3^- reduction to NO_2^- step with denitrification but reduces NO_2^- to NH_4^+ (Simon and Klotz, 2013) (Figure 2.8.).

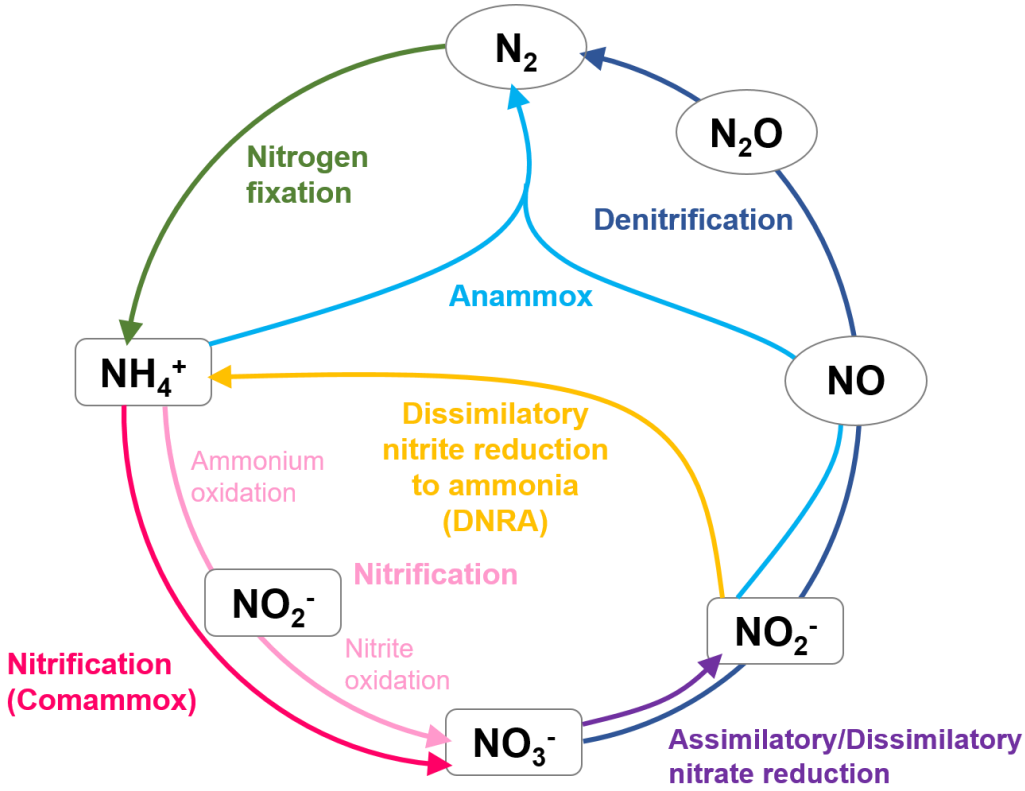

Figure 2.8. Schematic representation of the N biogeochemical cycle. Adapted from Daims et al. (2016).

Anthropogenic activities, such as the invention of the Haber Bosch process, have increased the presence of N in agricultural soils due to the application of synthetic N fertilizers in the so-called "green revolution", causing an imbalance of the N cycle equilibrium. In fact, around 90 to 130 millions of tons of N per year are accumulated in form of NO_3^- or NH_4^+ that cannot be removed by denitrification neither anammox, resulting in an increase of NO_3^- concentrations in soils, waters or sediments, leading serious environmental problems. In addition, to the large scale of synthetic fertilizers production, the consumption of fossil fuels also causes a negative effect on the global N cycle (Galloway et al., 2008).

Alterations in the N cycle have a negative impact on climate change, human health and the functioning of ecosystems reducing biodiversity, especially in aquatic systems and in soils where N concentration is increasing, causing eutrophication of lakes and rivers, causing 'dead' of anoxic zones due to proliferation of algae, as well as the contamination of surface water and its accumulation in groundwater (Howarth, 2004). At the level of public health, the consumption of these NO_3^--contaminated

waters has been associated with the development of methaemoglobinemia, the cause of the blue baby syndrome (Greer and Shannon, 2005), respiratory diseases and gastric cancer associated with the endogenous formation of toxic *N*-nitrosated compounds by bacteria in the gastrointestinal tract (van Grinsven et al., 2010). At an environmental level, the most direct effect is the eutrophication of aquatic ecosystems, whose result is an increase in primary production (photosynthesis), with consequences on the composition, structure and dynamics of the ecosystem. On the other hand, NO_3^- accumulated in soils or water surface may return to the atmosphere in the form of NO and N_2O, greenhouse gases that contribute to the depletion of the ozone layer. Besides, NO can be chemically oxidized to nitrogen dioxide (NO_2), which in turn can be hydrated to form nitrous and nitric acids (HNO_2 and HNO_3), which fall to the earth as components of acid rain (Zumft, 1997). N_2O is a potent greenhouse gas (GHG) and one of the main causes of ozone depletion, with a life in the atmosphere of 114 years and a warming potential 300 times higher than CO_2 due to its radiative capacity (Intergovernmental Panel on Climate Change, IPCC, 2014). In this context, it is essential to develop agricultural practices that sustain high productivity while decreasing the negative impact caused by the use of fertilizers. Microbial fertilizers become important as an alternative to chemical fertilizers, as an environmentally friendly agricultural practice. Legume crops are a key protein resource for human and animal foods. Thanks to their capacity to establish a symbiotic relationship with (N_2)-fixing rhizobia, it can contribute to natural N soil enrichment while reducing the need for chemical fertilization. Therefore, symbiotic N_2 fixation is considered a process with economic, ecological and agricultural importance. In this process a mutualist association between soil bacteria, commonly known as rhizobia, and plants of *Leguminosae* family is stablished.

The *Leguminosae* (or *Fabaceae*) is a family of herbs, shrubs, vines or trees in mainly terrestrial habitats, being part of most of the world's kind of vegetation. Legume family includes around 19,300 species within 750 genera and it is divided into three sub-families: the Caesalpinioideae, Mimosoideae and Papilionoideae (reviewed by Andrews and Andrews, 2017). Nevertheless, it has been proposed a new classification of the legumes, which includes six sub-families founded on the plastid

matK gene sequences from about 20% of all legume species across ~90% of all identified genera. These sub-families are: Caesalpinioideae, Cercidoideae, Detarioideae, Dialioideae, Duparquetioideae and Papilionoideae (The Legume Phylogeny Working Group, LPWG, 2017). *Leguminosae* is the third family with the greatest diversity of species, including species very important in human and animal nutrition, as soybeans, beans, peas, lentils, peanuts or forages, as alfalfa and clover. Soybean is the most widely grown legume, since it contains 40% protein, 21% in fat and a high concentration of isoflavones in its seeds. In fact, soybean crops contribute 77% of the total N_2 fixed in cultivated soils (16.4 Tg of fixed N_2), and 11% of N_2 biologically fixed on the planet (Herridge et al., 2008). Soybean is cultivated in 120-130 million hectares each year, being the most important protein content and oilseed crop in the world. The three most important soybean producers are Argentina, Brazil, and United States, where soybean crops are routinely inoculated with symbiotic N_2-fixing *Bradyrhizobium* spp.

Rhizobia are α- and β-Proteobacteria that belong to the genera *Rhizobium*, *Ensifer*, *Mesorhizobium*, *Bradyrhizobium*, *Allorhizobium*, *Azorhizobium*, *Blastobacter*, *Methylobacterium*, *Devosia*, *Phyllobacterium, Ochrobactrum, Burkholderia and Cupriavidus*. Rhizobia induce nodules formation in the roots of the plants and some in the stems, which are specialized structures where N_2 fixation takes place (reviewed by Poole et al., 2018).

For the establishment of the symbiosis, there is an exchange of molecular signals between both partners that leads to the formation of the nodule. In the symbiosis, the plant supplies sucrose to the plant host cells containing rhizobia, where it is transformed to dicarboxylic acids that are supplied to the bacteroids, the differentiated forms of rhizobia, to produce the energy required to reduce N_2 to NH_4^+ by the nitrogenase enzyme. Then, NH_4^+ is assimilated to amides or ureides and transfered to the plant (reviewed by Graham and Vance, 2003; Udvardi and Poole, 2013; Poole et al., 2018; Schwember et al., 2019).

2.3.2. Nodulation process

The establishment of an effective symbiosis is a complex process in which the exchange of specific signals between the symbionts is essential. The communication

between the micro- and macrosymbiont begins with the release by the plant of several compounds contained in their seed and root exudates, mainly flavonoids, aldonic acids and betaines. Flavonoids induce *nod* genes in rhizobia that produce lipochitooligosaccharides (Nod factors) (Figure 2.9.). Nod factors are key molecular signals that bind to specific plant receptor kinases on the plasma membrane and induce a Ca^{2+}-signaling route, that initiates the transcription of genes implicated in nodule development. Rhizobia attach to root hairs and are entrapped by root hair curling, which results in the formation of an infection pocket (Figure 2.9.). Rhizobia secrete a cellulase to bore a hole in the root hair through which they enter into a plant-derived infection thread that separates rhizobia from plant cells (Robledo et al., 2008). Infection threads ramify within the root cortical tissue and, eventually, unload their bacteria within cortical cells though endocytosis. In this step, rhizobia are liberated into the cytoplasm of the infected cortical cells, and they are surrounded by a plant membrane, termed the symbiosome membrane. In this way, bacteria are contained inside a vesicle, called symbiosome. Eventually, bacteria are differentiated into a N_2-fixing form, known as bacteroids (reviewed by Udvardi and Poole, 2013; Jones et al., 2007; Poole et al., 2018).

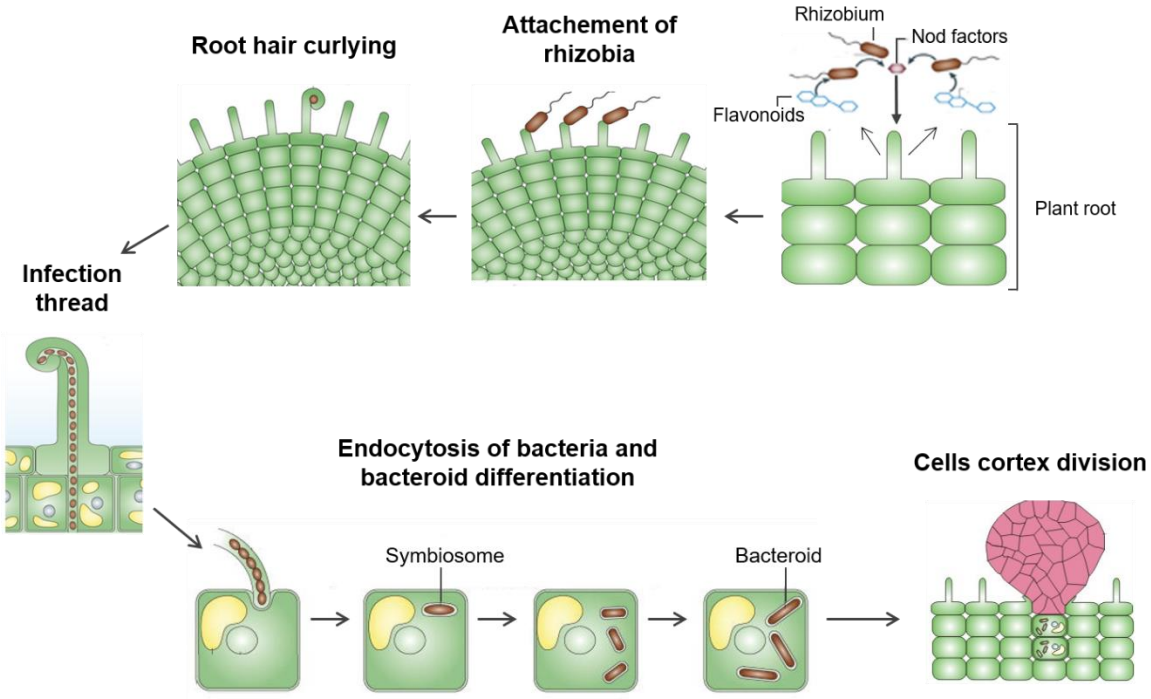

Figure 2.9. Schematic illustration of nodule formation. Adapted from Jones et al. (2007).

The formation of the nodule depends on the host plant, and can be grouped into two types of nodules, according to their structure and morphology. The first type are indeterminate nodules, present in pea, alfalfa or clover plants. This type of nodule presents a persistent meristem and well-differentiated longitudinal sections according to their degree of maturation. Indeterminate nodules have several zones: the distal zone I includes the nodule meristem, in which new plant cells are synthesized; zone II contains infection threads full of bacteria; in the interzone among zone II and III, bacteria are liberated from infection threads and surrounded by plant cells; zone III includes the mature, N_2-fixing bacteroids; and in zone IV, bacteroids senesce. The second type of nodules are determined, they are found in plants, such as soybeans, beans or lotus, and have a globular shape. These nodules have a central zone formed by infected and uninfected cells, then, an inner cortex of small cells with large intercellular spaces, surrounded by a layer of tightly packed cells, the outer cortex contains large cells laxely packed and large intercellular spaces, and, sometimes, they are surrounded by a peridermis. Rhizobia inside the infected cells differentiate and induce the formation of new enzymes (such as nitrogenase or the high-affinity terminal oxidase cytochrome *c* oxidase *cbb*$_3$). Rhizobia differenciation to bacteroides also undergo morphological changes into larger and more extended cells. For all these reasons, the term bacteroid is used to refer to the intracellular microsymbiont (reviewed by Terpolilli et al., 2012; Poole et al., 2018).

2.3.3. Nitrogenase. Genes involved in N_2 fixation and their regulation

Symbiotic N_2 fixation genes can be classified into: *nod*, *nif*, and *fix* genes. The *nod* genes products are necessary in the early stages in nodule formation (see above). The *nif* genes include nitrogenase structural genes, genes that are required for the nitrogenase biosynthesis, and regulatory genes. The *fix* genes, together with *nif* genes, are essential for N_2 fixation in symbiotic bacteria.

The structural *nifH* and *nifDK* genes encode the Mo-nitrogenase complex of all known diazotrophs. This complex catalyzes the reduction of N_2 to NH_3 with the following stoichiometry:

$$\mathrm{N_2} + 8e^- + 8\mathrm{H^+} + 16\mathrm{MgATP} \rightarrow 2\mathrm{NH_3} + \mathrm{H_2} + 16\mathrm{MgADP} + 16\mathrm{P_i}$$

This equation shows that nitrogenase activity requires high energy due to the great stability of the N_2 triple bond.

Nitrogenases comprise two proteins, one being a reductase component, known as the Fe-protein (NifH), that contains a single 4Fe-4S cluster and two ATP binding sites. A second catalytic protein (NifDK), known as the MoFe-protein, VFe-protein or FeFe-protein, houses an electron transfer P cluster, as well as the active-site metal cofactor (FeMo-co, FeV-co, and FeFe-co) (Seefeldt et al., 2018). The Fe-protein, with two bound ATP molecules, associates with one-half of the MoFe protein, and this association initiates a series of events that result in the transfer of an electron from the Fe-protein to FeMo-co, the hydrolysis of two ATP molecules to two ADP and two Pi, release of phosphate, and, finally, the dissociation of the Fe-protein (oxidized and with two bound ADP) from the MoFe-protein (reduced by one electron) (reviewed by Rubio and Ludden, 2008; Sickerman et al., 2017) (Figure 2.10.). In all microbes studied, the direct electron donor to nitrogenase is either a ferredoxin (Fd) or a flavodoxin (Fld). Fds coordinate Fe-S clusters, whereas Flds use a flavin mononucleotide (FMN) to mediate electron transfer. The Fld, NifF, has been shown to be the sole electron donor to nitrogenase in the γ-proteobacterium, *Klebsiella pneumoniae*, but in other bacteria, Fds or a combination of Fds and Flds have been implicated in electron transfer to nitrogenase (reviewed by Poudel et al., 2018). The electron-transfer complex FixABCX bifurcates electrons from NADH to generate reduced quinone and reduced Fd or Fld (Ledbetter et al., 2017; Fixen et al., 2018).

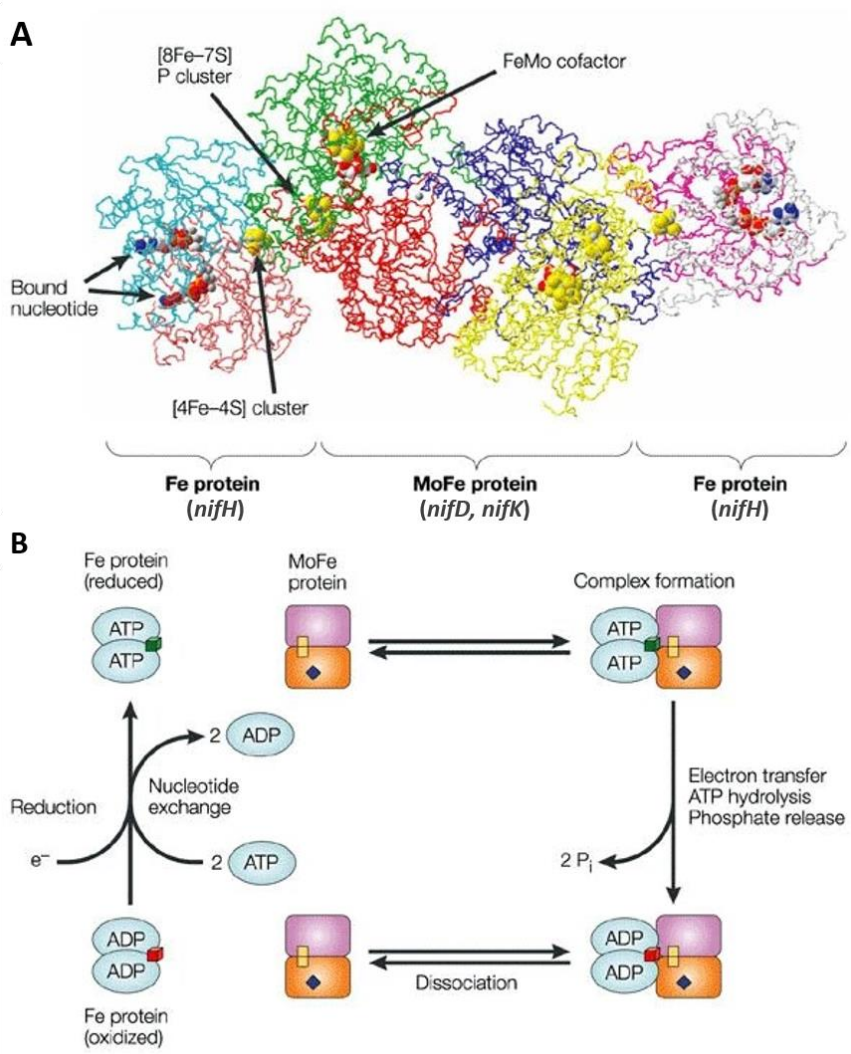

Figure 2.10. Nitrogenase enzyme. A. Structure of the nitrogenase complex that is formed between the Fe protein and MoFe proteins of *Azotobacter vinelandii*. **B.** Schematic representation of the nitrogenase complex reaction. The Fe protein dimer is represented in light blue with the cube showing the [4Fe-4S] cluster in green to indicate the reduced form and red to simbolized the oxidized form. The α and β subunits of the MoFe proteins are represented in orange and pink, respectively, the yellow squares depict the P cluster and the blue diamond shows the FeMo cofactor. Dixon and Kahn (2004).

2.3.3.1. Regulation of N_2 fixation

Microoxia is a requirement not only for nitrogenase activity, but for the whole induction of N_2 fixation and the expression of genes related to symbiosis (*nif* and *fix*) (Fischer, 1994). The detection and transduction of the "low O_2 signal" is mediated by proteins conserved and integrated in regulatory networks of each species of rhizobia (see reviews Fischer, 1994; Dixon and Kahn, 2004; Terpolilli et al., 2012; Poole et al., 2018; Rutten and Poole, 2019). In symbiotic diazotrophs, the transcription of *nif* and *fix*

genes is controlled by the master regulator NifA, that acts in combination with the sigma factor σ^{54} of the RNA polymerase (encoded by *rpoN*). The NifA protein shows a typical three-domain structure. The N-terminal GAF domain is a ubiquitous signaling motif found in signaling and sensory proteins from all three kingdoms of life (Ho et al., 2000). The central domain interacts with the σ^{54}-RNA polymerase and possesses ATPase activity, while the C-terminal domain shows a helix-turn-helix (HTH) motif involved in DNA-binding. In non-symbiotic diazotrophs, including *K. pneumoniae* and *Azotobacter vinelandii*, the GAF domain plays an important role in NifA repression by NifL binding. This interaction between NifA and NifL integrates multiple regulatory signals in *K. pneumoniae*. Expression of *nifL* is activated by NtrC in response to low N availability. NifL regulation of NifA, thus, combines a N signal at the level of *nifL* transcription and an O_2 signal at the protein level. No homolog of NifL is found in rhizobial diazotrophs and the role of the GAF domain in these organisms is unknown. In rhizobia, the activity of NifA is directly sensitive to O_2. In addition, the *nifA* gene is also subjected to transcriptional regulation, although the mechanisms vary depending on the rhizobial strain. For example, in *E. meliloti*, *nifA* expression is activated by the FixLJ two-component regulatory system (TCS) in response to low O_2. FixLJ system comprises a haem-containing O_2-binding sensor protein, FixL, that initiates a phosphorylation cascade under low O_2 tension, which activates the cognate transcriptional regulatory protein FixJ. In *B. diazoefficiens*, the regulation of *nifA* and *fixK* is split in two separate pathways, the redox-responsive TCS RegSR that activates *the fixR-nifA* operon, and the FixLJ TCS that is responsible for the activation of *fixK* (Bauer et al*.,* 1998; Dixon and Kahn, 2004). Interestingly, not all rhizobia employ FixLJ to activate expression of *fixK* and *nifA*. Particulary, in *Rhizobium etli* CFN42 and *Rhizobium leguminosarum* bv. viciae VF39, FixL is an orphan hybrid histidine kinase (hFixL) without predicted transmembrane segments. This gene is located on *R. etli* plasmid pCFN42f in a region that contains copies of the *fixK, fixNOQP* and *fixG* genes, which are reiterated in the symbiotic plasmid (Girard et al., 2000). *R. etli* hFixL initiates the regulatory circuit of *fix* genes in coordination with FxkR, a novel response regulator that belongs to the OmpR/PhoB family, and without the participation of FixJ (Zamorano-Sánchez et al., 2012). Interestingly, *E. meliloti* SM11 encodes both the FixL-FixJ-FixK and the hFixL-FxkR-FixKa regulatory systems. Genetic and functional

characterization of the regulatory module composed of hFixL and FxkR in *E. meliloti* SM11, demonstrated that this regulatory circuitry limits N_2 fixation and its absence results in an increase of the *fix* and *nif* genes expression, that are regulated by FixLJ (Reyes-González et al., 2016). Rhizobia generally display only one *nifA* copy, but one exception has been described for *Mesorhizobium loti*, which contains two *nifA* genes, *nifA*1 and *nifA*2, both located in the symbiotic island (Nukui et al., 2006). Another example of the presence of two *nifA* genes has emerged with the analysis of the genome sequence of the non-photosynthetic *Bradyrhizobium* sp. DOA9 strain (Okazaki et al., 2015). In this bacterium, both NifA proteins are exchangeable during symbiosis for the activation of *nif* genes, but not during free-living growth (Wongdee et al., 2018).

In *B. diazoefficiens*, the FixL protein, unlike other rhizobia, does not have a transmembrane section and is, therefore, a soluble protein (Gilles-González et al., 1994; Rodgers, 1999). Only a moderate decrease in the concentration of O_2, to 5%, is sufficient for FixL autophosphorylation and the consequent phosphorylation of FixJ. *B. diazoefficiens* FixLJ activates transcription of the CRP/FNR type regulators $FixK_2$ and $FixK_1$. $FixK_2$ is considered a key protein in the expression of the genes responsible for N_2 fixation and denitrification, since a *fixK*$_2$ mutant strain is not able to fix N_2 in symbiosis with soybean plants and does not grow anoxically with NO_3^- as the final electron acceptor (Nellen-Anthamatten et al., 1998). In addition to the transcriptional control of the *fixK*$_2$ gene by FixJ, this gene is subjected to negative regulation by the $FixK_2$ protein itself (reviewed by Fernández et al., 2016). $FixK_2$ also has a complex post-transcriptional regulation. First, it has a single cysteine in position 183 that is subjected to oxidization to sulfonic or sulfinic acid (Mesa et al., 2009). Secondly, $FixK_2$ has a regulation by proteolysis, through general degradation mediated by the chaperone protease system ClpAP1 (Bonnet et al., 2013), and specific proteolysis at the C-terminal end of the protein (reviewed by Fernández et al., 2016). $FixK_2$ proteolysis could be a mechanism to regulate protein levels in the cell, since despite the evident induction of *fixK*$_2$ gene expression under microoxic conditions, $FixK_2$ protein levels remain constant regardless of growth conditions (Nellen-Anthamatten et al., 1998; Mesa et al., 2009). It should be noted that this observation was recently verified by the use of an integrated

study of transcriptomics, proteomics and immunodetection using antibodies (Fernández et al., 2019), and it has been suggested the existence of a more general post-transcriptional control mechanism in microoxic conditions for a group of 91 genes/proteins, not only in the case of $FixK_2$.

Under microoxic conditions, $FixK_2$ controls a large regulon including genes involved in the synthesis of the high-affinity cytochrome oxidase *cbb*$_3$ (*fixNOQP*, *fixGHIS*) denitrification genes (*nap*, *nirK*, *nos*, *nnrR*), *rpoN*$_1$ (which codes for the factor σ^{54}) and *fixK*$_1$, among others (Nellen-Anthamatten et al., 1998; Mesa et al., 2008). Substantial part of the regulon of $FixK_1$ also belongs, but regulated opposite, to the NifA regulon, thus, interconnecting the cascades of FixLJ/$FixK_2$-$FixK_1$ and NifA. Moreover, expression of the NifA dependent genes requires the σ^{54} factor, that is controlled by $FixK_2$ (Bauer et al., 1998). This interconnection could allow an adequate activation of the essential genes for N_2 fixation. When the concentration of O_2 falls to micro-oxic levels, lower than 0.5%, the accumulation of active NifA is able to overcome the repression of $FixK_1$, in this way a fine adjustment of the N_2 fixation genes expression is achieved (Mesa et al., 2008).

In *B. diazoefficiens, nifA* and up to 250 other genes are controlled by the TCS redox sensor RegSR (Lindemann et al., 2007). RegSR belongs to redox responsive TCS family described in bacteria. In *B. diazoefficiens*, RegR (the response regulator) induces expression of the *fixR-nifA* operon (responsible for NifA synthesis) (Barrios et al., 1995; Barrios et al., 1998; Bauer et al., 1998) under all O_2 conditions. When the O_2 concentration decreases to very low levels (≤0.5%), NifA together with RNAP-containing RpoN (σ^{54}) improves its own synthesis. In *B. diazoefficiens*, RpoN is encoded by *rpoN*$_1$ and *rpoN*$_2$ genes (Kullik et al., 1991). The FixLJ-$FixK_2$-$FixK_1$ and RegSR-NifA cascades are connected by *rpoN*$_1$ because this gene is controlled by $FixK_2$.

2.3.4. Oxygen control in the nodule

Because nitrogenase is inactivated at atmospheric O_2 concentrations, within the nodule, the O_2 tension must be maintained at levels of 5 to 30 nM (Appleby, 1984), extremely low compared to the O_2 concentration in the atmosphere (250 μM). The sensitivity of nitrogenase to O_2 is conferred by the surface exposure of the [4Fe-4S]

group, which is linked to the two subunits of the NifH dimer. As mention above, a low concentration of O_2 is the main signal for the activation of the *nif* and *fix* genes.

The low O_2 concentration in the nodule is subject to a delicate balance, since O_2 is needed to synthesize all the ATP that nitrogenase activity demands, but it must not reach levels that inactivate this enzyme. These antagonistic needs are solved thanks to the function of three systems mainly: i) the variable oxygen diffusion barrier in the nodule endodermis; ii) the presence of leghaemoglobin (Lb); iii) the expression of the *cbb*$_3$ terminal oxidase. The oxygen diffusion barrier maintains the microaerobic environment within the infected zone of the nodules. It is composed by a complex structure that occludes the intercellular space in the middle part of the cortex, limiting O_2 permeability. It involves several morphological and metabolic mechanisms in different areas of the nodule, such as the presence of occlusions in the intercellular spaces of the middle cortex, an osmotic mechanism in the internal cortex, and a precision oxygen diffusion control mechanism that occurs in the infection zone (reviewed by Minchin, 1997, 2008). Lb is a high O_2 affinity plant carrier, which buffers free O_2 around 7-11 nM. This protein is the most abundant protein in nodules (~300 µM) and in very active nodules its concentration is 2-3 mM (Davies et al., 1999). Lb is itself present at a concentration several orders of magnitude higher than free O_2 (Ott et al., 2005). Most O_2 within nodules is therefore bound by Lb, which transports O_2 through the cytosol of infected cells to the membranes of the symbiosomes at steady-state concentrations to ensure bacteroids respiration, while protects nitrogenase activity (reviewed by Downie, 2005). A strong correlation between the Lb content and N_2 fixation activity of nodules has been demonstrated (Dakora, 1995). The *cbb*$_3$ oxidase has high affinity by O_2 (K_M = 7 nM) and is encoded by the *fixNOQP* genes (see the regulation of its expression above), which allows microaerobic respiration of the bacteroid during N_2 fixation (reviewed by Preisig et al., 1996; Delgado et al., 1998).

2.4. NO metabolism in the Rhizobium-Legume symbiosis

2.4.1. *Ensifer meliloti-Medicago truncatula*

E. meliloti is a symbiotic N_2-fixing soil bacterium which associates with plants of the genera *Medicago*, *Melilotus* and *Trigonella*. *M. truncatula* is a model legume because

of its advantageous features, such as diploid genetics, small genome (~500 Mbp), ease of transformation, brief life cycle and high-levels of natural diversity (Cook, 1999). *E. meliloti* 1021 is the model strain for investigating the interaction between the model symbiotic system *E. meliloti-M. truncatula*, whose molecular, biochemical and genetic characterization has been widely studied (Jones et al., 2007; Young et al., 2011). *E. meliloti* 1021 genome sequence is composed of three replicons: a 3.65 Mb chromosome and two megaplasmids, pSymA (1.35 Mb) and pSymB (1.68 Mb) (Galibert et al., 2001). pSymA includes genes that are implicated in symbiosis and genes likely responsible for N and C metabolism, transport, stress and resistance responses that confer *E. meliloti* a benefit for the symbiotic interaction (Barnett et al., 2001). pSymA also contains genes for denitrification: *napEFDABC*, *nirK*, *norECBQD* and *nosRZDFYLX* genes (Barnett et al., 2001). *E. meliloti* denitrification genes are induced under microoxic and symbiotic conditions (Becker et al., 2004). This bacterium is a partial denitrifier since it is unable to grow under anaerobic conditions with NO_3^- or NO_2^- as terminal electron acceptors, despite having and expressing the entire set of denitrification genes. However, it was shown that *E. meliloti napA*, *nirK*, *norC* and *nosZ* structural genes are functional under specific growth conditions (initial O_2 concentrations of 2% and initial cell density of 0.20-0.25) (Torres et al., 2011, 2014b). By using a robotized incubation system, it has been confirmed the inability of *E. meliloti* to reduce NO_3^- or NO_2^- to N_2O or N_2 under anaerobic conditions. On the contrary, *E. meliloti* was able to grow during anaerobic respiration by reducing externally provided N_2O to N_2 (Bueno et al., 2015). Recently, it has been shown that overexpression of *napEFDABC* genes (Nap+) confers to *E. meliloti* the capacity to grow through anaerobic NO_3^- respiration. These results suggest that the inability of *E. meliloti* to grow under anaerobic conditions using NO_3^- as electron acceptor can be attributed to a limitation in the expression of the periplasmic nitrate reductase (Torres et al., 2018).

2.4.1.1. NO in *M. truncatula* nodules

NO is produced during *E. meliloti-M. truncatula* symbiosis. Although the role of NO during the symbiotic interaction is not fully understood, it has been shown that NO can have a positive role during the infection steps, while it can inhibit the bacterial

nitrogenase enzyme responsible for N_2 fixation, and the plant glutamine synthetase involved in N assimilation in mature nodules (Trinchant and Rigaud, 1982; del Giudice et al., 2011; Melo et al., 2011; Blanquet et al., 2015). NO has also been shown to be a signal for nodule senescence (Cam et al., 2012; reviewed by Bruand and Meilhoc, 2019). Hence, to maintain efficient infection and N_2 fixation, the level of NO inside legume root nodules must be finely tuned. NO levels in the nodules result from a balance between NO synthesis and consumption, two processes which rely on both partners (Hichri et al., 2016). In the root nodules, both the bacterial and plant partners are responsible for NO production (reviewed by Hichri et al., 2015; Berger et al., 2018). From the plant side, NO is synthesized by the plant nitrate reductase (NR), nitrite (NO_2^-): NO reductase activity associated with the mitochondrial electron transport chain (ETC), and the NO synthase (NOS)-like activity (for a review see Chamizo-Ampudia et al., 2017; Astier et al., 2018) (Figure 2.11.).

In addition to plant sources, *E. meliloti napA* and *nirK* denitrification genes were reported to be involved in NO formation, at least in mature nodules (Horchani et al., 2011). In this context, NO-detoxification systems in nodules are essential for keeping a low steady-state intracellular NO concentration to maintain an efficient symbiosis. From the plant side, non-symbiotic and symbiotic plant haemoglobins have been proved to be implicated in NO detoxification in nodules (reviewed by Berger et al., 2018). From the bacterial perspective, the bacterial NO reductase, that catalyzes the reduction of NO into N_2O in the denitrification pathway, is also involved in NO consumption in *M. truncatula* nodules (Blanquet et al., 2015). In addition to Nor, a combined role for *E. meliloti* flavohaemoglobin (Hmp), and $NnrS_1$ and $NnrS_2$ proteins in NO degradation has been reported in *M. truncatula* nodules. In fact, *E. meliloti* mutans in those systems increased NO levels in the nodules and they affected the maintenance of an efficient symbiosis with *M. truncatula* (Blanquet et al., 2015). Although *E. meliloti* denitrification remains the main enzymatic way to produce NO, recent studies have suggested that the NO_3^- assimilatory pathway involving the nitrate reductase (NarB) and nitrite reductase (NirB) participates indirectly to NO synthesis by cooperating with the denitrification pathway (Ruiz et al., 2019).

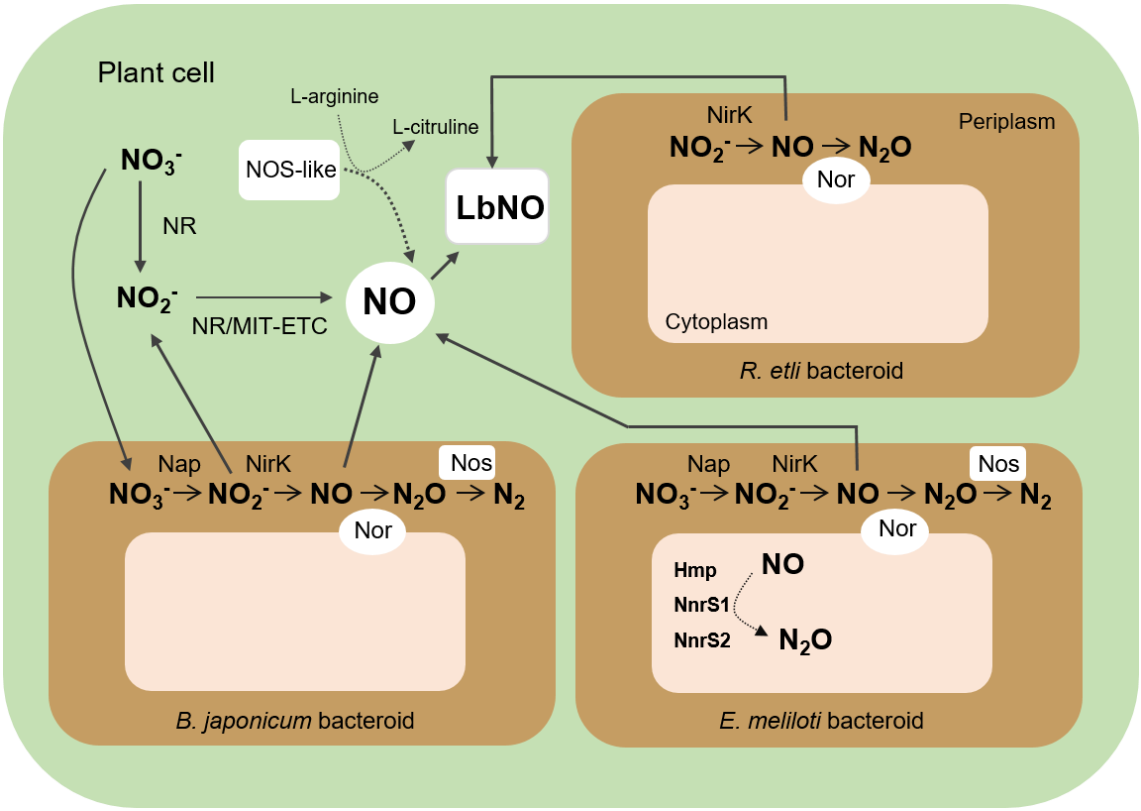

Figure 2.11. Illustration of NO and N_2O metabolism in root nodules from *G. max*-*B. diazoefficiens*, *M. truncatula*-*E. meliloti* and *P. vulgaris*-*R. etli* symbiosis. Adapted from Torres et al. (2016).

2.4.2. *Rhizobium etli- Phaseolus vulgaris*

R. etli is a N_2-fixing soil bacterium that stablishes symbiotic associations with *Phaseolus vulgaris* L., or common bean. In addition to being the main source of protein for hundreds of millions of people (Broughton et al., 2003), *P. vulgaris* is a model specie for the research of the symbiotic association of common bean with N_2-fixing bacteria from the genus *Rhizobium*. The genome of *R. etli* CFN42 contains a chromosome and six large plasmids (pCFN42a to pCFN42f) whose sizes range from 184.4 to 642.45 kb (González et al., 2006). Plasmid d corresponds to the symbiotic plasmid (pSym) and includes several genes implicated in nodulation and N_2-fixation processes. Plasmid pCFN42f contains a gene cluster that includes the *nirK* and *norCBQD* denitrification genes (Girard et al., 2000; González et al., 2006). This bacterium does not have *nap*, *nar* and *nos* denitrification genes and is incapable of respiring NO_3^- or carrying out a complete denitrification pathway. The presence of NirK and Nor-coding regions in *R. etli* suggests an NO-detoxifying function for these enzymes, avoiding accumulation

of NO inside free-living cells or in the nodules (Figure 2.11.). *In vivo* assays showed that NirK is necessary for NO_2^- reduction to NO and that Nor is essential to degrade NO under free-living conditions (Bueno et al., 2005; Gómez-Hernández et al., 2011). Moreover, in common bean nodules, NirK contributes to NO formation and Nor to NO removal in response to NO_3^-, as levels of LbNO complexes in nodules exposed to NO_3^- raised in nodules produced by a *R. etli norC* mutant and decreased in those from a *nirK* mutant, compared to LbNO levels from wild-type (WT) nodules (Gómez-Hernández et al., 2011). Interestingly, the presence of NO_3^- in the plant nutrient solution reduced nitrogenase-specific activity in WT and *norC* nodules. Nevertheless, the inhibition of nitrogenase activity by NO_3^- was not detected in *nirK* nodules, probably due to the low levels of cytotoxic NO in those nodules (Gómez-Hernández et al., 2011). These results showed the ability of common bean nodules to produce NO from NO_3^- included in the nutrient solution. *R. etli* genome contains a gene (RHE_CH01780) encoding for a putative assimilatory nitrate reductase, which is annotated as *narB*. Recently, it has been demonstrated that, under free-living microoxic conditions, NO_2^- produced by NarB from assimilatory NO_3^- reduction is detoxified by NirK and cNor denitrifying enzymes to produce NO and N_2O, respectively (Hidalgo-García et al., 2019). Thus, NarB (from the bacterial side) and the plant nitrate reductase (NR) (from the plant side) should be considered as candidates to reduce NO_3^- to NO_2^-, acting as source of NO_3^--dependent NO production in common bean nodules. The contribution of these enzymes to NO production in *P. vulgaris* nodules is currently under investigation.

2.4.3. *Bradyrhizobium diazoefficiens*-soybean

2.4.3.1. *B. diazoefficiens* as a model of rhizobial denitrification

B. diazoefficiens is the most widely used species in commercial inoculants for soybean crops. *B. diazoefficiens* occupies two distinct niches: the soil in free life and the root nodules in symbiotic association with *Glycine max* (soybean), *Macroptilium atropurpureum* (siratro), *Vigna unguiculata* (cowpea) and *Vigna radiata* (green soybean) (Göttfert et al., 1990). *B. diazoefficiens* USDA 110, which was originally isolated from soybean nodules in Florida (United States) in 1957, has been universally used for research into its molecular genetics, physiology and ecology. The genome of *B. diazoefficiens* USDA 110 is composed of a single circular chromosome about

9.1 million pairs of bases in length, it does not contain plasmids, but it has a region of 410 kb groups of genes involved in biological N_2 fixation that has been called symbiotic island (Kaneko et al., 2002). Until 2013, *B. diazoefficiens* USDA 110 was classified within the species *Bradyrhizobium japonicum*, whose type strain is USDA 6, however, morphophysiological, genetic and genomic differences between both resulted in the reclassification as *B. diazoefficiens* USDA 110 (Delamuta et al., 2013).

B. diazoefficiens is the only rhizobia species that, in addition to fixing N_2, has the ability to grow under anoxic conditions by reducing NO_3^- through the denitrification pathway, a process widely studied in this bacterium both in free-living conditions and in symbiosis (reviewed by Bedmar et al., 2013). *B. diazoefficiens* possesses the complete set of *napEDABC* (Delgado et al., 2003), *nirK* (Velasco et al., 2001), *norCBQD* (Mesa et al., 2002) and *nosRZDFYLX* (Velasco et al., 2004) denitrification genes, which encode the periplasmic nitrate reductase (Nap), copper nitrite reductase (NirK), nitric oxide reductase type c (cNor) and nitrous oxide reductase (Nos), respectively (for a detailed description of Nap, NirK, Nor and Nos enzymes see Chapters 2.2.1.1.1., 2.2.1.1.1.1., 2.2.2.2. and 2.2.1.1.1.1., respectively).

Phenotypic characterization of a *B. diazoefficiens napA* mutant revealed its inability to grow anaerobically and to express periplasmic NR activity (Delgado et al., 2003). The sequencing of the *B. diazoefficiens* genome (Kaneko et al., 2002) has confirmed that it does not possess *nar* genes responsible for the synthesis of the membrane-bound respiratory nitrate reductase. Therefore, Nap is the only enzyme responsible for NO_3^- respiration and initiates denitrification in *B. diazoefficiens* (Delgado et al., 2003). A *B. diazoefficiens nirK* deficient strain was unable to grow in anaerobiosis with NO_3^-, lacking respiratory nitrite reductase activity and accumulating NO_2^- in the medium (Velasco et al., 2001). The *B. diazoefficiens* soluble cytochrome c_{550} is the intermediary in the electronic transport between the bc_1 complex and the respiratory nitrite reductase NirK (Bueno et al., 2008). *B. diazoefficiens* mutant strains defective in the *norC* or *norB* genes are unable to grow under denitrifying conditions. Under these conditions, these mutants accumulate NO (Mesa et al., 2002). Finally, mutant strains of *B. diazoefficiens* for the *nosR* and *nosZ* genes were able to grow under denitrifying conditions, however, they accumulated large amounts of N_2O

(Velasco et al., 2004). The involvement of the periplasmic cyrochrome c_{550} (CycA) in the activity of the nitrous oxide reductase has been recently reported (Jiménez-Leiva et al., 2019).

2.4.3.2. NO metabolism in soybean nodules

By using transcriptional fusions and analysing β-galactosidase activity in the nodules *in situ*, expression of *B. diazoefficiens* denitrification genes in soybean nodules has been reported (Mesa et al., 2004). In plants depending exclusively on N_2 fixation, β-galactosidase activity from a *nirK-lacZ*, *norC-lacZ*, or *nosZ-lacZ* fusions was detected in bacteroids isolated from root nodules. Levels of β-galactosidase activity were similar in both bacteroids and nodule sections from plants that were solely N_2-dependent or grown in the presence of 4 mM KNO_3. These findings suggest that O_2, and not NO_3^-, is the main factor controlling expression of the denitrification genes in soybean nodules (Mesa et al., 2004). In fact, some environmental stresses, such as flooding, that causes a reduction in the O_2 concentration in the nodule, significantly increased the expression and activity of denitrification enzymes in soybean nodules, being more significant the increased of the periplasmic nitrate reductase (Sánchez et al., 2010).

Inoculation of soybean plants with *B. diazoefficiens* denitrification mutants did not affect symbiotic N_2 fixation when plants growth was exclusively dependent on BNF (Mesa et al., 2004). However, when KNO_3 was added to the medium, the number and dry weight of the nodules in plants inoculated with a *nirK* or a *norC* mutant strains were lower than those observed in plants inoculated with the WT strain (Mesa et al., 2004). Under these growth conditions, it has been suggested that denitrification enzymes play a role in nodule formation rather than in nodule function (Mesa et al., 2004). However, when plants were subjected to flooding conditions, inoculation with the *nirK* mutant had a slight advantage for N_2 fixation over the WT or the *norC* mutant (Sánchez et al., 2011b). These findings allowed Sánchez and colleagues (2011b) to suggest that NO formed by NirK in soybean nodules, in response to flooding, has a negative effect on nitrogenase activity. In this context, it has been shown that NO_3^- and flooding induce NO formation in soybean nodules (Meakin et al., 2007; Sánchez et al., 2010), causing a strong inhibition of nitrogenase activity and expression (Kato et al., 2010; Sánchez et al., 2010). In nodules, NO can also bind Lb, contributing to the

formation of nitrosyl-leghaemoglobin (LbNO) complexes, that have a major role in detoxifying either NO_2^- or NO (Sánchez et al., 2010). Recently, it has been shown that NO_3^- and flooding can also increase the production of the potent greenhouse gas N_2O by soybean nodules (Tortosa et al., 2015). Denitrification in the bacteroids has been proposed as the main process responsible for NO and N_2O production in soybean nodules, since levels of gases emitted are significantly reduced in nodules produced by a *B. diazoefficiens napA* null strain, where denitrification is blocked (Sánchez et al., 2010). However, basal levels of NO and N_2O were still detected in nodules from a *napA* mutant (Sánchez et al., 2010; Tortosa et al., 2015). These observations suggested that, besides denitrification, other mechanisms give rise to NO and N_2O in nodules. In addition to denitrification, a coordinated NO_3^- assimilation and NO detoxification system encoded by the *narK-bjgb-flp-nasC* operon has been proposed recently to be also involved in NO homeostasis within *B. diazoefficiens* free-living cells (Figure 2.12.). This cluster codes for the assimilatory nitrate reductase (NasC), a NO_3^-/NO_2^- transporter (NarK), a FAD-dependent NAD(P)H oxidoreductase (Flp) and a putative single domain haemoglobin (Bjgb). Bjgb mitigates the NO produced by NasC as by-product of NO_3^-/NO_2^- assimilation (Cabrera et al., 2016) (Figure 2.12.). Thus, a role for Bjgb in protecting *B. diazoefficiens* free-living cells from nitrosative stress has been proposed (Cabrera et al., 2016). However, the capacity of Bjgb to bind NO *in vitro* is unknown. As reported in free-living cells, Bjgb may also be involved in NO detoxification inside the nodules and, consequently, to protect nitrogenase against NO. However, the function of *B. diazoefficiens* Bjgb in soybean nodules remains to be investigated.

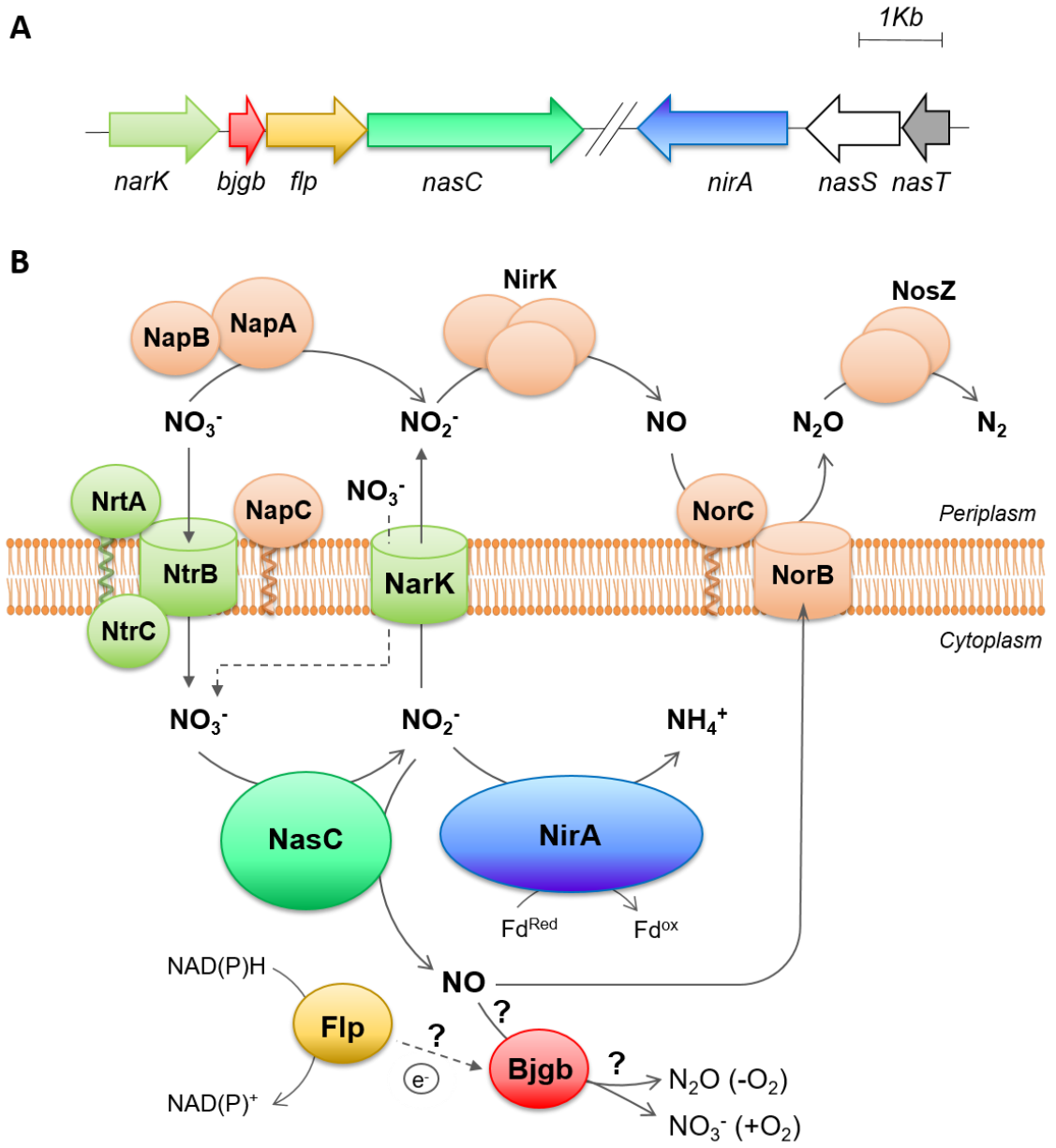

Figure 2.12. NO_3^- assimilation and NO detoxification in *B. diazoefficiens*. A. Organisation of regulatory and structural genes for the assimilatory pathway in *B. diazoefficiens*. **B.** Biochemical pathway for the coordinated NO_3^- assimilation and NO detoxification system, and denitrification in *B. diazoefficiens*. Adapted from Cabrera et al. (2016).

3

OBJETIVOS

3. OBJETIVOS

B. diazoefficiens es la única bacteria del orden *Rhizobiales* que es capaz no sólo de establecer simbiosis fijadoras de N_2 con plantas de soja, sino también de llevar a cabo una desnitrificación completa tanto en vida libre como en simbiosis. Además, esta bacteria puede crecer en vida libre con NO_3^- como única fuente de N a través del proceso de asimilación. Por ello, *B. diazoefficiens* se considera un modelo para estudiar la interrelación entre fijación de N_2, desnitrificación y asimilación de NO_3^-, procesos clave del ciclo del N.

Estudios previos, llevados a cabo en el Grupo del Metabolismo del Nitrógeno del Departamento de Microbiología del Suelo y Sistemas Simbióticos de la Estación Experimental del Zaidín, han demostrado que la hipoxia y el NO_3^- inducen la formación de NO en nódulos de soja, siendo la desnitrificación de los bacteroides el principal proceso implicado en la síntesis de NO (Sánchez et al., 2010). Estos estudios revelaron que el NO inhibe la actividad de la nitrogenasa, enzima clave en la fijación simbiótica de N_2, y la expresión del gen *nifH*, responsable de su síntesis (Sánchez et al., 2010). Por tanto, la presencia de sistemas de destoxificación de NO en nódulos es clave para una simbiosis eficiente. La enzima desnitrificante óxido nítrico reductasa (Nor) de los bacteroides es la principal implicada en la eliminación de NO en nódulos de soja en respuesta a NO_3^- y encharcamiento (Sánchez et al., 2010). Además de la desnitrificación, se ha demostrado en *B. diazoefficiens* la existencia de un sistema coordinado de asimilación de NO_3^- y destoxificación de NO codificado por el operón *narK-bjgb-flp-nasC* (Cabrera et al., 2016). Esta unidad transcripcional codifica para un transportador de NO_3^-/NO_2^- (NarK), una hemoglobina de dominio único (Bjgb), una flavoproteína dependiente de NAD(P)H (Flp) y una nitrato reductasa asimilativa (NasC). Cerca de estos genes se encuentra otro operón que incluye un gen que codifica para una nitrito reductasa asimilativa (NirA) y genes para un regulador de respuesta a NO_3^-/NO_2^- (NasST) (Cabrera et al., 2016) (Figura 2.12.). La proteína Bjgb presenta homología con el dominio N-terminal que contiene hemo de la flavohemoglobina (Hmp) de *E. coli*, así como con el dominio único de las hemoglobinas de *V. stercoraria* y *C. jejuni* (Sánchez et al., 2011a). La Flp es una proteína reductora dependiente de NAD(P)H que posee un motivo flavin mononucleótido (FMN) similar al dominio de unión FAD/NAD

de la Hmp de *E. coli*. Resultados previos a esta Tesis Doctoral han propuesto que Bjgb y Flp podrían eliminar el NO producido por la enzima NasC como producto de la asimilación de NO_3^-/NO_2^- (Cabrera et al., 2016). De hecho, Cabrera y colaboradores demostraron que Bjgb y Flp tienen un papel importante en la protección de células de *B. diazoefficiens* en vida libre frente al estrés nitrosativo. Se ha sugerido que Bjgb y Flp podrían formar un sistema de dos componentes que destoxificaría el NO generado como producto de la reducción de NO_3^- en condiciones de vida libre o en el interior de los nódulos de soja. Sin embargo, al inicio de esta Tesis Doctoral se desconocía el papel *in vitro* de las proteínas Bjgb y Flp en la destoxificación del NO, así como la implicación de la hemoglobina Bjgb y de las enzimas de asimilación de NO_3^- (NasC y NirA) en la interacción simbiótica con soja y en la homeostasis de NO en los nódulos. De acuerdo a los antecedentes presentados, para la realización de esta Tesis Doctoral se establecieron los siguientes objetivos:

1. Determinar la función *in vitro* de la hemoglobina de dominio único (Bjgb) y la flavoproteína (Flp) de *Bradyrhizobium diazoefficiens* en la destoxificación de óxido nítrico (NO).
2. Analizar el papel de la hemoglobina de dominio único (Bjgb) de *B. diazoefficiens* en la fijación simbiótica de nitrógeno (N_2) y en la homeostasis del NO en nódulos de soja.
3. Establecer la función de la nitrato reductasa asimilativa (NasC) y la nitrito reductasa asimilativa (NirA) de *B. diazoefficiens* en la fijación simbiótica de N_2.

---

1. To determine the function *in vitro* of the single domain haemoglobin (Bjgb) and the flavoprotein (Flp) from *Bradyrhizobium diazoefficiens* in nitric oxide (NO) detoxification.
2. To analyze the role of the single domain haemoglobin (Bjgb) from *B. diazoefficiens* in symbiotic nitrogen (N_2) fixation and NO homeostasis in soybean nodules.
3. To establish the function of the assimilatory nitrate reductase (NasC) and nitrite reductase (NirA) from *B. diazoefficiens* in symbiotic N_2 fixation.

4

MATERIALES Y MÉTODOS

4. MATERIALES Y MÉTODOS

4.1. Materiales

4.1.1. Cepas bacterianas

Las cepas de *B. diazoefficiens* y *E. coli* usadas en esta tesis, junto con sus características más importantes, se muestran a continuación (Tabla 4.1.).

Tabla 4.1. Cepas bacterianas.

Cepa	Descripción relevante	Referencia
E. coli		
DH5α	*supE44*, *ΔlacU169*, f80, *lacZΔM*, *5hsdR171*, *recA1*, *endA1*, *gyrA96*, *thi1*, *relA1*	Bethesda Research Laboratories Inc., Gaithersburg, Maryland,
S17.1	Sm^r, Spc^r; *thi*, *pro*, *recA*, *hsdR*, *hsdM*, RP4Tc::Mu, Km::Tn7	Simon et al. (1983)
BL21 (DE3)	F^- *ompT hsdS*$_B$ (r_B^- m_B^-) *gal dcm* (DE3)	Novagen®
B. diazoefficiens		
USDA 110	Cm^r; cepa silvestre	Departamento de Agricultura, Beltsville, Maryland, Estados Unidos
110*spc*4	Cm^r, Spc^r; cepa silvestre	Regensburger y Hennecke (1983)
4001	Cm^r; Δblr2807 (*bjgb*)	Cabrera et al. (2016)
4003	Cm^r; Δblr2809 (*nasC*)	Cabrera et al. (2016)
4011	Cm^r; Δbll4571 (*nirA*)	Cabrera et al. (2016)
GRPA1	Cm^r Spc^r Sm^r; *napA*::Ω (*napA*)	Delgado et al. (2003)
GRC131	Cm^r, Km^r; *norC*::*aphII*-PSP (*norC*)	Mesa et al. (2002)
H1	Cm^r, Spc^r, Km^r; *nifH*::Tn5 (*nifH*)	Hahn et al. (1984)
USDA 110-(pBBR1MCS-2)	Cm^r, Km^r; USDA 110 con pBBR1MCS-2	Este trabajo

Cepa	**Descripción relevante**	**Referencia**
4001-(pBBR1MCS-2)	Cm^r, Km^r; 4001 con pBBR1MCS-2	Este trabajo
4001-4023	Cm^r, Km^r; 4001 con pDB4023	Este trabajo
4001-4027	Cm^r, Km^r; 4001 con pDB4027	Este trabajo
4001-2499	Cm^r, Tc^r; 4001::P*norC-lacZ*	Cabrera et al. (2016)
4001-2499-(pBBR1MCS-2)	Cm^r, Tc^r, Km^r; 4001-2499 con pBBR1MCS-2	Este trabajo
4001-2499-4023	Cm^r, Tc^r, Km^r; 4001-2499 con pDB4023	Este trabajo
4001-2499-4027	Cm^r, Tc^r, Km^r; 4001-2499 con pDB4027	Este trabajo
GRC131	Cm^r, Km^r; *norC*::*aphII*-PSP (*norC*)	Mesa et al. (2002)
GRC131-(pBBR1MCS-5)	Cm^r, Km^r, Gm^r; GRC131 con pBBR1MCS-5	Este trabajo
GRC131-4028	Cm^r, Km^r, Gm^r; GRC131 con pDB4028	Este trabajo
GRC131-4029	Cm^r, Km^r, Gm^r; GRC131 con pDB4029	Este trabajo

4.1.2. Plásmidos

En la Tabla 4.2. se describen los plásmidos empleados durante el desarrollo de esta tesis.

Tabla 4.2. Plásmidos.

Plásmido	Descripción relevante	Referencia
pBBR1MCS-2	Km^r; *lacZ mob*$^+$, vector de clonación	Kovach et al. (1994)
pBBR1MCS-5	Gm^r; *lacZ mob*$^+$, vector de clonación	Kovach et al. (1994)
pBluescript KS (+)	Ap^r; *lacZ*, *ori f1*, vector de clonación	Stratagene®
pET-24a(+)	Km^r; Vector de expresión	Novagen®
pDB4008	Km^r; [pET-24a(+)] con un fragmento que contiene los genes completos *bjgb* (blr2807) y *flp* (blr2808) de *B. diazoefficiens*	Este trabajo
pDB4010	Km^r; [pET-24a(+)] con un fragmento que contiene el gen completo *flp* de *B. diazoefficiens*	Este trabajo
pDB4023	Km^r; (pBBR1MCS-2) con un fragmento que contiene el gen completo *bjgb* de *B. diazoefficiens*	Este trabajo
pDB4024	Ap^r; [pBS (KS)] con un fragmento que contiene el gen completo *bjgb* de *B. diazoefficiens* procedente de pDB4023	Este trabajo
pDB4025	Ap^r; [pBS (KS)] con un fragmento que contiene el gen completo *bjgb* de *B. diazoefficiens* mutado en la posición 52 (lisina-52) por QuickChange	Este trabajo
pDB4027	Km^r; (pBBR1MCS-2) con un fragmento que contiene el gen completo *bjgb* de *B. diazoefficiens* mutado en la posición 52 (lisina-52) por QuickChange, procedente de pDB4025	Este trabajo
pDB4028	Gm^r; (pBBR1MCS-5) con un fragmento que contiene el gen completo *bjgb* de *B. diazoefficiens* procedente de pDB4023	Este trabajo
pDB4029	Gm^r; (pBBR1MCS-5) con un fragmento que contiene el gen completo *bjgb* de *B. diazoefficiens* mutado en la posición 52 (lisina-52) por QuickChange, procedente de pDB4027	Este trabajo

4.1.3. Oligonucleótidos

En la siguiente tabla se presentan los oligonucleótidos empleados durante el desarrollo de esta tesis.

Tabla 4.3. Oligonucleótidos.

Nombre oligonucleótido	**Secuencia de ADN (5' → 3')**	**Referencia**
Complementación con el gen *bjgb* de *B. diazoefficiens*		
blr2807_For	GAGAAGCTTTCGCAACGACGCGGACAAAGG[(1)]	Este trabajo
blr2807_Rev	GAGGGATCCACGATGACCAGCGGTTCACTC[(1)]	Este trabajo
Construcción de los plásmidos de expresión de Bjgb-His$_6$ y Flp-His$_6$		
blr2807-8_His_For	CACACGCTAGCAGAGGATCGCATCACCATCACCATCACGGATC CATCGAGGGAAGGACGCCCGAACAGATTACCCTCATCCAG[(1)]	Este trabajo
blr2807-8_His _Rev	GCAAAGCTTTCAAGCCGCCTTGGAAGGACGCGC[(1)]	Este trabajo
blr2808_His_For	CACACGCTAGCATGGCGCTCAGGCGCAGGC[(1)]	Este trabajo
blr2808_His_Rev	GCAAAGCTTCCTTCCCTCGATAGCCGCCTTGGAAGGACGC[(1)]	Este trabajo
Mutagénesis puntual dirigida (QuickChange^{TM}) del gen *bjgb* de *B. diazoefficiens*		
blr2807(K52A)_For	CATGACCGAGCAGCGCAAG**GC**GCTGATGGGCATGCTCGCC[(2)]	Este trabajo
blr2807(K52A)_Rev	GGCGAGCATGCCCATCAG**CG**CCTTGCGCTGCTCGGTCATG[(2)]	Este trabajo
qRT-PCR		
fixN4_For	CGGGATCCCGACTCCTATCCGGTCGAGGAC	Mesa et al. (2005)
fixN4_Rev	CGGAATTCCGGGTCATGGATTTGGAGATGG	Mesa et al. (2005)
nifH_For	CGGCAGACCGACAAGGAA	Sánchez et al. (2010)
nifH_Rev	ATCAGTTGAGTGCCAAGCTTCTT	Sánchez et al. (2010)
narK_For	TATCGGCTTCTCGGTCTGG	Este trabajo
narK_Rev	GCTGGTCGGTGGTGTAATG	Este trabajo
norC_3_For	GCAGATGCCGCAGTTCAAC	Torres et al. (2014a)
norC_3_Rev	TGATCGTGCTCACCCATTG	Torres et al. (2014a)
16S_qRT_For	GCAGGCTTAACACATGCAAGTC	Torres et al. (2017)

Nombre oligonucleótido	**Secuencia de ADN (5' → 3')**	**Referencia**
16S_qRT_Rev	AGGTACGTTCCCACGCGTTACTC	Torres et al. (2017)
Otros		
pTXB1-1	GGGAATTGTGAGCGGATAAC	Sigma
pET28a-1_rev	CAGCTTCCTTTCGGGCTTTG	Sigma
M13_For	GTAAAACGACGGCCAGT	Sigma
M13_Rev	AACAGCTATGACCATGATTACG	Sigma

(1) Subrayada se indica la secuencia de los sitios de restricción añadida a la secuencia de los oligonucleótidos.

(2) En negrita se señalan las bases que se modificaron en la secuencia original del gen *bjgb* de *B. diazoefficiens* para introducir la mutación.

4.1.4. Medios de cultivo

La composición, elaboración y utilidad de los diferentes medios empleados para el desarrollo experimental de esta tesis se detallan en la siguiente tabla (Tabla 4.4.).

Tabla 4.4. Medios de cultivo.

Medio de cultivo	Composición	Utilidad	Referencia
E. coli			
LB (Luria-Bertani)	NaCl, 5 g; triptona, 10 g; extracto de levadura, 5 g; H_2O desionizada, enrasar a 1 l. pH 7	Medio de cultivo de rutina para *E. coli*	Miller (1972)
B. diazoefficiens			
PSY (Peptone- Salts-Yeast extract)	KH_2PO_4, 0,3 g; Na_2HPO_4, 0,3 g; $CaCl_2 \cdot 2H_2O$, 0,05 g; $MgSO_4 \cdot 7H_2O$, 0,1 g; extracto de levadura, 1 g; peptona, 3 g; ******solución (100×) de elementos traza, 10 ml; *****L-arabinosa, 0,1%; H_2O desionizada, enrasar a 1 l. pH 7	Medio de cultivo de rutina para *B. diazoefficiens*	Regensburger y Hennecke (1983)
Bergersen	K_2HPO_4, 0,23 g; $MgSO_4 \cdot 7H_2O$, 0,1 g; glicerol, 4 ml; glutamato sódico, 1,1 g; ******solución (100×) de elementos traza, 10 ml; H_2O desionizada, enrasar a 1 l. pH 7	Medio mínimo para *B. diazoefficiens*	Bergersen (1977)
BSN3	Medio Bergersen en el que se sustituye el glicerol por 10 mM de succinato y el glutamato sódico por 10 mM de KNO_3	Medio empleado para el cultivo en condiciones microóxicas de asimilación de nitrato	Cabrera et al. (2016)

Para la preparación de medios de cultivo sólidos, se añadió 15 g de agar bacteriológico por litro de medio, tras haber medido el pH.

La esterilización de todos los medios de cultivo se llevó a cabo en un autoclave a 121℃ durante 20 min. La arabinosa se adicionó al medio PSY, al igual que los antibióticos, cuando fue necesario, siempre después del autoclavado.

*****L-arabinosa: se prepara al 10% y se esteriliza por filtración con un filtro Minisart® NML (Sartorius) de 0,2 µm de tamaño de poro. Se conserva a 4°C.

******Solución concentrada de elementos traza (100×): H_3BO_3, 1 g; $ZnSO_4 \cdot 7H_2O$, 0,1 g; $CuSO_4 \cdot 5H_2O$, 0,05 g; $MnCl_2$, 0,05 g; $Na_2MoO_4 \cdot 2H_2O$, 0,01 g; $FeCl_3$, 0,1 g; H_2O desionizada, 1 l.

4.1.5. Antibióticos

La adición de antibióticos a los medios de cultivo se realizó a partir de soluciones concentradas de los mismos en H_2O desionizada y posterior esterilización con unidades de filtración Minisart® NML (Sartorius) de 0,2 µm de tamaño de poro. Las soluciones de tetraciclina y de cloramfenicol no se esterilizaron por filtración debido a que se utilizó alcohol o una mezcla hidroalcohólica para disolver dichos antibióticos. La concentración final de los diferentes antibióticos se indica en la Tabla 4.5.

Tabla 4.5. Antibióticos.

		Cultivos de *B. diazoefficiens*		**Cultivos de *E. coli* (liq. y sol.) (µg/ml)**
Nombre		**Líquido (µg/ml)**	**Sólido (µg/ml)**	
Espectinomicina	**Spc**	100	200	25
Tetraciclina*	**Tc**	25	50	10
Sulfato de kanamicina	**Km**	100	200	25
Ampicilina	**Ap**	-	-	200
Cloramfenicol**	**Cm**	20	20	50
Gentamicina	**Gm**	100	100	30

*****La solución concentrada de Tc se preparó en metanol:agua (1:1) o metanol absoluto dependiendo de la concentración de la misma (1 o 10 mg/ml, respectivamente).

******Para la solución concentrada de Cm se utilizó etanol.

4.1.6. Soluciones, tampones y reactivos

Las soluciones, tampones y reactivos utilizados en esta tesis se detallan en la siguiente tabla (Tabla 4.6.).

Tabla 4.6. Soluciones, tampones y reactivos.

Solución	Composición	Uso
Métodos microbiológicos		
Tampón de lavado	Tris-HCl 40 mM; KCl 150 mM. pH 7	Fraccionamiento de las células de *B. diazoefficiens*
Tampón de fraccionamiento	Tampón de lavado adicionado con AEBSF* 1 mM; DNAsaI 20 µg/ml *4-[2-Aminoethyl] benzenesulfonyl fluoride hydrochloride	
Métodos analíticos		
Tampón Z	$Na_2HPO_4 \cdot 2H_2O$ 60 mM; $NaH_2PO_4 \cdot H_2O$ 40 mM; KCl 10 mM; $MgSO_4$ 1 mM. pH 7. El día que se va a utilizar se añade β-mercaptoetanol 50 mM	Determinación de actividad β-galactosidasa
Solución de ONPG	2-nitrofenil-β-D-galactopiranósido, 4 mg/ml de tampón fosfato	
Tampón fosfato	A: $Na_2HPO_4 \cdot 2H_20$ (0,1 mM), 1,245 g/70 ml; B: $NaH_2PO_4 \cdot H_20$ (0,1 mM), 0,689 g/50 ml. Mezclar 61 ml de A y 39 ml de B	
Gel de resolución SDS-PAGE 14%	H_2O destilada 1,31 ml; Tris-HCl 1,5 M (pH 8,8) 1,25 ml; acrilamida 30% (37,5:1) 2,34 ml; SDS 10% 50 µl; APS* 10% (preparado fresco) 31,25 µl; TEMED 6,6 M 2,5 µl *Persulfato amónico $(NH_4)_2S_2O_8$)	SDS-PAGE
Gel de empaquetado SDS-PAGE 4%	H_2O destilada 0,91 ml; Tris-HCl 0,5 M (pH 6,8) 0,375 ml; acrilamida 30% (37,5:1) 0,2 ml; SDS 10% 15 µl; APS* 10% (preparado fresco) 30 µl; TEMED 6,6 M 1,25 µl *Persulfato amónico $(NH_4)_2S_2O_8$)	
Tampón de desarrollo SDS-PAGE	Glicina 14,41 g/l; Tris-Base 3,03 g/l; SDS 1 g/l. pH 8,3	
Tampón de carga SDS-PAGE	Tris-HCl 125 mM (pH 6,8); SDS 4%; DTT 0,1 M; glicerol 20%; azul de bromofenol 0,02%	

Solución	Composición	Uso
Tampón de transferencia	Tris 30 g/l; glicina 14,4 g/l; metanol 200 ml. pH 8,3	Transferencia de proteínas desde el gel de poliacrilamida a la membrana de nitrocelulosa
Solución de Coomassie	Coomassie Brilliant Blue R250 1 g; metanol 400 ml; ácido acético 100 ml; H_2O destilada 500 ml	Detección de proteínas en gel de poliacrilamida con Coomassie
Solución de desteñido	Metanol 250 ml; ácido acético 100 ml; H_2O destilada 650 ml	
Métodos de biología molecular		
Tampón TE	Tris-HCl 10 mM; EDTA 1 mM. pH 8	Obtención de ADN plasmídico de *E. coli* (miniprep TENS)
Solución TENS	NaOH 0,1 M; SDS 0,5%; ARNasaA en TE 1 µl	
Solución de neutralizado	Acetato sódico 3 M. Equilibrado con ácido acético glacial a pH 5,2	
Solución ARNasa A	2 mg/ml de ARNasa A en Tris-HCl 10 mM (pH 7,4); NaCl 0,1 M; glicerol 20%. Hervir durante 10 min para eliminar ADNasas	
Solución de lavado	NaCl 1 M; Sarcosil 1%	Obtención de ADN plasmídico de *B. diazoefficiens*
Solución MAXI	Tris-HCl 25 mM; glucosa 50 mM; EDTA 10 mM. pH 8	
Solución de lisis	NaOH 0,2 M; SDS 1%	
Solución de neutralizado	Acetato sódico 3 M. Equilibrado con ácido acético glacial a pH 4,8	
Tampón A	NaOAc 20 mM (pH 5,5); EDTA 1 mM (pH 8); H_2O desionizada-DEPC*****. *****Añadir DEPC 0,1% y dejar en agitación durante una noche. Autoclavar al día siguiente	Aislamiento de ARN total de nódulos de soja
H_2O destilada-DEPC	H_2O desionizada, DEPC 0,1%. Se deja en agitación durante 24 h y se autoclava posteriormente	
Tampón de carga de ADN o ARN 6×	Sacarosa 40%; azul de bromofenol 0,025%	Electroforesis en geles de agarosa
Tampón TBE 0,5×	Tris-HCl 45 mM; borato 45 mM; EDTA 1 mM. pH 8	Electroforesis en geles de agarosa para ADN

Solución	Composición	Uso
Tampón TAE 1×	Tris-acetato 40 mM; EDTA 1 mM. pH 8	Electroforesis en geles de agarosa para ARN
Tampón TFB1	Acetato potásico 30 mM; $MnCl_2 \cdot 4H_2O$ 50 mM; RbCl 100 mM; $CaCl_2 \cdot 2H_2O$ 10 mM; glicerol 15%. pH 5,8.	Preparación de células competentes de *E. coli*
Tampón TFB2	MOPS 10 mM; RbCl 10 mM; $CaCl_2 \cdot 2H_2O$ 75 mM; glicerol 15%. pH 6,8. Cubrir con papel de aluminio para proteger de la luz y conservar a 4°C	
Sobreexpresión y purificación de las proteínas Bjgb-His$_6$ y Flp-His$_6$ Todos los tampones empleados para la purificación de proteínas se filtraron usando filtros de nitrato de celulosa de 0,45 µm de tamaño de poro (Sartorius), acoplados a una bomba de vacío. Se conservaron a 4°C.		
Tampón A1	Na_2HPO_4 20 mM; $NaH_2PO_4 \cdot 2H_2O$ 20 mM; NaCl 150 mM; imidazol 25 mM. pH 7,5	Purificación Bjgb-His$_6$
Tampón B1	Na_2HPO_4 20 mM; $NaH_2PO_4 \cdot 2H_2O$ 20 mM; NaCl 150 mM; imidazol 500 mM. pH 7,5	
Tampón A2	HEPES 50 mM; EDTA 1 mM; glicerol 10%. pH 7	
Tampón B2	NaCl 1 M; HEPES 50 mM; EDTA 1 mM; glicerol 10%. pH 7	
Tampón C	Tris 20 mM; NaCl 150 mM; DTT 2 mM (preparado fresco); imidazol 25 mM; glicerol 10%. pH 7	Purificación Flp-His$_6$
Tampón D	Tris 20 mM; NaCl 150 mM; DTT 2 mM (preparado fresco); imidazol 500 mM; glicerol 10%. pH 7	
Tampón de diálisis	Tris 20 mM; NaCl 150 mM; DTT 2 mM (preparado fresco); EDTA 1 mM; glicerol 10%. pH 7	
Determinaciones analíticas y enzimáticas en nódulos de soja		
Medio de extracción de Lb	$Na_2HPO_4 \cdot 2H_2O$/$NaH_2PO_4 \cdot H_2O$ 50 mM (pH 7,4); $K_3Fe(CN)_6$ 0,02%; $NaHCO_3$ 0,1% Cubrir con papel de aluminio y conservar a 4°C hasta su empleo	Contenido de Lb en los nódulos
Tampón Na_2HPO_4/NaH_2PO_4	A: $Na_2HPO_4 \cdot 2H_2O$ (50 mM),0,8003 g/90 ml; B: $NaH_2PO_4 \cdot H_2O$ (50 mM), 0,1725 g/25 ml. Mezclar 81 ml de A y 19 ml de B. pH 7,4	

Solución	Composición	Uso
Tampón de extracción de bacteroides	Tampón Tris-HCl 50 mM, pH 7,5 (conservar a 4°C hasta su empleo); manitol 250 mM (añadir en el momento de uso)	Aislamiento de bacteroides de los nódulos
Mezcla NR	Tampón Tris-HCl 20 mM; KNO_3 20 mM; metil viológeno 0,4 mM. pH 7,5	Actividad nitrato reductasa de los bacteroides
Sulfanilamida	Sulfanilamida, 10 g en 200 ml de HCl concentrado (12 N). Enrasar a 1 l con H_2O desionizada. Cubrir con papel de aluminio para proteger de la luz y conservar a 4°C	Determinación de NO_2^-
NNEDA	Ácido N-naftil-etilén-diamino, 200 mg/l (0,77 mM). Cubrir con papel de aluminio para proteger de la luz y conservar a 4°C	
Solución de fenol-nitroprusiato	34 mg de nitroprusiato sódico en 70 ml de H_2O desionizada. Añadir 7 g de fenol. Ajustar el volumen a 100 ml. Conservar en oscuridad a 4°C	Contenido de NH_4^+en los bacteroides
Solución de hipoclorito	2,96 g NaOH; 29,74 g $Na_2HPO_4 \cdot 12H_2O$ en 140 ml de H_2O desionizada. Añadir 16,6 ml de NaOCl 12%. Ajustar a pH 12 con NaOH y el volumen a 200 ml con H_2O desionizada. Conservar en oscuridad a temperatura ambiente	

4.1.7. Preparación de una solución saturada de NO

Para preparar una solución saturada de NO (con una concentración de 5 mM aproximadamente), se siguió el protocolo que se detalla a continuación, desarrollado en el grupo de investigación del Dr. Andrew J. Gates (University of East Anglia, Norwich, Reino Unido):

1.- Añadir 4 ml de tampón de diálisis sin DTT (Tabla 4.6.) a un bote de cristal de 5 ml.

2.- Cerrar el bote con un tapón de goma perforable y sellar el tapón con película autosellante.

3.- Gasear con N_2 durante 20 min para eliminar todo el O_2.

4.- En una campana de extracción de gases, adicionar al tampón de diálisis 6 ml de NO gas con una jeringa Hamilton[a], contenido en un matraz con hidróxido de sodio (NaOH)[b]. La solución de NaOH se emplea para lavar el NO antes de inyectarlo en el tampón de diálisis.

5.- Agitar vigorosamente durante 5 min el bote para asegurar que el tampón de diálisis se satura con NO.

6.- Cuantificar la concentración de NO presente en la muestra, empleando un analizador de NO (Nitric Oxide Analyzer-NOA 280i. Sievers).

[a] Para inyectar el NO se usa una jeringa Hamilton hermética, antes de su uso esta jeringa se lava 5-7 veces con H_2O desionizada libre de O_2 para eliminar todo el O_2 de la misma. Para ello, se añaden 4 ml de H_2O a un bote de cristal (5 ml), el cual se cierra con un tapón de goma perforable y se sella con película autosellante, a continuación, el bote se gasea con N_2 durante 20 min y, por último, se realizan los lavados de la jeringa. Inmediatamente después de estos lavados, se cierra la llave que cierra herméticamente la jeringa para impedir la entrada de O_2 en la misma.

[b] Para preparar la solución de NaOH 0,1 M para el lavado de NO, se llena un matraz de 100 ml al máximo de su capacidad (120 ml aproximadamente) con una solución de NaOH 0,1 M. El matraz se cierra con un tapón de goma perforable y se sella con película autosellante. Posteriormente, se gasea con N_2 durante 30-50 min para eliminar todo el O_2 del mismo. Por último, se inyecta NO gas puro en el matraz, de modo que la atmósfera de éste se reemplaza por NO puro. Se sella de nuevo el tapón de goma perforable con película autosellante y se coloca el matraz en posición invertida en un soporte seguro.

4.2. Métodos microbiológicos

4.2.1. Conservación de cepas bacterianas

La conservación de las diferentes cepas se realizó según la metodología establecida en nuestro grupo de investigación. Para ello, se emplearon criotubos que contenían alícuotas de cultivos en fase logarítmica de crecimiento, a dichos criotubos se adicionó glicerol estéril (con una concentración final del 50%). Para la preparación de los

cultivos se inocularon 10 ml de LB, para *E. coli*, o 20 ml de PSY, para *B. diazoefficiens*, a los que se añadió sus correspondientes antibióticos y se inocularon con una sola colonia aislada que procedía de una placa fresca. Los cultivos se incubaron a 37℃ durante una noche para *E. coli* o a 30℃ durante 4 o 5 días para *B. diazoefficiens*. Posteriormente, los cultivos se centrifugaron y lavaron una vez con medio sin antibiótico. Los pellets se resuspendieron con 2,25 ml del medio correspondiente sin antibiótico y, finalmente, se alicuotaron en tres criotubos. De los tres criotubos preparados, uno se conservó a -20℃ para uso individual y dos a -80℃ para la colección del grupo.

Para el transporte y envío de cepas bacterianas a otros laboratorios se inocularon criotubos con medio de cultivo sólido en pico de flauta, LB o PSY para *E. coli* o *B. diazoefficiens*, respectivamente, suplementado con los antibióticos adecuados.

4.2.2. Cultivo de células de *B. diazoefficiens*

4.2.2.1. Cultivos en medio sólido y líquido

Los cultivos de células de *B. diazoefficiens* en medio sólido se iniciaron a partir de los criotubos conservados de las cepas. Las placas de medio PSY sólido con los antibióticos convenientes se estrían con asa de siembra con la de cepa de *B. diazoefficiens* adecuada. Las células se incuban aeróbicamente a 30℃ durante 4-7 días. Los precultivos líquidos se obtuvieron a partir de estos cultivos sólidos. Para ello, se inocularon con colonias aisladas de cultivos sólidos en matraces de 250 ml que contenían 50 ml de medio PSY líquido con sus antibióticos adecuados. Las células se incubaron aeróbicamente a 30℃, en un agitador orbital (170 r.p.m.), durante 4-5 días, hasta alcanzar una densidad óptica a 600 nm (DO_{600nm}) ∼1.

Para la inoculación de los cultivos en medio mínimo se procedió de la siguiente forma: los precultivos líquidos se centrifugaron y los pellets resultantes se lavaron dos veces con el medio de destino. A continuación, los pellets se resuspendieron en 1/20 del volumen inical, obteniéndose una suspensión de células concentradas. Se midió la DO_{600nm} de las diluciones 1:20 de las suspensiones celulares concentradas. Los cultivos se inocularon a una DO_{600nm} inicial de 0,1 a 0,3 para ser posteriormente incubados en las condiciones necesarias para cada experimento.

4.2.2.2. Cultivos aeróbicos

Los cultivos aeróbicos se iniciaron a partir de precultivos líquidos en PSY. Para ello, se inocularon matraces de 250 ml con 50 ml de medio BSN3. Estos cultivos se inocularon a una DO_{600nm} inicial de 0,35 y se incubaron con agitación (170 r.p.m.) a 30°C durante 2 días hasta alcanzar la fase exponencial. Estos cultivos se emplearon para la inoculación de las semillas de soja.

4.2.2.3. Cultivos microaeróbicos

Para el cultivo microaeróbico de *B. diazoefficiens* se emplearon tubos de 17 ml o matraces de 250 o 500 ml provistos de tapón de goma perforable y conservando la proporción 1:5 entre medio y fase gaseosa. La atmósfera gaseosa del recipiente se sustituyó al inicio de la incubación por una mezcla gaseosa de 2% de O_2 en N_2, el tiempo de gaseo dependió del volumen de la atmósfera del recipiente. Para evitar posibles contaminaciones durante el gaseo, se usaron filtros Minisart NML (Sartorius) de 0,2 µm de tamaño de poro. Estos cultivos se inocularon a una DO_{600nm} inicial de 0,1-0,3 y se incubaron con agitación (170 r.p.m.) a 30°C durante 1-4 días hasta alcanzar la fase exponencial. Estos cultivos se emplearon para análisis de pruebas enzimáticas.

4.2.3. Obtención de la fracción soluble (citosol) y particulada (membranas) de *B. diazoefficiens*

Los cultivos celulares de *B. diazoefficiens* se centrifugaron a 8.000 × *g* (10 min, 4°C) y se lavaron dos veces con tampón de lavado (Tabla 4.6.). El pellet resultante se resuspendió en 2 ml de tampón de lisado (Tabla 4.6.). Para la obtención de citosol y membranas de *B. diazoefficiens* se empleó una prensa de French (SLM), con la que se rompieron las células por diferencia de presión, siguiendo la metodología indicada por Fernández-López et al. (1994):

1.- Antes de la rotura de las células, la célula de la prensa se preenfria manteniéndola en una cámara frigorífica. Se procede al ensamblaje de la célula de la prensa, que consta de pistón, émbolo, tapa, llave y grifo.

2.- Posteriormente, se aplica la suspensión celular en la célula de la prensa y se lleva a cabo el lisado de las bacterias aplicando una presión constante de 120 MPa y dejando salir la suspensión lentamente por el grifo. Este proceso se repite tres veces.

3.- Se centrifuga el extracto de células resultante de la prensa a 8.000 × *g* (10 min, 4℃) para sedimentar las células que no se hayan roto. Se recoge el sobrenadante y se recentrifuga a 250.000 × *g* (1 h, 4℃).

4.- El sobrenadante resultante se consideró como la fracción soluble (citosol) y el sedimento translúcido como la fracción particulada (membranas). El sedimento se resuspendió en 100 µl de tampón Tris-HCl 50 mM (pH 7,5) con ayuda de un asa de plástico.

4.3. Métodos analíticos

4.3.1. Determinación de la producción de óxido nitroso (N_2O)

La producción de N_2O se midió mediante cromatografía gaseosa. Para ello, se prepararon tubos, cerrados herméticamente, que contenían cultivos celulares (sección 4.2.2.) (Cabrera et al., 2016) o nódulos (apartado 4.9.7) (Tortosa et al., 2015). Inmediatamente después de preparar dichos tubos, se adicionó al espacio de cabeza de cada tubo acetileno 10% (v/v) para inhibir la actividad de la enzima óxido nitroso reductasa (Yoshinari y Knowles, 1976). En este momento comenzó la incubación (tiempo 0). Transcurrido el tiempo de incubación[1] adecuado, se tomaron alícuotas de 1 ml del espacio gaseoso de cada tubo y se inyectaron en un cromatógrafo de gases HP modelo 4890D equipado con un detector de captura de electrones y una columna metálica empaquetada con PorapaK Q 80/100 MESH. Las temperaturas del inyector, columna y detector fueron de 125, 60 y 375℃, respectivamente. Como gas portador se empleó N_2 a un flujo de 28 ml/min. Los picos de N_2O se identificaron por comparación con el correspondiente patrón, cuya concentración era del 2% (v/v) de N_2O. La concentración de N_2O en las muestras se calculó tomando como referencia la curva patrón, construída con volúmenes conocidos de N_2O. Para calcular la concentración total de N_2O presente en el vial que contenía el cultivo o los nódulos, se estrapoló la concentración del espacio de cabeza con la solubilidad del N_2O en el medio y la temperatura, aplicando la ley de Henry (Sander, 1999).

Los valores de producción de N_2O por cultivos celulares se expresaron como: µM de N_2O producidos.

La preparación de los tubos con nódulos y sus cálculos se detallan en el apartado 4.9.7.

[1] Los cultivos celulares se incubaron a 30°C y con agitación (170 r.p.m.) durante 96 h y se tomaron muestras gasosas de los mismos a las 24, 48, 72 y 96 h de incubación. Los nódulos se incubaron a 30°C y sin agitación durante 6 h y se tomaron muestras a las 4 y 6 h de incubación.

4.3.2. Determinación de actividad β-galactosidasa

La actividad β-galactosidasa se determinó con un protocolo modificado al descrito en Sambrook y Russell (2001), el cual se detalla a continuación:

1.- Tomar alícuotas de 3 ml de cultivo de *B. diazoefficiens* (DO_{600nm} = 0,3-0,5) en tubos de microcentrífuga. Centrifugar a 13.000 r.p.m. durante 5 min, eliminar el sobrenadante y resuspender el pellet en 300 µl de medio de cultivo nuevo (200 µl se emplean para la reacción y 100 µl para determinar la DO_{600nm}), obteniendo de esta forma cultivo concentrado.

2.- Medir la DO_{600nm} del cultivo concentrado, a partir del cual se determina la actividad β-galactosidasa. Para ello, hay que diluir los 100 µl anteriores convenientemente con H_2O destilada y, a continuación, medir su DO_{600nm}. Considerar las diluciones realizadas y rectificarlas en la DO_{600nm}.

3.- Adicionar a cada tubo de reacción, que contiene 200 µl de cultivo (concentrado), 400 µl de tampón Z (Tabla 4.6.), 100 µl de cloroformo y 50 µl de SDS al 0,1% en tampón Z. Agitar en vórtex durante 15 s. La solución debe ponerse turbia y blanquecina. Incubar a 30°C durante 5 a 10 min para templar la reacción y separar las dos fases.

4.- Para iniciar la reacción, añadir a cada tubo 150 µl de la solución de ONPG (2-nitrofenil-β-D-galactopiranósido) (Tabla 4.6.). Comenzar el cronometraje de la reacción, mezclar ligeramente e incubar los tubos a 30°C hasta que aparezca un color amarillo moderado.

5.- Para detener la reacción, adicionar a cada tubo 350 µl de Na_2CO_3 1 M. Anotar el tiempo de incubación transcurrido entre la adición del ONPG (inicio de la reacción) y la adición del Na_2CO_3 (fin de la reacción).

6.- Centrifugar los tubos de reacción a 13.000 r.p.m. durante 5 min. Sin arrastrar restos celulales, transferir 300 µl de cada tubo a diferentes pocillos de una placa ELISA y medir a DO_{420nm}.

La actividad β-galactosidasa se expresa en unidades Miller (UM), de acuerdo con la fórmula siguiente:

$$UM = \frac{\{1000 \times DO_{420nm}\}}{\{t(minutos) \times V(ml) \times DO_{600nm}\}}$$

Donde:

DO_{420nm} = valor de DO de la reacción a 420 nm

DO_{600nm} = valor de DO a 600 nm de la alícuota de cultivo concentrada que se prepara al inicio del experimento

t= tiempo de incubación

V= volumen de cultivo (200 µl para este protocolo. Debido a que el cultivo tenía una DO_{600nm} muy baja, se tomó una alícuota de 3 ml cultivo y se concentró por centrifugación)

La actividad β-galactosidasa también se puede expresar considerando la concentración de proteína con la siguiente fórmula:

$$UM = \frac{\{1000 \times DO_{420nm}\}}{\{0{,}0045 \times t(minutos) \times V(ml) \times [prot.](mg/ml)\}}$$

0,0045 = absorbancia de 1 nmol de ONPG

4.3.3. Determinación de proteína

La concentración de proteína en células enteras, extractos celulares, soluciones de proteína pura y bacteroides, se determinó mediante el empleo del reactivo de

Bradford 5× (Bio-Rad), según las especificaciones de la casa comercial. Para células enteras y bacteroides es necesario llevar a cabo, previamente a la determinación de proteína, el siguiente tratamiento de lisis:

1.- Añadir 1 volumen de NaOH 1 M a 1 volumen de cultivo. Agitar en vórtex y hervir durante 20 min. Centrifugar a 12.000 r.p.m., durante 5 min, y a temperatura ambiente, para eliminar los restos celulares. Tomar alícuotas de 25 a 50 µl del extracto resultante y completar con H_2O destilada hasta 500 µl. Desde este paso, el protocolo es igual para todo tipo de muestras.

2.- Tomar alícuotas de las muestras convenientemente diluídas y completar con H_2O destilada hasta un volumen final de 800 µl.

3.- Añadir 200 µl de reactivo de Bradford 5× (Bio-Rad) y agitar en vórtex.

4.- Incubar la mezcla anterior entre 2 y 60 min.

5.- Medir la absorbancia de cada muestra a DO_{595nm} frente a un blanco, preparado con 800 µl de H_2O y 200 µl del reactivo de Bradford 5× (Bio-Rad).

La concentración de proteína en las muestras se calculó por interpolación de los valores de absorbancia obtenidos para cada muestra respecto a una curva patrón, la cual se prepara con cantidades conocidas de albúmina sérica bovina (Sigma).

4.3.4. Detección de citocromos tipo *c* en membranas de *B. diazoefficiens*

Para la detección de proteínas de membrana de *B. diazoefficiens* que contienen grupos hemo *c*, se siguió la técnica de detección de actividad peroxidasa, intrínseca a estos citocromos, descrita en Vargas et al. (1993) y Delgado et al. (2003).

4.3.4.1. Electroforesis en geles de poliacrilamida (SDS-PAGE)

Para la realización de geles de poliacrilamida y electroforesis de proteínas se utilizó el material incluido en el sistema Mini-Protean Tetra Handcast (Bio-Rad). Se emplearon geles de 1 mm de grosor con una concentración de poliacrilamida del 14% para el gel de resolución y del 4% para el de empaquetado (Tabla 4.6.). Los geles se prepararon entre los cristales, previamente montados sobre sus soportes, sobre los que se vertió 4,5 ml de la solución del 14% de poliacrilamida inmediatamente después de adicionar el persulfato amónico (APS) y tetrametilendiamina (TEMED). Para nivelar el gel se

adicionó sobre el mismo 1 ml de isopropanol. Pasados 45 min aproximadamente, se eliminó el isopropanol, se lavó con H_2O y se vertió 1 ml de la solución de poliacrilamida al 4% justo después de adicionar el APS y TEMED. Por último, se colocó el peine para hacer los pocillos, teniendo la precaución de no introducir burbujas.

Para el montaje del sistema de electroforesis, se encajaron dos geles enfrentados en el casete formando un vaso. A continuación, el sistema se introdujo en la cubeta de electroforesis y se rellenó con tampón de desarrollo (Tabla 4.6.), tanto el vaso creado por los cristales como la cubeta.

En cada carril se cargaron 10 µg de proteínas de membrana mezclados con tampón de carga (Tabla 4.6.). En uno de los carriles del gel se cargaron 5 µl de marcador de peso molecular PageRuler Plus Prestained Protein Ladder (Thermo).

La electroforesis se desarrolló a 20 mA (4°C) hasta que el frente alcanzó el final del gel.

4.3.4.2. Transferencia a membranas de nitrocelulosa

Para la detección de citocromos *c*, las proteínas del gel de poliacrilamida se transfirieron a una membrana de nitrocelulosa. Antes de comenzar la transferencia, la membrana se lavó durante 5 min en tampón de transferencia (Tabla 4.6.). También se empaparon en tampón de transferencia dos esponjas del sistema de electroforesis Miniprotean II (Bio-Rad) y dos papeles Whatman 3MM (del mismo tamaño que las esponjas). A continuación, se preparó un sándwich formado por una esponja, un papel Whatman, el gel de poliacrilamida, la membrana de nitrocelulosa, otro papel Whatman y otra esponja. La composición anterior se empaquetó y se situó en la cubeta de electroforesis (rellena con tampón de transferencia, Tabla 4.6.), considerando que las proteínas migrarán hacia el polo positivo. La trasferencia se realizó a 10 mA durante 3 h (4°C).

4.3.4.3. Detección de citocromos tipo *c*

La detección de los citocromos *c* adheridos a la membrana de nitrocelulosa se realizó incubando dicha membrana durante 3 min con 600 µl de la mezcla de reactivos SuperSignal West Pico Chemiluminescent Substrate (Thermo). Seguidamente, para la detección de la emisión de luz, se colocó una película fotográfica (Hyperfilm β-max,

Amersham) sobre la membrana de nitrocelulosa durante 10 min. Por último, la película se reveló con líquidos revelador y fijador (Tetenal), siguiendo las instrucciones del producto. La película se escaneó y se analizó con el programa ImageLab (Bio-Rad) (Tabla 4.10.).

4.3.5. Detección del hemo *b* en la proteína pura Bjgb

Para la detección del grupo hemo *b* de la proteína pura Bjgb (protocolo de purificación detallado en el apartado 4.5.), se desarrolló una metodología modificada a la descrita en Thomas et al. (1976).

4.3.5.1. Electroforesis en geles de poliacrilamida (SDS-PAGE)

Para la preparación de los geles de poliacrilamida y electroforesis de proteínas se empleó el material incluido en el sistema Mini-Protean Tetra Handcast (Bio-Rad), según se detalla en la sección 4.3.4.1.

En el carril que contenía la muestra de proteína Bjgb pura se cargaron 10 µg de proteína pura mezclados con tampón de carga (Tabla 4.6.) sin DTT. En otro carril del gel se cargaron 5 µl de marcador de peso molecular PageRuler Plus Prestained Protein Ladder (Thermo).

4.3.5.2. Detección de hemo *b*

En primer lugar, para la visualización del grupo hemo *b*, se preparó en fresco una solución de 3,3',5,5'-Tetrametilbencidina (TMBZ) 6,3 mM en metanol. A continuación, se mezclaron 3 partes de la solución TMBZ con 7 partes de acetato de sódico 0,25 M, pH 5. El gel se sumergió en esta mezcla a temperatura ambiente y en oscuridad. Después de 1 hora, durante la cual la mezcla se agitó cada 10-15 min, se añadió peróxido de hidrógeno (H_2O_2) a una concentración final de 30 mM. La tinción comenzó a detectarse pasados 3 min e incrementó en intensidad en los 30 min siguientes. En este momento, el gel se sumergió durante al menos 1 hora en una mezcla isopropanol:acetato sódico (0,25 M, pH 5), en una relación 3:7. Esta mezcla se renovó dos veces para eliminar el TMBZ precipitado y para mejorar la intensidad de la tinción. Por último, se tomó una fotografía del gel.

Para eliminar el TMBZ del gel de poliacrilamida, se incubó entre 1 y 3 h en una solución de sulfito de sodio (Na_2SO_3) a una concentración final de 70 mM, la solución

se mezcló cada 10-15 min. Seguidamente, se reemplazó la solución de Na_2SO_3 por una solución de isopropanol 30% (v/v). La solución de isopropanol se renovó 2-3 veces para asegurar la retirada del Na_2SO_3, que puede interferir en la tinción de proteínas. Finalmente, para visualizar las proteínas, el gel de poliacrilamida se tiñó con Azul de Coomassie. Para ello, el gel de poliacrilamida se incubó en una solución de Coomassie (Tabla 4.6.) durante 15 min. Posteriormente, se lavó con una solución de desteñido (Tabla 4.6.) durante 2 h y, por último, con H_2O destilada. Para el revelado de los geles se utilizó el sistema GelDoc XR (Bio-Rad) y el software de análisis de imagen Quantity One (Bio-Rad) e ImageLab (Bio-Rad) (Tabla 4.10.).

4.4. Métodos de biología molecular

4.4.1. Obtención de ADN total de *B. diazoefficiens*

4.4.1.1. Lisados por calor

Para la selección por PCR de los diferentes candidatos, tanto de cepas de *E. coli* como de *B. diazoefficiens,* se obtuvieron preparaciones de ADN total mediante lisados celulares por calor. Para ello, se usó el procedimiento que se describe a continuación, desarrollado en nuestro grupo de investigación:

1.- Preparar tubos de microcentrífuga con 200 µl de H_2O ultrapura. Resuspender una cantidad pequeña de células procedentes de cultivos sólidos o 25 µl de cultivo líquido en fase estacionaria de crecimiento.

2.- Hervir cada tubo durante 10 min a 100℃.

Antes de su empleo, los extractos celulares obtenidos se han de enfriar en hielo. Se utiliza un volumen de lisado celular equivalente al 10% de la mezcla de reacción de PCR. Las muestras se pueden preservar durante una semana a 4℃.

4.4.1.2. Método comercial

Para obtener mayor pureza de ADN total de *B. diazoefficiens* de la obtenida por los lisados por calor, se utilizó el kit de Realpure® Spin Plantas y Hongos (Real). El protocolo empleado fue el descrito por el fabricante. Todas las soluciones usadas están incluidas en el kit.

1.- Centrifugar a 8.000 × *g* (10 min, 4℃) 50 ml de cultivo de *B. diazoefficiens* crecido hasta fase exponencial. Eliminar el sobrenadante.

2.- Resuspender el sedimento celular en 1 ml de tampón de extracción, adicionar 200 µl de solución PVP y homogeneizar con vórtex.

3.- Añadir 200 µl de solución SDS y homogeneizar con vórtex. Centrifugar la muestra a 13.000 r.p.m. durante 5 min y transferir el sobrenadante a un nuevo tubo de microcentrífuga.

4.- Adicionar 200 µl de solución de precipitado e incubar durante 3 min en hielo. Centrifugar la muestra a 13.000 r.p.m. durante 5 min y pasar el sobrenadante a un tubo nuevo de microcentrífuga.

5.- Añadir un volumen de solución de lisis con proteinasa K, mezclar e incubar a 70℃ durante 10 min. Adicionar 300 µl de isopropanol y transferir la mezcla a una columna proporcionada por el kit. Centrifugar a 12.000 r.p.m. y descartar el eluyente.

6.- Adicionar 500 µl de solución de desinhibición, centrifugar y descartar el líquido eluyente. Lavar dos veces con 500 µl de solución de lavado. Por último, centrifugar la columna sin añadir nada a 13.000 r.p.m. durante 2 min.

7.- Eluir el ADN con 50 µl de H_2O ultrapura precalentada a 70℃, dejar que se hidrate la columna durante 1 min y después centrifugar a 13.000 r.p.m. durante 1 min. Finalmente, se cuantifica la concentración de ADN con un Nanodrop (apartado 4.4.8.).

4.4.2. Obtención de ADN plasmídico de *E. coli* (“minipreps”)

4.4.2.1. Método TENS

La extracción de ADN plasmídico de *E. coli* para la selección de candidatos correctos durante la clonación de fragmentos de ADN en plásmidos, se llevó a cabo como se describe a continuación:

1.- Preparar 3 ml de medio LB suplementado con los antibióticos adecuados. A continuación, inocular el medio anterior con la cepa de *E. coli*. Incubar a 37℃ durante una noche.

2.- Centrifugar el cultivo celular a 13.000 r.p.m. durante 5 min. Eliminar el sobrenadante.

3.- Resuspender el sedimento celular en 300 µl de solución TENS (Tabla 4.6.), adicionar 150 µl de ácido acético 3 M a pH 5,2 (solución de neutralizado; Tabla 4.6.) e inmediatamente agitar en vórtex durante 5 s.

4.- Centrifugar la muestra a 13.000 r.p.m. durante 10 min y pasar el sobrenadante a un nuevo tubo de microcentrífuga.

5.- Adicionar 1 ml de etanol absoluto frío, mezclar y centrifugar durante 5 min. Descartar el sobrenadante y lavar con 200 µl de etanol al 70% (frío).

6.- Secar el sedimento obtenido durante 10 min al vacío. Resuspender en 100 µl de H_2O ultrapura y añadir 1 µl de solución ARNasa (Tabla 4.6.).

Estas preparaciones de ADN se utilizaron para digestiones de ADN por endonucleasas de restricción y en las reacciones de amplificación por PCR. La muestra que se añadió correspondía al 10% del volumen final de la reacción.

4.4.2.2. Método comercial

Se requiere mayor pureza en las preparaciones de ADN plasmídico cuando éste se destina a secuenciación o se utiliza para clonajes posteriores, también cuando el método TENS no permite obtener el ADN suficientemente puro o a concentraciones necesarias para la selección de candidatos en determinados clonajes. En estos casos se emplea el método comercial QIAprep® Spin Miniprep Kit (Qiagen), siguiendo las instrucciones de la casa comercial. Las soluciones utilizadas vienen incluidas en el kit.

1.- Inocular, con la cepa de *E. coli*, 3 ml de medio LB suplementado con los correspondientes antibióticos. Incubar a 37°C durante una noche.

2.- Centrifugar el cultivo celular a 13.000 r.p.m. durante 1 min. Eliminar el sobrenadante.

3.- Resuspender el pellet en 250 µl de solución P1. Seguidamente, adicionar 250 µl de solución P2, y, por último, 350 µl de solución N3. Mezclar por inversión.

4.- Centrifugar a 13.000 r.p.m. durante 10 min. Pasar el sobrenadante a una columna proporcionada por el kit. Centrifugar a 13.000 r.p.m. durante 1 min y descartar el líquido eluyente.

5.- Añadir 500 µl de solución PB a la columna. Centrifugar a 13.000 r.p.m durante 1 min y eliminar el eluyente. Adicionar 750 µl de solución PE a la columna. Centrifugar a 13.000 r.p.m. durante 1 min y descartar el eluyente. Por último, centrifugar la columna sin añadir nada a 13.000 r.p.m. durante 1 min para eliminar los restos de etanol.

6.- Hidratar el ADN con 50 µl de H_2O ultrapura durante 1 min. Eluir el ADN, en un tubo de microcentrífuga nuevo, por centrifugación a 13.000 r.p.m. durante 1 min.

7.- Cuantificar la concentración de ADN con el Nanodrop (apartado 4.4.8.).

4.4.3. Obtención de ADN plasmídico de *B. diazoefficiens*

Para comprobar la presencia de plásmidos que se introducen en *B. diazoefficiens* mediante conjugación con *E. coli*, se aisló ADN plasmídico según el siguiente protocolo:

1.- Preparar matraces con 20 ml de medio PSY suplementado con los antibióticos adecuados. Inocular dicho medio con la cepa de *B. diazoefficiens*. Incubar a 30°C hasta que alcance la fase exponencial tardía de crecimiento.

2.- Centrifugar 5 ml de cultivo celular y descartar el sobrenadante.

3.- Resuspender el sedimento celular en 500 µl de solución de lavado (Tabla 4.6.). Lavar dos veces con esta solución.

4.- Resuspender el sedimento en 200 µl de solución MAXI (Tabla 4.6.). Añadir 400 µl de solución de lisis (Tabla 4.6.). Mezclar por inversión de los tubos. Esperar entre 10 y 15 min hasta que se alcance una lisis adecuada.

5.- Adicionar 200 µl de solución de neutralizado (Tabla 4.6.) y mezclar por inversión. Incubar en hielo durante 15 min. Centrifugar a 13.000 r.p.m. durante 3 min, pasar el sobrenadante a un tubo nuevo y añadir un volumen de isopropanol. Centrifugar a 13.000 r.p.m. durante 15 min y eliminar el sobrenadante.

6.- Añadir 1 ml de etanol al 70%. Centrifugar a 14.000 r.p.m. durante 2 min. Descartar el sobrenadante y secar el precipitado al vacío.

7.- Resuspender el precipitado en 20 µl de H_2O ultrapura.

4.4.4. Aislamiento de ARN total de nódulos de soja

La extracción de ARN total de los nódulos se llevó a cabo siguiendo la metodología descrita por Pessi et al. (2007):

Preparación previa:

- El día anterior del aislamiento, preparar un tubo de centrífuga (50 ml) RNasa free (Labcon) con bolas de carburo de wolframio (3 mm; Quiagen) sumergidas en ∼25 ml de cloroformo.

- Colocar tubos de microcentrígufa (1,5 ml) en una gradilla usando pinzas previamente lavadas con cloroformo, y colocar la gradilla a -20℃ para preenfriar los tubos.

- Para cada extracción de ARN, preparar tubos de centrífuga (15 ml) RNasa free (Labcon) con las siguientes soluciones:

F1.1: 160 µl SDS 10%; 2 ml tampón A; 3,5 ml fenol ácido

F1.2: 3,5 ml fenol ácido

F2: 3 ml (fenol/cloroformo/alcohol isoamílico)

F3: 2,5 ml cloroformo

F4**:** tubo vacío

Mantener todos los tubos, exepto el F1.1, en hielo.

1.- Coger una bola de carburo de wolframio con unas pinzas previamente lavadas en cloroformo. Secar la bola al aire (∼5-10 s) e introducirla en un tubo de microcentrígufa (2 ml). Una vez preparados los tubos necesarios, conservarlos en hielo.

Preparar 2 tubos de microcentrígufa (2 ml) para cada extracción de ARN.

2.- Transferir los nódulos (que estaban almacenados a -80℃) a los tubos de microcentrígufa (2 ml) con unas pinzas, lavadas previamente con cloroformo. En cada tubo de microcentrígufa, los nódulos (10 nódulos aproximadamente) deben ocupar un 1/4 del volumen del tubo. Cerrar los tubos, congelarlos rápidamente en nitrógeno líquido e introducirlos en los bloques del TissueLyzer Mixer Mill MM 301 (Retsch GmbH, Haan, Germany).

3.- Homogeneizar los nódulos en el TissueLyzer, a 30 Hercios durante 50 s (repetir este proceso tres veces). Congelar rápidamente los tubos en nitrógeno líquido entre cada pase por el TissueLyzer. El orden de los tubos debe invertirse en los bloques del TissueLyzer después del primer pase. Comprobar si el tejido nodular está suficientemente homogeneizado (color rosa-verdoso).

4.- Transferir los tubos, que contienen los nódulos lisados, a hielo. Sacar la bola de cada tubo con pinzas, previamente esterilizadas con cloroformo. Añadir 750 µl de tampón A (Tabla 4.6.) a cada tubo de microcentrígufa que contiene los nódulos lisados, cerrar los tubos e invertirlos con cuidado 3 veces. Verter la solución de los nódulos lisados de dos tubos de microcentrígufa a un tubo que contiene la solución F1.1 precalentada (65℃ durante 7-10 min).

5.- Agitar mediante vórtex 30 s, incubar 2 min a 65℃, agitar 1 min, incubar durante 5 min. Centrifugar la suspensión durante 5 min a 9.000 r.p.m. (4℃) y transferir la fase acuosa (superior) a un tubo con solución F1.2 (fenol ácido).

Este paso es importante para la separación del ARN en la fase acuosa y proteínas y ADN en la fase orgánica e interfase. Asegurarse que no se altera la interfase. Es preferible dejar parte de la fase acuosa en el tubo.

6.- Agitar mediante vórtex (30 s) y centrifugar la suspensión a 9.000 r.p.m durante 5 min a 4℃. Transferir con cuidado la fase acuosa a un tubo con solución F2 (fenol/cloroformo/alcohol isoamílico). Agitar mediante vórtex (30 s). Centrifugar la suspensión a 9.000 r.p.m durante 5 min a 4℃.

7.- Transferir con cuidado la fase acuosa a un tubo con solución F3 (cloroformo). Agitar mediante vórtex (30 s). Centrifugar la suspensión a 9.000 r.p.m durante 5 min a 4℃.

8.- Transferir con cuidado la fase acuosa (superior) a un tubo vacío (F4).

9.- Extraer 10 µl de ARN y mantener en hielo. Esta muestra de ARN se usará para comprobar la integridad del ARN en un gel de agarosa (2%).

10.- Adicionar el 10% de NaOAc 3 M (pH 5,5) y 2 volúmenes de etanol frío al 96% (almacenado a -20℃) a la muestra de ARN. Mezclar por inversión.

11.- Distribuir la muestra de ARN en tubos de microcentrígufa (1,5 ml) preenfriados a -20℃. Precipitar el ARN a -80℃ durante una noche.

Precipitación del ARN:

1.- Centrifugar los tubos de microcentrígufa (1,5 ml), que contienen la muestra de ARN, a 13.000 r.p.m. durante 30 min a 4℃.

2.- Descartar con cuidado el sobrenadante. Para lavar los pellets de ARN, añadir 1 ml de etanol al 80% (H_2O-DEPC) a cada tubo y centrifugar a 13.000 r.p.m. durante 15 min a 4℃.

3.- Eliminar con cuidado el etanol con una punta azul (de 1 ml). Tener cuidado de no eliminar el pellet blanco que contiene el ARN. Dar un centrifugado breve (spin) y eliminar el etanol residual con una punta amarilla (de 200 µl).

4.- Dejar los tubos abiertos para secar al aire los pellets de ARN durante ∼10 min.

Es necesario que el pellet esté completamente seco, de lo contrario podría contener etanol, que inhibe las reacciones enzimáticas posteriores. Sin embargo, el pellet no debe secarse en exceso, de lo contrario será difícil redisolverlo.

5.- Resuspender los pellets de ARN en 100 µl de H_2O libre de ARNasas (Sigma).

6.- Medir la concentración de ARN (sección 4.4.8.). Idealmente, la concentración de ARN que se debería obtener es > 1 µg/µl.

7.- Alicuotar las siguientes muestras de ARN para usos posteriores:

- Para electroforesis en gel de agarosa (2%): ∼1,5 µg de ARN total
- Para PCR control (-ADNasa): 500 ng de ARN total

4.4.5. Tratamiento con ADNasa

Para eliminar el ADN contaminante en las muestras de ARN, se llevó a cabo un tratamiento con ADNasa, según las instrucciones de la casa comercial:

1.- Preparar la mezcla de reacción:

- 10 µl de tampón de reacción 10×
- 2 µl de inhibidor de ARNasas (40 U/µl. Roche)

- 4 µl de ADNasa I (1 U/µl. Invitrogen)

- x µl de muestra de ARN (hasta 60 µg como máximo)

- Hasta 100 µl de H_2O ultrapura libre de ARNasas (Sigma)

2.- Incubar la reacción a 37ºC durante 1 h. Transferir al hielo para la posterior purificación de ARN.

4.4.5.1. Purificación de ARN

Las muestras de ARN se purificaron con el kit comercial RNeasy® Mini Kit (Quiagen). Se siguieron las intrucciones facilitadas por el fabricante. Las soluciones y las columnas usadas vienen incluidas en el kit.

Consideraciones previas:

- Añadir β-Mercaptoetanol al tampón RLT (10 µl β-Mercaptoetanol / 1 ml RLT) antes de su uso.

- Todos los pasos de centrifugación se realizan a temperatura ambiente.

- Dado que la capacidad máxima de unión de las columnas (Qiagen RNA easy columns) es de 100 µg de ARN, se recomienda no sobrecargar las columnas, ya que esto puede provocar la pérdida de ARN y afectar a la pureza de las muestras de ARN. Dependiendo de la cantidad de material de partida, se cargarán las soluciones de ARN en 2 columnas independientes (100 µg de ARN) o alternativamente se cargarán las muestras una después de otra en una única columna (<100 µg de ARN).

1.- Añadir 350 µl de tampón RLT a 100 µl de la reacción de digestión con ADNasa. Mezclar por pipeteo.

2.- Adicionar 250 µl de etanol (96-100%) a la solución de ARN. Mezclar por pipeteo.

3.- Transferir 700 µl de la mezcla anterior a una columna (Qiagen RNA easy column), colocada en un tubo de microcentrífuga de 2 ml. Cerrar el tubo y centrifugar durante 15 s a 13.000 r.p.m. Descartar el eluido.

4.- Transferir la columna a un tubo de microcentrífuga nuevo (2 ml). Añadir 500 µl de tampón RPE (contiene etanol) a la columna. Cerrar el tubo y centrifugar durante 15 s a 13.000 r.p.m. para lavar la columna. Eliminar el eluido.

5.- Adicionar otros 500 µl de tampón RPE a la columna. Cerrar el tubo y centrifugar durante 2 min a 13.000 r.p.m. para secar la membrana de gel de sílice de la columna.

6.- Para eliminar el etanol restante, se lleva a cabo un paso de centrifugación adicional. Colocar la columna en un tubo de microcentrífuga nuevo (2 ml). Centrifugar a 13.000 r.p.m. durante 1 min.

7.- Eluir el ARN de la columna, en un tubo de microcentrígufa nuevo, con 30 µl de H_2O ultrapura libre de ARNasas (Sigma). Cerrar el tubo y centrifugar durante 1 min a 13.000 r.p.m. Pipetear el eluido y cargar de nuevo sobre la columna. Centrifugar 1 min a 13.000 r.p.m. Este último paso permitirá obtener mayor cantidad de ARN de la columna.

8.- Desechar la columna y rápidamente colocar el tubo que contiene el ARN purificado en hielo.

9.- Cuantificar la concentración de ARN en el Nanodrop (apartado 4.4.8.).

10.- Alicuotar las siguientes muestras de ARN para usos posteriores:

- Para electroforesis en gel de agarosa (2%): ~1,5 µg de ARN total
- Para PCR control (+ADNasa): 500 ng de ARN total

11.- Alicuotar las muestras de ARN (con 20 µg de ARN por alícuota) para evitar ciclos de congelación y descongelación. Congelar las alícuotas con nitrógeno líquido y conservarlas a -80°C.

12.- Comprobar la integridad del ARN mediante electroforesis en gel de agarosa (2%) (sección 4.4.12.).

13.- Comprobar la presencia de ADN en las muestras de ARN mediante una reacción de PCR con ADN polimerasa Dream Taq. La PCR se realiza igual que una PCR de rutina (apartado 4.4.10.), sustituyendo el ADN molde por ARN (500 ng). Como control positivo de la reacción se emplea ADN genómico de *B. diazoefficiens* 110*spc*4 (50 ng) y como control negativo H_2O ultrapura. Los oligonucleótidos usados para esta comprobación fueron fixN4_For y fixN4_Rev (Tabla 4.3.). La ausencia de ADN en las muestras de ARN debe ser total.

4.4.6. Reverso transcripción

El ADN complementario (ADNc) se obtuvo desde ARN total mediante reacción de reverso transcripción. Para esta reacción se utilizó la enzima SuperScript® II Reverse Transcriptase (200 U/µl. Invitrogen). Las reacciones de reverso transcripción se llevaron a cabo en un termociclador de tapa calefactable Mastercycler 5333 (Eppendorf). La metodología empleada, bien establecida en nuestro grupo de investigación, fue la siguiente:

1.- La mezcla de reacción, que se prepara en un tubo de PCR, contiene: 2 µg de ARN total, 4 µl del oligonucleótido aleatorio (75 ng/µl), 5 µl de dNTPs (10 mM) y hasta 37 µl de H_2O ultrapura libre de ARNasas (Sigma). Mezclar por pipeteo. Incubar a 65℃ durante 5 min. Transferir a hielo.

2.- Adicionar a la mezcla de reacción anterior: 12 µl de tampón de reacción 5×, 6 µl de solución de DTT 0,1 M y 2 µl de inhibidor de ARNasas (40 U/µl. Roche). Mezclar por pipeteo. Incubar a 25℃ durante 2 min.

3.- Añadir a la mezcla de reacción anterior 3 µl de reverso transcriptasa. Mezclar por pipeteo. Incubar a 25℃ durante 10 min, 42℃ durante 50 min y 70℃ durante 15 min.

4.- Eliminar el ARN de la muestra por lisis alcalina adicionando por reacción 20 µl de NaOH 1 M. Mezclar por pipeteo e incubar a 65℃ durante 30 min. Seguidamente, neutralizar el pH añadiendo 20 µl de HCl 1 M por reacción y mezclar por pipeteo. Purificar el ADNc de igual manera que se purifican los productos de PCR (sección 4.4.13.). Adicionar alícuotas de 5 µl de ácido acético 3 M (pH 5,2), hasta que el indicador de pH del tampón PB vire a amarillo.

5.- Cuantificar la concentración de ADN con el Nanodrop (apartado 4.4.8.).

4.4.7. PCR cuantitativa a tiempo real (qRT-PCR)

Mediante la técnica de qRT-PCR se amplifica el ADNc (obtenido por reverso transcripción del ARN, sección 4.4.6.) y, simultáneamente, se cuantifica de forma relativa el producto de la amplificación. Esta técnica se llevó a cabo en el sistema iQTM5 Optical System (Bio-Rad, Foster City, CA, United States).

Las reacciones de qRT-PCR se prepararon en placas de 96 pocillos de 0,1 ml de volumen, siguiendo las especificaciones de la iQ™ SYBR Green Supermix. Cada pocillo contenía la mezcla para una reacción. Cada reacción se ensayó por triplicado en un volumen total de 19 µl, que contenía:

- 9,5 µl iQ™ SYBR Green Supermix (Bio-Rad)

- 4,5 µl de mezcla de oligonucleótidos For y Rev (2 µM de concentración final de cada oligonucleótido)

- 5 µl de ADNc a 2 ng/µl (10 ng total), 0,2 ng/µl (1 ng total) ó 0,02 ng/µl (0,1 ng total)

El programa de PCR incluía una desnaturalización inicial y activación de la ADN polimerasa durante 5 min a 95℃, seguido de 40 ciclos de 15 s a 95℃, 45 s a 60℃ y 45 s a 72℃. La especificidad de la amplificación se verificó mediante el análisis de las curvas de melting (70℃ durante 10 min).

Los cambios relativos en la expresión génica se calcularon según la metodología de Pfaffl (2001). Los niveles de expresión de los genes de interés se normalizaron frente a la expresión del gen constitutivo *16S rRNA* (Torres et al., 2017).

4.4.8. Determinación de la concentración de ADN y ARN

La concentración de ADN y ARN se estimó con el equipo NanoDrop ND-1000 (Thermo) mediante espectrofotometría, determinando la absorbancia a 260 nm de soluciones acuosas. En primer lugar, se elige el tipo de ácido nucleico que se va a medir, ARN o ADN de cadena doble o sencilla. Posteriormente, se limpia el pedestal y se deposita sobre éste una gota de H_2O ultrapura para ajustar el equipo. Seguidamente, se realiza el blanco colocando sobre el pedestal una gota de entre 1 y 2 µl de la solución donde esté diluido el ácido nucleico de la muestra y se selecciona el botón que corresponde al blanco. Una vez obtenida la línea base, se deposita sobre el pedestal de 1 a 2 µl de muestra y se pulsa el botón de medida. Después de que el equipo realice la medida, se obtiene el espectro de absorbancia a 260 y 280 nm (A_{260} y A_{280}), junto a los datos de concentración en ng/µl y los ratios 260/280 y 260/230. Estos ratios indican el grado de pureza de la muestra. El ratio 260/280 deber ser ∼1,8 en muestras de ADN y ∼2 en muestras de ARN, si son inferiores indican una posible contaminación por proteínas o

disolventes orgánicos. El ratio 260/230 debe estar comprendido entre 1,8 y 2,2, valores que no estén en este intervalo indican la presencia de contaminantes co-purificados con la muestra.

4.4.9. Digestión de ADN con endonucleasas de restricción

En el proceso de clonaje de fragmentos de ADN en vectores y verificación de las diferentes construcciones, es necesario realizar digestiones de ADN con endonucleasas de restricción. El perfil de digestión obtenido se compara con el perfil teórico de clonaje, el cual se simula con el software Clone Manager.

Para las digestiones de ADN se utilizaron las enzimas endonucleasas de restricción FastDigest (Thermo), siguiendo las especificaciones del fabricante.

La reacción de restricción se preparó en tubos de microcentrífuga con hasta 1 µg de ADN plasmídico ó 0,2 µg de ADN de PCR, 1 µl de tampón de reacción, 0,5 µl de endonucleasa y H_2O ultrapura hasta un volumen final de 10 µl. Si se realizan reacciones con varias endonucleasas, el volumen de las enzimas se ajusta para que no supere el 10% del volumen de la reacción. Las reacciones se incuban a 37℃ durante el tiempo requerido. Cuando el fragmento digerido se emplea para su clonación, las endonucleasas deben inactivarse térmicamente (Tabla 4.7.).

La siguiente tabla (Tabla 4.7.) incluye todas las endonucleasas utilizadas durante este trabajo junto con sus características más importantes.

Tabla 4.7. Endonucleasas de restricción.

Nombre	Diana	Tiempo de reacción (min)		Inactivación
		Plásmidos 1 µg	PCR 0,2 µg	
***Bam*HI**	G/GATCC	5	5	5 min/80℃
***Eco*RI**	G/AATTC	5	20	5 min/80℃
***Eco*RV**	GAT/ATC	5	5	---
***Hin*dIII**	A/AGCTT	5	20	10 min/80℃
***Nhe*I**	G/CTAGC	15	5	5 min/65℃
***Sal*I**	G/TCGAC	5	≥60	10 min/65℃
***Xba*I**	T/CTAGA	5	5	20 min/65℃
***Xho*I**	C/TCGAG	5	5	5 min/80℃

Se muestra la secuencia diana indicando el sitio de corte en la hebra 5' - 3'.

4.4.10. Amplificación de ADN por reacción en cadena de la polimerasa (PCR)

Mediante la técnica de PCR se amplificó ADN, el cual su usó con varios objetivos:

- Obtención de fragmentos de ADN para su clonación en vectores.
- Verificación de construcciones de plásmidos.
- Comprobación de cepas recombinantes.
- Comprobación de ausencia de contaminación de ADN en muestras de ARN.
- Obtención de mutaciones puntuales dirigidas.

En función de la finalidad con la que se lleva a cabo la amplificación de ADN, se usaron ADN polimerasas diferentes:

- Dream Taq (Thermo): para PCR de rutina de comprobación de clones, verificación de especificidad de oligonucleótidos y comprobación de contaminación de ADN en muestras de ARN.
- Phusion (Thermo): para reacciones de PCR en las que se precisa máxima fidelidad de la secuencia de ADN amplificada y amplicones de mayor tamaño, que se emplearán para su clonaje en vectores.
- *Pfu* (Thermo): para determinados casos en los que no se obtiene el resultado deseado con la Phusion ADN polimerasa, en sustitución de ésta.

La composición de la mezcla de reacción de PCR (para una reacción de 20 µl) para cada una de las ADN polimerasas, se muestra en la tabla siguiente (Tabla 4.8.). La composición de las diferentes reacciones de PCR se calculó siguiendo las especificaciones de cada polimerasa.

Tabla 4.8. Mezclas de reacción de PCR para Dream Taq, Phusion y *Pfu* ADN polimerasas.

Componente	**Dream Taq**	**Phusion**	***Pfu***
Tampón	2 µl	4 µl	2 µl
dNTPs (10 mM cada uno)	0,4 µl	0,4 µl	0,4 µl
Oligonucleótido For (10 µM)	1,6 µl	1,6 µl	2 µl
Oligonucleótido Rev (10 µM)	1,6 µl	1,6 µl	2 µl
ADN polimerasa (5 U/µl)	0,1 µl	0,1 µl	0,1 µl
ADN molde	50-100 ng	20 ng	100 ng
DMSO (opcional)	1 µl	–	–
H_2O ultrapura	Hasta 20 µl	Hasta 20 µl	Hasta 20 µl

Las reacciones de PCR se llevaron a cabo en termocicladores de tapa calefactable Mastercycler 5333 (Eppendorf), GeneAmp 2400 (PerkinElmer) y Px2 (Thermo). El programa de PCR se diseñó siguiendo las especificaciones cada polimerasa. En la Tabla 4.9. se muestran los programas de PCR adecuados para cada polimerasa:

Tabla 4.9. Programas de PCR para Dream Taq, Phusion y *Pfu* ADN polimerasas.

Etapa	**Ciclos**	**Dream Taq**	**Phusion**	***Pfu***
Desnaturalización	**1**	95℃ – 3 min	98℃ – 5 min	95℃ – 3 min
Desnaturalización	**30**	95℃ – 30 s	98℃ – 10 s	95℃ – 30 s
Anillamiento		(Tm - 5℃) – 30 s	Tm – 30 s	(Tm - 5℃) – 30 s
Extensión		72℃ – 1 min/kb	72℃ – 30 s/kb	72℃ – 2 min/kb
Extensión	**1**	72℃ – 10 min	72℃ – 10 min	72℃ – 10 min
Almacenamiento	**∞**	4℃	4℃	4℃

4.4.11. Mutación puntual dirigida (QuickChange™)

La técnica QuickChange Site-Directed Mutagenesis (Stratagene) se empleó para introducir una mutación puntual mediante intercambio de una lisina (lisina-52, K52) por alanina en el triplete AAG del gen *bjgb* del plásmido molde pDB4024 (Tabla 4.2.).

Para ello:

1. Diseñar una pareja de oligonucleótidos complementarios antiparalelos [blr2807(K52A)_For y blr2807(K52A)_Rev; Tabla 4.3.], que contengan en su zona central el nucleótido que se quiere sustituir.
2. Amplificar mediante PCR el ADN del plásmido en estado circular que contiene la secuencia en la que se desea efectuar la mutación. Para la reacción de PCR se usó la *Pfu* ADN polimerasa (sección 4.4.10.).
3. Digerir enzimáticamente los productos de PCR con *Dpn*I (1 µl, 10 U/µl, New England Biolabs®). Esta enzima sólo digiere el ADN sintetizado por *E. coli* y no el mutagenizado sintetizado de *novo* en la reacción de PCR.
4. Verificar por electroforesis en gel de agarosa (apartado 4.4.12.) utilizando 5 µl de los amplicones digeridos y no digeridos con *Dpn*I.
5. Transformar células competentes de *E. coli* DH5α (sección 4.4.16.2.) con 5 µl de ADN digerido y sembrar en placas de LB suplementado con los antibióticos adecuados.
6. Seleccionar colonias, aislar su ADN plasmídico y comprobar mediante secuenciación (apartados 4.4.2. y 4.4.14., respectivamente) si la mutación puntual dirigida está presente. Para la secuenciación se emplearon oligonucleótidos específicos (M13_For y M13_Rev; Tabla 4.3.). Se descartaron posibles mutaciones aleatorias no deseadas.
7. Después de la secuenciación, se escogió un plásmido con la mutación puntual deseada (pDB4025; Tabla 4.2.), el cual se utilizó como base para experimentos posteriores.

4.4.12. Electroforesis de ADN y ARN en geles de agarosa

Para la preparación y realización de electroforesis en geles de agarosa se siguió el protocolo descrito en Sambrook y Russell (2001).

Para separar y visualizar fragmentos de ADN procedentes de PCR, miniprep o digestión, se utilizó la electroforesis horizontal en geles de agarosa preparados en TBE 0,5× (Tabla 4.6.). La concentración de agarosa fue del 0,7% para electroforesis de rutina o 1% para diferenciar fragmentos inferiores a 500 pb. El sistema empleado fue Mini-Sub Cell GT (Bio-Rad) con TBE 0,5× (Tabla 4.6.) como tampón de desarrollo para la realización de la electroforesis. Las muestras se mezclaron con tampón de carga 6× (Tabla 4.6.) y, a continuación, se cargaron en el gel de agarosa. La electroforesis se desarrolló a 100 V, hasta que el frente alcanzó el último cuarto de la longitud del gel.

Para comprobar la integridad de muestras de ARN total se utilizó el mismo tipo de electroforesis en geles de agarosa al 2% en TAE 1× (preparado con H_2O destilada-DEPC) (Tabla 4.6.). Las muestras de ARN se mezclaron con el mismo tampón de carga 6× (Tabla 4.6.) empleado para las muestras de ADN y, seguidamente, se cargaron en el gel de agarosa. Se usó TAE 1× (Tabla 4.6.) como tampón de desarrollo. La electroforesis se desarrolló a 80 V durante 30-45 min.

Para visualizar las muestras de ADN o ARN, el tampón de carga contenía GelRed (Biotium) al 2%. El GelRed es un fluoróforo intercalante de ácidos nucleicos que emite luz a 605 nm cuando está unido a los ácidos nucleicos y se excita por luz ultravioleta a 250 nm. El revelado de los geles se realizó en el sistema GelDoc XR (Bio-Rad) y el software de análisis de imagen utilizado fue Quantity One (Bio-Rad) e ImageLab (Bio-Rad) (Tabla 4.10.).

4.4.13. Purificación de fragmentos de PCR

Cuando el fragmento de ADN procedente de una PCR se va a digerir con endonucleasas de restricción o clonar directamente en un vector, es preciso purificar el ADN para eliminar restos de tampón, oligonucleótidos, dNTPs o el ADN molde de la reacción de PCR.

Si se obtiene un único producto como resultado de la reacción de PCR, éste se puede purificar empleando el kit QIAquick PCR Purification (Qiagen). Se siguen las especificaciones del fabricante y las soluciones usadas vienen incluidas en el kit.

1.- Añadir 5 volúmenes de tampón PB al producto de PCR, mezclar y verificar que la mezcla permanece amarilla, debido a un indicador de pH que contiene el tampón.

2.- Verter la mezcla en una columna proporcionada por el kit y centrifugar a 13.000 r.p.m. durante 1 min. Descartar el eluyente.

3.- Lavar la columna con 750 µl de tampón PE, centrifugar a 13.000 r.p.m. durante 1 min y eliminar el eluyente. Centrifugar de nuevo la columna a 13.000 r.p.m. durante 1 min para eliminar restos de etanol.

4.- Añadir 30 µl de tampón EB o H_2O ultrapura, dejar hidratar el ADN de la columna durante 1 min. Eluir el producto, en un nuevo tubo de microcentrífuga, por centrifugación a 13.000 r.p.m. durante 1 min.

5.- Determinar la concentración de ADN con el Nanodrop (sección 4.4.8.).

4.4.14. Secuenciación de ADN

Para la comprobación del correcto clonaje o mutagénesis en los diferentes plásmidos, se secuenció la región de interés de éstos por el método Sanger. Esta técnica se llevó a cabo en el Instituto de Parasitología y Biomedicina López Neyra (Granada). Las mezclas de secuenciación se prepararon siguiendo las instrucciones del servicio. Para ello, en un tubo de microcentrífuga de 500 µl se añadieron entre 400 y 800 ng de ADN plasmídico, o entre 10 y 80 ng de producto de PCR, 6,4 pmoles de un único oligonucleótido desde el que se inicia la lectura de secuenciación y se completó hasta 12 µl con H_2O ultrapura. Los resultados recibidos del servicio de secuenciación se analizaron con programas informáticos como Clone Manager.

4.4.15. Ligación de fragmentos de restricción en vectores de clonación

4.4.15.1. Ligación en vectores de clonación

Para la ligación entre un fragmento de ADN y un vector, ambos digeridos con enzimas de restricción compatibles, se usó una proporción de vector:inserto de al menos 1:3 (moles). La suma de la cantidad de ADN vector y la cantidad de ADN inserto (x + y)

debe ser de al menos 100 ng. La reacción de ligación se preparó según un protocolo modificado al descrito en Sambrook y Russell (2001). Se añade en un tubo de microcentrígufa:

- x µl de ADN vector
- y µl de ADN inserto
- 1 µl de ligasa (T4 DNA ligase, 1 U/µl. Roche)
- 1 µl de tampón de ligasa 10×
- H_2O ultrapura hasta un volumen final de 10 µl

Una vez que se prepara la reacción, se mezcla suavemente y se centrifuga (1 pulso). Por último, se incuba a temperatura ambiente durante 1 h o a 4℃ durante toda la noche.

4.4.15.2. Desfosforilación de vectores de clonación

El tratamiento con fosfatasa alcalina se empleó para desfosforilar un vector digerido, con el fin de impedir la religación y la ligación entre dos moléculas del vector digerido. Para ello, se siguió una metodología adaptada a la descrita en Sambrook y Russell (2001). Con el vector digerido previamente (apartado 4.4.9.) con las endonucleasas de restricción apropiadas, se prepara la reacción de desfosforilación:

- Hasta 1 µg de vector digerido
- 1 µl de tampón de la fosfatasa alcalina 10×
- 0,5 µl de fosfatasa alcalina de camarón (Shrimp Alkaline Phosphatase, SAP, 1 U/µl. Thermo)
- H_2O ultrapura hasta un volumen final de 10 µl

Seguidamente, se mezcla suavemente y se centrifuga (1 pulso). Se incuba la reacción a 37℃ durante 30 min para extremos 5’ protuberantes o 60 min para extremos 3’ protuberantes o romos. Finalmente, se detiene la reacción por inactivación térmica, incubando durante 15 min a 65℃.

4.4.16. Transferencia de ADN a células de *E. coli*

4.4.16.1. Preparación de células competentes con cloruro de rubidio (RbCl)

La células competentes de *E. coli* se prepararon siguiendo la técnica descrita por Hanahan (1983), como se indica a continuación:

1.- Inocular un matraz de 500 ml, que contiene 100 ml de medio LB precalentado a 37℃, con 5 ml de un cultivo de células de *E. coli* crecido durante la noche anterior. Incubar a 37℃, con agitación (170 r.p.m.), hasta que el cultivo alcance una DO_{600nm} de 0,4-0,6 (fase logarítmica). Colocar el cultivo en hielo durante 15 min para detener el crecimiento celular.

2.- Centrifugar el cultivo celular en tubos estériles a 8.000 × *g* (10 min, 4℃). Eliminar el sobrenadante.

3.- Resuspender suavemente el sedimento de células en 30 ml de solución TFB1 (Tabla 4.6.) estéril y fría a 4℃. Incubar la suspensión celular en hielo durante 15 min. Centrifugar a 8.000 × *g* (10 min, 4℃). Desechar el sobrenadante.

4.- Resuspender el sedimento celular obtenido en 4 ml de solución TFB2 (Tabla 4.6.) fría. Alicuotar en tubos de microcentrífuga preenfriados a 4℃, añadir 100 µl de suspensión de células por tubo. Conservar las alícuotas a -80℃.

Las células competentes son muy delicadas, por ello hay que tener en cuenta una serie de precauciones para evitar la lisis celular: todos los pasos se realizan en frío y sin estrés mecánico, se debe pipetear con suavidad y sin utilizar el vórtex.

4.4.16.2. Transformación de células competentes de *E. coli*

La transformación de células competentes con ADN plasmídico se realizó siguiendo la metodología descrita por Rodríguez y Tait (1983), modificada como se detalla:

1.- Descongelar en hielo alícuotas de 100 µl de células competentes (10 a 15 min).

2.- Añadir 50-100 ng de ADN de ligación o 25 ng de plásmido puro con el que se vaya a transformar. Mezclar suavemente e incubar en hielo durante 30 min.

3.- Calentar a 42℃ (choque térmico) durante 45 s. Incubar en hielo otros 5 min.

4.- Adicionar 4 volúmenes de medio LB e incubar a 37°C con agitación (170 r.p.m.) durante 1 h. Preparar placas Petri con medio LB suplementado con los antibióticos convenientes. Si se realiza una selección por color se añade al medio 40 µl de 5-Bromo-4-cloro-3-indolil-β-D-galactopiranósido (X-Gal) a una concentración de 20 mg/ml, diluido en dimetilformamida, y 4 µl de 1-Isopropil-β-D-1-tiogalactopiranósido (IPTG) a una concentración de 200 mg/ml.

5.- Sembrar las placas con las células transformadas e incubar a 37°C durante una noche.

4.4.17. Transferencia de ADN a células de *B. diazoefficiens* mediante conjugación

La transferencia de ADN a células de *B. diazoefficiens* se llevó a cabo mediante conjugación biparental desde la cepa donadora de *E. coli* S17.1, que contiene el plásmido que se pretende transferir, siguiendo la metodología que se describe a continuación, bien establecida en nuestro grupo de investigación:

1.- Cultivar la cepa de *B. diazoefficiens* (cepa receptora) en un matraz con 50 ml de PSY suplementado con los correspondientes antibióticos hasta que alcance la fase exponencial tardía de crecimiento (4-5 días).

Preparar un cultivo de la cepa donadora (*E. coli* S17.1) en un tubo con 3 ml de medio LB con los antibióticos adecuados, incubar durante una noche.

2.- Previamente a la conjugación, refrescar el cultivo de la cepa donadora en un tubo con 3 ml de LB con los antibióticos convenientes, para ello, se inocula dicho medio con 150 µl del cultivo preparado el día anterior. Cultivar hasta alcanzar la fase logarítmica (DO_{600nm} entre 0,6-0,8), aproximadamente 3 h después.

3.- Centrifugar 5 ml de la cepa receptora (*B. diazoefficiens*) y 1 ml de la cepa donadora (*E. coli* S17.1). Descartar el sobrenadante. Lavar dos veces con 1 ml de medio PSY.

4.- Resuspender el sedimento de células en 100 µl de PSY. La suspensión resultante se coloca en el centro de la placa de PSY sin antibióticos. Una vez que la gota se haya secado, incubar durante 48 h a 30°C.

5.- Preparar dos placas de PSY con los antibióticos correspondientes para el cribado de los transconjugantes. Para evitar el crecimiento de las células de *E. coli*, adicionar al medio PSY de las placas cloranfenicol 20 µg/ml.
6.- Con ayuda del asa de siembra, recoger la masa celular de la gota y resuspender en 1 ml PSY sin antibióticos, dentro de un tubo de microcentrífuga.
7.- Sembrar 30 y 200 µl de la suspensión celular obtenida mediante conjugación en cada una de las placas de PSY con los antibióticos adecuados. Incubar a 30°C hasta que aparezcan colonias (8-10 días).
8.- Una vez que se obtienen colonias, se siembran en estría en placas con los mismos antibióticos para su comprobación posterior.

4.5. Sobreexpresión y purificación de las proteínas Bjgb-His_6 y Flp-His_6

La expresión y posterior purificación de las proteínas Bjgb y Flp se llevaron a cabo a partir de los plásmidos pDB4008 y pDB4010 (Tabla 4.2.), respectivamente. En cada uno de estos plásmidos, la región codificante del gen *bjgb* o *flp* está fusionada en fase en su extremo 5' o 3', respectivamente, a la secuencia de la etiqueta de seis histidinas (procedente de uno de los oligonucleótidos empleados para la amplificación del gen de interés o del vector, respectivamente), que posibilita su purificación posterior mediante cromatografía de afinidad, como proteína recombinante Bjgb-His_6 o Flp-His_6. En la cromatografía de afinidad, la proteína queda retenida a la columna a través de la formación de un enlace de coordinación entre los iones metálicos níquel (inmovilizados en la columna) y los residuos de histidina de la proteína, posteriormente, la proteína se eluye como proteína pura.

El plásmido de expresión empleado, pET24a(+), permite la sobreexpresión de la proteína bajo el control del promotor de T7 y se induce en presencia de IPTG.

4.5.1. Inducción de las células para purificación

Para la producción de las proteínas Bjgb y Flp, se utilizó la cepa de *E. coli* BL21 (DE3) (Tabla 4.1.), la cual contiene el gen de la ARN polimerasa T7 del fago λDE3. Las células competentes de *E. coli* BL21 (DE3) se transformaron (apartado 4.4.16.2.) con el plásmido pDB4008 o pDB4010 (Tabla 4.2.). A partir de las placas sembradas con células de esta cepa de *E. coli* transformadas, se prepararon criotubos que contenían alícuotas

de cultivo en fase logarítmica de crecimiento y glicerol para su conservación a -20℃ (sección 4.2.1.). El protocolo para la inducción de las células para purificación se ha desarrollado en esta Tesis Doctoral y consiste en:

1.- Preparar placas Petri con medio sólido LB suplementado con antibiótico. Sembrar con la cepa adecuada de *E. coli* BL21 (DE3), que contiene el plásmido de expresión pDB4008 o pDB4010. Incubar las células a 37℃ durante una noche.

2.- Desde los cultivos sólidos anteriores, inocular un tubo de 20 ml que contiene 10 ml de LB líquido, suplementado con antibiótico, con una sola colonia aislada. Incubar las células aeróbicamente a 37℃ durante una noche en un agitador orbital (170 r.p.m).

3.- Desde los cultivos líquidos anteriores, inocular un matraz de 250 ml que contiene 100 ml de LB líquido, suplementado con el antibiótico conveniente, con 2 ml del cultivo preparado el día anterior. Incubar las células aeróbicamente a 37℃ durante una noche en un agitador orbital (170 r.p.m).

4.- Desde los cultivos líquidos anteriores, inocular un matraz de 2,5 l que contiene 1 l de LB líquido, suplementado con antibiótico, con 20 ml del cultivo preparado el día anterior. Incubar las células aeróbicamente a 37℃ en un agitador orbital (170 r.p.m) hasta alcanzar una DO_{600nm} ~0,5.

5.- Tomar 5 ml del cultivo y recoger células mediante centrifugación a 5.100 r.p.m. durante 5 min (4℃) para su posterior comprobación en geles de poliacrilamida (SDS-PAGE) (apartado 4.5.4.).

6.- Inducir la expresión de la proteína a purificar mediante la adición de 1 ml de IPTG**[a]** a 1 M (Cf = 1 mM). Para inducir la expresión de proteínas que contienen citocromos, adicionalmente, se añade 1 ml de clorhidrato de ácido δ-aminolevulínico**[a]** a 500 mM (Cf = 500 µM) y 250 µl de citrato férrico**[a]** a 40 mM (Cf = 10 µM), como precursores de la síntesis de citocromos.

[a] *El IPTG, clorhidrato de ácido δ-aminolevulínico y el citrato férrico se prepararon en fresco. Se disolvieron en H_2O desionizada y se esterilizaron con una unidad de filtración Minisart® NML (Sartorius) de 0,2 µm de tamaño de poro.*

7.- Incubar las células aeróbicamente a 30℃ en un agitador orbital (170 r.p.m) durante una noche. Las células se incuban a 30℃ porque éstas se tienen que adaptar a las condiciones bajo las cuales la inducción de la proteína-His_6 por IPTG tiene lugar.

8.- Tomar 5 ml del cultivo y recoger células mediante centrifugación a 5.100 r.p.m. durante 5 min (4℃) para su comprobación en geles de poliacrilamida (SDS-PAGE) (sección 4.5.4).

9.- Recoger las células, después de ∼20 h de incubación, mediante centrifugación a 5.100 r.p.m. (20 min, 4℃). Si la purificación de proteína no se va a realizar el mismo día, congelar el pellet sumergiéndolo en nitrógeno líquido. Conservarlo a -80℃ hasta su uso.

4.5.2. Fraccionamiento celular

El protocolo para el fraccionamiento celular se ha puesto a punto en esta Tesis Doctoral y consiste en:

1.- Descongelar lentamente el pellet de células inducidas procedentes de 1 l de cultivo.

2.- Resuspender el sedimento celular en 15 ml de tampón A1 o tampón C (Tabla 4.6.), según la proteína que se vaya a purificar.

3.- Lisar las células aplicando una presión constante de 1.000 psi con una prensa de French (SLM Aminco, Jessup). Repetir este proceso 3 veces.

4.- Suplementar el lisado de células con DNasaI (bovine pancreas, Sigma), RNasa A (bovine pancreas, Sigma) e inhibidor de proteasas (complete ULTRA Tablets, EDTA-free, Roche), siguiendo las especificaciones de la casa comercial.

5.- Centrifugar el extracto celular a 43.000 r.p.m. durante 45 min (4℃) para sedimentar las células que no se hayan lisado y residuos celulares insolubles.

6.- Tomar 20 µl de lisado de células para analizarlo mediante electroforesis en gel de poliacrilamida (SDS-PAGE) (apartado 4.5.4.).

4.5.3. Purificación de las proteínas Bjgb-His_6 y Flp-His_6

La purificación de las proteínas Bjgb y Flp se llevó a cabo mediante cromatografía líquida, empleando un equipo de cromatografía ÄKTA pure (consultar las

especificaciones del fabricante para su correcto uso). A continuación, se presentan los dos protocolos (para las proteínas Bjgb y Flp) desarrollados en esta Tesis Doctoral:

a) Purificación de la proteína Bjgb-His_6

La proteína Bjgb-His_6 se purificó mediante cromatografía de afinidad por iones metálicos inmovilizados (IMAC), seguida de una cromatografía de intercambio iónico. Todo el proceso de purificación se llevó a cabo a temperatura ambiente.

a.1) Cromatografía de afinidad:

En primer lugar, se prepara la columna de afinidad (5 ml) (Ni^{2+}-IMAC column; HiTrap Chelating HP, GE Healthcare Life Sciences). Para ello, se carga la columna con 1 volumen de columna (CV) (5 ml) de sulfato de níquel ($NiSO_4$) 0,2 M**[a]**, se lava con 10 CV de tampón de elución B1 (Tabla 4.6.) para eliminar el exceso de $NiSO_4$ que no se ha unido a la matriz y se equilibra con 10 CV de tampón de unión A1 (Tabla 4.6.). Todos estos pasos previos se llevan a cabo a un flujo de 5 ml/min.

[a] *Esta solución se filtra usando un filtro de nitrato de celulosa de 0,45 µm de tamaño de poro (Sartorius), acoplado a una bomba de vacío.*

Una vez preparada la columna se procede según se detalla a continuación:

1. Filtrar el lisado de células con una unidad de filtración Minisart® NML (Sartorius) de 0,2 µm de tamaño de poro.
2. Conectar la columna de afinidad al equipo ÄKTA pure y cargar el lisado de células en dicha columna a un flujo de 5 ml/min.
3. Lavar la columna con 10 CV de tampón A1 (Tabla 4.6.), a un flujo de 5 ml/min, para eluir las proteínas que no se han unido a la columna.
4. Generar un gradiente lineal de imidazol (Sigma-Aldrich) de 25 a 500 mM con 10 CV de una mezcla de tampón A1 y B1 (a un flujo de 1 ml/min). Este paso se realiza para eluir la proteína de interés, que está unida al níquel de la columna por la cola de histidina.
5. Comprobar la presencia de la proteína pura y su pureza en las diferentes fracciones del eluido mediante electroforesis SDS-PAGE (sección 4.5.4.). Para ello, se toma una alícuota de 20 µl de cada fracción del eluido en la que se haya

identificado la presencia de proteína a partir del cromatograma generado por el sistema.

6. Mezclar las fracciones que contienen la proteína pura. Identificar dichas fracciones con el cromatograma generado por el sistema durante la cromatografía de afinidad.

a.2) Cromatografía de intercambio iónico:

Antes de comenzar, se equilibra la columna (5 ml) (HiTrap Q HP anion-exchange column; GE Healthcare Life Sciences) con 10 CV de tampón de unión A2 (Tabla 4.6.), a un flujo de 5 ml/min. Posteriormente:

7. Diluir 10 veces la muestra anterior (procedente del punto 6) con el tampón de unión A2 (Tabla 4.6.), que se utilizará para la cromatografía de intercambio iónico. Con esta cromatografía se eliminará el imidazol e impurezas procedentes de la cromatografía de afinidad.
8. Conectar la columna de intercambio iónico al equipo ÄKTA pure y cargar la muestra, previamente preparada en el punto 7, en dicha columna a un flujo de 5 ml/min.
9. Lavar la columna con 10 CV de tampón de unión A2 (Tabla 4.6.) a un flujo de 5 ml/min.
10. Generar un gradiente entre 0 y 1 M de NaCl con 10 CV de una mezcla de tampón A2 y B2 (a un flujo de 0,5 ml/min). Este paso se realiza para eluir la proteína de interés (con carga negativa), que está unida a los cationes sodio (Na^+) de la columna por interacción con éstos.
11. Comprobar el grado de pureza de la proteína en las diferentes fracciones del eluido mediante electroforesis SDS-PAGE (apartado 4.5.4.). Para ello, tomar una alícuota de 20 µl de cada fracción del eluido en la que se haya identificado la presencia de proteína a partir del cromatograma generado por el sistema.
12. Mezclar las fracciones que contienen la proteína pura. Identificar dichas fracciones con el cromatograma generado por el sistema durante la cromatografía de intercambio iónico.
13. Intercambiar el tampón en el que está la proteína purificada (tampón de elución B2, Tabla 4.6.) por el tampón de unión A2 (sin cloruro de sodio, NaCl)

(Tabla 4.6.). Para ello, concentrar la muestra de proteína pura por centrifugación con un filtro para centrífuga Millipore Amicon™ acoplado a un tubo de centrífuga (ver especificaciones del fabricante). Concentrar la muestra hasta un volumen final de 2 ml. Finalmente, mezclar los 2 ml de muestra de proteína concentrada con 4 ml de tampón A2.

14. Comprobar el grado de pureza de la proteína en el eluido mediante electroforesis SDS-PAGE (sección 4.5.4.).
15. Determinar la concentración de proteína pura en el eluido (apartado 4.3.3.).
16. Realizar un espectro completo ultravioleta-visible (UV/Vis) de la proteína pura. Para ello, 1 ml de muestra de proteína pura diluida se deposita en una cubeta de cuarzo de 0,1 mm de longitud de paso, a continuación, la cubeta se introduce en el espectro para medir la absorbancia de la muestra.

    Con los datos de absorbancia obtenidos de la muestra de proteína pura mediante UV/Vis, se representan gráficamente las unidades de absorbancia (eje y) frente a la longitud de onda (eje x).
17. Preparar alícuotas de la proteína pura de 500 µl en tubos de microcentrífuga. Congelar dichas alícuotas sumergiéndolas en nitrógeno líquido. Almacenarlas a -80℃ hasta su uso.

Una vez que finaliza la purificación, añadir a las columnas de afinidad e intercambio iónico etanol 20% para su conservación a 4℃.

b) Purificación de la proteína Flp-His_6

Esta proteína se purificó mediante cromatografía de afinidad por iones metálicos inmovilizados (IMAC) (a temperatura ambiente), seguida de una diálisis (a 4℃).

b.1) Cromatografía de afinidad:

En primer lugar, se prepara la columna. Se carga la columna de afinidad (5 ml) (Ni^{2+}-IMAC column; HiTrap Chelating HP, GE Healthcare Life Sciences) con 1 CV de $NiSO_4$ 0,2 M[a], se lava con 10 CV de tampón de elución D (Tabla 4.6.) para eliminar el exceso de $NiSO_4$ y se equilibra con 10 CV de tampón de unión C (Tabla 4.6.). Todos los pasos se realizan a un flujo de 5 ml/min.

[a] *Esta solución se filtra usando un filtro de nitrato de celulosa de 0,45 µm de tamaño de poro (Sartorius), acoplado a una bomba de vacío.*

Una vez preparada la columna se procede según se detalla a continuación:

1. Filtrar el lisado de células con una unidad de filtración Minisart® NML (Sartorius) de 0,2 µm de tamaño de poro.
2. Conectar la columna de afinidad al equipo ÄKTA pure y cargar el lisado de células en dicha columna a un flujo de 5 ml/min.
3. Lavar la columna con 10 CV de tampón C (Tabla 4.6.), a un flujo de 5 ml/min, para eluir las proteínas que no se han unido a la columna.
4. Generar un gradiente lineal de imidazol (Sigma-Aldrich) de 25 a 500 mM con 10 CV de una mezcla de tampón C y D, a un flujo de 1 ml/min. Este paso se lleva a cabo para eluir la proteína de interés, que está unida al níquel de la columna por la cola de histidina.
5. Comprobar el grado de pureza de la proteína en las diferentes fracciones del eluido mediante electroforesis SDS-PAGE (sección 4.5.4.). Para ello, tomar una alícuota de 20 µl de cada fracción del eluido en la que se haya identificado la presencia de proteína a partir del cromatograma generado por el sistema.
6. Mezclar las fracciones que contienen la proteína pura. Identificar dichas fracciones con el cromatograma generado por el sistema durante la cromatografía de afinidad.

   b.2) Diálisis:

7. Para retirar de la muestra final de proteína pura el imidazol, procedente de la cromatografía de afinidad, y restos de contaminantes proteicos, se intercambia mediante diálisis el tampón en el que está la proteína purificada (tampón de elución D, Tabla 4.6.) por el tampón de diálisis (Tabla 4.6.). Para la diálisis se usó un casete con una membrana con un tamaño de poro de 10 kDa (Slide-A-Lyzer® Dyalisis Cassettes -Thermo Scientific).

   (7.1) Preparar 4 l de tampón de diálisis y enfriar a 4°C.

   (7.2) Sumergir el casete de diálisis en el tampón de diálisis durante 5 min.

(7.3) Centrifugar a 13.000 r.p.m durante 10 min (4℃) la muestra de proteína para comprobar que no ha precipitado.

(7.4) Inyectar la muestra de proteína, con ayuda de una aguja acoplada a una jeringa, en el casete de diálisis. Seguir indicaciones del fabricante.

(7.5) Dejar el casete sumergido en el tampón de diálisis durante una noche con agitación suave.

(7.6) Extraer del casete la muestra de proteína dializada. Seguir indicaciones del fabricante.

(7.7) Comprobar mediante centrifugación a 13.000 r.p.m durante 10 min (4℃) si la proteína ha precipitado.

8. Comprobar el grado de pureza de la proteína mediante electroforesis SDS-PAGE (apartado 4.5.4.).
9. Determinar la concentración de proteína pura (sección 4.3.3.).
10. Realizar un espectro de absorbancia completo (UV/Vis) de la proteína pura. Para ello, 1 ml de muestra de proteína pura se deposita en una cubeta de cuarzo de 0,1 mm de longitud de paso, a continuación, la cubeta se introduce en el espectro para medir la absorbancia de la muestra.

    Con los datos de absorbancia obtenidos de la muestra de proteína pura mediante UV/Vis, se representan gráficamente las unidades de absorbancia (eje y) frente a la longitud de onda (eje x).
11. Preparar alícuotas de la proteína pura de 500 µl en tubos de microcentrífuga. Congelar dichas alícuotas sumergiéndolas en nitrógeno líquido. Almacenarlas a -80℃ hasta su uso.

Para el lavado de las bombas peristálticas del cromatógrafo (previo y posterior a las purificaciones), así como para la recogida de los eluidos, se siguieron las indicaciones del fabricante del equipo de cromatografía líquida ÄKTA pure.

4.5.4. Electroforesis y visualización de proteína en geles de poliacrilamida (SDS-PAGE)

4.5.4.1. Preparación de las muestras

- *Análisis de la fracción soluble procedente del proceso de sobreexpresión de proteína:* se toma una alícuota de 1 ml de células, se centrifuga a 13.000 r.p.m. durante 5 min (temperatura ambiente) y, seguidamente, se resuspende cada unidad de densidad óptica en 100 µl de tampón de carga (Tabla 4.6.), para que la proteína sea equiparable en cada muestra analizada.

- *Análisis de la fracción soluble en todas las etapas de purificación de proteína:* se tomaron 20 µl de cada fracción y se mezclaron con tampón de carga (Tabla 4.6.).

Todas las muestras se calentaron a 95℃ durante 5 min y, a continuación, se centrifugaron a 13.000 r.p.m. durante 5 min (temperatura ambiente) antes de cargarlas en el gel.

4.5.4.2. Electroforesis de proteína en geles de poliacrilamida

Para la preparación de los geles de poliacrilamida se utilizó el material incluido en el sistema Mini-Protean Tetra Handcast (Bio-Rad) (apartado 4.3.4.1.). Los geles empleados eran de 1 mm de grosor y la concentración de poliacrilamida fue del 14% para el gel de resolución y del 4% para el de empaquetado (Tabla 4.6.).

En cada carril se cargaron 10 µl de cada muestra. En un carril se cargaron 5 µl de marcador de peso molecular PageRuler Plus Prestained Protein Ladder (Thermo).

La electroforesis se desarrolló a un voltaje constante de 180 V, a temperatura ambiente, hasta que el frente alcanzó el final del gel.

4.5.4.3. Visualización de proteínas en geles de poliacrilamida con azul de Coomassie

Después de la electroforesis, las proteínas se detectaron mediante tinción con Azul de Coomassie. Para ello, el gel de poliacrilamida se incubó en solución de Coomassie (Tabla 4.6.) durante 15 min. Posteriormente, el gel se lavó con una solución de desteñido (Tabla 4.6.) durante 2 h y, por último, con H_2O destilada. Para el revelado de

los geles se utilizó el sistema GelDoc XR (Bio-Rad) y el software de análisis de imagen Quantity One (Bio-Rad) e ImageLab (Bio-Rad) (Tabla 4.10.).

4.6. Técnicas espectroscópicas: ensayos *in vitro*

El procedimiento llevado a cabo para los ensayos *in vitro* de interacción de proteínas puras mediante UV/Vis se ha desarrollado en este trabajo. Las muestras se prepararon en una cámara de anaerobiosis Unilab^{plus} ECO mBRAUN con una atmósfera de N_2 en la que la concentración de O_2 era <0,5 ppm. Las muestras se prepararon en una cubeta de cuarzo de 0,1 mm de longitud de paso cerrada con un tapón de goma perforable, el tapón se selló con película autosellante. Posteriormente, se midió el espectro completo UV/Vis (250-800 nm) de las muestras en un espectrofotómetro (VARIAN Cary4000).

a) Estudio de la capacidad de la proteína Flp de reducir a la proteína Bjgb:

Para ensayar la capacidad de la proteína Flp de actuar como donador fisiológico de electrones de la proteína Bjgb se siguió el siguiente protocolo:

1.- Reconstituir la proteína Flp (concentración en la muestra final de 10 µM) con el cofactor flavín adenín dinucleótido (FAD) (concentración en la muestra final de 10 µM). Añadir la proteína Bjgb (concentración en la muestra final de 10 µM) en su forma férrica. Para ello, adicionar a la cubeta de cuarzo en el siguiente orden:

- 970 µl de proteína Flp (10 µM)
- 10 µl FAD (1 mM)
- 10 µl proteína Bjgb (1 mM)

Cerrar la cubeta con un tapón de goma perforable y sellar el tapón con película autosellante. Mezclar con suavidad por inversión 4-5 veces. Obtener un espectro completo UV/Vis de la muestra.

2.- Adicionar a la muestra anterior 10 µl de un stock de nicotinamida adenina dinucleótida (NADH) a 0,5 mM, siendo la concentración final de NADH en la muestra 5 µM. El NADH actúa como poder reductor.

Cerrar la cubeta con un tapón de goma perforable y sellar el tapón con película autosellante. Mezclar con suavidad por inversión 4-5 veces. Obtener un espectro completo UV/Vis de la muestra.

3.- Preparar 7 muestras iguales a las preparadas en los pasos 1 y 2, modificando la concentración final de NADH (10, 15, 20, 25, 30, 35 y 40 µM) en cada muestra.

Obtener un espectro completo UV/Vis de cada una de las 7 muestras.

Los espectros de las diferentes muestras se obtuvieron frente a un blanco (tampón de diálisis, Tabla 4.6.).

b) Estudio de la capacidad de unión del NO al grupo hemo reducido de la proteína Bjgb:

1.- Añadir a la cubeta de cuarzo la proteína Bjgb en tampón de diálisis (concentración en la muestra final de 10 µM) y ditionito sódico (concentración en la muestra final de 50 µM). El ditionito actúa como donador químico de electrones. Para ello, adicionar a la cubeta de cuarzo en el siguiente orden:

- 970 µl de tampón de diálisis
- 10 µl proteína Bjgb (1 mM)
- 10 µl ditionito sódico (5 mM)

Cerrar la cubeta con un tapón de goma perforable y sellar el tapón con película autosellante. Mezclar con suavidad por inversión 4-5 veces. Obtener un espectro completo UV/Vis de la muestra.

2.- Adicionar a la muestra anterior 10 µl de un stock de NO a 5 mM (sección 4.1.7.), siendo la concentración final de NO en la muestra 50 µM.

Cerrar la cubeta con tapón de goma perforable y sellar el tapón con película autosellante. Mezclar con suavidad por inversión 4-5 veces. Obtener un espectro completo UV/Vis de la muestra.

Repetir el ensayo anterior sustituyendo el ditionito sódico (donador químico de electrones) por la proteína Flp (donador fisiológico de electrones):

1.- Reconstituir la proteína Flp (concentración en la muestra final de 10 µM) con el cofactor flavín adenín dinucleótido (FAD) (concentración en la muestra final de 10 µM). Añadir la proteína Bjgb (concentración en la muestra final de 10 µM) y NADH (concentración en la muestra final de 5 µM). Para ello, adicionar a la cubeta de cuarzo en el siguiente orden:

- 960 µl de proteína Flp (10 µM)
- 10 µl FAD (1 mM)
- 10 µl proteína Bjgb (1 mM)
- 10 µl NADH (0,5 mM)

Cerrar la cubeta con tapón de goma perforable y sellar el tapón con película autosellante. Mezclar con suavidad por inversión 4-5 veces. Obtener un espectro completo UV/Vis de la muestra.

2.- Adicionar a la muestra anterior 10 µl de un stock de NO a 5 mM (apartado 4.1.7.), siendo la concentración final de NO en la muestra 50 µM.

Cerrar cubeta con tapón de goma perforable y sellar con película autosellante. Mezclar con suavidad por inversión 4-5 veces. Obtener un espectro completo UV/Vis de la muestra.

Los espectros de las diferentes muestras se obtuvieron frente a un blanco (tampón de diálisis, Tabla 4.6.).

Finalmente, con los datos de absorbancia obtenidos de cada muestra analizada mediante UV/Vis, se representaron gráficamente las unidades de absorbancia (eje y) frente a la longitud de onda (eje x).

4.7. Inoculación y cultivo de plantas de soja con *B. diazoefficiens*

4.7.1. Esterilización y germinación de semillas de soja

Para la esterilización superficial y germinación de las semillas de soja se siguió el protocolo que se detalla a continuación, el cual se ha puesto a punto en nuestro grupo de investigación:

1.- Colocar las semillas que se deseen esterilizar en un matraz de 500 ml, previamente autoclavado. No esterilizar más de 200 semillas por matraz.

2.- Sumergir las semillas en 100 ml de etanol absoluto durante 5 min. Agitar el matraz durante este tiempo. Eliminar el etanol.

3.- Sumergir las semillas en 100 ml de H_2O_2 al 30% (v/v) durante 15 min. Agitar el matraz durante este tiempo. Eliminar el H_2O_2.

4.- Lavar las semillas 10 veces con 100 ml de H_2O destilada (en cada lavado) y estéril (1-2 min/lavado).

5.- Colocar las semillas en placas Petri que contienen 25 ml de agar-H_2O (1%) (p/v) (8-9 semillas/placa).

6.- Geminar las semillas en oscuridad a 30℃ durante 72 h.

Todos los pasos anteriores se realizan en condiciones de esterilidad, en una cabina de flujo laminar.

4.7.2. Soluciones nutritivas para el cultivo de las plantas

Se empleó una solución mineral derivada de la descrita por Rigaud y Puppo (1975), con la siguiente composición:

- Macroelementos (por litro de agua): KH_2PO_4, 68 mg; K_2HPO_4, 44 mg; $SO_4Mg{\cdot}7H_2O$, 123 mg; K_2SO_4, 174 mg; SO_4Ca, 173 mg; EDTA Férrico (Secuestrene), 25 mg.
- Microelementos (por litro de agua): $MoO_4Na_2{\cdot}2H_2O$, 0,11 mg; BO_3H_3, 2,85 mg; $SO_4Mn{\cdot}4H_2O$, 3,07 mg; $SO_4Zn{\cdot}7H_2O$, 0,55 mg; $SO_4Cu{\cdot}5H_2O$, 0,2 mg.

La solución se esterilizó en autoclave a 121℃ durante 30 min. Para las plantas cultivadas con nitrato (NO_3^-), se adicionó a la solución nutritiva 4 mM de nitrato de potasio (KNO_3).

4.7.3. Cultivo de las plantas en jarras Leonard

Las semillas de soja germinadas se plantaron en jarras Leonard (Leonard, 1943). La jarra Leonard estaba formada por dos componentes: una base de vidrio (inferior) y una botella de vidrio invertida (superior). La base contenía 0,5 l de solución nutritiva de Rigaud y Puppo modificada y la parte superior se rellenó de vermiculita (que retiene la

humedad y los nutrientes). La parte superior también contenía una tira doble de papel de filtro, que sobresalía por la parte inferior de la botella, entrando en contacto con la solución nutritiva de las plantas[1]. En cada jarra Leonard se sembraron dos plántulas que se inocularon en el momento de la siembra con 1 ml de suspensión de la cepa bacteriana adecuada de *B. diazoefficiens* (10^8 células/ml inóculo) (Figura 4.1.).

Posteriormente, las plántulas se cubrieron con vermiculita y sobre la vermiculita se depositó una fina capa de perlita (previamente autoclavada), que evita la contaminación ambiental y refleja la luz, evitando un calentamiento excesivo de las semillas que pudiera provocar una alteración de su desarrollo. Las jarras se envolvieron en papel opaco a la luz, para proteger a las raíces de la luz (Figura 4.1.).

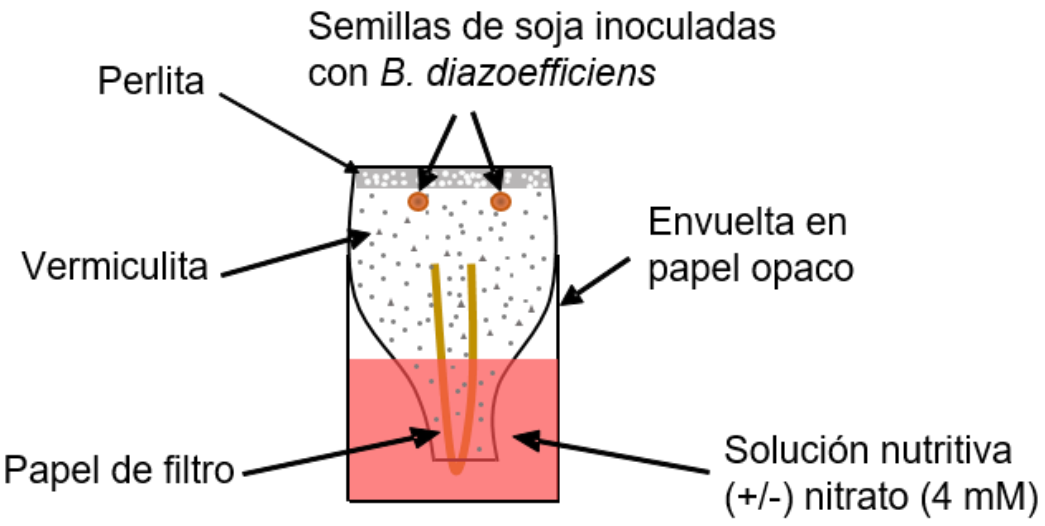

Figura 4.1. Jarra Leonard para el cultivo de plantas de soja. Jarra Leonard que contiene dos semillas de soja, cada una inoculada con 1 ml de suspensión bacteriana de la cepa bacteriana de *B. diazoefficiens* correspondiente.

Las jarras Leonard se trasladaron a una cámara de crecimiento de plantas, que tenía las condiciones ambientales controladas: ciclo día/noche de 16/8 h, 26/22℃ de temperaturas día/noche y una densidad de flujo de fotones fotosintéticos de 128-148 µmol fotones × m^{-2} × s^{-1}. Las plantas se cosecharon a los 35 días después de la inoculación.

[1] Una vez preparadas las jarras Leonard, se esterilizaron (sin solución mineral) en autoclave a 121℃ durante 40 min. La solución mineral, previamente autoclavada, se añadió en el momento de la siembra en condiciones de esterilidad.

4.7.4. Tratamientos de las plantas

Como se menciona anteriormente, cuando las plantas se trataron con NO_3^-, la solución nutritiva se suplementó con 4 mM de KNO_3. Después de 28 días de crecimiento, un conjunto de plantas se sometió a encharcamiento durante 7 días. Para ello, las plantas se sacaron de la parte superior de la jarra Leonard y se colocaron en la base de la jarra. La base se llenó al límite de su capacidad con solución nutritiva con o sin NO_3^-, de forma que las raíces y los nódulos quedaron cubiertos por dicha solución, según se describe en Sánchez et al. (2010) (Figura 4.2.B.). Las plantas no sometidas a encharcamiento se cultivaron durante todo tiempo en jarras Leonard (Figura 4.2.A.).

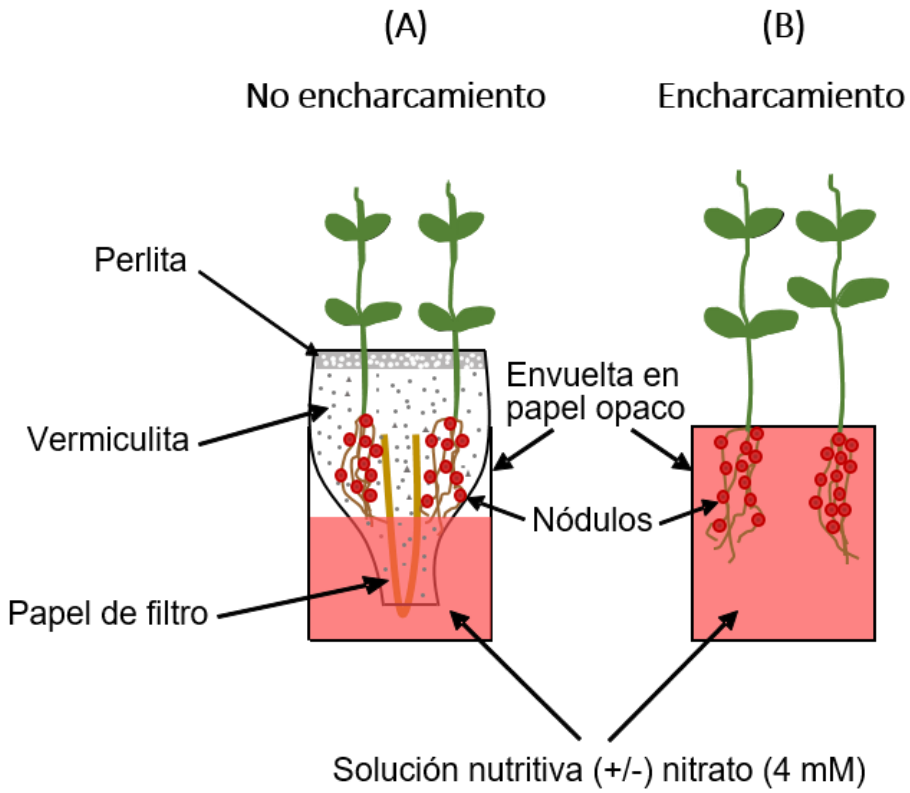

Figura 4.2. Jarras Leonard con plantas de soja noduladas. A. Tratamiento sin encharcamiento y **B.** Tratamiento con encharcamiento.

Para la determinación del contenido de N de la planta proveniente de la fijación biológica de N_2, las plantas se trataron con 4 mM KNO_3 marcado con ^{15}N (Potassium nitrate-^{15}N; 5 atom% ^{15}N). Para ello, el KNO_3 marcado se adicionó a la solución mineral en el momento de su preparación.

Tras el período de cultivo, las plantas se cosecharon de las jarras Leonard, la vermiculita se lavó de las raíces con abundante H_2O y se secaron con papel de filtro. Por un lado, se cosecharon los nódulos para realizar las diferentes determinaciones y, por otro lado, se llevó a cabo un análisis de los parámetros fisiológicos de las plantas de soja.

4.7.5. Cosecha de nódulos

Para la determinación de la actividad reductora de acetileno (ARA) y producción de NO y N_2O por los nódulos, éstos se separaron de las raíces de las plantas de soja e, inmediatamente, se prepararon las diferentes muestras para dichos análisis, que se realizaron el mismo día de la cosecha de los nódulos. Para el resto de determinaciones, los nódulos se cosecharon, se prepararon alícuotas de los mismos en tubos de centrífuga e, inmediatamente, se congelaron sumergiendo los tubos en nitrógeno líquido. Se conservaron a -80°C hasta su empleo para las diferentes determinaciones.

4.8. Determinación de los parámetros fisiológicos de las plantas de soja

4.8.1. Número de nódulos, peso seco de nódulos y peso seco de planta

El día de la cosecha se cuantificó el número de nódulos por planta (NNP). También se determinó el peso seco de nódulos por planta (PSNP) y el peso seco de planta (PSP). Para la determinación del PSNP y del PSP, los nódulos y las plantas se secaron en una estufa a 70°C durante 3 días y, posteriormente, se pesaron.

El PSNP se expresó en gramos ⁄ planta: (g × planta^{-1}). El PSP se expresó en gramos (g).

4.8.2. Contenido en N total y del N proveniente de la fijación biológica de N_2

Para la determinación del contenido en N total y N de la fijación biológica de N_2, se siguió el procedimiento descrito en Sánchez et al. (2011b). Estos análisis se realizaron por el servicio de 'Análisis de Nitrógeno y Carbono' de la Estación Experimental del Zaidín (Consejo Superior de Investigaciones Científicas), Granada, España, y por el

grupo de investigación de 'Biogeoquímica de Isótopos Estables' del Instituto Andaluz de Ciencias de la Tierra (Consejo Superior de Investigaciones Científicas), Granada, España, respectivamente. En primer lugar, las plantas de soja (la parte aérea sin las raíces), secadas en una estufa a 70℃ durante 3 días, se pesaron y se molieron en un molino IKA A 11 (Rose Scientific Ltd., Alberta, Canada). A continuación, se pesaron muestras de 3 mg y se analizaron para cuantificar su contenido en N total (TN) y el enriquecimiento en N-15 (%átomos de ^{15}N en exceso). Para ello, se usó un analizador elemental (EA1500 NC, Carlo Erba, Milan, Italy) combinado con un espectrómetro de masas de relación isotópica (Delta Plus XL, ThermoQuest, Bremen, Germany).

Los valores de TN se expresaron en mg de N ⁄ g de planta: (mg N × g^{-1}).

La proporción de N derivado del N_2 atmosférico (%Ndfa) se calculó como:

$$\%Nfda = 100 \times [1 - (\mathrm{A}/\mathrm{B})]$$

Donde:

A = %átomos de ^{15}N en exceso en plantas inoculadas

B = %átomos de ^{15}N en exceso en plantas no inoculadas

%Átomos de ^{15}N en exceso = %átomos de ^{15}N en el tratamiento marcado - %átomos de ^{15}N en el tratamiento no marcado

Para calcular el %átomos de ^{15}N en exceso, un conjunto de plantas se mantuvo en condiciones de fijación de N_2 para obtener el %átomos de ^{15}N del tratamiento no marcado.

El contenido de N_2 fijado (FN) se calculó como:

$$FN = (\%\mathrm{Ndfa} \times \mathrm{TN})/100$$

El FN se expresó como mg de N fijado ⁄ g de planta: (mg N × g^{-1}).

4.9. Determinaciones analíticas y enzimáticas en nódulos de soja

Las determinaciones análiticas y enzimáticas que se detallan a continuación se llevaron a cabo en los nódulos procedentes de 15-20 plantas de cada tratamiento.

4.9.1. Actividad reductora de acetileno de los nódulos

La fijación de N_2 se determinó como producción de etileno por la nitrogenasa a partir de acetileno, es decir, como actividad reductora de acetileno (ARA). Para la determinación de ARA en nódulos de soja, éstos se incubaron en viales de 20 ml cerrados herméticamente (SUPELCO®) y, posteriormente, se cuantificó el etileno (C_2H_4) producido en el espacio de cabeza de los viales a lo largo del tiempo mediante cromatografía gaseosa. Para ello, se siguió la metodología establecida en nuestro grupo de investigación, que consiste en:

1.- Introducir en la base de cada vial un pequeño papel de filtro. Tarar los viales (sin el tapón y con el papel de filtro incorporado) para calcular, posteriormente, el peso fresco de los nódulos por vial.

2.- Introducir entre 20-30 nódulos por vial. Pesar los viales para saber el peso fresco de nódulos en cada uno de ellos.

3.- Humedecer el papel de filtro de cada vial con 100 µl de solución nutritiva de plantas con 4 mM KNO_3, para mantener la humedad de este sistema cerrado. Cerrar el vial herméticamente con un tampón que incorpora goma perforable.

4.- Añadir 1 ml de acetileno puro a cada vial. Incubar los viales a 30°C y en oscuridad. En este momento comienza la incubación (tiempo 0).

5.- Analizar las muestras gaseosas en el cromatógrafo[a] transcurridas 2 h desde el inicio de la incubación (T1). Para ello, tomar una alícuota de 0,5 ml del espacio gaseoso del vial e inyectar en el cromatógrafo.

6.- Una vez realizadas las medidas correspondientes al T1 de todos los viales, volver a incubar los viales a 30°C y en oscuridad.

7.- Analizar las muestras gaseosas en el cromatógrafo transcurridas 4 h desde el inicio de la incubación (T2). Para ello, tomar una alícuota de 0,5 ml del espacio gaseoso del vial e inyectar en el cromatógrafo.

8.- Calcular el ARA determinando el incremento en la producción de etileno en el espacio de cabeza de cada vial. La emisión de etileno se mide en el rango lineal de producción de etileno, que se comprueba previamente al representar gráficamente los

valores obtenidos en función del tiempo. En nuestro caso, este rango estaba comprendido entre el tiempo de incubación T1 (2 h) y el tiempo de incubación T2 (4 h), y se calculó como: Δ C_2H_4 nmol (4-2 h) ⁄ Δ tiempo (4-2 h).

Los valores de ARA se expresaron como: [nmol C_2H_4 producidos × min^{-1} × $(g\ PFN)^{-1}$].

[a] Las muestras se inyectaron en un cromatógrafo de gases Hewlett Packard modelo 5890, equipado con detector de ionización de llama y una columna metálica (180 cm × 3,2 mm) empaquetada con Porapak Q de 80-100 mesh. Las temperaturas del horno, inyector y detector fueron 60, 90 y 110℃, respectivamente. Como gas portador se empleó N_2 a un flujo de 60 ml/min. Los picos de etileno se identificaron por comparación con el correspondiente patrón. La concentración de etileno en cada muestra se calculó tomando como referencia la curva patrón, construida con volúmenes conocidos de etileno.

4.9.2. Contenido de leghemoglobina en los nódulos

El contenido de leghemoglobina (Lb) en los nódulos se cuantificó mediante fluorimetría, siguiendo el protocolo descrito por Sánchez et al. (2010), que consiste en:

1.- Homogeneizar 0,3 g de nódulos en 6 ml de medio de extracción de Lb (Tabla 4.6.) suplementado con 0,1 g de polivinilpolipirrolidona (PVPP). Enfriar previamente el mortero y el medio de extracción de Lb.

2.- Centrifugar el extracto resultante a 14.000 r.p.m. durante 20 min a 4℃.

3.- Tomar alícuotas de 50 µl del sobrenadante y añadir 3,15 ml de una solución saturada de ácido oxálico (6,6 g/100 ml) en tubos de cristal con rosca de 17 ml. Preparar cuatro alícuotas de cada muestra: tres serán réplicas analíticas y una será el control, que no se autoclava.

4.- Calentar las muestras a 120℃ durante 30 min en un autoclave.

5.- Enfriar las muestras a temperatura ambiente.

6.- Determinar la fluorescencia emitida por los grupos hemo de las soluciones.

Para la medida de la fluorescencia se empleó un fluorímetro Shimadzu (Shimadzu Scientific Instruments, Kyoto, Japan) equipado con una lámpara xenón-

mercurio y un fotomultiplicador sensible al rojo, RF-540. La longitud de onda de excitación fue de 405 nm y la del selector monocromático de emisión de 650 nm.

Las diferencias existentes entre los valores de la fluorescencia emitidos por las muestras control (no calentadas) y calentadas son proporcionales a la cantidad de hemoproteínas existentes y, por tanto, indicativo de la cantidad de leghemoglobina en las muestras. El contenido de Lb en cada muestra se calculó usando como referencia una curva patrón construída a partir de hemoglobina de plasma humano.

El contenido de Lb se expresó como: [mg Lb × $(g\ PFN)^{-1}$].

4.9.3. Aislamiento de bacteroides de los nódulos

El aislamiento de los bacteroides de los nódulos de soja se realizó según el protocolo que se presenta a continuación (Arrese-Igor et al., 1998):

1.- Colocar ∼1 g de nódulos en un mortero previamente enfriado en hielo.

2.- Homogeneizar los nódulos con 7 ml de tampón de extracción de bacteroides (Tabla 4.6.).

3.- Filtrar el homogenado a través de 4 capas de gasa hidrófila para eliminar los restos de células vegetales. Centrifugar a 1.500 r.p.m. durante 5 min a 4℃.

4.- Centrifugar de nuevo el sobrenadante a 8.000 r.p.m. durante 10 min a 4℃, para obtener el pellet de bacteroides.

5.- Lavar dos veces el precipitado (bacteroides) con 30 ml de tampón Tris-HCl 50 mM (pH 7,5).

6.- Resuspender el pellet de bacteroides en 1,5 ml del mismo tampón empleado en el paso anterior.

4.9.4. Lisado de bacteroides

La metodología para el lisado de bacteroides se ha puesto a punto en esta Tesis Doctoral. Para ello, se partió de una resuspensión que contenía bacteriodes aislados, obtenida como se detalla en la sección 4.9.3. Para el fraccionamiento de los bacteroides se usó una prensa de French (SLM). Antes de la rotura de los bacteroides, la célula de la prensa se preenfrió manteniéndola en una cámara frigorífica. Se

procedió al ensamblaje de la célula de la prensa, que consta de pistón, émbolo, tapa, llave y grifo. A continuación, se aplicó la suspensión de bacteroides en la célula de la prensa y se procedió al lisado de los mismos aplicando una presión constante de 120 MPa, dejando salir la suspensión lentamente por el grifo. Este proceso se repitió tres veces.

El extracto celular resultante se centrifugó a 8.000 × *g* (10 min, 4°C) para sedimentar restos celulares y bacteroides que no se habían roto. El sobrenadante se utilizó para las determinaciones analíticas.

4.9.5. Detección de NO en los nódulos

La detección de NO en los nódulos se realizó mediante fluorescencia, siguiendo el método descrito por Nagata et al. (2008) con algunas modificaciones. El protocolo utilizado consistió en:

1.- Introducir 5 nódulos por tubo (tubo de 17 ml provisto con tampón de rosca). Elegir 5 nódulos que tengan un tamaño similar. Preparar dos series de tubos por cepa y tratamiento: uno para el tratamiento con el fluoróforo y otro para el tratamiento con H_2O desionizada.

Con el tratamiento con el fluoróforo se detecta la fluorescencia emitida por la autofluorescencia del nódulo y la debida a la unión específica entre el NO y el fluoróforo. Mientras que con el tratamiento con H_2O desionizada se detecta sólo la autofluorescencia del nódulo.

2.- Añadir 200 µl de una solución 7 µM de diacetato de 4,5-diaminofluoresceína (DAF-2DA) por tubo (tratamiento con fluoróforo).

Adionar 200 µl de una solución 7 µM de diacetato de 4,5-diaminofluoresceína (DAF-2DA) a un tubo sin nódulos (se usará como blanco).

3.- Añadir 200 µl de H_2O desionizada por tubo (tratamiento con H_2O desionizada).

4.- Cerrar todos los tubos e incubar a 30°C en agitación (170 r.p.m) durante 2 h en oscuridad.

5.- Transferir la solución de DAF-2DA y H_2O desionizada de cada tubo a un tubo de microcentrígufa. Mantener los tubos de microcentrígufa en hielo y preservados de la luz.

6.- Para la medida de la fluorescencia, se adiciona 120 µl de la solución DAF-2DA/H_2O desionizada a una cubeta de cuarzo de 10 mm de longitud de paso. A continuación, se determinan las unidades relativas de fluorescencia de la solución DAF-2DA/H_2O desionizada empleando un fluorímetro MD-5020 Photon Technology International (Birmingham, NJ, U.S.A.) con una longitud de onda de 495 nm de excitación y 515 nm de emisión (2 nm de amplitud de banda).

7.- Secar los nódulos en una estufa a 70℃ durante 3 días. Pesar los nódulos (peso seco de nódulos).

A las unidades de fluorescencia (RFU) emitidas por la solución 7 µM de DAF-2DA incubada con nódulos se les restó el blanco, es decir, la fluorescencia emitida por la solución 7 µM de DAF-2DA (tubo sin nódulos con 200 µl de solución 7 µM de DAF-2DA). Al último valor obtenido se le restó la autofluorescencia del nódulo, esto es, la fluorescencia emitida por los nódulos incubados en H_2O (tubo con nódulos conteniendo 200 µl de H_2O desionizada).

La acumulación de NO en los nódulos se expresó como unidades relativas de fluorescencia (RFU) ⁄ mg de peso seco de nódulo (PSN): [RFU × $(mg\ PSN)^{-1}$].

4.9.6. Tratamiento de los nódulos con un secuestrador de NO

Para confirmar que la fluorescencia detectada con el fluoróforo DAF-2DA era debido al NO, los nódulos se trataron con un secuestrador de NO, de acuerdo a la metodología descrita por Shimoda et al. (2009), modificada como se indica a continuación:

1.- Introducir 5 nódulos por tubo (tubo de 17 ml provisto con tampón de rosca). Elegir 5 nódulos que tengan un tamaño similar.

2.- Añadir 200 µl de una solución 3 mM de 2-[4-carboxifenil]-4,4,5,5-tetrametilimidazolina-1-oxil-3-óxido (c-PTIO) por tubo. Cerrar los tubos e incubar a 30℃ en agitación (170 r.p.m) durante 1 h en oscuridad.

3.- Retirar el c-PTIO y añadir 200 µl de una solución 7 µM de diacetato de 4,5-diaminofluoresceína (DAF-2DA) por tubo. Cerrar los tubos e incubar a 30°C en agitación (170 r.p.m) durante 2 h en oscuridad.

4.- Transferir la solución de DAF-2DA de cada tubo a un tubo de microcentrígufa. Mantener los tubos de microcentrígufa en hielo y preservados de la luz.

5.- Para la medida de la fluorescencia, se adicionó 120 µl de la solución DAF-2DA a una cubeta de cuarzo de 10 mm de longitud de paso. A continuación, se determinan las unidades relativas de fluorescencia de la solución DAF-2DA empleando un fluorímetro con una longitud de onda de 495 nm de excitación y 515 nm de emisión (2 nm de amplitud de banda).

6.- Secar los nódulos en una estufa a 70°C durante 3 días. Pesar los nódulos (peso seco de nódulos).

Los valores de fluorescencia obtenidos en el fluorímetro se trataron como se detalla en el apartado 4.9.5. La acumulación de NO se expresó como unidades relativas de fluorescencia (RFU) / mg de peso seco de nódulo (PSN): [RFU × $(mg\ PSN)^{-1}$].

4.9.7. Producción de N_2O por los nódulos

Para determinar la producción de N_2O por los nódulos de soja, éstos se incubaron en viales de 20 ml cerrados herméticamente (SUPELCO®) y, posteriormente, se cuantificó el N_2O producido en el espacio de cabeza de los viales a lo largo del tiempo mediante cromatografía gaseosa (sección 4.3.1.). Para ello, se siguió el método descrito por Tortosa et al. (2015) con algunas modificaciones, y consistió en:

1.- Colocar entre 20-30 nódulos por vial (cerrados herméticamente y provistos con un tampón que incorpora goma perforable) que contiene 100 µl (para nódulos procedentes del tratamiento sin encharcamiento) o 5 ml (para nódulos procedentes del tratamiento con encharcamiento) de solución nutritiva de plantas con 4 mM KNO_3.

2.- Añadir acetileno 10% (v/v) en cada vial para inhibir la enzima óxido nitroso reductasa (Yoshinari y Knowles, 1976).

3.- Incubar los viales a 30°C y en oscuridad. En este momento comienza la incubación (tiempo 0).

4.- Tomar una alícuota de 1 ml del espacio gaseoso del vial e inyectar en el cromatógrafo transcurridas 4 h desde el inicio de la incubación (T1).

5.- Una vez realizadas las medidas correspondientes al T1 de todos los viales, volver a incubar los viales a 30℃ y en oscuridad.

6.- Tomar una alícuota de 1 ml del espacio gaseoso del vial e inyectar en el cromatógrafo transcurridas 6 h desde el inicio de la incubación (T2).

7.- Calcular la producción de N_2O en el rango lineal de producción del mismo, que estaba comprendido entre las 4 y las 6 h, y se calculó como:

Δ concentración molar de N_2O (6-4 h) ⁄ Δ tiempo (6-4 h)

Los resultados se expresaron como: [nmol N_2O producidos × h^{-1} × $(g\ PSN)^{-1}$].

4.9.8. Actividad nitrato reductasa de los bacteroides

Previamente a la determinación de la actividad nitrato reductasa (NR), se procede al aislamiento de los bacteroides. Para ello se procedió de la siguiente manera:

1.- Colocar ∼1 g de nódulos en un mortero preenfriado en hielo.

2.- Aislar los bacteroides según el protocolo descrito en la sección 4.9.3. Determinar el contenido de nitrito (NO_2^-) en el sobrenadante obtenido después de cada lavado (ver descripción de determinación de NO_2^- al final de este apartado). Resuspender el pellet de bacteroides con tampón Tris-HCl 50 mM (pH 7,5), guardar una alícuota de suspensión de bacteroides para determinar proteína (sección 4.3.3.).

3.- Determinar la actividad NR siguiendo el procedimiento descrito por Delgado et al. (1992), que consiste en:

(3.1) Mezclar 250 µl de mezcla NR (Tabla 4.6.) con 100 µl de suspensión de bacteroides (0,3-0,5 mg de proteína).

(3.2) Comenzar la reacción añadiendo a la mezcla anterior 50 µl de ditionito sódico 46 mM en Tris-HCl 500 mM (pH 7,5). Mezclar suavemente y colocar los tubos a 30℃.

(3.3) Mantener la reacción a 30℃ durante 15-30 min, en este tiempo la coloración azul de la mezcla de reacción no debe desaparecer. La reacción se detiene agitando

mediante vórtex los tubos hasta que el color azul desaparece. Para obtener los controles, las mezclas de reacción se agitan mediante vórtex en el momento de la adición del ditionito sódico para conseguir su completa oxidación.

Una vez que la reacción se detiene, en ausencia completa de la coloración azul de los tubos, se determina el NO_2^- presente en cada tubo. Para la valoración del NO_2^- se empleó la reacción de diazotación de Griess-Yllosway, esta reacción utiliza la sulfanilamida y el ácido N-naftil-etilén-diamino (NNEDA) como reactivos. A un volumen de muestra se añaden volúmenes iguales de sulfanilamida y de NNEDA (Tabla 4.6.). Agitar e incubar a temperatura ambiente durante 20 min. Posteriormente, se mide la absorbancia a DO_{540nm} y se ajusta a una curva patrón preparada a partir de concentraciones conocidas de nitrito sódico ($NaNO_2$).

Los resultados se expresaron como: [nmol NO_2^- producidos × min^{-1} × (mg proteína)$^{-1}$].

4.9.10. Contenido de amonio en los bacteroides

Para la medida del contenido de amonio (NH_4^+) en los bacteroides, se empleó ∼1 g de nódulos de cada cepa y tratamiento. Previamente a la determinación de NH_4^+, se llevó a cabo el aislamiento (sección 4.9.3.) y lisado (sección 4.9.4.) de los bacteroides. El contenido de NH_4^+ se midió siguiendo el método descrito por Witte y Medina-Escobar (2001) con algunas modificaciones, y consistió en:

1.- Tomar 400 µl de la fracción soluble de bacteroide y depositar en un tubo de microcentrífuga.

2.- Añadir 100 µl de solución de fenol-nitroprusiato y 200 µl de solución de hipoclorito (Tabla 4.6.). Cerrar el tubo y mezclar por inversión.

3.- Incubar a 50ºC durante 20 min.

4.- Medir la absorbancia a 639 nm.

El contenido de NH_4^+ se calculó por referencia a la curva patrón, construida con concentraciones conocidas de cloruro de amonio (NH_4Cl). Los valores de NH_4^+ se expresaron como: [µM NH_4^+ × (g PFN)$^{-1}$].

4.10. Estadística

Para los parámetros analizados estadísticamente, se realizaron análisis estadísticos descriptivos (media y desviación estándar) y se comprobó que los datos seguían una distribución normal. Los análisis de varianza (ANOVA) para los tratamientos que utilizan el test de post-hoc Tukey-Kramer ($P \leq 0,05$) se usaron como análisis estadísticos inferenciales empleando el software abierto GNU-PSPP v0.9.0 (disponible en https://www.gnu.org/software/pspp/).

4.11. Métodos bioinformáticos

Las herramientas bioinformáticas empleadas en el desarrollo de esta Tesis Doctoral se presentan en la siguiente tabla (Tabla 4.10.):

Tabla 4.10. Programas bioinformáticos.

Programa	Descripción	Referencia
BLAST (Basic Local Alignment Search Tool)	Programa para alinear secuencias de ADN, ARN o proteínas, basado en la base de datos del NCBI	Altschul et al. (1990)
Clone Manager	Programa para la simulación de clonajes, restricciones, representación gráfica de plásmidos y diseño de oligonucleótidos	Sci-Ed Software
Clustal W	Programa para el alineamiento múltiple de secuencias	Thompson et al. (1994)
ImageLab	Programa para análisis de imagen de geles de ADN o proteína	Bio-Rad
Quantity One	Programa para la obtención, análisis y cuantificación de imagen de geles obtenidas por equipos de Bio-Rad	Bio-Rad
iQ5 Optical System Software	Software para la adquisición y análisis de los datos de qRT-PCR	Bio-Rad

5

RESULTS

Chapter 5.1

The *Bradyrhizobium diazoefficiens* single domain haemoglobin Bjgb binds NO

5. RESULTS

5.1. The *Bradyrhizobium diazoefficiens* single domain haemoglobin Bjgb binds NO

5.1.1. Abstract

B. diazoefficiens is a soil bacterium that establishes N_2-fixing symbiotic associations with soybean plants. This bacterium is also able to denitrify and grow under free-living conditions with NO_3^- or NO_2^- as the sole N source. In addition to the denitrification pathway, *B. diazoefficiens* possesses an integrated system for NO_3^- assimilation and NO detoxification, encoded by the *narK-bjgb-flp-nasC* operon. This cluster codes for a putative haemoglobin (Bjgb), an assimilatory nitrate reductase (NasC), a NO_3^-/NO_2^- transporter (NarK) and an FAD-dependent NAD(P)H oxidoreductase (Flp) (Cabrera et al., 2016).

Bjgb shares 37 and 32% amino acid identity with sdHbs from *V. stercoraria* (Vgb) and *C. jejuni* (Cgb), respectively, that have been implicated in NO detoxification. Bjgb also showed 34, 35 and 33% identity with the haem-binding domain of fHbs from *E. coli*, *S.* Typhimurium and *E. meliloti* 1021, respectively, but it does not possess the binding sites for FAD and NAD(P)H typical from fHbs (Sánchez et al., 2011a). Flp is a NAD(P)H reducing protein, with a flavin mononucleotide (FMN) moiety with an analogous function to that of the fHb-like FAD/NAD-binding domain. A role for Bjgb and Flp in protecting *B. diazoefficiens* cells from nitrosative stress under free-living conditions has been recently demonstrated (Cabrera et al., 2016). Cabrera and colleagues (2016) have proposed that Bjgb and Flp might form a NO detoxification system analogous to fHbs, where Flp would supply electrons from NAD(P)H to Bjgb. Nevertheless, the function *in vitro* of Bjgb-Flp in NO detoxification and the end-products of NO turnover are unknown.

Here, we report the overexpression, purification and *in vitro* biophysical characterization of *B. diazoefficiens* Bjgb and Flp. Results from this work showed that Bjgb is reduced by electrons supplied by Flp following oxidation of NADH. The reduced

b-type haem cofactor from Bjgb has the ability to bind NO. The role *in vivo* of a key amino acid residue (lysine-52) from Bjgb has also been investigated.

5.1.2. Reduction of Bjgb by Flp and NO binding

5.1.2.1. Expression and purification of Bjgb

5.1.2.1.1. Construction of pDB4008 expression plasmid

In order to express N-terminally His_6-tagged Bjgb and Flp proteins, a fragment of 1719 bp, which contains the *bjgb* (blr2807) and *flp* (blr2808) genes, was amplified by PCR using the primer pairs 2807-8_His_For/2807-8_His_Rev (Table 4.3.). The PCR-amplified DNA fragment was purified and quantified, then, it was digested with *Nhe*I and *Hin*dIII restriction endonucleases and ligated to plasmid pET-24a(+) (5252 bp), that was pre-digested with the aforementioned enzymes (Table 4.2.). The resulting plasmid includes *bjgb* fused in its 5' end with the histidine tag and *flp*. The correct insertion of the PCR fragment into the vector, as well as the amplified sequence fidelity, were confirmed by sequencing using primers pTXB1-1 and pET28a-1_rev (Table 4.3.). The final construction yielded plasmid pDB4008 (Figure 5.1.1.).

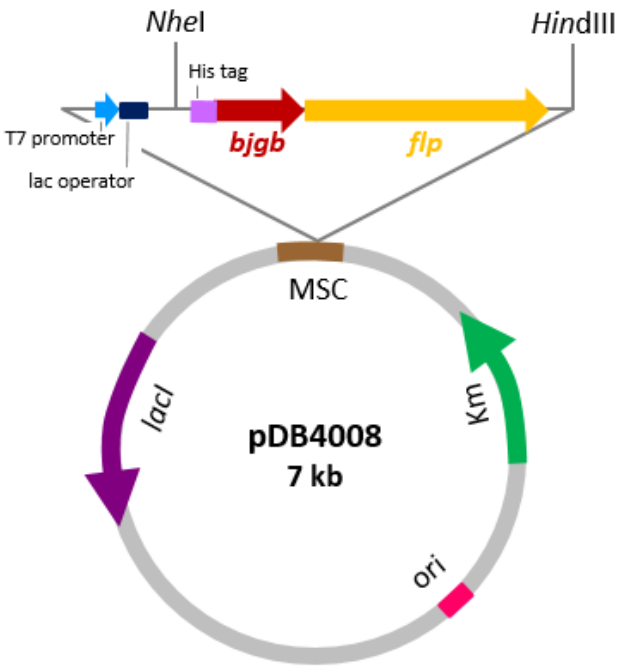

Figure 5.1.1. Construction of plasmid pDB4008 for Bjgb-Flp-His_6 expression. Map of pDB4008. Insertion of *bjgb* and *flp* to yield recombinant proteins fused with a histidine tag at their amino terminal end under the control of the T7 promoter. MCS: Multiple Cloning Site.

5.1.2.1.2. Expression of Bjgb in *E. coli* BL21 (DE3)

E. coli BL21 (DE3) competent cells transformed with pDB4008 (Table 4.2.) were incubated at 37℃ until the cell culture reached an OD_{600nm} ~0.5 (approximately 2 h) (section 4.5.1.). At this time, an aliquot (5 ml) was taken from the culture. Next, 1 mM IPTG, 500 µM δ-aminolevulinic acid hydrochloride and 10 µM of ferric citrate were added to the culture, that was incubated again at 30℃ overnight. Then, cells were harvested by centrifugation. After cell lysis (see section 4.5.2.), SDS-PAGE analysis of soluble protein extracts showed overexpression of Bjgb protein, at approximately 15 kDa, when IPTG was added to cell culture (Figure 5.1.2., lane 2). However, overexpression of a band that should correspond to Flp (~45 kDa) was not observed in the presence of IPTG by using plasmid pDB4008 (Figure 5.1.2., lane 2).

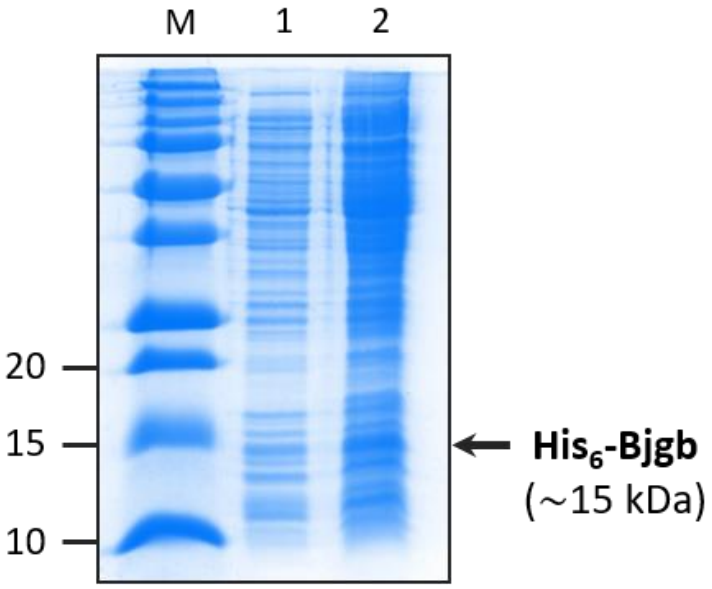

Figure 5.1.2. Overexpression of Bjgb. *E. coli* BL21 (DE3) cells with pDB4008 were incubated at 37℃ for 2 h. After adding IPTG, δ-aminolevulinic acid hydrochloride and ferric citrate to the cell culture, cells were lysated and subjected to SDS-PAGE. Then, the gel was stained with Coomassie Blue. A sample was taken from the culture before IPTG induction (lane 1) and after overnight IPTG incubation (lane 2). On the right margin, the band (~15 kDa) corresponding to overexpressed Bjgb is indicated. Lane 'M' corresponds to protein molecular marker PageRuler™ Plus Prestained Protein Ladder. The molecular size, in kDa, and the position of the marker proteins are indicated on the left margin.

5.1.2.1.3. Purification of Bjgb

For Bjgb purification, 5 l of *E. coli* BL21 (DE3) competent cells transformed with pDB4008 were used. After cell fractionation, soluble extracts were subjected to affinity chromatography (detailed procedure in section 4.5.3.*a.1.*) and the absorbance was followed at 280 nm (protein absorbance) and 412 nm (for haem protein absorbance) during chromatography (Figure 5.1.3.A.). Then, a linear gradient of 25-500 mM imidazole was applied to the column and two elution peaks were detected (Figure 5.1.3.A.). SDS-PAGE analysis of the elution fractions showed the presence of Bjgb (~15 kDa), while contaminants of varying size were eluted earlier, at relatively low imidazole concentration (Figure 5.1.3.C.). Flp protein was not bound to the affinity matrix (Figure 5.1.3.C.). Fractions containing Bjgb (Figure 5.1.3.C., lanes 3 to 11) were pooled and loaded onto an anion exchange column (section 4.5.3.*a.2.*) to remove the excess of imidazole and contaminating proteins (Figure 5.1.3.B.). The column was developed with a linear gradient of 0-1 M NaCl and elution fractions were monitored at 280 and 412 nm, resulting in a unique peak (Figure 5.1.3.B.). SDS-PAGE of eluted protein fractions gave a single band of about 15 kDa that corresponds to Bjgb (Figure 5.1.3.C., lanes 13 to 15). An additional band at 30 kDa was observed, which corresponds to the dimeric state of Bjgb (Figure 5.1.3.C., lane 13). Fractions containing Bjgb (Figure 5.1.3.C., lanes 13 to 15) were pooled and concentrated (section 4.5.3.*a.2.*). Then, 10 µg of pure Bjgb was analysed by SDS-PAGE resulting in a single band of about 15 kDa (Figure 5.1.3.C., lane 16). The yield of pure protein was 4.6 mg/l per culture.

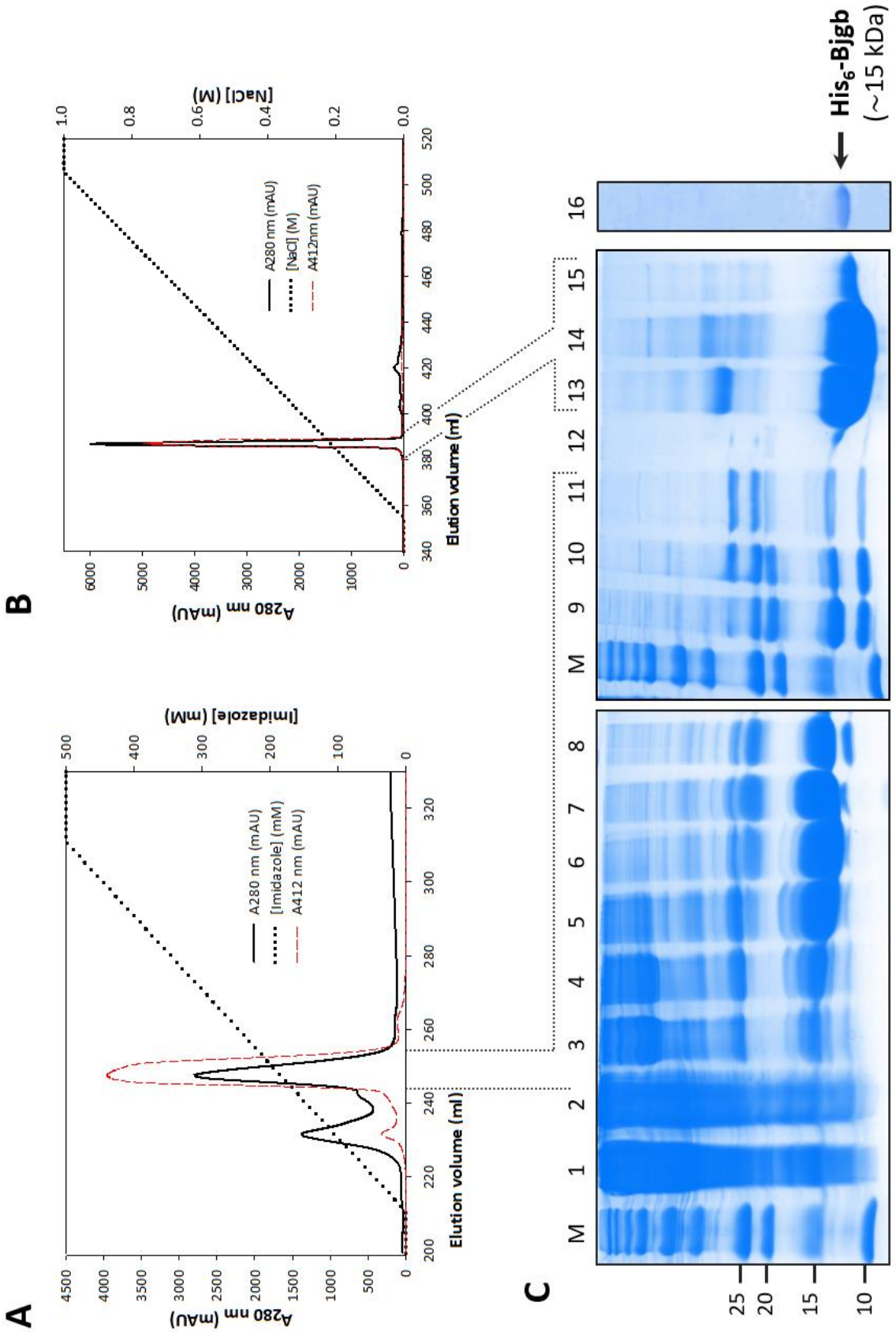
A
B
C
A280 nm (mAU)
[Imidazole] (mM)
A280 nm (mAU)
[NaCl] (M)
Elution volume (ml)
A280 nm (mAU)
A412 nm (mAU)
A280 nm (mAU)
[NaCl] (M)
A412nm (mAU)
M
1
2
3
4
5
6
7
8
9
10
11
12
13
14
15
16
His6-Bjgb
(~15 kDa)
25
20
15
10

Figure 5.1.3. Purification of Bjgb. A. Chromatogram obtained during the affinity purification of Bjgb from soluble cell extracts. The absorbance at 280 nm (continuous black line, $A_{280\ nm}$) and at 420 nm (dashed red line, $A_{412\ nm}$) were monitored during chromatography, as well as the imidazole gradient (dotted black line, [imidazole]). **B.** Chromatogram obtained during the anion-exchange chromatography. The absorbance at 280 (continuous black line, $A_{280\ nm}$) and at 420 nm (dashed red line, $A_{412\ nm}$) were monitored during the chromatography, as well as the NaCl gradient (dotted black line, [NaCl]). **C.** Coomassie Blue staining of SDS-PAGE proteins obtained after the affinity and anion-exchange chromatography. Lane 1, cell extract; lane 2, cell extract eluted from the affinity column; lane 3 to 11, elution fractions from the affinity column after imidazole gradient loading into the column; lane 12, eluted proteins from the anion-exchange column after loading fractions 3 to 11 into the column; lanes 13 to 15, eluted proteins from the anion-exchange column after NaCl gradient loading into the column; lane 16, corresponds to SDS-PAGE of purified Bjgb after concentration of proteins from fractions 13 to 15. On the right margin the band (~15 kDa) corresponding to Bjgb is indicated. 'M' corresponds to protein molecular marker PageRuler™ Plus Prestained Protein Ladder. The molecular size, in kDa, and the position of the marker proteins are indicated on the left margin.

Absorption spectra of diluted purified Bjgb, in air, showed a Soret peak at 410 nm (Figure 5.1.4., dotted purple line). The position of the Soret peak at 410 nm indicated the presence of the haem cofactor in the oxidised state, suggesting formation of a hexacoordinated haem (Figure 5.1.4., dotted purple line). The spectrum of the reduced derivative was obtained in the presence of excess of sodium dithionite and showed a Soret band at 426 nm and α and β peaks at 560 and 530 nm, respectively (Figure 5.1.4., continuous pink line), indicating that Bjgb is a *b*-type haem protein.

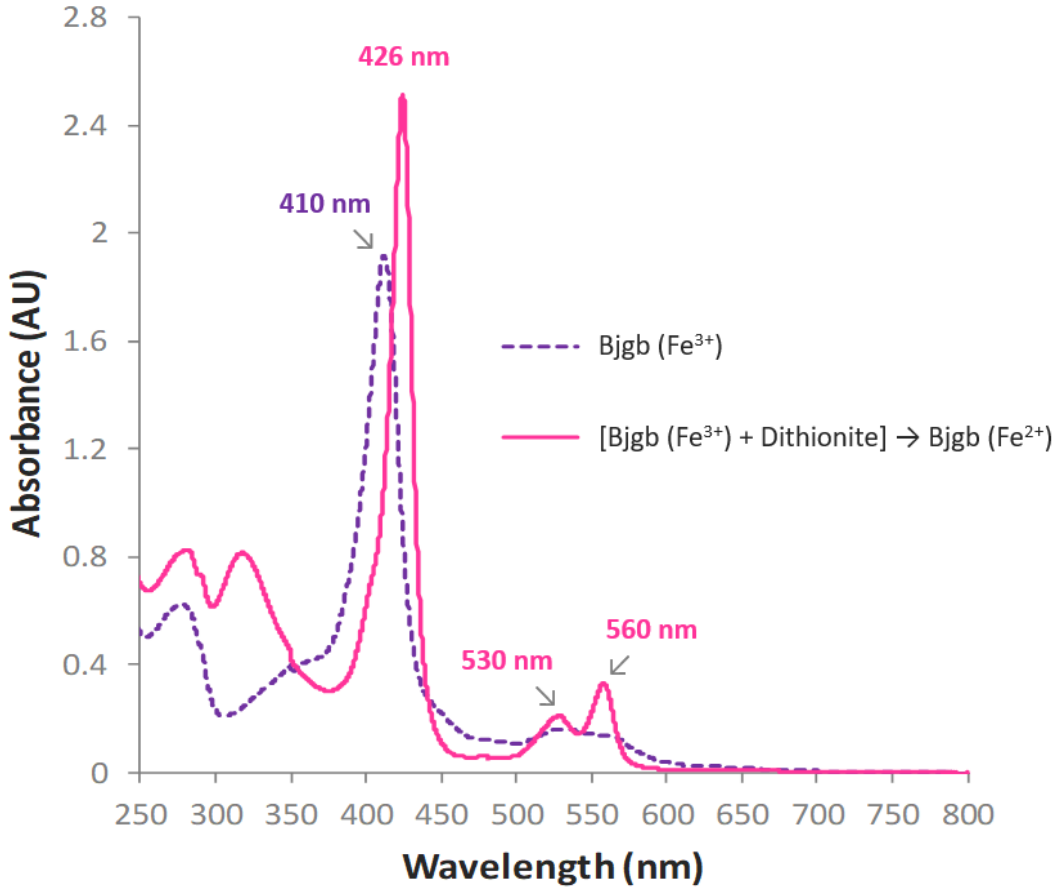

Figure 5.1.4. UV/Vis spectrum of purified Bjgb. Spectrum of oxidized Bjgb (Fe^{3+}) (15 µM) (dotted purple line) and fully reduced Bjgb (Fe^{2+}) (continuous pink line) is shown. Sodium dithionite was added at a final concentration of 50 µM.

Haem-staining of purified Bjgb allowed us to detect a band of about 15 kDa, which corresponds to Bjgb containing a haem cofactor (Figure 5.1.5., lane 'Haem Staining'). An additional haem band, corresponding to dissociated cofactors, was observed at the end of the gel (Figure 5.1.5., lane 'Haem Staining'), suggesting that the haem cofactor is not covalently bound to the Bjgb peptide, as would be the case for a *c*-type cytochrome and, therefore, it is lost despite applying semi-denaturing conditions, consistent with a *b*-type haem protein behaviour in SDS-PAGE.

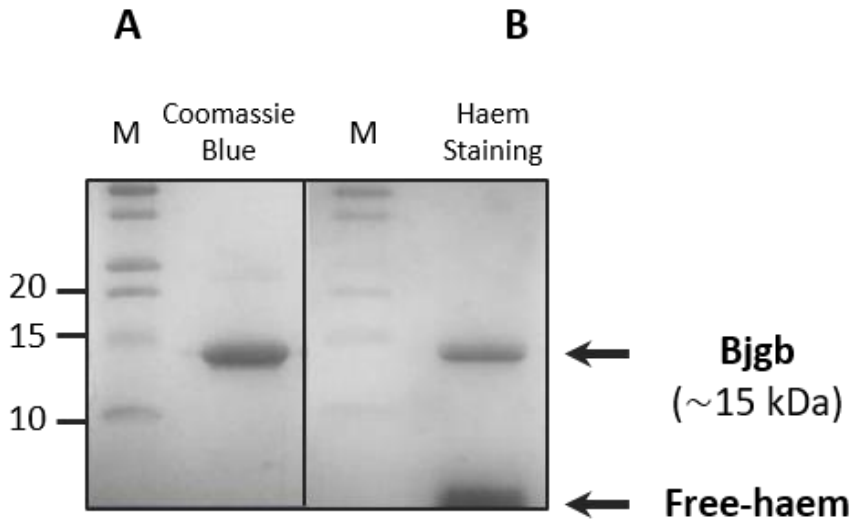

Figure 5.1.5. Haem-staining of Bjgb. SDS-PAGE analysis of purified Bjgb were subjected to Coomassie Blue **(A)** and haem **(B)** staining on replica gels. On the right, the band (~15 kDa), corresponding to Bjgb, is indicated. 'M' corresponds to protein molecular marker PageRuler™ Plus Prestained Protein Ladder. The molecular size, in kDa, and the position of the marker proteins are indicated on the left margin.

5.1.2.2. Expression and purification of Flp

5.1.2.2.1. Construction of the expression plasmid pDB4010

In order to express C-terminally fused His_6-tagged Flp protein, a fragment of 1286 bp, which contains the *flp* (blr2808) gene, was amplified by PCR from pDB4008 using the primer pair 2808_His_For/2808_His_Rev (Table 4.3.). The PCR-amplified DNA fragment was purified and quantified, then, it was digested with *Nhe*I and *Hin*dIII restriction endonucleases and ligated to plasmid pET-24a(+) (5252 bp), that was pre-digested with the aforementioned enzymes (Table 4.2.). The resulting plasmid includes *flp* fused in its 3' end with the histidine tag coding sequence. The correct insertion of the PCR fragment into the vector, as well as the amplified sequence fidelity, were confirmed by sequencing using primers pTXB1-1 and pET28a-1_rev (Table 4.3.). The final construction yielded plasmid pDB4010 (Figure 5.1.6.).

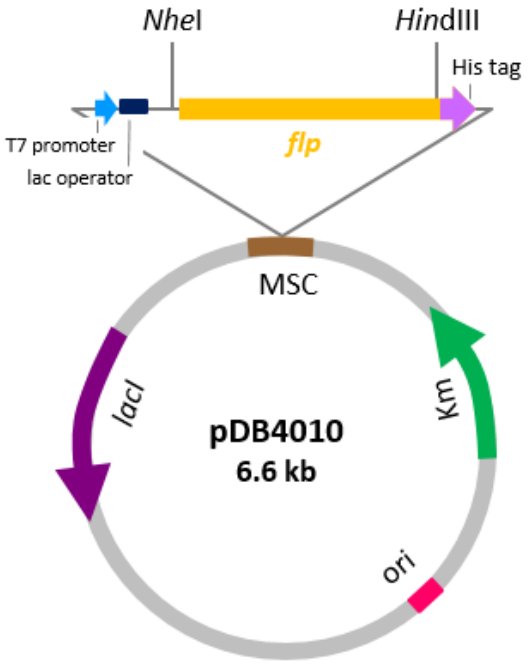

Figure 5.1.6. Construction of the Flp-His$_6$ expression plasmid pDB4010. Plasmid map of plasmid pDB4010. Insertion of *flp* to yield a recombinant protein fused with a histidine tag at its carboxyl terminal end under the control of the T7 promoter. MCS: Multiple Cloning Site.

5.1.2.2.2. Expression of Flp in *E. coli* BL21 (DE3)

E. coli BL21 (DE3) competent cells transformed with plasmid pDB4010 (Table 4.2.) were incubated at 37°C until the cell culture reached an OD_{600nm} ~0.5 (approximately 2 h) (section 4.5.1.). At this time, an aliquot (5 ml) was taken from the culture. Next, 1 mM IPTG was added to the culture, that was incubated at 30°C overnight. After cell harvesting and lysis (see section 4.5.2.), SDS-PAGE analysis of soluble protein extracts showed overexpression of Flp, at approximately 45 kDa, when IPTG was added to the cell culture (Figure 5.1.7., lane 2).

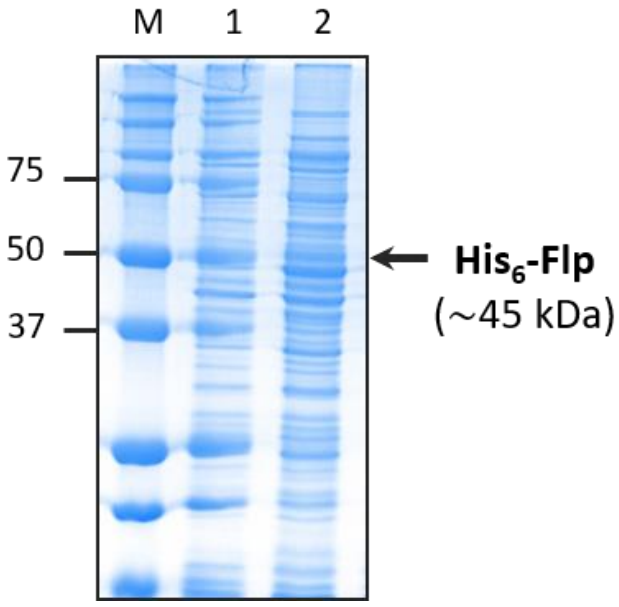

Figure 5.1.7. Overexpression of Flp. *E. coli* BL21 (DE3) cells containing pDB4010 were incubated at 37°C for 2 h. After adding IPTG to the cell culture, cells were lysated and subjected to SDS-PAGE. Then, the gel was stained with Coomassie Blue. A sample was taken from the culture before IPTG induction (lane 1) and another sample after the overnight IPTG incubation (lane 2). On the right margin the band (~45 kDa) corresponding to overexpressed Flp is indicated. 'M' corresponds to protein molecular marker PageRuler™ Plus Prestained Protein Ladder. The molecular size, in kDa, and the position of the marker proteins are indicated on the left margin.

5.1.2.2.3. Purification of Flp

To purify Flp protein, 5 l of *E. coli* BL21 (DE3) competent cells containing plasmid pDB4010 were used. After cell fractionation, soluble extracts containing overexpressed Flp were subjected to affinity chromatography (Figure 5.1.8.A.) (detailed procedure in section 4.5.3.*b.1*). Then, a linear gradient of 25-500 mM imidazole was applied to the column and absorbance at 280 nm was followed. Two peaks at 280 nm corresponding to protein absorbance were observed (Figure 5.1.8.A.). Next, SDS-PAGE analysis of the eluted column fractions allowed the identification of those containing Flp (lanes 14 to 20, Figure 5.1.8.B.). These fractions were pooled and dialyzed using a membrane with 10 kDa molecular mass cut off to remove the excess of imidazole and smaller contaminating proteins (section 4.5.3.*b.2*). After the dialysis, purified Flp gave a single band on SDS-PAGE with an estimated molecular mass ~45 kDa (lane 21, Figure 5.1.8.B.). A yield of 1.4 mg/l of pure protein per culture was obtained.

Absorption spectrum of purified Flp did not show any peak indicative of the presence of a flavin cofactor (Figure 5.1.8.C.). Consequently, Flp had to be reconstituted with FAD for the *in vitro* assays.

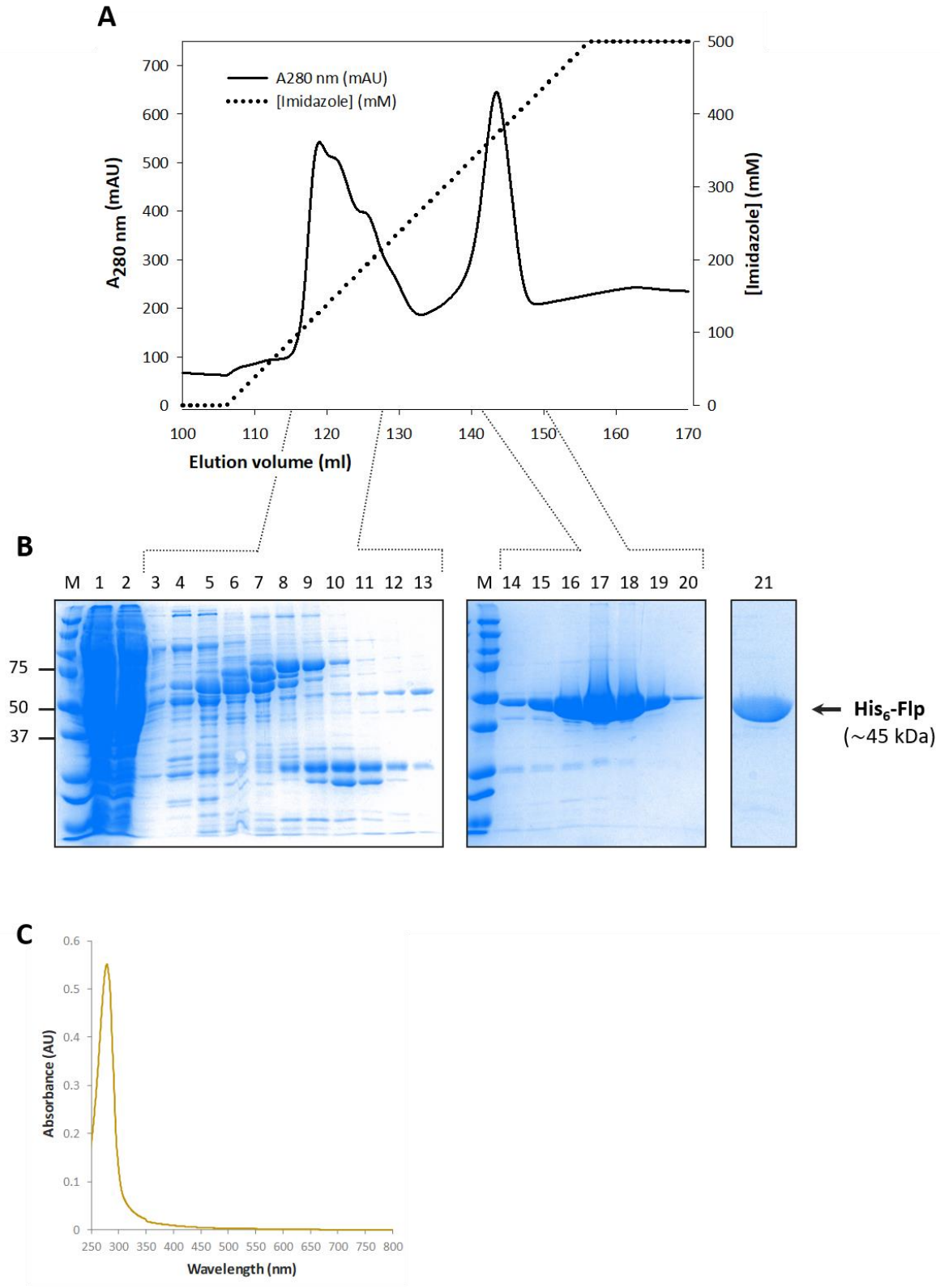

Figure 5.1.8. Purification of Flp. A. Chromatogram obtained during the affinity chromatography of soluble cell extract enriched in Flp. The absorbance at 280 nm (continuous black line, $A_{280\ nm}$) and the imidazole gradient (dotted black line, [imidazole]) were monitored during the chromatography. **B.** After the affinity chromatography, proteins were detected by SDS-PAGE, using Coomassie Blue staining. Lane 1, cell extract; lane 2, cell extract eluted from the affinity column; lane 3 to 20, cell extract eluted from the affinity column after the addition of imidazole gradient; lane 21, purified Flp obtained after the dialysis step. On the right margin, the band (~45 kDa) corresponding to Flp is indicated. 'M' corresponds to protein molecular marker PageRuler™ Plus Prestained Protein Ladder. The molecular size, in kDa, and the position of the marker proteins are indicated on the left margin. **C.** UV/Vis spectrum of purified Flp.

5.1.2.3. Reduction of Bjgb by Flp and NO binding

In order to investigate the role of Flp as redox partner of Bjgb, a spectrum of Bjgb incubated with Flp reconstituted with FAD in the presence of excess of NADH was measured. Before adding Flp to the sample, a control spectrum containing only Bjgb, FAD and NADH was carried out. As shown in Figure 5.1.10.A. (dotted purple line), the haem cofactor remained oxidised (Bjgb Fe^{3+}). However, addition of Flp to the sample resulted in a Bjgb reduced spectrum (Bjgb Fe^{2+}) (Figure 5.1.10.A., continuous red line) similar to that obtained in the presence of excess of sodium dithionite (Figure 5.1.4., continuous pink line), showing a Soret band at 426 nm and α and β peaks at 560 and 530 nm, respectively (Figure 5.1.10.A., continuous red line). These results clearly demonstrated that Flp is essential for flavin-mediated NADH reduction of Bjgb haem cofactor.

In order to determine the NADH concentration needed for a complete Bjgb reduction by Flp, a range of NADH concentrations ranging from 0 to 40 µM was added to the sample mixture containing equimolar concentrations of Bjgb, Flp and FAD (10-15 µM) and a spectrum of each sample was carried out (Figure 5.1.10.A., inset). The absorbance ratio at 556/420 nm of the sample containing each NADH concentration was plotted. As shown in Figure 5.1.10.A. (inset), after ½ equivalent of NADH, full reduction of Bjgb was observed. By performing this assay, we found that 5-7.5 µM was the optimal NADH concentration necessary for full reduction of Bjgb without an excess of electrons. Once Bjgb was reduced with Flp, FAD and NADH (Figure 5.1.10.B., continuous red line), pure NO gas was added to the mixture. As shown in Figure 5.1.10.B. (dotted green line), the addition of NO to the reduced protein yielded

a spectrum with a peak at 420 nm and a broad band in the visible region, which suggested the formation of a five-coordinate NO-bound haem similar to that typical of other NO sensors (Price et al., 2007; Giardina et al., 2008; Rinaldo et al., 2014; Ebert et al., 2017). Similar results were obtained when NO was added to Bjgb reduced with sodium dithionite (Figure 5.1.9., dotted green line). Addition of NO to the incubation mixture caused a change in the Bjgb spectrum similar to that observed in Figure 5.1.10.B. (dotted green line), where Bjgb was first reduced with Flp, FAD and NADH. These spectroscopic results are consistent with the hypothesis that haem-containing Bjgb is reduced by NADH-dependent FAD-reconstituted Flp and binds NO forming a NO derivative typical of a haem protein.

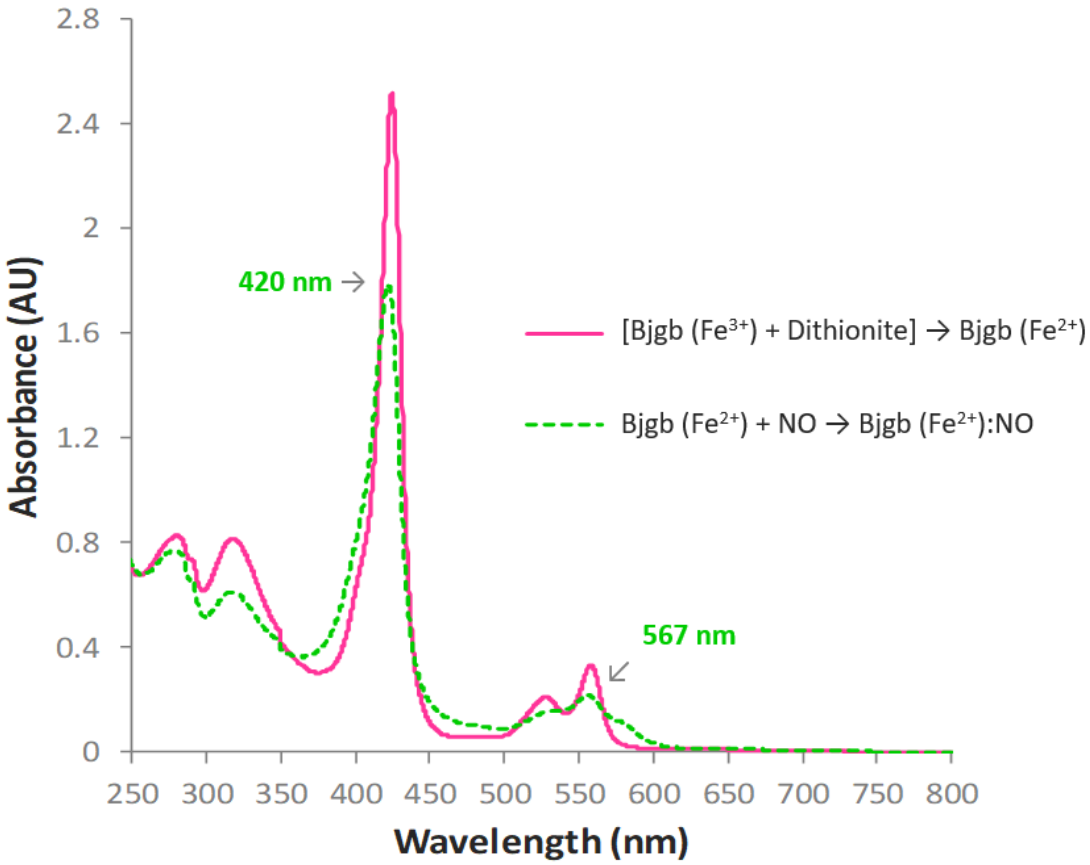

Figure 5.1.9. Influence of NO on the spectroscopic properties of reduced Bjgb. UV/Vis spectrum of reduced Bjgb (Fe^{2+}) with sodium dithionite at a final concentration of 50 µM (continuous pink line). NO was added from a saturated solution (at a final concentration of 50 µM) and the spectrum was recorded again (dotted green line).

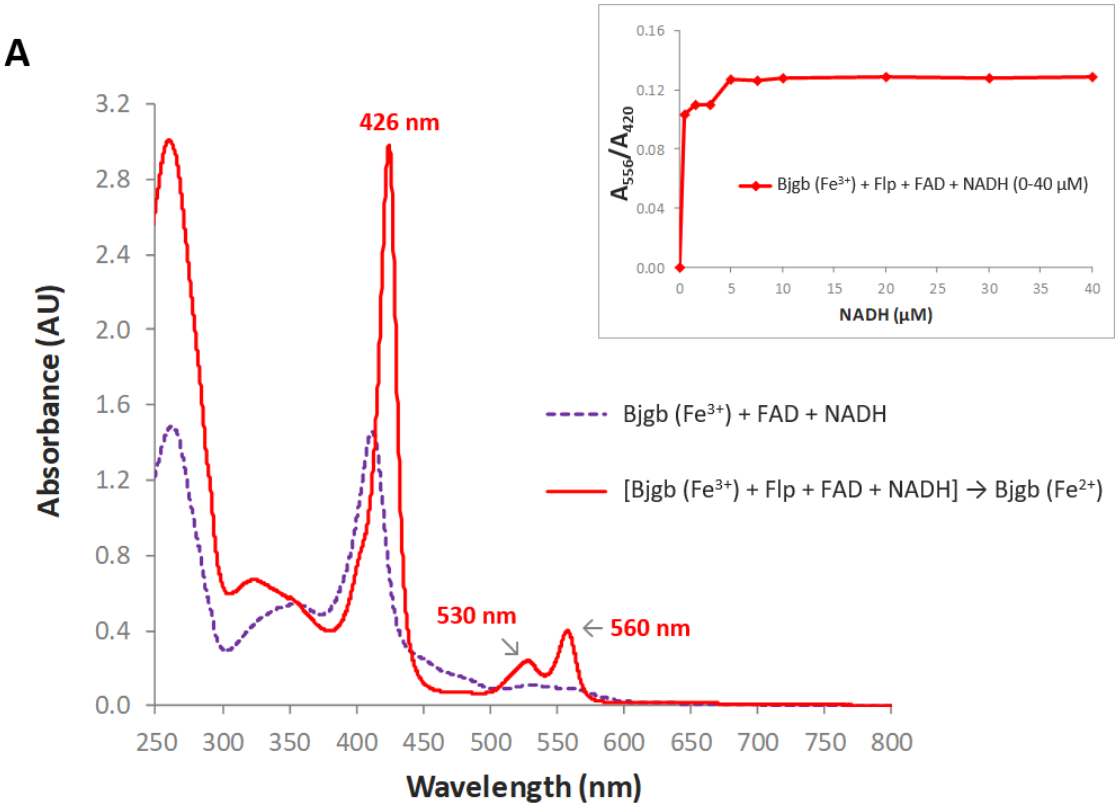
A
426 nm
530 nm
560 nm
Absorbance (AU)
Wavelength (nm)
Bjgb (Fe3+) + FAD + NADH
[Bjgb (Fe3+) + Flp + FAD + NADH] → Bjgb (Fe2+)
A556/A420
Bjgb (Fe3+) + Flp + FAD + NADH (0-40 µM)
NADH (µM)

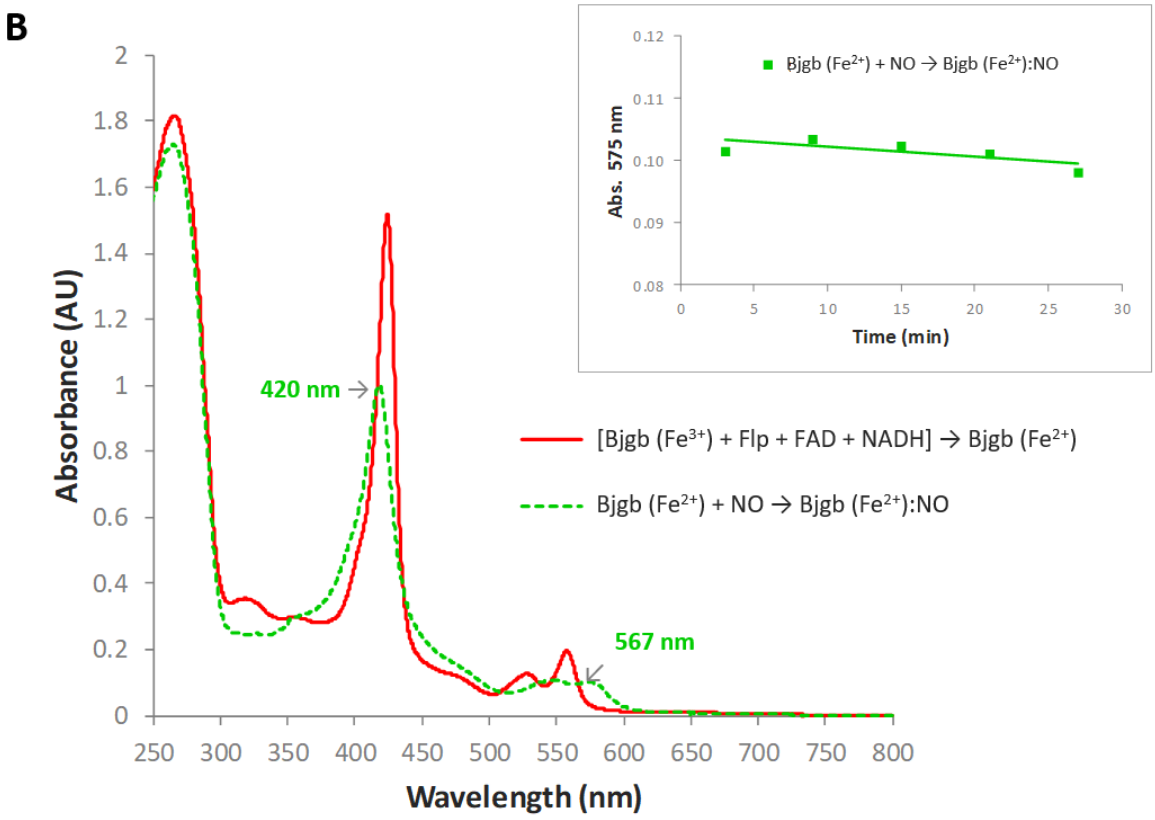
B
420 nm
567 nm
Absorbance (AU)
Wavelength (nm)
[Bjgb (Fe3+) + Flp + FAD + NADH] → Bjgb (Fe2+)
Bjgb (Fe2+) + NO → Bjgb (Fe2+):NO
Abs. 575 nm
Time (min)

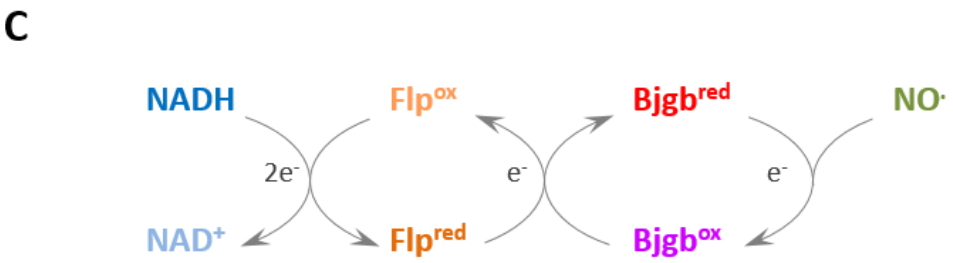

Figure 5.1.10. Influence of Flp and NO on the spectroscopic properties of purified Bjgb. A. UV/Vis spectrum of purified Bjgb (Fe^{3+}) (12 µM) in the presence of FAD (12 µM) and NADH (40 µM) (dotted purple line). UV/Vis spectrum of reduced Bjgb (15 µM) by Flp (15 µM), which was reconstituted with FAD (15 µM), in the presence of NADH (40 µM) (continuous red line). Inset, the ratio A_{556nm}/A_{420nm} of separate reactions [Bjgb (Fe^{3+}) + Flp + FAD + NADH] with different NADH concentrations. NADH concentration ranged from 0 to 40 µM. **B.** UV/Vis spectrum of reduced Bjgb (10 µM) by Flp (10 µM), which was reconstituted with 10 µM of FAD, in the presence of 5 µM of NADH (continuous red line). NO was added from a saturated solution (at a final concentration of 50 µM) and a UV/Vis spectrum was recorded again (dotted green line). Inset, time course of the absorbance at 575 nm after adding NO to the sample. **C.** Schematic representation of the reactions assayed in A and B.

5.1.3. Role of the lysine-52 haem-iron ligand in NO homeostasis *in vivo*

5.1.3.1. Importance of the lysine-52 from Bjgb

A bioinformatic analysis of the *B. diazoeficciens* Bjgb primary amino acid sequence and the predicted gene products for other Hbs homologues from diverse bacteria, confirmed the previously reported presence of the proximal F8 histidine (His^{81}) and CD1 phenylalanine (Phe^{42}) residue (Figure 5.1.11.) (Sánchez et al., 2011a). These residues are considered to be key residues and they are very conserved in bacterial and non-bacterial Hbs (Gardner, 2005). The sequence alignment showed that Bjgb has a lysine-52 (in red in Figure 5.1.11.) that is not conserved in other Hbs (Figure 5.1.11.). Interestingly, the recently *in vitro* structure of *C. reinhardtii* trHb (THB1) exhibited the coordination of the haem Fe by a histidine 77 (proximal) and a lysine-53 (distal), in both the Fe (III) (ferric) and Fe (II) (ferrous) states (Rice et al., 2015). The distal lysine ligation in TrHb1 is related to the ability to coordinate both Fe (III) and Fe (II) and establishing a moderately negative reduction potential to the haem Fe. It has been proposed that this lysine-53 coordination is related to the capacity of THB1 to detoxify NO efficiently (Johnson et al., 2018). Similarly, as it has been demonstrated in

C. reinhardtii, regarding the role of lysine-53 coordination of THB1 in NO detoxification, we can speculate that lysine-52 from Bjgb might have a similar function. To prove this hypothesis, site directed mutation to replace the lysine-52 from Bjgb with a alanine was performed.

```
Q89RG5 Bjgb      -MTPEQITLIQQSFAK---VA-----PISETAAVLFYDRLFEVAPSVRAMFPED---MTE
Q0P842 Cgb       -MTKEQIQIIKDCVPI---LQ-----KNGEDLTNEFYKIMFNDYPEVKPMFNMEKQISGE
P04252 Vgb       MLDQQTINIIKATVPV---LK-----EHGVTITTTFYKNLFAKHPEVRPLFDMGRQESLE
A8JAR4 THB1      --------MAADTAPADSLYSRMGGEAAVEKAVDVFYERIVA-DPQLAPFFANVDMKKQR
P24232 EcfHb     MLDAQTIATVKATIPL---LV-----ETGPKLTAHFYDRMFTHNPELKEIFNMSNQRNGD
Q7WUM8 SmfHb     MLTQKTKDIVKATAPV---LA-----QHGYAIIQHFYKRMFQAHPELKNIFNMAHQERGE
                                              **. :.   *.:  :*

Q89RG5 Bjgb      QRKKLMGMLAAV--VGGLSNLDSILPAASALAKRHVAYGAKAEHYPVVGATLLWTLEKGL
Q0P842 Cgb       QPKALAMAILMA--AKNIENLENMRSFVDKVAITHVNLGVKEEHYPIVGACLLKAIKNLL
P04252 Vgb       QPKALAMTVLAA--AQNIENLPAILPAVKKIAVKHCQAGVAAAHYPIVGQELLGAIKEVL
A8JAR4 THB1      -RKQVAFMTYVFGGSGAYEGRD-LGASH---RRLIREQGMNHHHFDLVAAHLDSTLQELG
P24232 EcfHb     QREALFNAIAAY--ASNIENLPALLPAVEKIAQKHTSFQIKPEQYNIVGEHLLATLDEMF
Q7WUM8 SmfHb     QQQALARAVYAY--AANIENPESLSAVLKDIAHKHASLGVRPEQYPIVGEHLLASIKEVL
                   : :             ..   :                  :: :*.  *  ::.:

Q89RG5 Bjgb      GEAW-----TPELATAWTDAYGVLSGYMISEAYGAQAQAAE
Q0P842 Cgb       NPD-------EATLKAWEVAYGKIAKFYIDIEKKLYDK---
P04252 Vgb       GDAA-----TDDILDAWGKAYGVIADVFIQVEADLYAQAVE
A8JAR4 THB1      VAQELKAEAMAIVASARPLIFGT-------GEAGAAN----
P24232 EcfHb     SPG-------QEVLDAWGKAYGVLANVFINREAEI------
Q7WUM8 SmfHb     GDAA-----TDEIISAWAQAYGNLADILAGMES--------
                        *    :*
```

Figure 5.1.11. Sequence alignment of *B. diazoefficiens* Bjgb with other bacterial Hbs. Sequence alignment of *B. diazoefficiens* USDA 110 sdHb (Bjgb, Q89RG5) with sdHbs from *C. jejuni* (Cgb, Q0P842) and *V. stercoraria* (Vgb, P04252), the haem domain of fHbs from *E. coli* (EcfHb, P24232) and *E. meliloti* 1021 (SmfHb, Q7WUM8), and the trHb from *C. reinhardtii* (THB1, A8JAR4). Identical amino acids are shown by an asterisk. Proximal F8 histidine (His^{81}) and CD1 phenylalanine (Phe^{42}) residues are shown in bold. Lysine-52 from *B. diazoefficiens* USDA 110 Bjgb is shown in red. Lysine-53 from *C. reinhardtii* THB1 is shown in blue. Sequences were obtained from UniProt database (http://www.uniprot.org/) using the accession numbers given in parentheses above. Sequences were aligned by using the Clustal Omega (http://www.ebi.ac.uk/).

5.1.3.2. Strains and plasmids construction

The *bjgb* gene was amplified from genomic DNA isolated from *B. diazoefficiens* USDA 110 by PCR using primers blr2807_For/blr2807_Rev (Table 4.3.), which contained sequences for *Hin*dIII and *Bam*HI restriction sites. DNA fragment containing the relevant ORF and Shine-Dalgarno sequence was cloned into pBBR1MCS-2 (Table 4.2.), that was pre-digested with the aforementioned enzymes, yielding plasmid pDB4023 (Table 4.2.). This plasmid was transferred into *B. diazoefficiens bjgb* mutant

(strain 4001) (Cabrera et al., 2016) by conjugation using *E. coli* S17.1 as donor strain, yielding strain 4001-4023 (Table 4.1.). To construct control strains, the empty vector pBBR1MCS-2 was also transferred into *B. diazoefficiens* USDA 110 and *bjgb* mutant by conjugation using *E. coli* S17.1 as donor strain, generating USDA 110-(pBBR1MCS-2) and 4001-(pBBR1MCS-2) strains (Table 4.1.).

In a second step, *bjgb* gene was isolated from pDB4023 by digesting this plasmid with *Hin*dIII and *Bam*HI and, then, it was cloned into pBS(KS) vector (Table 4.2.), previously digested with the same enzymes, yielding pDB4024 (Table 4.2.). In order to exchange the codon for lysine-52 against an alanine codon, the QuickChange Site-Directed Mutagenesis method was used (see section 4.4.11. for details; Figure 5.1.12.). For this purpose, the complementary primer pairs blr2807(K52A)_For/blr2807(K52A)_Rev (Table 4.3.) and pDB4024 (Table 4.2.) were used. Following this strategy, we obtained plasmid pDB4025 (Table 4.2.), which contained *bjgb* with lysine-52 changed to alanine (K52A). Then, plasmid pDB4025, containing K52A mutated *bjgb* gene, was digested with *Hin*dIII and *Xba*I and cloned into pBBR1MCS-2, yielding plasmid pDB4027 (Table 4.2.). This plasmid was transferred to *B. diazoefficiens bjgb* mutant by conjugation using *E. coli* S17.1 as donor strain, generating strain 4001-4027 (Table 4.1.).

To perform the experiments designed to monitor *norC* expression, plasmids pBBR1MCS-2, pDB4023 and pDB4027 (Table 4.2.) were transferred to *B. diazoefficiens bjgb* mutant containing the transcriptional fusion *norC-lacZ* (4001-2499; Table 4.1.) by conjugation using *E. coli* S17.1 as donor strain. As result of the conjugation, we obtained 4001-2499-(pBBR1MCS-2), 4001-2499-4023 and 4001-2499-4027 strains, respectively (Table 4.1.).

The correct nucleotide sequence of all PCR-amplified fragments cloned into the appropriate plasmids was confirmed by sequencing. The correct insertion of all plasmids transferred into the corresponding recipient strain was confirmed by plasmid extraction and checked by PCR analyses.

Figure 5.1.12. Mutation strategy to replace lysine-52 from Bjgb with alanine. Scheme showing the QuickChange Site-Directed Mutagenesis of two nucleotides (marked in red) in the coding region of the *bjgb* gene. For this purpose, the complete plasmid containing the *bjgb* gene (pDB4024) was amplified using two antiparallel oligonucleotides, that include the mutation in the centre of their sequence. The selection of newly synthesized plasmids was carried out by digestion with *Dpn*I (de novo synthesized DNA presented methylated *Dpn*I targets, so it is not susceptible to digestion).

5.1.3.3. Involvement of lysine-52 in NO homeostasis *in vivo*

In order to establish the role *in vivo* of the lysine-52 from Bjgb, plasmids pDB4023 and pDB4027 (Table 4.2.) overexpressing the native Bjgb or the K52A Bjgb mutant, respectively, were transferred into the *bjgb* mutant (Table 4.1.) for complementation studies. Previous studies have reported that inactivation of the *B. diazoefficiens bjgb* gene provoked an induction of the expression of *nor* genes, encoding the nitric oxide reductase (Cabrera et al., 2016). To further investigate the role of the K52A mutation on *nor* expression, a *norC-lacZ* transcriptional fusion was integrated in the chromosome of the *bjgb* mutant containing plasmids pDB4023 and pDB4027, that overexpress native Bjgb or K52A Bjgb, respectively (Table 4.2.). As controls, the WT USDA 110 and the *bjgb* mutant strains containing pBBR1MCS-2 were also included in the analyses. As reported previously (Cabrera et al., 2016), a significant increase of *norC-lacZ* expression was observed in the *bjgb* mutant compared to WT levels (Figure 5.1.13.A.). However, in the *bjgb* mutant overexpressing the native Bjgb (*bjgb* + Bjgb), a decrease about 8-fold of *norC-lacZ* expression was observed, compared to the expression levels observed in the *bjgb* mutant. By contrast, β-galactosidase activity of the *norC-lacZ* transcriptional fusion was only ∼2-fold lower in the *bjgb* mutant overexpressing K52A Bjgb (*bjgb* + K52A Bjgb) compared to those values reached by the *bjgb* mutant, and no difference was found compared to the WT values (Figure 5.1.13.A.). It has been previously demonstrated that the haem *c* binding NorC component of the nitric oxide reductase corresponds to a protein of about 16 kDa (Mesa et al., 2002; Cabrera et al., 2016). To confirm *nor* expression results, relative amount of NorC was determined by haem-staining analysis of proteins isolated from membranes (Figure 5.1.13.B.). As shown in Figure 5.1.13.B., NorC was induced in membranes from the *bjgb* mutant, compared to the very weak level of this protein detected in membranes from the *bjgb* + Bjgb mutant, containing plasmid pDB4023 that overexpresses Bjgb (Figure 5.1.13.B., lanes 2 and 4). However, when K52A Bjgb was overexpressed in the *bjgb* mutant (*bjgb* + K52A Bjgb) a significant induction of NorC expression was observed, compared to that from membranes of the *bjgb* mutant complemented with the native Bjgb protein (*bjgb* + Bjgb) (Figure 5.1.13.B, lanes 2 and 3).

Finally, we analyzed the effect of K52A Bjgb mutant in Nor activity by measuring the capacity of the cells to produce N_2O, the product of NO reduction catalysed by NorCB reductase. As previously reported by Cabrera and colleagues (2016), the *bjgb* mutant produced more N_2O than WT cells (~3-fold) (Figure 5.1.13.C.). However, the *bjgb* + Bjgb mutant, overexpressing the native Bjgb, produced very low levels of N_2O, probably as a consequence of the very low expression of the *norC-lacZ* fusion, as well as the low levels of NorC observed in this mutant (Figure 5.1.13.A. and B, lane 2). Interestingly, the *bjgb* mutant overexpressing K52A Bjgb (*bjgb* + K52A Bjgb) showed a significant induction (~15-fold) of N_2O production capacity, compared to the very weak N_2O levels produced by the *bjgb* + Bjgb mutant, overexpressing the native Bjgb (Figure 5.1.13.C.). Taken together, these results suggest that the lysine-52 haem-Fe ligand from Bjgb has a critical role in *nor* expression and, consequently, in NO homeostasis *in vivo*.

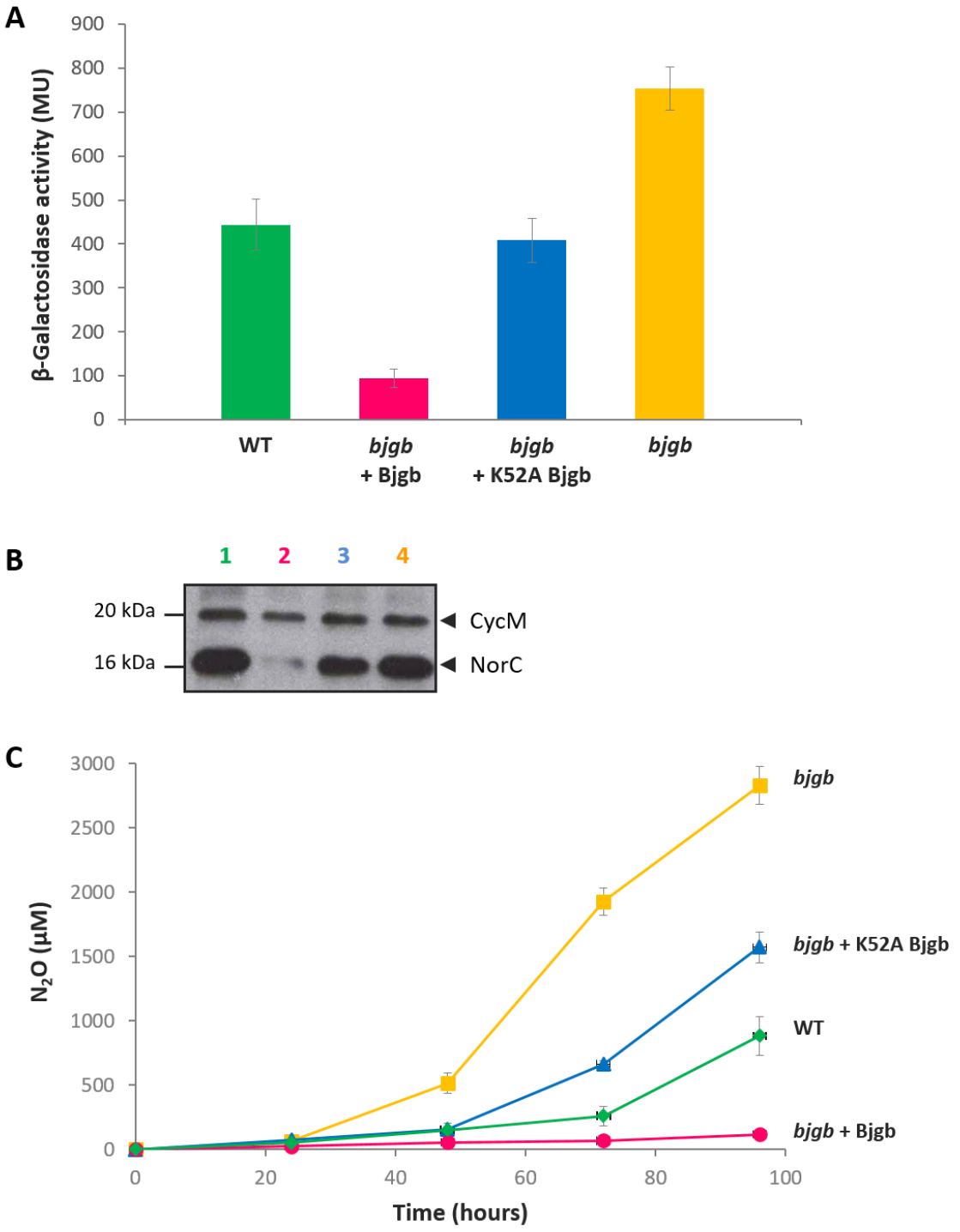

Figure 5.1.13. Effect of K52A Bjgb mutation in nitric oxide reductase expression.
A. β-galactosidase activity from a *norC-lacZ* transcriptional fusion integrated in the chromosome of WT, *bjgb*, *bjgb* + Bjgb and *bjgb* + K52A Bjgb *B. diazoefficiens* strains. **B.** Haem-staining SDS-PAGE analysis of membrane fractions from WT (lane 1), *bjgb* (lane 4), *bjgb* + Bjgb (lane 2) and *bjgb* + K52A Bjgb (lane 3) *B. diazoefficiens* strains. Each lane contains ~10 µg of total protein. Haem-staining bands corresponding to NorC and CycM, which were previously identified, are indicated. **C.** N_2O production. In A and C, data are expressed as mean values with standard deviations from at least two different cultures assayed in triplicate. Cells were cultured in BSN3 minimum medium under 2% O_2 initial concentration and NO_3^- as sole N source.

Chapter 5.2

The haemoglobin Bjgb from *Bradyrhizobium diazoefficiens* controls NO homeostasis in soybean nodules to protect symbiotic nitrogen fixation

Ana Salas, Germán Tortosa, Alba Hidalgo-García, Antonio Delgado, Eulogio J. Bedmar, David J. Richardson, Andrew J. Gates and María J. Delgado

Modified version of manuscript published in *Frontiers in Microbiology* on 10 jan, 2020

Doi: 10.3389/fmicb.2019.02915

5.2. The haemoglobin Bjgb from *Bradyrhizobium diazoefficiens* controls NO homeostasis in soybean nodules to protect symbiotic nitrogen fixation

5.2.1. Abstract

Legume-rhizobia symbiotic associations have beneficial effects on food security and nutrition, health and climate change. Hypoxia induced by flooding produces NO in nodules from soybean plants cultivated in NO_3^--containing soils. As NO is a strong inhibitor of nitrogenase expression and activity, this negatively impacts symbiotic N_2 fixation in soybean and limits crop production. In *B. diazoefficiens*, denitrification is the main process involved in NO formation by soybean flooded nodules. In addition to denitrification, NO_3^- assimilation is another source of NO in free-living *B. diazoefficiens* cells, and a single domain haemoglobin (Bjgb) has been shown to have a role in NO detoxification during NO_3^--dependent growth. However, the involvement of Bjgb in protecting nitrogenase against NO in soybean nodules remains unclear. In this work, we have investigated the effect of inoculation of soybean plants with a *bjgb* mutant on BNF. By analyzing the proportion of N in shoots derived from N_2-fixation using the ^{15}N isotope dilution technique, we found that plants inoculated with the *bjgb* mutant strain had higher tolerance to flooding than those inoculated with the parental strain. Similarly, reduction of nitrogenase activity and *nifH* expression by flooding was less pronounced in *bjgb* than in WT nodules. These beneficial effects are probably due to the reduction of NO accumulation in *bjgb* flooded nodules compared to the WT nodules. This decrease is caused by an induction of expression and activity of the denitrifying nitric oxide reductase enzyme in *bjgb* bacteroids. As *bjgb* deficiency promotes NO-tolerance, the negative effect of NO on nitrogenase is partially prevented and, thus, it demonstrates that inoculation of soybean plants with the *B. diazoefficiens bjgb* mutant confers protection of symbiotic N_2 fixation during flooding.

5.2.2. Bacterial strains

B. diazoefficiens strains used in this study and their description are listed in Table 4.1. Primers sequences in this work are listed in Table 4.3.

5.2.3. Loss of *B. diazoefficiens* Bjgb confers tolerance of soybean symbiotic nitrogen fixation to flooding

After 35 days of growth, nodule number per plant (NNP), nodule dry weight per plant (NDWP) and plant dry weight (PDW) were analyzed (Table 5.2.1.). As previously reported (Mesa et al., 2004), the presence of NO_3^- in the nutrient solution did not inhibit NNP or NDWP in plants inoculated with either the WT or the *bjgb* mutant (Table 5.2.1.). Flooding treatment did not significantly alter NNP in plants grown either in the presence or in the absence of NO_3^-, independently of the strain used as inoculum (Table 5.2.1.). On the contrary, flooding provoked a significant inhibition of NDWP of plants cultivated with or without NO_3^-. Interestingly, those plants inoculated with the *bjgb* mutant and grown with NO_3^- showed higher NDWP in response to flooding (about 30%) than plants that were inoculated with the WT (Table 5.2.1.). As expected, the presence of NO_3^- increased PDW compared to non- NO_3^- treated plants. As shown in Table 5.2.1., in the absence of NO_3^-, flooding did not significantly affect PDW in plants inoculated with any of the strains. However, in NO_3^--treated plants, flooding provoked a negative effect on PDW that was only significant (about 28%) in those plants inoculated with the WT strain, but not in those inoculated with the *bjgb* mutant (Table 5.2.1.). As control of symbiotic N_2 fixation, a set of uninoculated plants were included in the analyses. After 35 days growth, nodulation did not take place in uninoculated plants and very low levels of PDW were observed in those plants grown without NO_3^- (Table 5.2.1.). In plants that were only NO_3^- dependent, flooding decreased PDW about 36% (Table 5.2.1.).

Table 5.2.1. Nodule number per plant (NNP), nodule dry weight per plant (NDWP), and plant dry weight (PDW) of plants inoculated with *B. diazoefficiens* USDA 110 (WT) or 4001 (*bjgb* mutant) strains. Nodules were isolated from plants grown in the absence (-Nitrate) or the presence of 4 mM KNO_3 (+Nitrate). Seven days before harvesting, plants were subjected (+F) or not (-F) to flooding conditions. Values (means ± standard deviations) in a column within the same treatment marked with the same lower-case letter, and values in a column within the same strain followed by the same capital letter, are not significantly different as determined by the ANOVA test at $P \leq 0.05$ (n = 6).

		- Nitrate			+Nitrate		
Strain	**Treatment**	**NNP**	**NDWP (g plant^{-1})**	**PDW (g)**	**NNP**	**NDWP (g plant^{-1})**	**PDW (g)**
USDA 110 (WT)	- F	53 ± 11 aA	0.174 ± 0.046 aA	1.95 ± 0.83 aA	57 ± 8 aA	0.161 ± 0.012 bA	3.40 ± 0.51 aA
	+F	41 ± 12 aA	0.088 ± 0.020 aB	1.66 ± 0.39 aA	48 ± 11 aA	0.057 ± 0.007 bB	2.45 ± 0.26 aB
4001 (*bjgb*)	- F	49 ± 14 aA	0.169 ± 0.048 aA	1.93 ± 0.70 aA	61 ± 9 aA	0.192 ± 0.011 aA	3.61 ± 0.64 aA
	+F	45 ± 9 aA	0.096 ± 0.010 aB	1.49 ± 0.27 aA	52 ± 13 aA	0.081 ± 0.010 aB	2.74 ± 0.96 aA
Uninoculated	- F	-	-	0.65 ± 0.07 bA	-	-	3.25 ± 0.53 aA
	+F	-	-	0.66 ± 0.08 bA	-	-	2.09 ± 0.49 aB

As is indicated in Table 5.2.2., flooding stress provoked a significant decrease in the total N content (TN) of shoots from inoculated plants grown with 4 mM KNO_3 (Table 5.2.2.). Nevertheless, plants inoculated with *bjgb* showed an increase of about 12% in TN compared to plants where the WT was used as inoculum (Table 5.2.2.). In uninoculated plants cultured with NO_3^-, flooding did not affect TN (Table 5.2.2.). In order to differentiate between N acquired from N_2-fixation or NO_3^- assimilation, we used the ^{15}N isotope dilution technique, that allowed us to determine the proportion of N derived from the atmosphere (%Ndfa) in plants that were cultivated with 4 mM ^{15}N-labelled KNO_3. Here, flooding decreased %Ndfa of plants, being this reduction significantly higher in plants inoculated with the WT compared to those inoculated with the *bjgb* mutant (55% *versus* 30%). Consequently, the content of fixed N (FN) of flooded plants inoculated with *bjgb* was about 47% higher than that of flooded plants inoculated with the WT (Table 5.2.2.). These results clearly indicate that inoculation of the plants with the *bjgb* mutant confers tolerance of symbiotic N_2 fixation to flooding. By using the ^{15}N isotope dilution technique, we also calculated the % of ^{15}N atom in excess (atom% ^{15}N excess) of the shoots. As shown in Table 5.2.2., ^{15}N excess in uninoculated plants was significantly higher compared to inoculated plants and no effect of flooding in ^{15}N excess of uninoculated plants was perceived. However, in plants inoculated either with the WT or *bjgb* mutant, flooding increased the % of ^{15}N excess. These results indicate that soybean N_2 fixation is more sensitive to flooding than NO_3^- assimilation, supporting previous findings (Bacanamwo and Purcell, 1999; Sánchez et al., 2011b).

Table 5.2.2. Atom ^{15}N excess, proportion of N derived from the atmosphere (%Ndfa), total N content (TN), and fixed-N content (FN) of shoot tissue of uninoculated plants or plants inoculated with *B. diazoefficiens* USDA 110 (WT) or 4001 (*bjgb* mutant) strains. Plants grown in the presence of 4 mM K $^{15}NO_3$ were subjected (+F) or not (-F) to flooding conditions for 7 days. Values (means ± standard deviations) in a column within the same treatment marked with the same lower-case letter, and values in a column within the same strain followed by the same capital letter, are not significantly different as determined by the ANOVA test at $P \leq 0.05$ (n = 6).

Strain	Treatment	Atom ^{15}N excess (%)	Ndfa (%)	TN (mg g^{-1})	FN (mg g^{-1})
USDA 110 (WT)	- F	2.66 ± 0.30 bB	39.32 ± 6.77 aA	27.97 ± 2.84 aA	10.98 ± 2.03 aA
	+F	3.40 ± 0.45 bA	17.87 ± 5.41 bB	14.94 ± 0.85 bB	2.63 ± 0.64 bB
4001 (*bjgb*)	- F	2.67 ± 0.55 bA	39.16 ± 12.52 aA	26.20 ± 2.55 aA	10.39 ± 2.01 aA
	+F	3.11 ± 0.84 bA	27.45 ± 4.70 aA	16.94 ± 0.90 aB	4.94 ± 0.90 aB
Uninoculated	- F	4.39 ± 0.77 aA	-	12.53 ± 1.41 bA	-
	+F	4.44 ± 0.12 aA	-	13.48 ± 1.54 bA	-

In order to confirm the flooding effect on N_2 fixation, nitrogenase activity was measured by determining ARA in nodules incubated for 2 and 4 h (Figure 5.2.1.). Values for C_2H_4 produced in nmol per min and g NFW (Figure 5.2.2.A.) showed a decrease in ARA (about 55%) for WT nodules isolated from plants submitted to flooding, compared to non-flooded nodules. However, nitrogenase activity only decreased about 30% in *bjgb* nodules from flooded plants, compared to non-flooded *bjgb* nodules (Figure 5.2.2.A.). Functionality of the nodules was also estimated by measuring the leghaemoglobin (Lb) content (Figure 5.2.2.B.). Consistent with ARA determinations, flooding provoked a smaller decrease of Lb content in nodules produced by the *bjgb* mutant (about 22%), compared to that observed in WT nodules (about 55%).

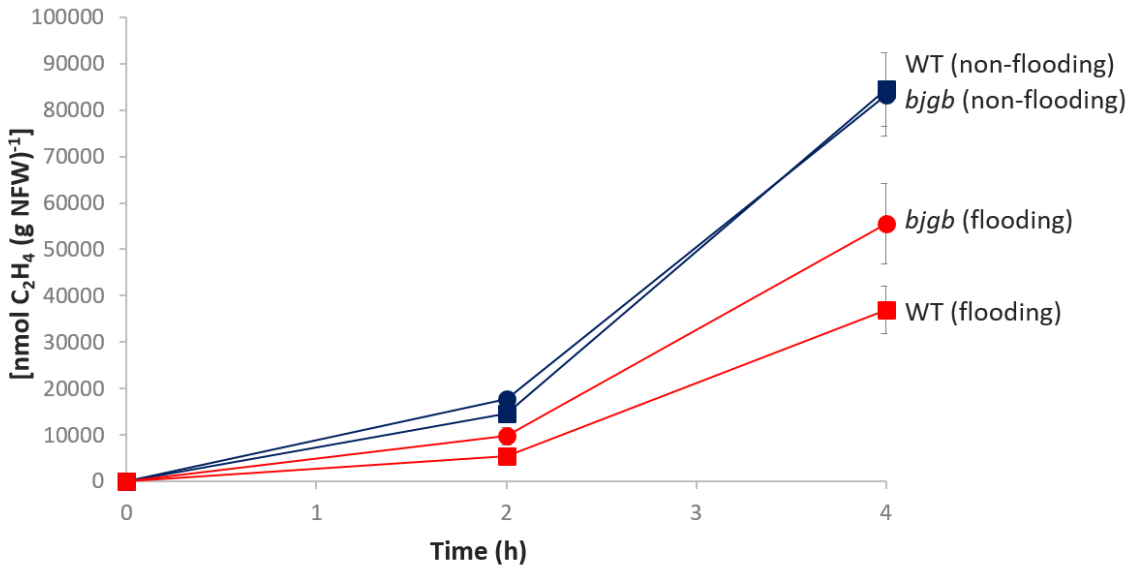

Figure 5.2.1. Ethylene emission by soybean nodules. Plants were inoculated with *B. diazoefficiens* USDA 110 (WT) (squares) or 4001 (*bjgb* mutant) (circles) strains. Nodules were isolated from non-flooded plants (blue symbols) or plants subjected to flooding conditions for 7 days (red symbols). Data are means with standard deviations from two independent experiments assayed by using six replicates.

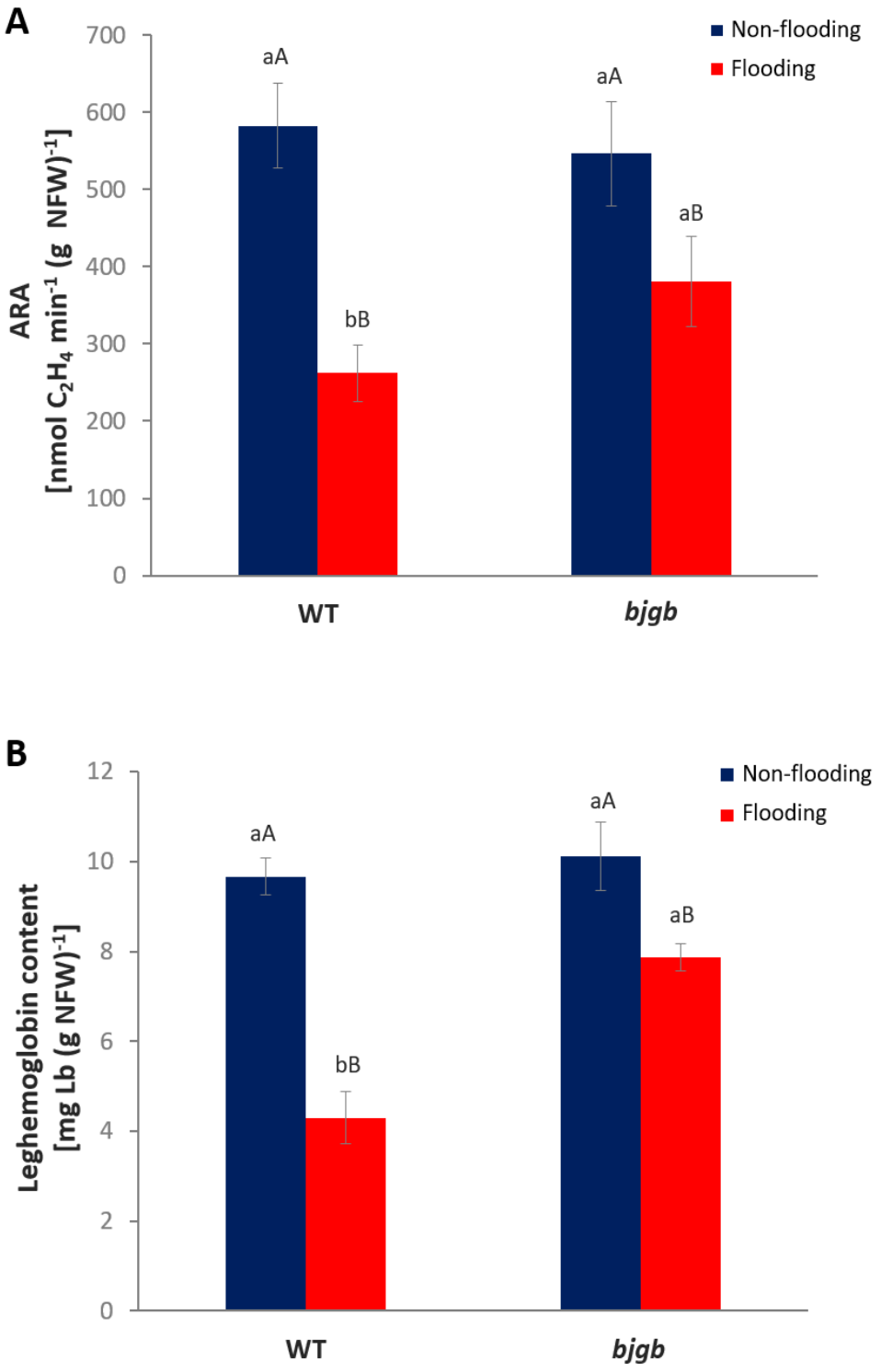

Figure 5.2.2. A. Acetylene reduction activity (ARA) and B. Leghaemoglobin (Lb) content of soybean nodules. Plants were inoculated with *B. diazoefficiens* USDA 110 (WT) or 4001 (*bjgb* mutant) strains. Nodules were isolated from non-flooded plants (blue bars) or plants subjected to flooding conditions for 7 days (red bars). Data are means with standard deviations from two independent experiments assayed by using six replicates. In individual graphs, bars within the same treatment marked with the same lower-case letter, and bars within the same strain followed by the same capital letter, are not significantly different as determined by the ANOVA test at $P \leq 0.05$.

Next, we tested the effect of deleting *bjgb* on the expression of the *nifH* gene, which is responsible for the synthesis of the Fe-protein from nitrogenase complex (Table 5.2.3.). Transcript levels for *nifH* were examined in WT or *bjgb* nodules by qRT-PCR. As observed in Table 5.2.3., *nifH* expression was not significantly affected in the nodules induced by the *bjgb* mutant (-1.31 fold-change) compared to WT nodules, both collected from non-flooded plants. Flooding decreased *nifH* expression by ∼16-fold in WT nodules, compared to that observed in WT non-flooded nodules. However, *nifH* mRNA levels decreased by ∼10-fold in *bjgb* flooded nodules, compared to those observed in WT non-flooded nodules.

Table 5.2.3. Expression of *narK*, *nifH* and *norC* in nodules measured by qRT-PCR. Nodules were harvested from plants inoculated with *B. diazoefficiens* USDA 110 (WT) or 4001 (*bjgb* mutant) strains. Plants were grown in the presence of 4 mM KNO_3 and subjected (or not) to flooding conditions for 7 days. Data are means ± standard deviations from there independent RNA samples assayed by using three replicates. nd, not determined, +, increased expression, -, decreased expression.

		Relative amount of transcript (fold-change)	
Strain	**Gene**	**No flooding**	**Flooding**
USDA 110 (WT)	*narK*	1.00 ± 0.00	+11.18 ± 1.85
4001 (*bjgb*)	*narK*	nd	nd
USDA 110 (WT)	*nifH*	1.00 ± 0.00	- 16.33 ± 3.07
4001 (*bjgb*)	*nifH*	-1.31 ± 0.28	-10.61 ± 1.91
USDA 110 (WT)	*norC*	1.00 ± 0.00	+67.53 ± 6.86
4001 (*bjgb*)	*norC*	+1.12 ± 0.28	+89.16 ± 8.59

In order to ascribe the effect of *bjgb* inoculation to the presence of Bjgb in the nodules, we checked the expression of the *bjgb* gene by analyzing transcript levels of *narK,* the lead gene of the *narK-bjgb-flp-nasC* transcriptional unit (Cabrera et al., 2016) (Table 5.2.3.). As shown in Table 5.2.3., *narK* expression increased ∼11-fold in flooded nodules compared to non-flooded nodules collected from plants inoculated with the WT strain.

5.2.4. Loss of *B. diazoefficiens* Bjgb reduces NO levels in soybean nodules in response to flooding

The contribution of *B. diazoefficiens* Bjgb in NO homeostasis in nodules was investigated by analyzing the capacity to accumulate NO, as well as to produce N_2O, the product of the nitric oxide reductase (Nor). To perform these experiments, we used nodules from plants grown under the conditions that induced NO and N_2O accumulation, as previously reported (Sánchez et al., 2010; Tortosa et al., 2015). Thus, nodules were collected from soybean plants inoculated with *B. diazoefficiens* USDA 110 (WT) or 4001 (*bjgb* mutant) strains, cultivated with 4 mM NO_3^- and submitted (or not) to flooding conditions for 7 days before harvesting. Free NO was detected by using the DAF-2DA specific fluorescent probe. As shown in Figure 5.2.3.A., very low levels of NO were observed in WT and *bjgb* nodules of non-flooded plants. However, flooding significantly induced NO formation in WT nodules, confirming previous results (Sánchez et al., 2010). This induction was also observed in nodules from plants inoculated with the *bjgb* mutant, that accumulated approximately 2-fold less NO than WT nodules in response to flooding conditions (Figure 5.2.3.A.). In order to prove that the increase of fluorescence perceived in flooded nodules was caused by NO, WT and *bjgb* flooded nodules were incubated with a NO scavenger (c-PTIO). After incubation of the nodules with c-PTIO, nodular NO accumulation was significantly reduced (Figure 5.2.3.A.), indicating that the fluorescence signal was mostly due to NO production.

We also analyzed Nor activity by measuring N_2O production by soybean nodules using gas chromatography. While non-flooded nodules produced by WT or *bjgb* strains showed basal levels of N_2O, flooding conditions induced N_2O production in *B. diazoefficiens* WT nodules, consistent with previous observations (Tortosa et al., 2015). Interestingly, nodules produced by the *bjgb* mutant accumulated about 2-fold

more N_2O than WT nodules in response to flooding (Figure 5.2.3.B.). The lower NO levels, as well as higher N_2O production capacity observed in the nodules from the *bjgb* mutant compared to WT levels (Figure 5.2.3.A. and B.), suggest that Nor activity, that reduces NO to N_2O, is induced in *bjgb* bacteroids. In order to establish if the differences of Nor activity observed between WT and *bjgb* bacteroids could be explained by changes in *nor* gene expression, *norC* transcripts were measured by performing qRT-PCR analyses. RNA was isolated from nodules harvested from soybean plants inoculated with *B. diazoefficiens* WT or *bjgb* mutant strains. In nodules from plants that were not subjected to flooding, *bjgb* mutation did not significantly affect *norC* expression compared to WT (+1.12 fold-change). Flooding provoked a notable increase of *norC* expression in either WT or *bjgb* flooded-nodules, compared to WT non-flooded nodules (+67.53 and +89.16 fold-change, respectively). Interestingly, the induction of *norC* expression by flooding was about 33% higher in *bjgb* nodules than in WT nodules (Table 5.2.3.).

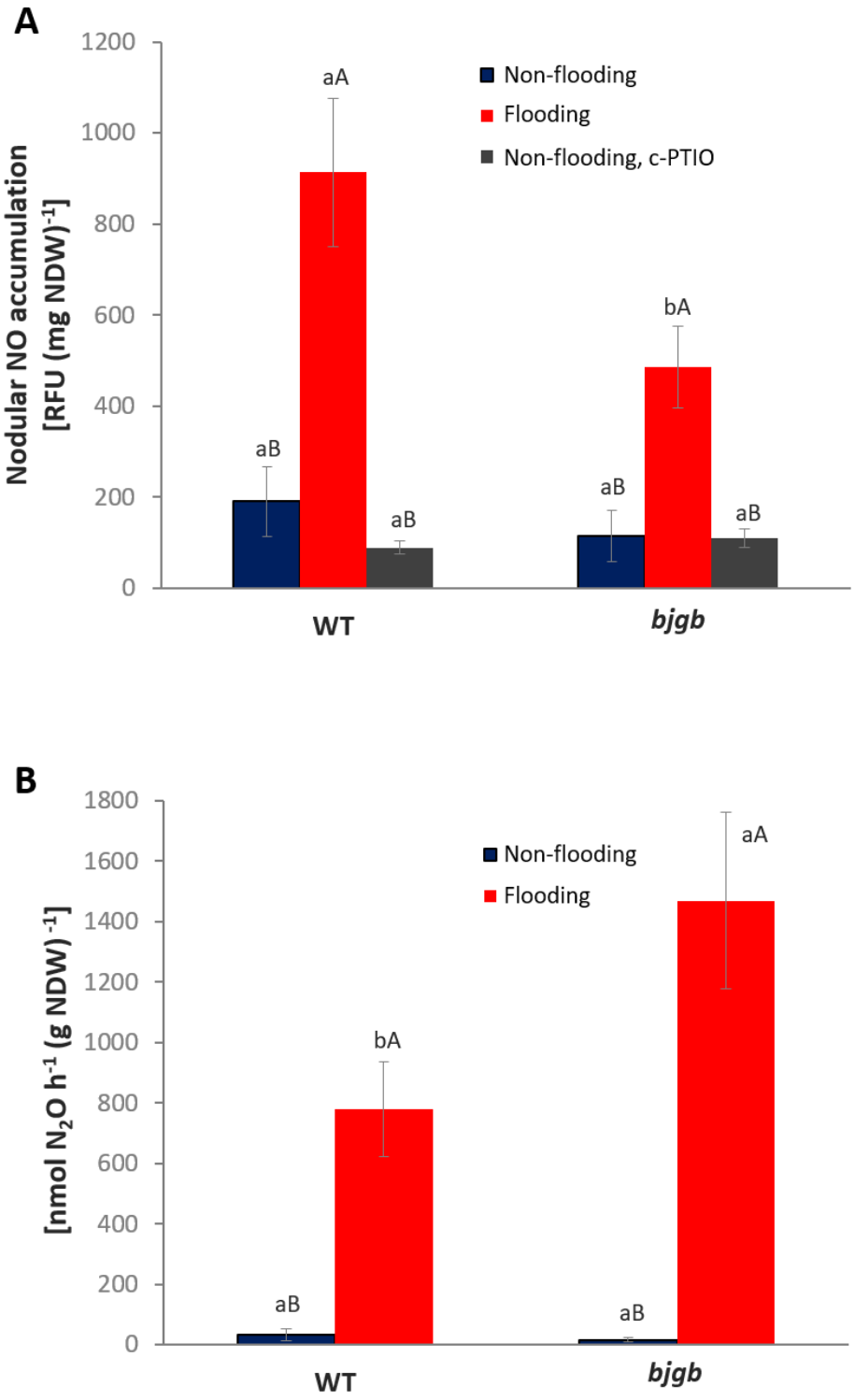

Figure 5.2.3. A. NO detection and B. N_2O production by soybean nodules. Plants were inoculated with *B. diazoefficiens* USDA 110 (WT) or 4001 (*bjgb* mutant) strains. Nodules were isolated from non-flooded plants (blue bars) or plants subjected to flooding conditions for 7 days (red bars). In A, flooded nodules were incubated with 3 mM c-PTIO (grey bars). Data are means with standard deviations from two independent experiments assayed by using six replicates. In individual graphs, bars within the same treatment marked with the same lower-case letter, and bars within the same strain followed by the same capital letter, are not significantly different as determined by the ANOVA test at $P \leq 0.05$.

Chapter 5.3

The role of nitrate assimilation in the *Bradyrhizobium diazoefficiens*-soybean symbiosis

5.3. The role of nitrate assimilation in the *Bradyrhizobium diazoefficiens*-soybean symbiosis

5.3.1. Abstract

Previous studies have reported that hypoxia induces the production of NO in nodules of soybean plants cultivated in NO_3^--containing soils. NO is a strong inhibitor of nitrogenase expression and activity. Consequently, NO accumulation negatively impacts symbiotic N_2 fixation. In soybean nodules, *B. diazoefficiens* denitrification is the main process involved in NO formation (Sánchez et al., 2010). In addition to denitrification, *B. diazoefficiens* free-living cells possess an integrated system for NO_3^- assimilation and NO detoxification, encoded by the *narK-bjgb-flp-nasC* operon. In this system, the assimilatory nitrate reductase, NasC, reduces NO_3^- to NO_2^-, and the nitrite reductase, NirA, reduces NO_2^- to NH_4^+ (Cabrera et al., 2016). In addition to reducing NO_3^- to NO_2^-, NasC also contributes to NO formation during NO_3^-/NO_2^- assimilation. However, to date, the role of NasC and NirA in soybean nodules remains unclear.

In this work, we have investigated the involvement of *B. diazoefficiens nasC* and *nirA* mutants on symbiotic N_2 fixation. By analyzing nitrogenase activity in nodules, we found that plants inoculated with a *nasC* mutant showed a similar response to flooding than those inoculated with the parental strain, while plants inoculated with *nirA* were more tolerant to flooding. Furthermore, nitrate reductase (NR) activity of *nasC* bacteroids from flooded nodules was similar to that observed from bacteroids induced by the parental strain. However, NR activity of bacteroids from plants inoculated with a *napA* mutant was undetectable. These results indicate that NasC has not a relevant role in NO_3^- reduction in bacteroids, being the periplasmic nitrate reductase (NapA) the main enzyme involved.

In this work, we also studied the involvement of NO_3^- assimilation in the symbiosis *B. diazoefficiens*-soybean by inoculating plants with a *nifH* mutant, where N_2 fixation does not take place. We measured the transcript levels of *narK*, which is the lead gene of the *narK-bjgb-flp-nasC* transcriptional unit (Cabrera et al., 2016). These results revealed that *narK* expression increased in *nifH* nodules from plants grown with NO_3^-, compared to parental nodules. Moreover, *nifH* nodules from plants treated with

NO_3^- showed a higher NH_4^+ content in the bacteroids than those from plants grown in the absence of NO_3^-. Taken together, these results suggest that assimilatory NO_3^- reduction might have a relevant role in soybean nodules in those cases in which N_2 fixation is impaired.

5.3.2. Bacterial strains

All *B. diazoefficiens* strains used in this work and their description are listed in Table 4.1. Sequence of primers used in this study are shown in Table 4.3. As parental strains (WT), *B. diazoefficiens* USDA 110 and *B. diazoefficiens* 110*spc*4 were used in this work. *B. diazoefficiens napA* (Delgado et al., 2003), *nasC* (Cabrera et al., 2016) and *nirA* (Cabrera et al., 2016) mutants were constructed previously from *B. diazoefficiens* USDA 110 (WT). While *B. diazoefficiens nifH* mutant was obtained from *B. diazoefficiens* 110*spc*4 by Hahn and colleagues (1984).

5.3.3. Involvement of *B. diazoefficiens* NasC and NirA in the response of soybean symbiotic nitrogen fixation to flooding

The *nasC* and *nirA* mutants were used to inoculate soybean germinated seeds, that were grown with 4 mM KNO_3 and subjected (or not) to flooding for 7 days before harvesting. As mention in Chapter 5.2., this NO_3^- concentration was selected based on a previous work (Mesa et al., 2004) because it does not inhibit nodule formation. After 35 days of growth, the effect of flooding on nodule biomass and plant dry weight (see Chapter 5.2.) was similar independently of the strain used as inoculant (data not shown). As we observed in Chapter 5.2., a decrease in ARA (about 55%) was observed in WT nodules from plants subjected to flooding, compared to non-flooded nodules. Similarly to WT nodules, flooding also provoked a significant decrease of nitrogenase activity (about 39%) in *nasC* nodules. By contrast, the ARA of nodules induced by the *nirA* mutant was not affected by flooding (Figure 5.3.1.A.). We also included in these analyses nodules from plants inoculated with a *napA* mutant, defective in the periplasmic nitrate reductase. Consistent with that previously reported by Sánchez and colleagues (2010), flooding did not affect nitrogenase activity in *napA* nodules (Figure 5.3.1.A.). Functionality of the nodules was also estimated by measuring the Lb content (Figure 5.3.1.B.). Consistent with ARA determinations, flooding provoked a significant decrease of Lb content in nodules produced by the WT or *nasC* mutant

(56% and 32%, respectively). However, Lb levels were not significantly affected by flooding either in *nirA* or *napA* nodules, compared to those levels observed in non-flooded nodules.

We also investigated the contribution of NasC and NapA to NR activity of the bacteroids. Previous studies have demonstrated that NR activity was not detectable in free-living cells of the *nasC* mutant cultured aerobically with NO_3^- as the only N source (Cabrera et al., 2016). On the contrary, in this work we have observed WT levels of NR activity in *nasC* bacteroids from flooded plants (Figure 5.3.1.C.). As previously reported (Sánchez et al., 2010), flooding induced about 2-fold bacteroidal NR activity in WT nodules, being this activity undetectable in *napA* nodules (Figure 5.3.1.C.). Taken together, these results suggest that NapA is the main enzyme responsible for NO_3^- reduction in bacteroids, while NasC does not have a relevant role. These observations would explain the weak effect of *nasC* inoculation on the response of symbiotic N_2 fixation to flooding.

A

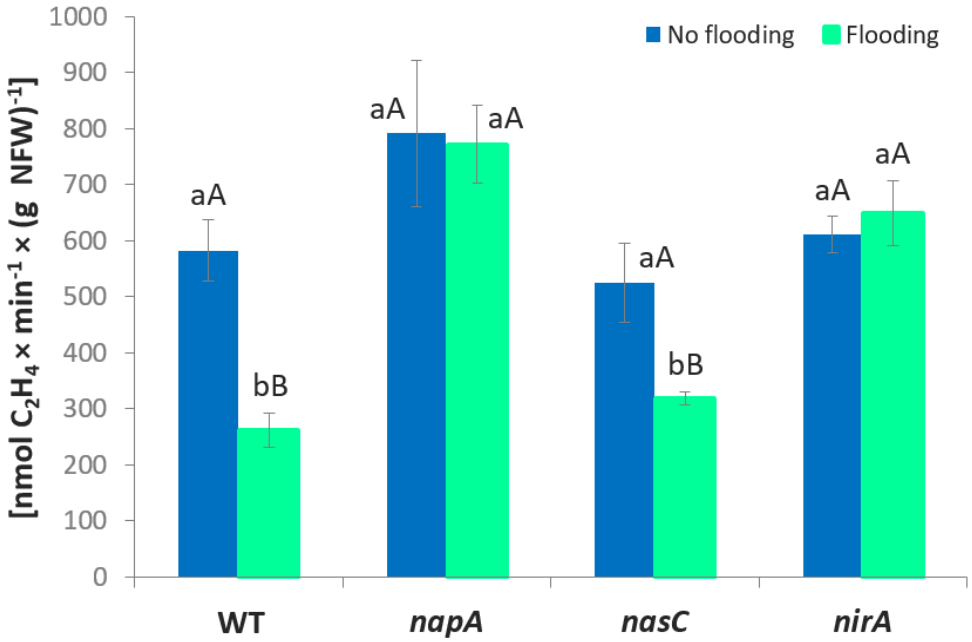

B

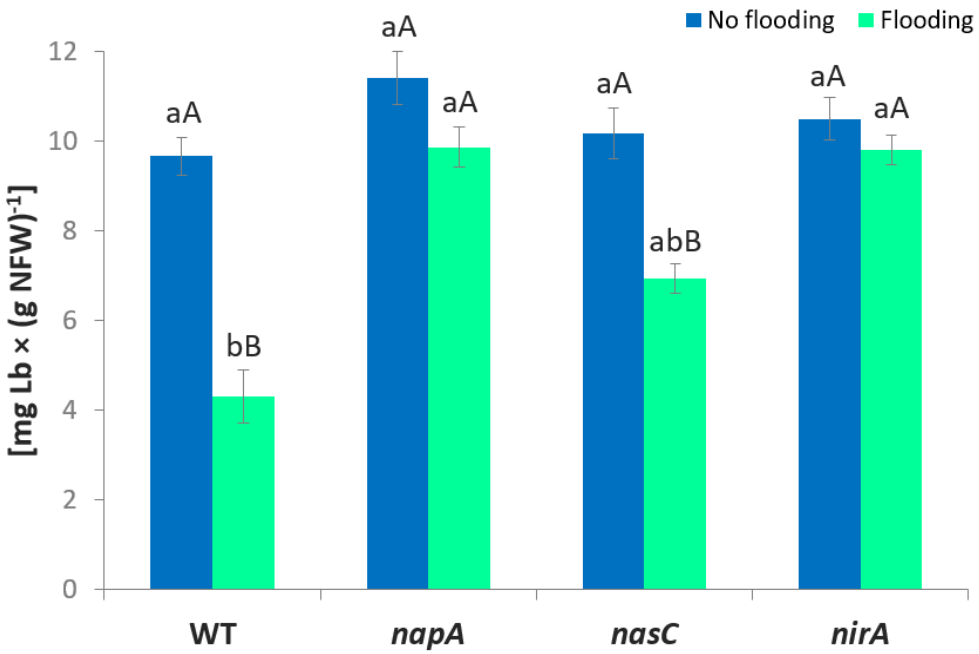

C

NR activity [nmol NO_2^- × min^{-1} × (mg protein)$^{-1}$]		
Strain	**No flooding**	**Flooding**
WT	5.26 ± 0.58 aB	8.38 ± 0.88 aA
napA	nd	nd
nasC	4.06 ± 0.46 aB	9.89 ± 0.64 aA

Figure 5.3.1. A. Acetylene reduction activity (ARA) B. Leghaemoglobin content (Lb) in nodules. C. Nitrate reductase (NR) activity in bacteroids. Plants were inoculated with *B. diazoefficiens* USDA 110 (WT), GRPA1 (*napA* mutant), 4003 (*nasC* mutant) or 4011 (*nirA* mutant) strains. Nodules were isolated from non-flooded plants or plants subjected to flooding for 7 days. Plants were grown in the presence of 4 mM KNO_3. Data are means with standard deviations from two independent experiments assayed by using six replicates. In individual graphs, bars within the same treatment marked with the same lower-case letter, and bars within the same strain followed by the same capital letter, are not significantly different as determined by the ANOVA test at $P \leq 0.05$. Values of table in a column within the same treatment marked with the same lower-case letter, and values in a column within the same strain followed by the same capital letter, are not significantly different as determined by the ANOVA test at $P \leq 0.05$ (n = 6). nd = not detected.

5.3.4. Role of nitrate assimilation in non-nitrogen fixing nodules

Results from Chapter 5.3.3. have revealed that assimilatory NO_3^- reduction to NO_2^- by NasC does not have a role in symbiotic N_2 fixation. This observation might be due to very low expression of NasC in the presence of NH_4^+, the product of nitrogenase. In fact, it is very well established in free-living bacteria that assimilatory NO_3^- reduction is repressed by NH_4^+ (Moreno-Vivián et al., 1999, 2007). In order to investigate the potential role of NO_3^- assimilation in nodules, we inoculated soybean plants with a *nifH* mutant that induces nodule formation, however, they are unable to reduce N_2 to NH_4^+ in the bacteroids (Hahn et al., 1984). After 35 days of plant growth, nodule number per plant (NNP), nodule fresh weight per plant (NFWP) and plant dry weight (PDW) were analyzed (Table 5.3.1.). Confirming previous results (Mesa et al., 2004), the presence of NO_3^- in the nutrient solution did not inhibit NNP or NFWP in plants inoculated with the WT (Table 5.3.1.). Inoculation with the *nifH* mutant did not alter NNP of plants grown either in the absence or in the presence of NO_3^-. Values obtained were very similar to those observed in plants inoculated with the parental strain (Table 5.3.1.). As previously reported (Hahn et al., 1984), plants inoculated with the *nifH* mutant and cultivated without NO_3^- showed lower NFWP (about 66%) than plants inoculated with the WT and grown under the same conditions (Table 5.3.1.). However, when NO_3^- was added to the nutrient solution, NFWP of plants inoculated with the *nifH* mutant was restored to WT levels (Table 5.3.1.). Interestingly, the individual weight of nodules (NFWP divided by NNP) from plants inoculated with the *nifH* increased significantly (about 52%), relative to those isolated from plants that grew only by N_2 fixation

(16 mg and 7.7 mg, respectively). As expected, plants inoculated with the *nifH* mutant and cultivated without NO_3^- presented 4-fold lower PDW, compared to those inoculated with the WT. The presence of NO_3^- increased PDW, compared to non-NO_3^- treated plants, and no differences were observed between plants inoculated with the WT and those inoculated with the *nifH* mutant (Table 5.3.1.).

Table 5.3.1. Nodule number per plant (NNP), nodule fresh weigth per plant (NFWP) and plant dry weigth (PDW) of plants inoculated with *B. diazoefficiens* 11*spc*4 (WT) or H1 (*nifH* mutant) strains. Plants were grown in the absence (-N) or the presence of 4 mM KNO_3 (+N). Values (means ± standard deviations) in a column within the same treatment marked with the same lower-case letter, and values in a column within the same strain followed by the same capital letter, are not significantly different as determined by the ANOVA test at $P \leq 0.05$ (n = 6).

Strain	Treatment	NNP	NFWP (g plant^{-1})	PDW (g)
WT	-N	32 ± 9 aA	0.70 ± 0.19 aA	2.01 ± 0.48 aB
	+N	38 ± 11 aA	0.65 ± 0.21 aA	3.32 ± 0.49 aA
nifH	-N	31 ± 6 aA	0.24 ± 0.05 bB	0.50 ± 0.07 bB
	+N	36 ± 7 aA	0.58 ± 0.13 aA	3.29 ± 0.46 aA

To estimate nodule functionality, Lb content was determined as an indicative parameter of the nodule N_2 fixing fitness. As expected, Lb content in *nifH* nodules decreased, compared to WT nodules from plants that were grown either without or with NO_3^-. Nitrate did not alter Lb content in nodules produced by either WT or *nifH* mutant (Figure 5.3.2.).

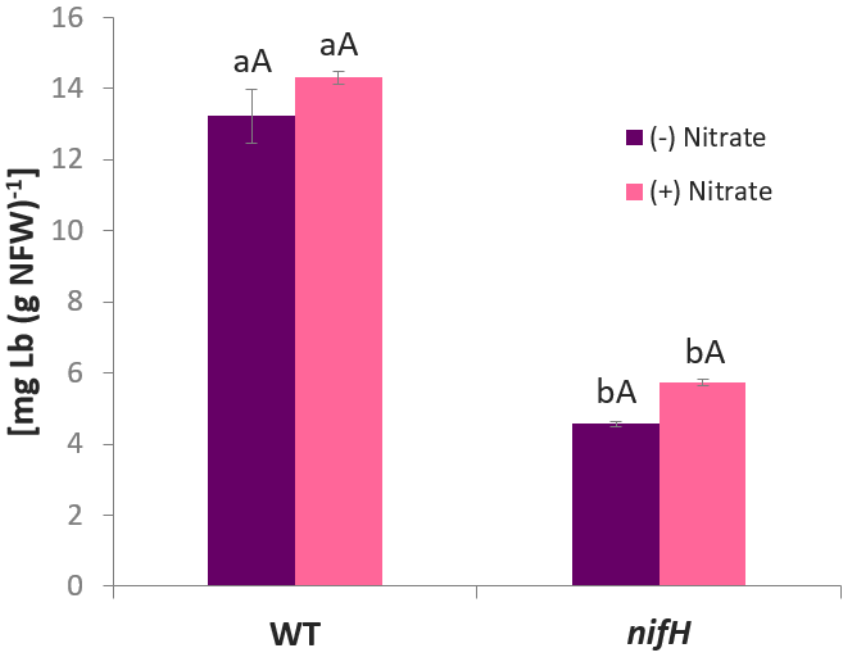

Figure 5.3.2. Leghaemoglobin content (Lb) in nodules. Plants were inoculated with *B. diazoefficiens* 11*spc*4 (WT) or H1 (*nifH* mutant) strains. Nodules were isolated from plants grown in the absence (-Nitrate) or the presence of 4 mM KNO_3 (+Nitrate). Data are means with standard deviations from two independent experiments assayed by using six replicates. In individual graphs, bars within the same treatment marked with the same lower-case letter, and bars within the same strain followed by the same capital letter, are not significantly different as determined by the ANOVA test at $P \leq 0.05$.

The contribution of bacteroidal NO_3^- assimilation in soybean nodules was also investigated by measuring the expression of *narK*, the lead gene of the *narK-bjgb-flp-nasC* transcriptional unit, in nodules produced by the *nifH* mutant. We also examined the production of NH_4^+, the product of NO_3^- assimilation and nitrogenase activity, in the bacteroids. Transcript levels of *narK* were analyzed after RNA isolation from nodules collected from NO_3^--treated soybean plants that were inoculated with *B. diazoefficiens* WT or *nifH* mutant. As shown in Table 5.3.2., *narK* expression increased ~88-fold in *nifH* nodules compared to parental nodules. NH_4^+ content was determined in bacteroids isolated from nodules of plants grown in the absence or the presence of NO_3^- (Figure 5.3.3.). As expected, bacteroids induced by the *nifH* mutant and isolated from nodules of plants grown under N_2 fixation dependent conditions were strongly impaired in their capacity to produce NH_4^+, due to the lack of

nitrogenase. However, when NO_3^- was present in the nutrient solution, *nifH* bacteroids showed significant levels of NH_4^+ that probably might be produced by the NO_3^- assimilatory pathway (Figure 5.3.3.).

Table 5.3.2. Expression of *narK* in nodules. Gene expression was measured by qRT-PCR in nodules from plants inoculated with *B. diazoefficiens* 11*spc*4 (WT) or H1 (*nifH* mutant) strains. Nodules were harvested from plants grown in the presence of 4 mM KNO_3. Data are means ± standard deviations from there independent RNA samples assayed by using three replicates.

	Relative amount of transcript	
Gene	**110*spc*4 (WT)**	***nifH***
narK	1.00 ± 0.00	+87.82 ± 18.70

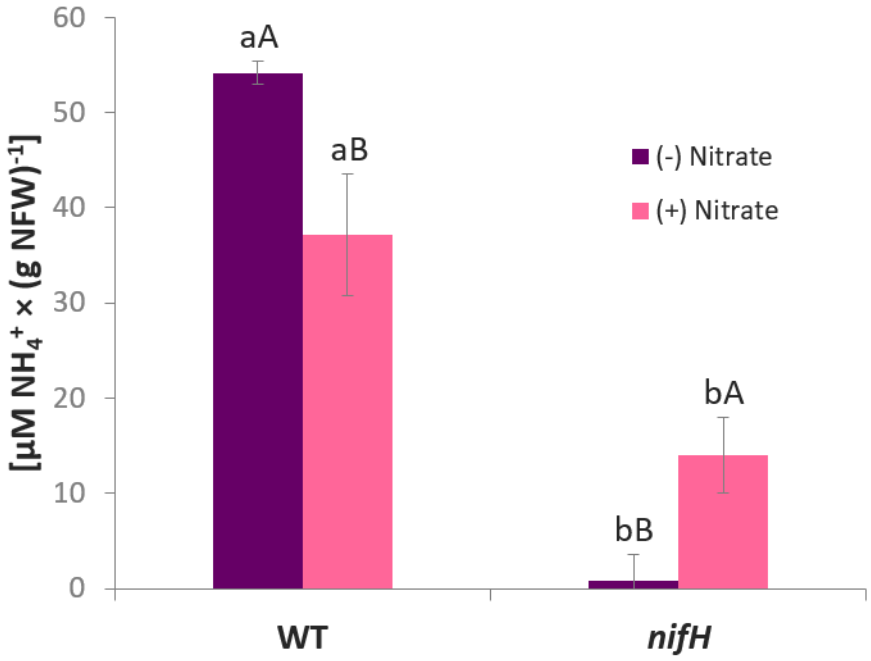

Figure 5.3.3. Ammonium (NH_4^+) content in bacteroids. Plants were inoculated with *B. diazoefficiens* 11*spc*4 (WT) or H1 (*nifH* mutant) strains. Nodules were isolated from plants grown in the absence (-Nitrate) or the presence of 4 mM KNO_3 (+Nitrate). Data are means with standard deviations from two independent experiments assayed by using six replicates. In individual graphs, bars within the same treatment marked with the same lower-case letter, and bars within the same strain followed by the same capital letter, are not significantly different as determined by the ANOVA test at $P \leq 0.05$.

6

DISCUSSION

6. DISCUSSION

6.1. The *in vitro* roles of Bjgb and Flp from *B. diazoefficiens* in NO detoxification

Bacteria use a large variety of proteins to eliminate NO. Among them, haemoglobins (flavohaemoglobins, single domain haemoglobins and trucanted haemoglobins) are the most important and well-characterized proteins involved in aerobic NO detoxification in bacteria (Poole, 2005; Stern and Zhu, 2014; Gell, 2018). In *B. diazoefficiens*, a single domain haemoglobin (Bjgb) (Cabrera et al., 2011; Sánchez et al., 2011a) has been identified. The gene encoding Bjgb (blr2807, *bjgb*) is included in the *B. diazoefficiens narK-bjgb-flp-nasC* operon, which contains other genes involved in NO_3^- assimilation (Cabrera et al., 2016). The *in vivo* function of Bjgb and Flp proteins in the protection of *B. diazoefficiens* cells from nitrosative stress has been recently demonstrated (Cabrera et al., 2016). However, the *in vitro* function of Bjgb and Flp is unknown. Bjgb is homologous to the N-terminal haem-containing domain of the fHb from *E. coli*, as well as to the sdHbs from *V. stercoraria* and *C. jejuni* (Sánchez et al., 2011a). Flp is a NAD(P)H reducing protein, with a flavin mononucleotide (FMN) moiety analogous to the fHb-like FAD/NAD-binding domain.

UV-Vis electronic absorbance spectroscopic assays, that were performed with purified Bjgb and Flp, revealed that Bjgb contains a haem *b* cofactor and it is reduced by Flp, that transfers electrons from NAD(P)H. Thus, Flp is a key protein that acts as a redox partner of Bjgb. Moreover, it has been shown that reduced Bjgb haem *b* can also bind NO. These results confirmed the role of Bjgb and Flp in NO metabolism and demostrated the *in vitro* capacity of Bjgb to bind NO.

Sequence alignment of Bjgb with other Hbs showed the presence of the proximal haem-coordinating F8 histidine residue (His^{81}), that is 100% conserved across the whole Hb superfamily (Figure 5.1.11.). *B. diazoefficiens* Bjgb sequence also possesses the CD1 phenylalanine (Phe^{42}), which makes π-stacking interactions with pyrrole ring C and is the second-most highly conserved globin residue after HisF8 (reviewed in Gell, 2018) (Figure 5.1.11.). On the contrary, instead of the conserved alanine (A) present in most of the other Hbs, Bjgb contains a lysine (K52) that is not conserved. Interestingly, *C. reinhardtii* trHb (THB1) exhibits a lysine (K53) as a haem Fe

ligand, that has been recently shown to be implicated in NO detoxification (Rice et al., 2015) (Figure 5.1.11.). In order to reveal the involvement of Bjgb K52 in NO metabolism, we performed a mutation strategy to replace lysine-52 from Bjgb with alanine (K52A) through QuickChange Site-Directed Mutagenesis method (Figure 5.1.12.). Previous studies have proposed that NO is the signalling molecule that activates transcription of *B. diazoefficiens nor* genes, encoding the respiratory nitric oxide reductase (Bueno et al., 2017). During NO_3^--dependent anaerobic growth, the Cu-containing respiratory nitrite reductase (NirK) generates NO in the periplasm and the assimilatory nitrate reductase (NasC) is responsible for NO production in the cytoplasm (Cabrera et al., 2016; Bueno et al., 2017). In this context, it has been proposed that Bjgb binds NO produced in the cytoplasm, that is generated by NasC as by-product of NO_3^-/NO_2^- assimilation (Cabrera et al., 2016). Confirming this hypothesis, we have demonstrated in this work the capacity of Bjgb to bind NO *in vitro*. Phenotypic *in vivo* characterization of a *bjgb* delection mutant showed an induction of Nor expression, probably due to increased intracellular NO levels that arise during assimilatory NO_3^- reduction (Cabrera et al., 2016). In this Thesis, we have investigated the role *in vivo* of the lysine-52 by analyzing the expression and activity of Nor in *B. diazoefficiens* cells expressing Bjgb K52A mutant, compared to those cells expressing the Bjgb native protein. We have determined Nor expression by using a *norC-lacZ* transcriptional fusion, by detecting NorC through haem-staining analyses and also by measuring the capacity of the cells to produce N_2O, the product of Nor activity. By following these three approaches, we found that overexpression of Bjgb in the *bjgb* mutant significantly reduced expression of Nor (Figure 5.1.13.). These results suggest that the complementation of the *bjgb* mutant with a plasmid overexpressing the native Bjgb, that bind NO, probably reduced the concentration of the signalling molecule (NO) and, consequently, expression of Nor is significantly decreased. However, when the *bjgb* mutant was complemented with a plasmid overexpressing the Bjgb K52A mutant, the strong reduction of Nor expression provoked by the presence of the native Bjgb was not observed (Figure 5.1.13.). These observations suggest that the capacity of Bjgb K52A mutant to bind NO is probably lower than that of the native Bjgb protein. Consequently, the presence of NO in the cytoplasm of the cells expressing Bjgb K52A resulted in the induction of Nor expression to WT levels.

Taken together, these results allowed us to conclude that the lysine-52 from Bjgb has a critical role for NO homeostasis *in vivo*.

Unlike the fHbs, such as Hmp from *E. coli*, which contain a central FAD binding domain and a C-terminal NADP-binding domain (Poole, 2005), sdHbs lack the oxidoreductase FAD/NAD-binding domain. There is evidence suggesting that, under aerobic conditions, sdHbs function generally as NO dioxygenase (NOD) enzymes where NO induces O_2-Hb^{2+} dioxygenation to form Hb^{3+}+NO_3^- (for a review see Tinajero-Trejo and Shepherd, 2013). However, the reductase that recycles Hb^{2+} from Hb^{3+} *in vivo* remains to be identified. In this Thesis, we have identified the redox partner of the *B. diazoefficiens* sdHb (Bjgb), since we have demonstrated *in vitro* that Flp is able to reduce Bjgb. However, further experiments are needed to demonstrate the NOD activity of Bjgb *in vitro*.

Similarly, as reported for sdHbs, Hmp converts NO into NO_3^- by a NOD activity under aerobic conditions (Gardner et al., 1998; Hausladen et al., 2001; Gardner, 2005). In addition to NOD activity, Hmp is also able to reduce NO to N_2O under anaerobic conditions (Kim et al., 1999). Regarding the role *in vivo* of Bjgb, it has been demonstrated that, under low oxygen NO_3^--dependent free-living conditions, a *bjgb* mutant showed substantial growth inhibition compared to WT cells, suggesting a NO detoxifying role (Cabrera et al., 2016). It might be possible that, as reported for Hmp, Bjgb has the capacity to reduce NO to N_2O. However, Cabrera and colleagues (2016) demonstrated that the denitrifying Nor enzyme is the only NO reductase, given the incapacity of a *B. diazoefficiens norC* mutant to produce N_2O. In order to confirm these observations, in this Thesis we transferred plasmid pDB4028, overexpressing native Bjgb, to *norC* mutant. Similarly, as it was previously observed, N_2O production could not be detected in a *norC* mutant overexpressing native Bjgb (data not shown). These results demonstrate that Bjgb is not implicated in N_2O production. Therefore, the respiratory NO-reductase enzyme is the main source of N_2O in *B. diazoefficiens*, as previously reported (Cabrera et al., 2016).

6.2. Function of the haemoglobin Bjgb from *B. diazoefficiens* in NO homeostasis in soybean nodules and in symbiotic nitrogen fixation

Several studies have shown that NO production in soybean nodules is induced by NO_3^- and hypoxia, that is promoted by flooding conditions (Meakin et al., 2007; Sánchez et al., 2010). This molecule is a potent inhibitor of nitrogenase activity and expression (Kato et al., 2010; Sánchez et al., 2010). In nodules, NO can also bind Lb contributing to the formation of nitrosyl-leghaemoglobin (LbNO) complexes, that have a major role in detoxifying RNS (Sánchez et al., 2010). It is also well established that the denitrification pathway in *B. diazoefficiens* is the major source of NO and N_2O in soybean nodules (Sánchez et al., 2010; Tortosa et al., 2015). Previous experiments revealed that in soybean plants inoculated with a *B. diazoefficiens napA* null strain, where denitrification is inhibited, basal levels of NO and N_2O were still detected in nodules (Sánchez et al., 2010; Tortosa et al., 2015). These observations suggested that, in addition to denitrification, other mechanisms give rise to NO and N_2O in nodules. The recently identified haemoglobin Bjgb is one such system, which has been reported to be involved in NO detoxification under free living conditions (Cabrera et al., 2011; Sánchez et al., 2011a; Cabrera et al., 2016), however, its function inside the nodules is unknown. In this work, the role of Bjgb in symbiotic N_2 fixation and NO homeostasis in the *B. diazoefficiens*-*Glycine max* symbiosis has been investigated by inoculating plants with a *bjgb* mutant. In order to induce NO formation in the nodules, soybean plants were grown in the presence of KNO_3 (4 mM) and 7 days before harvesting they were subjected to flooding, as previously reported (Mesa et al., 2004; Meakin et al., 2007; Sánchez et al., 2010). This NO_3^- concentration was selected based in a previous work (Mesa et al., 2004) where *Glycine max* L. Merr., cv. Williams inoculated with *B. diazoefficiens* USDA 110 was grown in the presence of 0, 1, 2, 3, 4, 5 and 6 mM KNO_3. Mesa and colleagues (2004) found that 4 mM KNO_3 resulted in the induction of bacteroidal denitrification by measuring N_2O formation in nodules, and this concentration did not inhibit either nodule formation or nitrogenase activity. Since the effect of flooding on NNP was similar independently of the strain used for inoculation, the increase in NDWP observed in plants where *bjgb* was used as inoculum is probably due to a higher individual nodule weight. This observation suggests that the *bjgb*

mutant has a beneficial effect on nodule development and growth, rather than on nodule number formation.

The impact of flooding on N_2 fixation was further investigated by calculating the amount of fixed N in shoots (FN) employing the ^{15}N isotope dilution method. Consistent with previous observations (Sánchez et al., 2011b), this approach was used to demonstrate the negative effect of flooding on N_2 fixation in plants grown in the presence of NO_3^-. The decrease of FN provoked by flooding was significantly less pronounced in plants that were inoculated with the *bjgb* mutant, indicating that the loss of Bjgb confers tolerance of N_2 fixation to flooding. These findings were confirmed by analysis of nitrogenase activity (ARA) and levels of leghaemoglobin (estimation of nodule functionality). As reported previously, flooding significantly inhibited ARA and Lb levels in WT nodules (Sánchez et al., 2010). However, the negative effect of flooding on ARA and Lb levels was smaller in nodules from plants inoculated with the *bjgb* mutant, compared to WT nodules.

In contrast to our findings, inoculation of *M. truncatula* plants with an *E. meliloti* strain lacking the flavohaemoglobin (Hmp) strongly inhibited ARA and provoked nodule senescence (Cam et al., 2012), as compared to those inoculated with the WT. The authors attributed this effect to an increase in the NO levels observed in nodules produced by the *hmp* mutant, which negatively affected N_2 fixation and increased root nodule senescence. Contrary to the higher NO levels observed in *M. truncatula* nodules induced by the *E. meliloti hmp* mutant compared to those produced by the WT (Cam et al., 2012), our results showed that NO formation was significantly lower in *bjgb* than in WT nodules in response to flooding. The apparent differences observed regarding the involvement of the *E. meliloti hmp* and *B. diazoefficiens bjgb* mutants in N_2-fixation and nodule NO formation could be due to the different plant growth conditions used by Cam et al. (2012) and in this work. While Cam and colleagues cultured *M. truncatula* in N-free medium, in the present work soybean plants were grown with NO_3^- and subjected to flooding for 7 days. In *B. diazoefficiens*, denitrification accounts for about 90% of NO present in flooded soybean nodules (Sánchez et al., 2010), while in *M. truncatula* nodules, *E. meliloti* produces only ~35% of NO detected (Cam et al., 2012). The apparent contradictory

observations found between the roles of *E. meliloti* Hmp and *B. diazoefficiens* Bjgb might be also due to metabolic differences in their NO_3^--reducing pathways. While *B. diazoefficiens* is a complete denitrifier which grows anoxically by NO_3^- respiration, *E. meliloti* is unable to respire NO_3^- under anoxic conditions (reviewed by Torres et al., 2016). Furthermore, it might also be possible that the nature of nodule-type supports different mechanisms of dealing with the nitrosative stress, considering that indeterminate nodules (*M. truncatula*) are characterized by a persistent meristem and a continuous growth, while determinate nodules (*G. max*) are characterized by a not persistent meristem and a limited growth potential.

The decreased levels of NO produced by *bjgb* nodules could explain the tolerance of N_2 fixation to flooding observed in plants inoculated with the *bjgb* mutant. In *B. diazoefficiens* there are two main processes involved in NO formation, which are denitrification and NO_3^- assimilation. Under low oxygen NO_3^--dependent free-living conditions, pathways for both respiratory denitrification and NO_3^- assimilation are active to promote bacterial survival. In fact, both respiratory (Nap) and assimilatory (NasC) nitrate reductases contribute similarly to the total activity. Under these conditions, a *bjgb* mutant showed substantial growth inhibition compared to WT cells, suggesting a NO detoxifying role for Bjgb (Cabrera et al., 2016). However, under symbiotic conditions, where growth is not needed, the contribution of assimilatory NO_3^- reduction in the bacteroids is only ~10% (Sánchez et al., 2010). Consequently, it may be possible that low NO concentrations arising from NO_3^- assimilation in the bacteroids cytoplasm does not present toxicity in nodules. These observations may also explain that, in contrast to the reported role in NO detoxification during NO_3^--dependent anaerobic growth, Bjgb would not be directly involved in NO detoxification inside nodules and, thus, it may instead act as an NO-buffer.

The assimilatory nitrate reductase (NasC) is encoded by the *narK-bjgb-flp-nasC* operon, that also contains the gene encoding the sdHb (Bjgb). Cabrera and colleagues (2016) reported that NO produced by NasC in the cytoplasm acts as signalling molecule, which activates expression of the denitrifying *nor* genes. In this context, it has been recently demonstrated that NO is the signalling molecule that induces *nor* genes in *B. diazoefficiens* (Bueno et al., 2017). Under free-living conditions, expression

of the respiratory Nor was significantly up-regulated in a *bjgb* mutant relative to WT, probably due to increased intracellular NO levels that arise during assimilatory NO_3^- reduction (Cabrera et al., 2016). In soybean nodules, NO produced by the periplasmic denitrifying enzyme NirK is the main source of NO, and Nor the principal system for NO removal (Sánchez et al., 2010). It might be possible that, as it has been demonstrated in free-living cells (Cabrera et al., 2016), NO produced in the cytoplasm from NO_3^- assimilation is increased in bacteroids induced by the *bjgb* mutant. Then, this molecule would act in the cytoplasm as a signal that induces *nor* genes expression. In fact, induction of *norC* expression by flooding was greater in the *bjgb* nodules than in WT nodules. Furthermore, analysis of Nor activity showed a higher N_2O formation capacity in *bjgb* nodules, compared to those of the parental strain.

It has been previously reported that soybean plants inoculated with a *B. diazoefficiens nirK* mutant, whose nodules do not produce NO from denitrification, were more tolerant to flooding than plants inoculated with the WT strain (Sánchez et al., 2011b). Similarly, results obtained in this work suggest that inoculation with the *bjgb* mutant partially diminished the negative effect of flooding on N_2 fixation observed in WT-inoculated plants. This advantage is probably due to the increased capacity of *bjgb* deficient nodules to induce expression of *nor* genes, whereby the gene product removes the NO produced by denitrification. The decreased levels of NO observed in *bjgb* nodules compared to WT nodules in response to flooding lead us to suggest that *B. diazoefficiens* Bjgb, instead of functioning as a direct NO-detoxifying protein in the nodules, it would contribute indirectly by modulating cytoplasmic NO levels, the signalling molecule required for induction of the denitrifying nitric oxide reductase enzyme, which is the major protein involved in NO removal in soybean nodules (see Figure 6.1.). In conclusion, this work reveals a strategy for nitrogenase protection and, consequently, for efficient symbiotic N_2 fixation, that requires the modulation of NO levels in root nodules by the microsymbiont. Therefore, using rhizobia strains that modulate NO levels in nodules is an important practice that would enhance legume production and promote sustainable agriculture. From this perspective, the contribution of *bjgb* mutation is positive for nitrogenase protection. However, elevated N_2O production resulting from increased NO reduction results in

release of a potent and stable greenhouse gas, that has a negative environmental impact and may contribute to climate change.

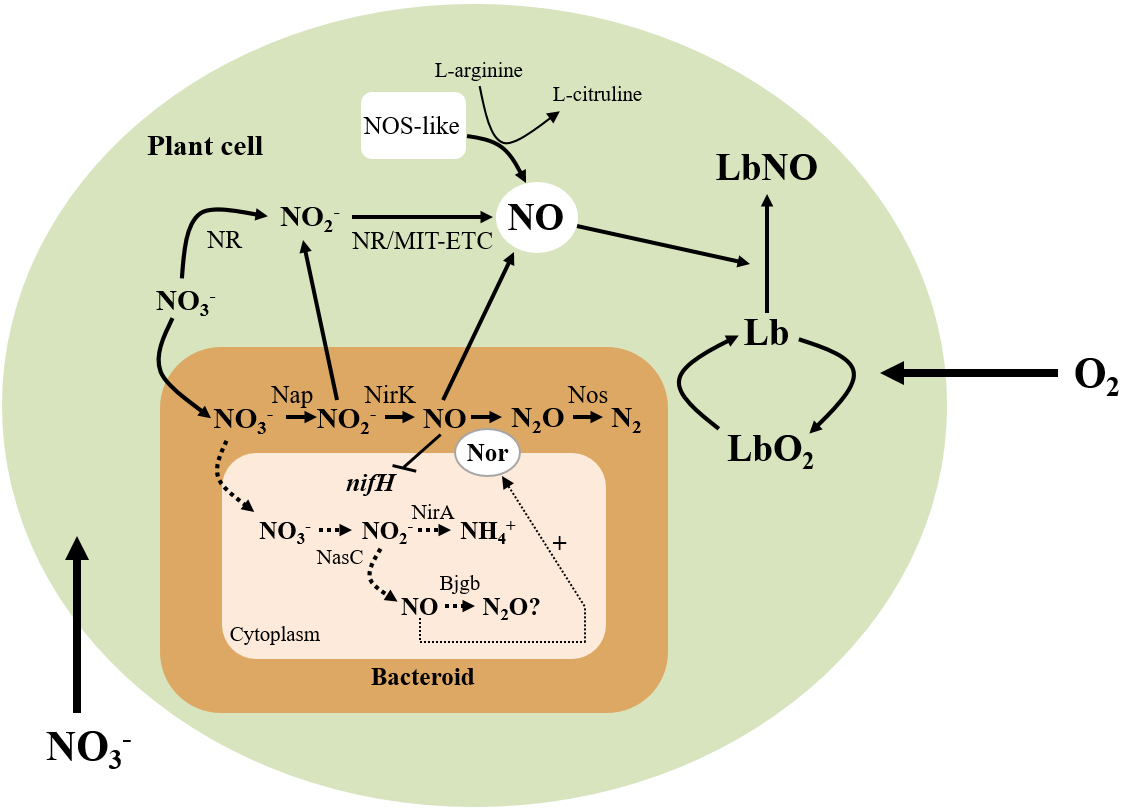

Figure 6.1. Proposed role of Bjgb in soybean nodules, alongside well-characterized sources of NO in nodules. The large green circle represents the plant cell, and the square represents the bacteroid, where the periplasm is shown in orange and the cytoplasm is shown in beige. Adapted from Torres et al. (2016).

As shown in Figure 6.1., in addition to the reported plant sources of NO in legume nodules, denitrification in the bacteroids also contributes to the formation of this molecule. During this process, NO_2^- and NO produced by Nap and NirK, respectively, can bind Lb producing LbNO complexes. It has also been reported that NO is an inhibitor of *nifH* expression. Results from this work suggest that, in addition to denitrification, assimilatory NO_3^- reduction by NasC might be another source of NO in nodules. NO produced in the bacteroid cytoplasm by this system would act as a signalling molecule to activate *nor* genes.

6.3. Role of nitrate assimilation in the *B. diazoefficiens*-soybean symbiosis

The capacity of *B. diazoefficiens* to assimilate NO_3^- under free-living conditions by reducing it to NO_2^- and NH_4^+ through the activity of the assimilatory nitrate (NasC) and nitrite (NirA) reductases, respectively, is well established (Cabrera et al., 2016). However, the involvement of NasC and NirA inside the nodules is unknown. In this work, the role of NasC and NirA in symbiotic N_2 fixation in the *B. diazoefficiens*-*Glycine max* symbiosis has been investigated by inoculating soybean plants with a *nasC* or *nirA B. diazoefficiens* mutants. Similarly to the experiments performed in Chapter 5.2., after inoculation, soybean plants were grown in the presence of KNO_3 (4 mM) and, 7 days before harvesting, they were subjected (or not) to flooding.

Regardless of the plant growth conditions, inoculation with the *nasC* or the *nirA* mutants did not affect nodulation or plant dry weight, relative to those plants inoculated with the WT strain (data not shown). By measuring acetylene reduction activity (ARA) in nodules, ARA of nodules from plants inoculated with a *nasC* mutant showed a similar response to flooding than that of those nodules isolated from plants inoculated with the parental strain. These results suggest that NasC does not show a relevant role in N_2 fixation. Supporting this suggestion, we have also observed in this Thesis that nitrate reductase (NR) activity of *nasC* bacteroids from flooded nodules was similar to that from bacteroids produced by the parental strain. In contrast, NR activity of bacteroids from plants inoculated with a *napA* mutant was not detected, as previously reported by Sánchez and colleagues (2010) (Figure 5.3.1.C.). Taking these results together, we conclude that the periplasmic NR (NapA), that initiates the denitrification process, is the main enzyme involved in NO_3^- reduction in *B. diazoefficiens* bacteroids.

By contrast to *nasC* nodules, nitrogenase activity of the nodules from plants inoculated with *nirA* was more tolerant to flooding, compared to those nodules from plants inoculated with the parental strain. These observations were confirmed by monitoring the levels of Lb, as a parameter indicative of the N_2 fixation activity of the nodules (Dakora, 1995). Since either the *nasC* or the *nirA* mutants are defective in NH_4^+ formation from NO_3^- (Cabrera et al., 2016), the different response of nitrogenase activity to flooding observed in the *nasC* or the *nirA* nodules cannot be attributed to

the lack of NH_4^+ production from NO_3^- assimilation. It has been previously demonstrated the capacity of NasC to produce NO from NO_2^- (Cabrera et al., 2016). In this context, Cabrera and colleagues (2016) reported that NO produced by NasC in the cytoplasm acts as signalling molecule, which activates expression of the denitrifying *nor* genes encoding the main enzyme involved in NO removal in the bacteroids. It is also well established that NO is a potent inhibitor of nitrogenase activity and expression (Kato et al., 2010; Sánchez et al., 2010). Results from Chapter 5.2. have shown that, in bacteroids of a *bjgb* mutant, increased intracellular NO levels, that arise from assimilatory NO_3^- reduction, induce expression of Nor. Consequently, NO levels in the nodules decreased, and protection of nitrogenase activity occurs. Cabrera and colleagues (2016) showed that, under free-living conditions, a *nirA* mutant is unable to use NO_2^- as N source and to grow by reducing it to NH_4^+. In addition to be the source of NirA, NO_2^- could be also the source of NasC to produce NO, as it has been reported for the new class of NO-forming nitrite reductases molybdoenzymes (for a review see Maia and Moura, 2015; Maia et al., 2017). In this context, it might be possible that increased NO_2^- levels in the cytoplasm of the *nirA* mutant provoke induction of NO formation by NasC. Similarly, as we have observed in nodules produced by the *bjgb* mutant, increased intracellular NO levels might induce expression of Nor, that removes NO produced through denitrification in the periplasm, and, consequently, inhibition of nitrogenase activity by this toxic molecule is prevented. However, more experiments need to fully support this hypothesis.

In this Thesis, we have also investigated the role of NO_3^- assimilation in the *B. diazoefficiens*-soybean symbiosis by using another approach consisting in the use of nodules induced by *B. diazoefficiens* mutants defective in N_2 fixation. For this purpose, we inoculated soybean plants with a *nifH* mutant, where N_2 fixation does not occur (Hahn et al., 1984). When plants were grown in the absence of NO_3^-, inoculation with the *nifH* mutant, defective in the Fe-protein from nitrogenase, induces the formation of bacteroids unable to produce NH_4^+ and provide it to the host plant, resulting in N-starved plants (Hahn et al., 1984). In fact, it has been recently reported that the amount of several ureides and its purine precursors was reduced in *nifH* nodules, likely

because no NH_4^+ is produced by the bacteroids, and, as a consequence, synthesis and transport of ureides is impaired (Lardi et al., 2016).

As previously reported by Hahn and colleagues (1984), inoculation of plants with the *nifH* mutant produced the same number of nodules (NNP) than the WT. In this work, we also found that nodule fresh weight (NFWP) was reduced 3-fold in plants inoculated with the *nifH* mutant, compared to those inoculated with the parental strain (Table 5.3.1.). These results suggest that nodule growth, estimated by calculating the individual weight of nodules by dividing NFWP between NNP, was significantly reduced in plants inoculated with the *nifH* mutant and grown without NO_3^-, compared to those inoculated with the WT. In contrast, in plants grown with NO_3^-, *nifH* nodules showed similar growth rates as WT nodules. According to these observations, it might be possible that NO_3^- assimilation by *nifH* nodules has a positive effect on nodule development. As expected, bacteroids produced by the *nifH* mutant were unable to produce NH_4^+ when plants only depended on N_2 fixation. Surprisingly, we found that in NO_3^--grown plants, bacteroids from nodules induced by the *nifH* mutant were able to produce NH_4^+ (Figure 5.3.3.). Consequently, it might be possible that the capacity to produce NH_4^+ from NO_3^- assimilation by the bacteroids has a positive effect on nodule growth and development. In order to investigate the relevance of NO_3^- assimilation by bacteroids in NO_3^--treated plants, we analyzed transcript levels of *narK*, which is the lead gene of the *narK-bjgb-flp-nasC* (blr2803-blr2809) transcriptional unit (Cabrera et al., 2016) that contains NO_3^- assimilation genes, such as *nasC*. We found that *narK* expression was significantly induced in *nifH* nodules from plants treated with NO_3^-, compared to parental nodules. Confirming our results, recent transcriptomic data with nodules induced by the *nifH* mutant showed an activation of the gene cluster blr2803-blr2809 and gene *nirA* (bll4571) encoding the assimilatory nitrite reductase (Cabrera et al., 2016; Lardi et al., 2016). Transcriptomic analyses made by Lardi and colleagues (2016) also showed an activation of the bacterial N stress response (Ntr) with two P-II proteins encoding genes (*glnB* and *glnK*), as well as the two-component response regulator *ntrC* gene, being strongly up-regulated in nodules infected by a *nifH* mutant (Lardi et al., 2016).

It has been reported that NtrC is a transcriptional activator of *nirA* (Franck et al., 2015) and *narK-bjgb-flp-nasC* operon (López et al., 2017). NtrC is required for the expression of assimilatory NO_3^- and NO_2^- reductase activities in *B. diazoefficiens* free living cells (López et al., 2017). It is well known that, in Gram-negative bacteria, the NO_3^- assimilation (*nas*) genes are subjected to dual control: ammonia repression by the general N regulatory (Ntr) system and specific NO_3^- or NO_2^- induction (Luque-Almagro et al., 2011). In *B. diazoefficiens* free-living cells, NtrC induces *narK-bjgb-flp-nasC* expression in the absence of NH_4^+ (López et al., 2017). In this bacterium, *nasTS-nirA* cluster encodes a NO_3^-/NO_2^- responsive TCS, NasS-NasT (Sánchez et al., 2014), and a NO_2^- ferredoxin-dependent reductase, NirA (Cabrera et al., 2016). The RNA-binding protein NasT has been shown to positively and directly regulate *narK-bjgb-flp-nasC* and *nirA* (Cabrera et al., 2016). NasS forms a complex with NasT, avoiding transcription antitermination activity of this protein in the absence of NO_3^-. In the presence of NO_3^-, NasS dissociates from NasT, enabling this protein to bind mRNA for its transcription antitermination effect (Luque-Almagro et al., 2013; Sánchez et al., 2014). In addition to NtrBC, NasST might also act as a transcriptional regulator of *narK-bjgb-flp-nasC* and *nirA* genes in soybean nodules.

By concluding, as result of all of the above mentioned observations, we suggest that, in NO_3^--treated soybean nodules induced by the *nifH* mutant, the absence of NH_4^+ and the presence of NO_3^- are the optimal conditions to induce expression of the NtrC dependent *narK-bjgb-flp-nasC* operon, that will produce NH_4^+ from NO_3^- assimilation and, consequently, might have a positive effect on nodule health and development. We propose that assimilatory NO_3^- reduction might have an important function in soybean nodules in those cases in which N_2 fixation is impaired and, consequently, NH_4^+ production in bacteroids is significantly reduced.

7

CONCLUSIONES/CONCLUSIONS

7. CONCLUSIONES

1. La hemoglobina (Bjgb) de *Bradyrhizobium diazoefficiens* contiene un grupo hemo *b* como cofactor que se une a óxido nítrico (NO) *in vitro*. La flavoproteína (Flp) actúa reduciendo a Bjgb *in vitro*.
2. La lisina-52 de la Bjgb de *B. diazoefficiens* tiene un papel crítico en la homeostasis de NO *in vivo*.
3. La inoculación de plantas de soja con una mutante *bjgb* de *B. diazoefficiens* confiere tolerancia a la fijación simbiótica de nitrógeno (N_2) al encharcamiento. Esta ventaja se debe a la capacidad de los nódulos deficientes de Bjgb de inducir la expresión de los genes *norCBQD*, que codifican la enzima respiratoria óxido nítrico reductasa (Nor), la principal proteína implicada en la eliminación de NO en los nódulos de soja.
4. La Bjgb de *B. diazoefficiens*, en lugar de funcionar como una proteína directamente implicada en la destoxificación de NO en los nódulos, puede contribuir indirectamente modulando los niveles citoplasmáticos de NO en los bacteroides, la molécula señal necesaria para la inducción de Nor.
5. La nitrato reductasa asimilativa de *B. diazoefficiens* (NasC) no tiene un papel relevante en los nódulos de la soja. La nitrato reductasa periplásmica (NapA) es la principal enzima que interviene en la reducción de nitrato (NO_3^-) en los bacteroides.
6. La delección del gen *nirA*, que codifica la nitrito reductasa asimilativa (NirA), protege a la fijación de N_2 en la simbiosis *B. diazoefficiens*-soja durante condiciones de encharcamiento.
7. En plantas tratadas con NO_3^-, la inoculación con una mutante *nifH* de *B. diazoefficiens* induce la expresión de la asimilación de NO_3^- en los bacteroides.
8. La reducción asimilativa de NO_3^- en los bacteroides puede tener un efecto positivo en el desarrollo y funcionalidad de los nódulos en aquellos casos en los que la fijación de N_2 se ve afectada.

CONCLUSIONS

1. *Bradyrhizobium diazoefficiens* haemoglobin (Bjgb) contains a *b*-type haem cofactor that binds nitric oxide (NO) *in vitro*. The flavoprotein (Flp) acts as a redox partner for Bjgb *in vitro*.
2. Lysine-52 from *B. diazoefficiens* Bjgb has a critical role for NO homeostasis *in vivo*.
3. Inoculation of soybean plants with a *B. diazoefficiens bjgb* mutant confers tolerance of symbiotic nitrogen (N_2) fixation to flooding. This advantage is due to the ability of Bjgb deficient nodules to induce the expression of *norCBQD* genes, which encodes the respiratory nitric oxide reductase (Nor) enzyme, the major protein involved in NO removal in soybean nodules.
4. *B. diazoefficiens* Bjgb, instead of functioning as a direct NO-detoxifying protein in the nodules, may contribute indirectly by modulating cytoplasmic NO levels in the bacteroids, the signalling molecule required for the induction of Nor.
5. *B. diazoefficiens* assimilatory nitrate reductase (NasC) does not have a relevant role in soybean nodules. Instead, the periplasmic nitrate reductase (NapA) remains the main enzyme involved in nitrate (NO_3^-) reduction in bacteroids.
6. Deletion of *nirA*, encoding the assimilatory nitrite reductase (NirA), protects N_2 fixation of *B. diazoefficiens*-soybean symbiosis during flooding conditions.
7. In NO_3^--treated plants, inoculation with a *B. diazoefficiens nifH* mutant induces expression of NO_3^- assimilation in the bacteroids.
8. Assimilatory NO_3^- reduction in bacteroids may have a positive effect on nodule health and development when N_2 fixation is impaired.

8

REFERENCES

8. REFERENCES

Agapie, T., Suseno, S., Woodward, J.J., Stoll, S., Britt, R.D., and Marletta, M.A. (2009). NO formation by a catalytically self-sufficient bacterial nitric oxide synthase from *Sorangium cellulosum*. *Proc Natl Acad Sci U S A* 106**,** 16221-16226.

Al-Attar, S., and de Vries, S. (2015). An electrogenic nitric oxide reductase. *FEBS Lett* 589**,** 2050-2057.

Altschul, S.F., Gish, W., Miller, W., Myers, E.W., and Lipman, D.J. (1990). Basic local alignment search tool. *J Mol Biol* 215**,** 403-410.

Andrews, M., and Andrews, M.E. (2017). Specificity in Legume-Rhizobia Symbioses. *Int J Mol Sci* 18.

Anjum, M.F., Stevanin, T.M., Read, R.C., and Moir, J.W. (2002). Nitric oxide metabolism in *Neisseria meningitidis*. *J Bacteriol* 184**,** 2987-2993.

Appleby, C.A. (1984). Leghemoglobin and *Rhizobium* respiration. *Ann Rev Plant Physiol* 35**,** 443-478.

Arcovito, A., Benfatto, M., Cianci, M., Hasnain, S.S., Nienhaus, K., Nienhaus, G.U., Savino, C., Strange, R.W., Vallone, B., and Della Longa, S. (2007). X-ray structure analysis of a metalloprotein with enhanced active-site resolution using *in situ* x-ray absorption near edge structure spectroscopy. *Proc Natl Acad Sci U S A* 104**,** 6211-6216.

Arrese-Igor, C., Gordon, A.J., Minchin, F.R., and Ford, D.R. (1998). Nitrate entry and nitrite formation in the infected region of soybean nodules. *J Exp Botany* 318**,** 41-48.

Arya, S., Sethi, D., Singh, S., Hade, M.D., Singh, V., Raju, P., Chodisetti, S.B., Verma, D., Varshney, G.C., Agrewala, J.N., and Dikshit, K.L. (2013). Truncated hemoglobin, HbN, is post-translationally modified in *Mycobacterium tuberculosis* and modulates host-pathogen interactions during intracellular infection. *J Biol Chem* 288**,** 29987-29999.

Astier, J., Gross, I., and Durner, J. (2018). Nitric oxide production in plants: an update. *J Exp Bot* 69**,** 3401-3411.

Bacanamwo, M., and Purcell, L.C. (1999). Soybean dry matter and N accumulation responses to flooding stress, N sources and hypoxia. *J Exp Bot* 50**,** 689-696.

Balasiny, B., Rolfe, M.D., Vine, C., Bradley, C., Green, J., and Cole, J. (2018). Release of nitric oxide by the *Escherichia coli* YtfE (RIC) protein and its reduction by the hybrid cluster protein in an integrated pathway to minimize cytoplasmic nitrosative stress. *Microbiology* 164**,** 563-575.

Bali, S., Palmer, D.J., Schroeder, S., Ferguson, S.J., and Warren, M.J. (2014). Recent advances in the biosynthesis of modified tetrapyrroles: the discovery of an alternative pathway for the formation of heme and heme d_1. *Cell Mol Life Sci* 71**,** 2837-2863.

Bang, I.S., Liu, L., Vázquez-Torres, A., Crouch, M.L., Stamler, J.S., and Fang, F.C. (2006). Maintenance of nitric oxide and redox homeostasis by the salmonella flavohemoglobin hmp. *J Biol Chem* 281**,** 28039-28047.

Baptista, J.M., Justino, M.C., Melo, A.M., Teixeira, M., and Saraiva, L.M. (2012). Oxidative stress modulates the nitric oxide defense promoted by *Escherichia coli* flavorubredoxin. *J Bacteriol* 194**,** 3611-3617.

Barnett, M.J., Fisher, R.F., Jones, T., Komp, C., Abola, A.P., Barloy-Hubler, F., et al. (2001). Nucleotide sequence and predicted functions of the entire *Sinorhizobium meliloti* pSymA megaplasmid. *Proc Natl Acad Sci U S A* 98**,** 9883-9888.

Barrios, H., Fischer, H.M., Hennecke, H., and Morett, E. (1995). Overlapping promoters for two different RNA polymerase holoenzymes control *Bradyrhizobium japonicum nifA* expression. *J Bacteriol* 177**,** 1760-1765.

Barrios, H., Grande, R., Olvera, L., and Morett, E. (1998). *In vivo* genomic footprinting analysis reveals that the complex *Bradyrhizobium japonicum fixRnifA* promoter region is differently occupied by two distinct RNA polymerase holoenzymes. *Proc Natl Acad Sci U S A* 95**,** 1014-1019.

Bartberger, M.D., Liu, W., Ford, E., Miranda, K.M., Switzer, C., Fukuto, J.M., Farmer, P.J., Wink, D.A., and Houk, K.N. (2002). The reduction potential of nitric oxide (NO) and its importance to NO biochemistry. *Proc Natl Acad Sci U S A* 99**,** 10958-10963.

Bartesaghi, S., and Radi, R. (2018). Fundamentals on the biochemistry of peroxynitrite and protein tyrosine nitration. *Redox Biol* 14**,** 618-625.

Bauer, E., Kaspar, T., Fischer, H.M., and Hennecke, H. (1998). Expression of the *fixR-nifA* operon in *Bradyrhizobium japonicum* depends on a new response regulator, RegR. *J Bacteriol* 180**,** 3853-3863.

Becker, A., Berges, H., Krol, E., Bruand, C., Ruberg, S., Capela, D., et al. (2004). Global changes in gene expression in *Sinorhizobium meliloti* 1021 under microoxic and symbiotic conditions. *Mol Plant Microbe Interact* 17**,** 292-303.

Bedmar, E.J., Bueno, E., Correa, D., Torres, M.J., Delgado, M.J., and Mesa, S. (2013). Ecology of denitrification in soils and plant-associated bacteria, in *Beneficial Plant-Microbial Interactions: Ecology and Applications* (González, M.B.R., González-López J., eds.) CRC Press, Florida, 164-182.

Bedmar, E.J., Robles, E.F., and Delgado, M.J. (2005). The complete denitrification pathway of the symbiotic, nitrogen-fixing bacterium *Bradyrhizobium japonicum*. *Biochem Soc Trans* 33**,** 141-144.

Bennett, S.P., Soriano-Laguna, M.J., Bradley, J.M., Svistunenko, D.A., Richardson, D.J., Gates, A.J., and Le Brun, N.E. (2019). NosL is a dedicated copper chaperone for assembly of the Cu_Z center of nitrous oxide reductase. *Chem Sci* 10**,** 4985-4993.

Bergaust, L.L., Hartsock, A., Liu, B., Bakken, L.R., and Shapleigh, J.P. (2014). Role of *norEF* in denitrification, elucidated by physiological experiments with *Rhodobacter sphaeroides*. *J Bacteriol* 196**,** 2190-2200.

Berger, A., Brouquisse, R., Pathak, P.K., Hichri, I., Singh, I., Bhatia, S., Boscari, A., Igamberdiev, A.U., and Gupta, K.J. (2018). Pathways of nitric oxide metabolism and operation of phytoglobins in legume nodules: missing links and future directions. *Plant Cell Environ* 41**,** 2057-2068.

Bergersen, F.J. (1977). A treatise on dinitrogen fixation. *Biology: Section III* (Hardy, R.W., and Silver, W. eds.) John Wiley & Sons, New York, 519-556.

Blanquet, P., Silva, L., Catrice, O., Bruand, C., Carvalho, H., and Meilhoc, E. (2015). *Sinorhizobium meliloti* controls nitric oxide-mediated post-translational modification of a *Medicago truncatula* nodule protein. *Mol Plant Microbe Interact* 28**,** 1353-1363.

Bonamore, A., and Boffi, A. (2008). Flavohemoglobin: structure and reactivity. *IUBMB Life* 60**,** 19-28.

Bonnet, M., Stegmann, M., Maglica, Ž., Stiegeler, E., Weber-Ban, E., Hennecke, H., and Mesa, S. (2013). $FixK_2$, a key regulator in *Bradyrhizobium japonicum*, is a substrate for the protease ClpAP *in vitro*. *FEBS Lett* 587**,** 88-93.

Borrero-De Acuña, J.M., Timmis, K.N., Jahn, M., and Jahn, D. (2017). Protein complex formation during denitrification by *Pseudomonas aeruginosa*. *Microb Biotechnol* 10**,** 1523-1534.

Brandes, N., Rinck, A., Leichert, L.I., and Jakob, U. (2007). Nitrosative stress treatment of *E. coli* targets distinct set of thiol-containing proteins. *Mol Microbiol* 66**,** 901-914.

Bricio, C., Álvarez, L., San Martin, M., Schurig-Briccio, L.A., Gennis, R.B., and Berenguer, J. (2014). A third subunit in ancestral cytochrome *c*-dependent nitric oxide reductases. *Appl Environ Microbiol* 80**,** 4871-4878.

Broughton, W.J., Hernández, G., Blair, M., Beebe, S., Gepts, P., and Vanderleyden, J. (2003). Beans (*Phaseolus* spp.)-Model food legumes. *Plant Soil* 252**,** 55-128.

Bruand, C., and Meilhoc, E. (2019). Nitric oxide in plants: pro- or anti-senescence. *J Exp Bot* 70**,** 4419-4427.

Buddha, M.R., Tao, T., Parry, R.J., and Crane, B.R. (2004). Regioselective nitration of tryptophan by a complex between bacterial nitric-oxide synthase and tryptophanyl-tRNA synthetase. *J Biol Chem* 279**,** 49567-49570.

Bueno, E., Bedmar, E.J., Richardson, D.J., and Delgado, M.J. (2008). Role of *Bradyrhizobium japonicum* cytochrome c_{550} in nitrite and nitrate respiration. *FEMS Microbiol Lett* 279**,** 188-194.

Bueno, E., Gómez-Hernández, N., Girard, L., Bedmar, E.J., and Delgado, M.J. (2005). Function of the *Rhizobium etli* CFN42 *nirK* gene in nitrite metabolism. *Biochem Soc Trans* 33**,** 162-163.

Bueno, E., Mania, D., Frostegård, Å., Bedmar, E.J., Bakken, L.R., and Delgado, M.J. (2015). Anoxic growth of *Ensifer meliloti* 1021 by N_2O-reduction, a potential mitigation strategy. *Front Microbiol* 6**,** 537.

Bueno, E., Robles, E.F., Torres, M.J., Krell, T., Bedmar, E.J., Delgado, M.J., and Mesa, S. (2017). Disparate response to microoxia and nitrogen oxides of the *Bradyrhizobium japonicum napEDABC*, *nirK* and *norCBQD* denitrification genes. *Nitric Oxide* 68**,** 137-149.

Burney, S., Niles, J.C., Dedon, P.C., and Tannenbaum, S.R. (1999). DNA damage in deoxynucleosides and oligonucleotides treated with peroxynitrite. *Chem Res Toxicol* 12**,** 513-520.

Butland, G., Spiro, S., Watmough, N.J., and Richardson, D.J. (2001). Two conserved glutamates in the bacterial nitric oxide reductase are essential for activity but not assembly of the enzyme. *J Bacteriol* 183**,** 189-199.

Cabello, P., Pino, C., Olmo-Mira, M.F., Castillo, F., Roldán, M.D., and Moreno-Vivián, C. (2004). Hydroxylamine assimilation by *Rhodobacter capsulatus* E1F1. requirement of the *hcp* gene (hybrid cluster protein) located in the nitrate assimilation *nas* gene region for hydroxylamine reduction. *J Biol Chem* 279**,** 45485-45494.

Cabrera, J.J., Salas, A., Torres, M.J., Bedmar, E.J., Richardson, D.J., Gates, A.J., and Delgado, M.J. (2016). An integrated biochemical system for nitrate assimilation and nitric oxide detoxification in *Bradyrhizobium japonicum*. *Biochem J* 473**,** 297-309.

Cabrera, J.J., Sánchez, C., Gates, A.J., Bedmar, E.J., Mesa, S., Richardson, D.J., and Delgado, M.J. (2011). The nitric oxide response in plant-associated endosymbiotic bacteria. *Biochem Soc Trans* 39**,** 1880-1885.

Calmels, S., Ohshima, H., and Bartsch, H. (1988). Nitrosamine formation by denitrifying and non-denitrifying bacteria: implication of nitrite reductase and nitrate reductase in nitrosation catalysis. *J Gen Microbiol* 134**,** 221-226.

Cam, Y., Pierre, O., Boncompagni, E., Herouart, D., Meilhoc, E., and Bruand, C. (2012). Nitric oxide (NO): a key player in the senescence of *Medicago truncatula* root nodules. *New Phytol* 196**,** 548-560.

Caranto, J.D., and Lancaster, K.M. (2017). Nitric oxide is an obligate bacterial nitrification intermediate produced by hydroxylamine oxidoreductase. *Proc Natl Acad Sci U S A* 114**,** 8217-8222.

Carreira, C., Pauleta, S.R., and Moura, I. (2017). The catalytic cycle of nitrous oxide reductase - The enzyme that catalyzes the last step of denitrification. *J Inorg Biochem* 177**,** 423-434.

Cébron, A., and Garnier, J. (2005). *Nitrobacter* and *Nitrospira* genera as representatives of nitrite-oxidizing bacteria: detection, quantification and growth along the lower Seine River (France). *Water Res* 39**,** 4979-4992.

Chamizo-Ampudia, A., Sanz-Luque, E., Llamas, A., Galván, A., and Fernández, E. (2017). Nitrate reductase regulates plant nitric oxide homeostasis. *Trends Plant Sci* 22**,** 163-174.

Chan, J., Xing, Y., Magliozzo, R.S., and Bloom, B.R. (1992). Killing of virulent *Mycobacterium tuberculosis* by reactive nitrogen intermediates produced by activated murine macrophages. *J Exp Med* 175**,** 1111-1122.

Clarke, T.A., Cole, J.A., Richardson, D.J., and Hemmings, A.M. (2007). The crystal structure of the pentahaem *c*-type cytochrome NrfB and characterization of its solution-state interaction with the pentahaem nitrite reductase NrfA. *Biochem J* 406**,** 19-30.

Clarke, T.A., Mills, P.C., Poock, S.R., Butt, J.N., Cheesman, M.R., Cole, J.A., Hinton, J.C., Hemmings, A.M., Kemp, G., Soderberg, C.A., Spiro, S., Van Wonderen, J., and Richardson, D.J. (2008). *Escherichia coli* cytochrome *c* nitrite reductase NrfA. *Methods Enzymol* 437**,** 63-77.

Cole, J. (1996). Nitrate reduction to ammonia by enteric bacteria: redundancy, or a strategy for survival during oxygen starvation? *FEMS Microbiol Lett* 136**,** 1-11.

Cole, J.A. (2017). CHAPTER 2: Nitric oxide production, damage and management during anaerobic nitrate reduction to ammonia, in *Metalloenzymes in Denitrification: Applications and Environmental Impacts* (Moura, I., Moura, J.J., Pauleta, S.R., Maia, L.B., eds.) The Royal Society of Chemistry, 11-38.

Cole, J.A. (2018). Anaerobic bacterial response to nitrosative stress. *Adv Microb Physiol* 72**,** 193-237.

Cook, D.R. (1999). *Medicago truncatula*-a model in the making! *Curr Opin Plant Biol* 2**,** 301-304.

Corker, H., and Poole, R.K. (2003). Nitric oxide formation by *Escherichia coli*. Dependence on nitrite reductase, the NO-sensing regulator Fnr, and flavohemoglobin Hmp. *J Biol Chem* 278**,** 31584-31592.

Cramm, R., Siddiqui, R.A., and Friedrich, B. (1994). Primary sequence and evidence for a physiological function of the flavohemoprotein of *Alcaligenes eutrophus*. *J Biol Chem* 269**,** 7349-7354.

Daims, H., Lucker, S., and Wagner, M. (2016). A new perspective on microbes formerly known as nitrite-oxidizing bacteria. *Trends Microbiol* 24**,** 699-712.

Dakora, F.D. (1995). A functional relationship between leghaemoglobin and nitrogenase based on novel measurements of the two proteins in legume root nodules. *Ann Bot* 75**,** 49-54.

Daskalakis, V., Ohta, T., Kitagawa, T., and Varotsis, C. (2015). Structure and properties of the catalytic site of nitric oxide reductase at ambient temperature. *Biochim Biophys Acta* 1847**,** 1240-1244.

Davies, M.J., Mathieu, C., and Puppo, A. (1999). Leghemoglobin: properties and reactions. *Adv Inorg Chem* 46**,** 495-542.

de Boer, A.P., van der Oost, J., Reijnders, W.N., Westerhoff, H.V., Stouthamer, A.H., and van Spanning, R.J. (1996). Mutational analysis of the *nor* gene cluster which encodes nitric-oxide reductase from *Paracoccus denitrificans*. *Eur J Biochem* 242**,** 592-600.

de Vries, S., and Pouvreau, L.A.M. (2007). CHAPTER 4: Nitric oxide reductase: structural variations and catalytic mechanism, in *Biology of the Nitrogen Cycle* (Ferguson, S.J., Newton, W.E, eds.) Elsevier, Amsterdam, 57-66.

del Giudice, J., Cam, Y., Damiani, I., Fung-Chat, F., Meilhoc, E., Bruand, C., et al. (2011). Nitric oxide is required for an optimal establishment of the *Medicago truncatula-Sinorhizobium meliloti* symbiosis. *New Phytol* 191**,** 405-417.

Delamuta, J.R., Ribeiro, R.A., Ormeno-Orrillo, E., Melo, I.S., Martínez-Romero, E., and Hungria, M. (2013). Polyphasic evidence supporting the reclassification of *Bradyrhizobium japonicum* group Ia strains as *Bradyrhizobium diazoefficiens* sp. nov. *Int J Syst Evol Microbiol* 63**,** 3342-3351.

Delgado, M.J., Bedmar, E.J., and Downie, J.A. (1998). Genes involved in the formation and assembly of rhizobial cytochromes and their role in symbiotic nitrogen fixation. *Adv Microb Physiol* 40**,** 191-231.

Delgado, M.J., Bonnard, N., Tresierra-Ayala, A., Bedmar, E.J., and Muller, P. (2003). The *Bradyrhizobium japonicum napEDABC* genes encoding the periplasmic nitrate reductase are essential for nitrate respiration. *Microbiology* 149**,** 3395-3403.

Delgado, M.J., Olivares, J., and Bedmar, E.J. (1992). Constitutive and nitrate-induced, membrane-bound nitrate reductase from *Bradyrhizobium japonicum*. *Curr Microbiol* 24**,** 121-124.

Dixon, R., and Kahn, D. (2004). Genetic regulation of biological nitrogen fixation. *Nat Rev Microbiol* 2**,** 621-631.

Downie, J.A. (2005). Legume haemoglobins: symbiotic nitrogen fixation needs bloody nodules. *Curr Biol* 15**,** 196-198.

Eady, R.R., Antonyuk, S.V., and Hasnain, S.S. (2016). Fresh insight to functioning of selected enzymes of the nitrogen cycle. *Curr Opin Chem Biol* 31**,** 103-112.

Earnshaw, A., and Greenwood, N. (1997). Chemistry of the Elements. Elsevier, Amsterdam, 1341.

Ebert, M., Schweyen, P., Broring, M., Laass, S., Hartig, E., and Jahn, D. (2017). Heme and nitric oxide binding by the transcriptional regulator DnrF from the marine bacterium *Dinoroseobacter shibae* increases *napD* promoter affinity. *J Biol Chem* 292**,** 15468-15480.

Eich, R.F., Li, T., Lemon, D.D., Doherty, D.H., Curry, S.R., Aitken, J.F., Mathews, A.J., Johnson, K.A., Smith, R.D., Phillips, G.N., Jr., and Olson, J.S. (1996). Mechanism of NO-induced oxidation of myoglobin and hemoglobin. *Biochemistry* 35**,** 6976-6983.

Einsle, O. (2011). Structure and function of formate-dependent cytochrome *c* nitrite reductase, NrfA. *Methods Enzymol* 496**,** 399-422.

Einsle, O., and Kroneck, P.M. (2004). Structural basis of denitrification. *Biol Chem* 385**,** 875-883.

Elvers, K.T., Wu, G., Gilberthorpe, N.J., Poole, R.K., and Park, S.F. (2004). Role of an inducible single-domain hemoglobin in mediating resistance to nitric oxide and nitrosative stress in *Campylobacter jejuni* and *Campylobacter coli*. *J Bacteriol* 186**,** 5332-5341.

Fernández-López, M., Olivares, J., and Bedmar, E.J. (1994). Two differentially regulated nitrate reductases required for nitrate-dependent, microaerobic growth of *Bradyrhizobium japonicum*. *Arch Microbiol* 162**,** 310-315.

Fernández, N., Cabrera, J.J., Salazar, S., Parejo, S., Rodríguez, M.C., Lindemann, A., Bonnet, M., Hennecke, H., Bedmar, E.J., and Mesa, S. (2016). Molecular determinants of negative regulation of the *Bradyrhizobium diazoefficiens* transcription factor $FixK_2$, in *Biological Nitrogen Fixation and Beneficial Plant-Microbe Interaction* (González-Andrés, F., James, E., eds.) Springer International Publishing, Cham, 57-72.

Fernández, N., Cabrera, J.J., Varadarajan, A.R., Lutz, S., Ledermann, R., Roschitzki, B., Eberl, L., Bedmar, E.J., Fischer, H.M., Pessi, G., Ahrens, C.H., and Mesa, S. (2019). An integrated systems approach unveils new aspects of microoxia-mediated regulation in *Bradyrhizobium diazoefficiens*. *Front Microbiol* 10**,** 924.

Figueiredo, M.C., Lobo, S.A., Sousa, S.H., Pereira, F.P., Wall, J.D., Nobre, L.S., and Saraiva, L.M. (2013). Hybrid cluster proteins and flavodiiron proteins afford protection to *Desulfovibrio vulgaris* upon macrophage infection. *J Bacteriol* 195**,** 2684-2690.

Fischer, H.M. (1994). Genetic regulation of nitrogen fixation in rhizobia. *Microbiol Rev* 58**,** 352-386.

Fixen, K.R., Pal Chowdhury, N., Martínez-Pérez, M., Poudel, S., Boyd, E.S., and Harwood, C.S. (2018). The path of electron transfer to nitrogenase in a phototrophic alpha-proteobacterium. *Environ Microbiol* 20**,** 2500-2508.

Franck, W.L., Qiu, J., Lee, H.I., Chang, W.S., and Stacey, G. (2015). DNA microarray-based identification of genes regulated by NtrC in *Bradyrhizobium japonicum*. *Appl Environ Microbiol* 81**,** 5299-5308.

Freitas, T.A., Hou, S., Dioum, E.M., Saito, J.A., Newhouse, J., González, G., Gilles-González, M.A., and Alam, M. (2004). Ancestral hemoglobins in archaea. *Proc Natl Acad Sci U S A* 101**,** 6675-6680.

Galibert, F., Finan, T.M., Long, S.R., Puhler, A., Abola, P., Ampe, F., et al. (2001). The composite genome of the legume symbiont *Sinorhizobium meliloti*. *Science* 293**,** 668-672.

Galloway, J.N., Townsend, A.R., Erisman, J.W., Bekunda, M., Cai, Z., Freney, J.R., Martinelli, L.A., Seitzinger, S.P., and Sutton, M.A. (2008). Transformation of the nitrogen cycle: recent trends, questions, and potential solutions. *Science* 320**,** 889-892.

Gardner, A.M., and Gardner, P.R. (2002). Flavohemoglobin detoxifies nitric oxide in aerobic, but not anaerobic, *Escherichia coli*. Evidence for a novel inducible anaerobic nitric oxide-scavenging activity. *J Biol Chem* 277**,** 8166-8171.

Gardner, A.M., Helmick, R.A., and Gardner, P.R. (2002). Flavorubredoxin, an inducible catalyst for nitric oxide reduction and detoxification in *Escherichia coli*. *J Biol Chem* 277**,** 8172-8177.

Gardner, P.R. (2005). Nitric oxide dioxygenase function and mechanism of flavohemoglobin, hemoglobin, myoglobin and their associated reductases. *J Inorg Biochem* 99**,** 247-266.

Gardner, P.R. (2012). Hemoglobin: a nitric-oxide dioxygenase. *Scientifica (Cairo)* 2012**,** 683729.

Gardner, P.R., Gardner, A.M., Martin, L.A., and Salzman, A.L. (1998). Nitric oxide dioxygenase: an enzymic function for flavohemoglobin. *Proc Natl Acad Sci USA* 95**,** 10378-10383.

Gates, A.J., Luque-Almagro, V.M., Goddard, A.D., Ferguson, S.J., Roldán, M.D., and Richardson, D.J. (2011). A composite biochemical system for bacterial nitrate and nitrite assimilation as exemplified by *Paracoccus denitrificans*. *Biochem J* 435**,** 743-753.

Gell, D.A. (2018). Structure and function of haemoglobins. *Blood Cells Mol Dis* 70**,** 13-42.

Giardina, G., Rinaldo, S., Johnson, K.A., Di Matteo, A., Brunori, M., and Cutruzzolà, F. (2008). NO sensing in *Pseudomonas aeruginosa*: structure of the transcriptional regulator DNR. *J Mol Biol* 378**,** 1002-1015.

Gibson, Q.H., and Roughton, F.J. (1957). The kinetics and equilibria of the reactions of nitric oxide with sheep haemoglobin. *J Physiol* 136**,** 507-524.

Gibson, Q.H., and Roughton, F.J. (1965). Further studies on the kinetics and equilibria of the reaction of nitric oxide with haemoproteins. *Proc R Soc Lond B Biol Sci* 163**,** 197-205.

Gilberthorpe, N.J., and Poole, R.K. (2008). Nitric oxide homeostasis in *Salmonella typhimurium*: roles of respiratory nitrate reductase and flavohemoglobin. *J Biol Chem* 283**,** 11146-11154.

Gilles-González, M.A., González, G., Perutz, M.F., Kiger, L., Marden, M.C., and Poyart, C. (1994). Heme-based sensors, exemplified by the kinase FixL, are a new class of heme protein with distinctive ligand binding and autoxidation. *Biochemistry* 33**,** 8067-8073.

Girard, L., Brom, S., Dávalos, A., López, O., Soberón, M., and Romero, D. (2000). Differential regulation of *fixN*-reiterated genes in *Rhizobium etli* by a novel *fixL-fixK* cascade. *Mol Plant Microbe Interact* 13**,** 1283-1292.

Goddard, A.D., Bali, S., Mavridou, D.A., Luque-Almagro, V.M., Gates, A.J., Roldán, M.D., Newstead, S., Richardson, D.J., and Ferguson, S.J. (2017). The *Paracoccus*

denitrificans NarK-like nitrate and nitrite transporters-probing nitrate uptake and nitrate/nitrite exchange mechanisms. *Mol Microbiol* 103**,** 117-133.

Goddard, A.D., Moir, J.W., Richardson, D.J., and Ferguson, S.J. (2008). Interdependence of two NarK domains in a fused nitrate/nitrite transporter. *Mol Microbiol* 70**,** 667-681.

Gomes, C.M., Vicente, J.B., Wasserfallen, A., and Teixeira, M. (2000). Spectroscopic studies and characterization of a novel electron-transfer chain from *Escherichia coli* involving a flavorubredoxin and its flavoprotein reductase partner. *Biochemistry* 39**,** 16230-16237.

Gómez-Hernández, N., Reyes-González, A., Sánchez, C., Mora, Y., Delgado, M.J., and Girard, L. (2011). Regulation and symbiotic role of *nirK* and *norC* expression in *Rhizobium etli*. *Mol Plant Microbe Interact* 24**,** 233-245.

González, P.J., Correia, C., Moura, I., Brondino, C.D., and Moura, J.J. (2006). Bacterial nitrate reductases: Molecular and biological aspects of nitrate reduction. *J Inorg Biochem* 100**,** 1015-1023.

González, P.J., Rivas, M., and Moura, J.J. (2017). CHAPTER 3: Structure, function and mechanisms of respiratory nitrate reductases, in *Metalloenzymes in Denitrification: Applications and Environmental Impacts* (Moura, I., Moura, J.J., Pauleta, S.R., Maia, L.B., eds.) The Royal Society of Chemistry, 39-58.

Göttfert, M., Grob, P., and Hennecke, H. (1990). Proposed regulatory pathway encoded by the *nodV* and *nodW* genes, determinants of host specificity in *Bradyrhizobium japonicum*. *Proc Natl Acad Sci U S A* 87**,** 2680-2684.

Graham, P.H., and Vance, C.P. (2003). Legumes: importance and constraints to greater use. *Plant Physiol* 131**,** 872-877.

Greer, F.R., and Shannon, M. (2005). Infant methemoglobinemia: the role of dietary nitrate in food and water. *Pediatrics* 116**,** 784-786.

Gusarov, I., and Nudler, E. (2005). NO-mediated cytoprotection: instant adaptation to oxidative stress in bacteria. *Proc Natl Acad Sci U S A* 102**,** 13855-13860.

Gusarov, I., Shatalin, K., Starodubtseva, M., and Nudler, E. (2009). Endogenous nitric oxide protects bacteria against a wide spectrum of antibiotics. *Science* 325**,** 1380-1384.

Gusarov, I., Starodubtseva, M., Wang, Z.Q., McQuade, L., Lippard, S.J., Stuehr, D.J., and Nudler, E. (2008). Bacterial nitric-oxide synthases operate without a dedicated redox partner. *J Biol Chem* 283**,** 13140-13147.

Hahn, M., Meyer, L., Studer, D., Regensburger, B., and Hennecke, H. (1984). Insertion and deletion mutations within the *nif* region of *Rhizobium japonicum*. *Plant Mol Biol* 3**,** 159-168.

Hallin, S., Philippot, L., Löffler, F.E., Sanford, R.A., and Jones, C.M. (2018). Genomics and Ecology of Novel N_2O-Reducing Microorganisms. *Trends Microbiol* 26**,** 43-55.

Hanahan, D. (1983). Studies on transformation of *Escherichia coli* with plasmids. *J Mol Biol* 166**,** 557-580.

Hartsock, A., and Shapleigh, J.P. (2010). Identification, functional studies, and genomic comparisons of new members of the NnrR regulon in *Rhodobacter sphaeroides*. *J Bacteriol* 192**,** 903-911.

Hausladen, A., Gow, A., and Stamler, J.S. (2001). Flavohemoglobin denitrosylase catalyzes the reaction of a nitroxyl equivalent with molecular oxygen. *Proc Natl Acad Sci USA* 98**,** 10108-10112.

Hausladen, A., Gow, A.J., and Stamler, J.S. (1998). Nitrosative stress: metabolic pathway involving the flavohemoglobin. *Proc Natl Acad Sci U S A* 95**,** 14100-14105.

Hein, S., Witt, S., and Simon, J. (2017). Clade II nitrous oxide respiration of *Wolinella succinogenes* depends on the NosG, -C1, -C2, -H electron transport module, NosB and a Rieske/cytochrome *bc* complex. *Environ Microbiol* 19**,** 4913-4925.

Hemschemeier, A., Duner, M., Casero, D., Merchant, S.S., Winkler, M., and Happe, T. (2013). Hypoxic survival requires a 2-on-2 hemoglobin in a process involving nitric oxide. *Proc Natl Acad Sci U S A* 110**,** 10854-10859.

Hendriks, J., Oubrie, A., Castresana, J., Urbani, A., Gemeinhardt, S., and Saraste, M. (2000). Nitric oxide reductases in bacteria. *Biochim Biophys Acta* 1459**,** 266-273.

Herold, S., and Rock, G. (2005). Mechanistic studies of the oxygen-mediated oxidation of nitrosylhemoglobin. *Biochemistry* 44**,** 6223-6231.

Herridge, D.F., Peoples, M.B., and Boddey, R.M. (2008). Global inputs of biological nitrogen fixation in agricultural systems. *Plant and Soil* 311**,** 1-18.

Heylen, K., and Keltjens, J. (2012). Redundancy and modularity in membrane-associated dissimilatory nitrate reduction in *Bacillus*. *Front Microbiol* 3**,** 371.

Hichri, I., Boscari, A., Castella, C., Rovere, M., Puppo, A., and Brouquisse, R. (2015). Nitric oxide: a multifaceted regulator of the nitrogen-fixing symbiosis. *J Exp Bot* 66**,** 2877-2887.

Hichri, I., Meilhoc, E., Boscari, A., Bruand, C., Frendo, P., and Brouquisse, R. (2016). Nitric oxide: Jack-of-all-trades of the nitrogen-fixing symbiosis?, in *Advances in botanical research* (Vol. 77) London & New York: Academic Press, 193–218.

Hidalgo-García, A., Torres, M.J., Salas, A., Bedmar, E.J., Girard, L., and Delgado, M.J. (2019). *Rhizobium etli* produces nitrous oxide by coupling the assimilatory and denitrification pathways. *Front Microbiol* 10**,** 980.

Hino, T., Matsumoto, Y., Nagano, S., Sugimoto, H., Fukumori, Y., Murata, T., Iwata, S., and Shiro, Y. (2010). Structural basis of biological N_2O generation by bacterial nitric oxide reductase. *Science* 330**,** 1666-1670.

Ho, Y.S., Burden, L.M., and Hurley, J.H. (2000). Structure of the GAF domain, a ubiquitous signaling motif and a new class of cyclic GMP receptor. *EMBO J* 19**,** 5288-5299.

Honisch, U., and Zumft, W.G. (2003). Operon structure and regulation of the *nos* gene region of *Pseudomonas stutzeri*, encoding an ABC-Type ATPase for maturation of nitrous oxide reductase. *J Bacteriol* 185**,** 1895-1902.

Horchani, F., Prevot, M., Boscari, A., Evangelisti, E., Meilhoc, E., Bruand, C., Raymond, P., Boncompagni, E., Aschi-Smiti, S., Puppo, A., and Brouquisse, R. (2011). Both plant and bacterial nitrate reductases contribute to nitric oxide production in *Medicago truncatula* nitrogen-fixing nodules. *Plant Physiol* 155**,** 1023-1036.

Horrell, S., Kekilli, D., Strange, R.W., and Hough, M.A. (2017). Recent structural insights into the function of copper nitrite reductases. *Metallomics* 9**,** 1470-1482.

Howarth, R.W. (2004). Human acceleration of the nitrogen cycle: drivers, consequences, and steps toward solutions. *Water Sci Technol* 49**,** 7-13.

Hu, Z., Wessels, H., van Alen, T., Jetten, M.S.M., and Kartal, B. (2019). Nitric oxide-dependent anaerobic ammonium oxidation. *Nat Commun* 10**,** 1244.

Hughes, M.N. (2008). Chemistry of nitric oxide and related species. *Methods Enzymol* 436**,** 3-19.

Hutfless, E.H., Chaudhari, S.S., and Thomas, V.C. (2018). Emerging roles of nitric oxide synthase in bacterial physiology. *Adv Microb Physiol* 72**,** 147-191.

Ilari, A., Bonamore, A., Farina, A., Johnson, K.A., and Boffi, A. (2002). The X-ray structure of ferric *Escherichia coli* flavohemoglobin reveals an unexpected geometry of the distal heme pocket. *J Biol Chem* 277**,** 23725-23732.

Jang, J., Ashida, N., Kai, A., Isobe, K., Nishizawa, T., Otsuka, S., Yokota, A., Senoo, K., and Ishii, S. (2018). Presence of Cu-type (NirK) and cd_1-type (NirS) nitrite reductase genes in the denitrifying bacterium *Bradyrhizobium nitroreducens* sp. nov. *Microbes Environ* 33**,** 326-331.

Jetten, M.S. (2008). The microbial nitrogen cycle. *Environ Microbiol* 10**,** 2903-2909.

Jetten, M.S., Niftrik, L., Strous, M., Kartal, B., Keltjens, J.T., and Op den Camp, H.J. (2009). Biochemistry and molecular biology of anammox bacteria. *Crit Rev Biochem Mol Biol* 44**,** 65-84.

Jiménez-Leiva, A., Cabrera, J.J., Bueno, E., Torres, M.J., Salazar, S., Bedmar, E.J., Delgado, M.J., and Mesa, S. (2019). Expanding the regulon of the *Bradyrhizobium diazoefficiens* NnrR transcription factor: new insights into the denitrification pathway. *Front Microbiol* 10**,** 1926.

Johnson, E.A., Rice, S.L., Preimesberger, M.R., Nye, D.B., Gilevicius, L., Wenke, B.B., Brown, J.M., Witman, G.B., and Lecomte, J.T. (2014). Characterization of THB1, a *Chlamydomonas reinhardtii* truncated hemoglobin: linkage to nitrogen metabolism and identification of lysine as the distal heme ligand. *Biochemistry* 53**,** 4573-4589.

Johnson, E.A., Russo, M.M., Nye, D.B., Schlessman, J.L., and Lecomte, J.T.J. (2018). Lysine as a heme iron ligand: A property common to three truncated hemoglobins from *Chlamydomonas reinhardtii*. *Biochim Biophys Acta Gen Subj* 1862**,** 2660-2673.

Johnson, E.G., Sparks, J.P., Dzikovski, B., Crane, B.R., Gibson, D.M., and Loria, R. (2008). Plant-pathogenic *Streptomyces* species produce nitric oxide synthase-derived nitric oxide in response to host signals. *Chem Biol* 15**,** 43-50.

Jones, K.M., Kobayashi, H., Davies, B.W., Taga, M.E., and Walker, G.C. (2007). How rhizobial symbionts invade plants: the *Sinorhizobium-Medicago* model. *Nat Rev Microbiol* 5**,** 619-633.

Justino, M.C., Almeida, C.C., Teixeira, M., and Saraiva, L.M. (2007). *Escherichia coli* di-iron YtfE protein is necessary for the repair of stress-damaged iron-sulfur clusters. *J Biol Chem* 282**,** 10352-10359.

Justino, M.C., Vicente, J.B., Teixeira, M., and Saraiva, L.M. (2005). New genes implicated in the protection of anaerobically grown *Escherichia coli* against nitric oxide. *J Biol Chem* 280**,** 2636-2643.

Kahle, M., ter Beek, J., Hosler, J.P., and Ädelroth, P. (2018). The insertion of the non-heme Fe_B cofactor into nitric oxide reductase from *P. denitrificans* depends on NorQ and NorD accessory proteins. *Biochim Biophys Acta Bioenerg* 1859**,** 1051-1058.

Kaneko, T., Nakamura, Y., Sato, S., Minamisawa, K., Uchiumi, T., Sasamoto, S., and Al., E. (2002). Complete genomic sequence of nitrogen-fixing symbiotic bacterium *Bradyrhizobium japonicum* USDA 110. *DNA Res* 9**,** 189-197.

Kapp, O.H., Moens, L., Vanfleteren, J., Trotman, C.N., Suzuki, T., and Vinogradov, S.N. (1995). Alignment of 700 globin sequences: extent of amino acid substitution and its correlation with variation in volume. *Protein Sci* 4**,** 2179-2190.

Kartal, B., de Almeida, N.M., Maalcke, W.J., Op den Camp, H.J., Jetten, M.S., and Keltjens, J.T. (2013). How to make a living from anaerobic ammonium oxidation. *FEMS Microbiol Rev* 37**,** 428-461.

Kastrau, D.H., Heiss, B., Kroneck, P.M., and Zumft, W.G. (1994). Nitric oxide reductase from *Pseudomonas stutzeri*, a novel cytochrome *bc* complex. Phospholipid requirement, electron paramagnetic resonance and redox properties. *Eur J Biochem* 222**,** 293-303.

Kato, K., Kanahama, K., and Kanayama, Y. (2010). Involvement of nitric oxide in the inhibition of nitrogenase activity by nitrate in *Lotus* root nodules. *J. Plant Physiol* 167**,** 238-241.

Kaur, R., Pathania, R., Sharma, V., Mande, S.C., and Dikshit, K.L. (2002). Chimeric *Vitreoscilla* hemoglobin (VHb) carrying a flavoreductase domain relieves nitrosative stress in *Escherichia coli*: new insight into the functional role of VHb. *Appl Environ Microbiol* 68**,** 152-160.

Kendrew, J.C., Dickerson, R.E., Strandberg, B.E., Hart, R.G., Davies, D.R., Phillips, D.C., and Shore, V.C. (1960). Structure of myoglobin: a three-dimensional Fourier synthesis at 2 A. resolution. *Nature* 185**,** 422-427.

Kern, M., and Simon, J. (2009). Electron transport chains and bioenergetics of respiratory nitrogen metabolism in *Wolinella succinogenes* and other Epsilonproteobacteria. *Biochim Biophys Acta* 1787**,** 646-656.

Kern, M., Volz, J., and Simon, J. (2011). The oxidative and nitrosative stress defence network of *Wolinella succinogenes*: cytochrome *c* nitrite reductase mediates the stress response to nitrite, nitric oxide, hydroxylamine and hydrogen peroxide. *Environ Microbiol* 13**,** 2478-2494.

Kim, S.O., Orii, Y., Lloyd, D., Hughes, M.N., and Poole, R.K. (1999). Anoxic function for the *Escherichia coli* flavohaemoglobin (Hmp): reversible binding of nitric oxide and reduction to nitrous oxide. *FEBS Lett* 445**,** 389-394.

Kits, K.D., Sedlacek, C.J., Lebedeva, E.V., Han, P., Bulaev, A., Pjevac, P., Daebeler, A., Romano, S., Albertsen, M., Stein, L.Y., Daims, H., and Wagner, M. (2017). Kinetic analysis of a complete nitrifier reveals an oligotrophic lifestyle. *Nature* 549**,** 269-272.

Kohanski, M.A., Dwyer, D.J., Hayete, B., Lawrence, C.A., and Collins, J.J. (2007). A common mechanism of cellular death induced by bactericidal antibiotics. *Cell* 130**,** 797-810.

Kovach, M.E., Phillips, R.W., Elzer, P.H., Roop, R.M., and Peterson, K.M. (1994). pBBR1MCS: a broad-host-range cloning vector. *Biotechniques* 16**,** 800-802.

Kraft, B., Strous, M., and Tegetmeyer, H.E. (2011). Microbial nitrate respiration--genes, enzymes and environmental distribution. *J Biotechnol* 155**,** 104-117.

Kullik, I., Fritsche, S., Knobel, H., Sanjuan, J., Hennecke, H., and Fischer, H.M. (1991). *Bradyrhizobium japonicum* has two differentially regulated, functional homologs of the σ^{54} gene (*rpoN*). *J Bacteriol* 173**,** 1125-1138.

Lardi, M., Murset, V., Fischer, H.M., Mesa, S., Ahrens, C.H., Zamboni, N., and Pessi, G. (2016). Metabolomic profiling of *Bradyrhizobium diazoefficiens*-induced root nodules reveals both host plant-specific and developmental signatures. *Int J Mol Sci* 17**,** 815.

Ledbetter, R.N., García Costas, A.M., Lubner, C.E., Mulder, D.W., Tokmina-Lukaszewska, M., Artz, J.H., et al. (2017). The electron bifurcating FixABCX protein complex from *Azotobacter vinelandii*: generation of low-potential reducing equivalents for nitrogenase catalysis. *Biochemistry* 56**,** 4177-4190.

Leonard, L.T. (1943). A simple assembly for use in the testing of cultures of Rhizobia. *J Bacteriol* 45**,** 523-527.

Lewinska, A., and Bartosz, G. (2006). Yeast flavohemoglobin protects against nitrosative stress and controls ferric reductase activity. *Redox Rep* 11**,** 231-239.

Lin, J.T., and Stewart, V. (1998). Nitrate assimilation by bacteria. *Adv Microb Physiol* 39**,** 1-30, 379.

Lindemann, A., Moser, A., Pessi, G., Hauser, F., Friberg, M., Hennecke, H., and Fischer, H.M. (2007). New target genes controlled by the *Bradyrhizobium japonicum* two-component regulatory system RegSR. *J Bacteriol* 189**,** 8928-8943.

Liu, L., Zeng, M., Hausladen, A., Heitman, J., and Stamler, J.S. (2000). Protection from nitrosative stress by yeast flavohemoglobin. *Proc Natl Acad Sci U S A* 97**,** 4672-4676.

Lockwood, C.W., Burlat, B., Cheesman, M.R., Kern, M., Simon, J., Clarke, T.A., Richardson, D.J., and Butt, J.N. (2015). Resolution of key roles for the distal pocket histidine in cytochrome *c* nitrite reductases. *J Am Chem Soc* 137**,** 3059-3068.

López, M.F., Cabrera, J.J., Salas, A., Delgado, M.J., and López-García, S.L. (2017). Dissecting the role of NtrC and RpoN in the expression of assimilatory nitrate and nitrite reductases in *Bradyrhizobium diazoefficiens*. *Antonie Van Leeuwenhoek* 110**,** 531-542.

Lu, C., Mukai, M., Lin, Y., Wu, G., Poole, R.K., and Yeh, S.R. (2007). Structural and functional properties of a single domain hemoglobin from the food-borne pathogen *Campylobactor jejuni*. *J Biol Chem* 282**,** 25917-25928.

Luque-Almagro, V.M., Gates, A.J., Moreno-Vivián, C., Ferguson, S.J., Richardson, D.J., and Roldán, M.D. (2011). Bacterial nitrate assimilation: gene distribution and regulation. *Biochem Soc Trans* 39**,** 1838-1843.

Luque-Almagro, V.M., Lyall, V.J., Ferguson, S.J., Roldán, M.D., Richardson, D.J., and Gates, A.J. (2013). Nitrogen oxyanion-dependent dissociation of a two-component complex that regulates bacterial nitrate assimilation. *J Biol Chem* 288**,** 29692-29702.

Maalcke, W.J., Dietl, A., Marritt, S.J., Butt, J.N., Jetten, M.S., Keltjens, J.T., Barends, T.R., and Kartal, B. (2014). Structural basis of biological NO generation by octaheme oxidoreductases. *J Biol Chem* 289**,** 1228-1242.

Mahinthichaichan, P., Gennis, R.B., and Tajkhorshid, E. (2018). Bacterial denitrifying nitric oxide reductases and aerobic respiratory terminal oxidases use similar delivery pathways for their molecular substrates. *Biochim Biophys Acta Bioenerg* 1859**,** 712-724.

Maia, L.B., Moura, I., and Moura, J.J. (2017). CHAPTER 1: Molybdenum and tungsten-containing enzymes: an overview, in *Molybdenum and Tungsten Enzymes: Biochemistry* (Hille, R., Schulzke, C., Kirk, M.L., eds.) The Royal Society of Chemistry, 1-80.

Maia, L.B., and Moura, J.J. (2011). Nitrite reduction by xanthine oxidase family enzymes: a new class of nitrite reductases. *J Biol Inorg Chem* 16**,** 443-460.

Maia, L.B., and Moura, J.J. (2014). How biology handles nitrite. *Chem Rev* 114**,** 5273-5357.

Maia, L.B., and Moura, J.J. (2015). Nitrite reduction by molybdoenzymes: a new class of nitric oxide-forming nitrite reductases. *J Biol Inorg Chem* 20**,** 403-433.

Maia, L.B., and Moura, J.J.G. (2018). Putting xanthine oxidoreductase and aldehyde oxidase on the NO metabolism map: Nitrite reduction by molybdoenzymes. *Redox Biol* 19**,** 274-289.

Mania, D., Heylen, K., Van Spanning, R.J., and Frostegard, A. (2014). The nitrate-ammonifying and *nosZ*-carrying bacterium *Bacillus vireti* is a potent source and sink for nitric and nitrous oxide under high nitrate conditions. *Environ Microbiol* 16**,** 3196-3210.

Martínez-Espinosa, R.M., Cole, J.A., Richardson, D.J., and Watmough, N.J. (2011). Enzymology and ecology of the nitrogen cycle. *Biochem Soc Trans* 39**,** 175-178.

Matsumoto, Y., Tosha, T., Pisliakov, A.V., Hino, T., Sugimoto, H., Nagano, S., Sugita, Y., and Shiro, Y. (2012). Crystal structure of quinol-dependent nitric oxide reductase from *Geobacillus stearothermophilus*. *Nat Struct Mol Biol* 19**,** 238-245.

McLean, S., Bowman, L.A., and Poole, R.K. (2010). Peroxynitrite stress is exacerbated by flavohaemoglobin-derived oxidative stress in *Salmonella typhimurium* and is relieved by nitric oxide. *Microbiology* 156**,** 3556-3565.

Meakin, G.E., Bueno, E., Jepson, B., Bedmar, E.J., Richardson, D.J., and Delgado, M.J. (2007). The contribution of bacteroidal nitrate and nitrite reduction to the formation of nitrosylleghaemoglobin complexes in soybean root nodules. *Microbiology* 153**,** 411-419.

Melo, P.M., Silva, L.S., Ribeiro, I., Seabra, A.R., and Carvalho, H.G. (2011). Glutamine synthetase is a molecular target of nitric oxide in root nodules of *Medicago truncatula* and is regulated by tyrosine nitration. *Plant Physiol* 157**,** 1505-1517.

Mesa, S., Alche , J.D., Bedmar, E., and Delgado, M.J. (2004). Expression of *nir*, *nor* and *nos* denitrification genes from *Bradyrhizobium japonicum* in soybean root nodules. *Physiol Plant* 120**,** 205-211.

Mesa, S., Hauser, F., Friberg, M., Malaguti, E., Fischer, H.M., and Hennecke, H. (2008). Comprehensive assessment of the regulons controlled by the FixLJ-$FixK_2$-$FixK_1$ cascade in *Bradyrhizobium japonicum*. *J Bacteriol* 190**,** 6568-6579.

Mesa, S., Reutimann, L., Fischer, H.M., and Hennecke, H. (2009). Posttranslational control of transcription factor $FixK_2$, a key regulator for the *Bradyrhizobium japonicum*-soybean symbiosis. *Proc Natl Acad Sci U S A* 106**,** 21860-21865.

Mesa, S., Ucurum, Z., Hennecke, H., and Fischer, H.M. (2005). Transcription activation in vitro by the *Bradyrhizobium japonicum* regulatory protein $FixK_2$. *J Bacteriol* 187**,** 3329-3338.

Mesa, S., Velasco, L., Manzanera, M.E., Delgado, M.J., and Bedmar, E.J. (2002). Characterization of the *norCBQD* genes, encoding nitric oxide reductase, in the nitrogen fixing bacterium *Bradyrhizobium japonicum*. *Microbiology* 148**,** 3553-3560.

Miller, J.H. (1972). Experiments in Molecular Genetics, Cold Spring Harbor Laboratory, New York.

Mills, P.C., Rowley, G., Spiro, S., Hinton, J.C., and Richardson, D.J. (2008). A combination of cytochrome *c* nitrite reductase (NrfA) and flavorubredoxin

(NorV) protects *Salmonella enterica* serovar Typhimurium against killing by NO in anoxic environments. *Microbiology* 154**,** 1218-1228.

Minchin, F.R. (1997). Regulation of oxygen diffusion in legume nodules. *Soil Biology and Biochemistry* 29**,** 88-89.

Minchin, F.R., James, E.K., and Becana, M. (2008). CHAPTER 11: Oxygen diffusion, production of reactive oxygen and nitrogen species, and antioxidants in legume nodules, in *Nitrogen-fixing leguminous symbioses* (Dilworth, M.J., James, E.K., Sprent, J.I., Newton, W.E., eds.) Springer, Dordrecht, 321-362.

Möller, M.N., Ríos, N., Trujillo, M., Radi, R., Denicola, A., and Álvarez, B. (2019). Detection and quantification of nitric oxide-derived oxidants in biological systems. *J Biol Chem* 294**,** 14776-14802.

Monk, C.E., Pearson, B.M., Mulholland, F., Smith, H.K., and Poole, R.K. (2008). Oxygen- and NssR-dependent globin expression and enhanced iron acquisition in the response of campylobacter to nitrosative stress. *J Biol Chem* 283**,** 28413-28425.

Moreno-Vivián, C., Cabello, P., Martínez-Luque, M., Blasco, R., and Castillo, F. (1999). Prokaryotic nitrate reduction: molecular properties and functional distinction among bacterial nitrate reductases. *J Bacteriol* 181**,** 6573-6584.

Moreno-Vivián, C., and Flores, E. (2007). CHAPTER 17: Nitrate assimilation in bacteria, in *Biology of the Nitrogen Cycle* (Ferguson, S.J., Newton, W.E., eds.) Elsevier, Amsterdam, 263-282.

Mowat, C.G., Gazur, B., Campbell, L.P., and Chapman, S.K. (2010). Flavin-containing heme enzymes. *Arch Biochem Biophys* 493**,** 37-52.

Mukhopadhyay, P., Zheng, M., Bedzyk, L.A., LaRossa, R.A., and Storz, G. (2004). Prominent roles of the NorR and Fur regulators in the *Escherichia coli* transcriptional response to reactive nitrogen species. *Proc Natl Acad Sci U S A* 101**,** 745-750.

Nagata, M., Murakami, E., Shimoda, Y., Shimoda-Sasakura, F., Kucho, K., Suzuki, A., Abe, M., Higashi, S., and Uchiumi, T. (2008). Expression of a class 1 hemoglobin gene and production of nitric oxide in response to symbiotic and pathogenic bacteria in *Lotus japonicus*. *Mol Plant Microbe Interact* 21**,** 1175-1183.

Nakano, M.M. (2002). Induction of ResDE-dependent gene expression in *Bacillus subtilis* in response to nitric oxide and nitrosative stress. *J Bacteriol* 184**,** 1783-1787.

Nakano, M.M. (2006). Essential role of flavohemoglobin in long-term anaerobic survival of *Bacillus subtilis*. *J Bacteriol* 188**,** 6415-6418.

Nardini, M., Pesce, A., Labarre, M., Richard, C., Bolli, A., Ascenzi, P., Guertin, M., and Bolognesi, M. (2006). Structural determinants in the group III truncated hemoglobin from *Campylobacter jejuni*. *J Biol Chem* 281**,** 37803-37812.

Nellen-Anthamatten, D., Rossi, P., Preisig, O., Kullik, I., Babst, M., Fischer, H.M., and Hennecke, H. (1998). *Bradyrhizobium japonicum* $FixK_2$, a crucial distributor in

the FixLJ-dependent regulatory cascade for control of genes inducible by low oxygen levels. *J Bacteriol* 180**,** 5251-5255.

Newton, E. (2007). CHAPTER 8: Physiology, biochemistry, and molecular biology of nitrogen fixation, in *Biology of the Nitrogen Cycle* (Ferguson, S.J., Newton, W.E., eds.) Elsevier, Amsterdam, 109-129.

Nojiri, M. (2017). CHAPTER 5: Structure and function of copper nitrite reductase, in *Metalloenzymes in Denitrification: Applications and Environmental Impacts* (Moura, I., Moura, J.J., Pauleta, S.R., Maia, L.B., eds.) The Royal Society of Chemistry, 91-113.

Nukui, N., Minamisawa, K., Ayabe, S., and Aoki, T. (2006). Expression of the 1-aminocyclopropane-1-carboxylic acid deaminase gene requires symbiotic nitrogen-fixing regulator gene *nifA2* in *Mesorhizobium loti* MAFF303099. *Appl Environ Microbiol* 72**,** 4964-4969.

Okazaki, S., Noisangiam, R., Okubo, T., Kaneko, T., Oshima, K., Hattori, M., et al. (2015). Genome analysis of a novel *Bradyrhizobium* sp. DOA9 carrying a symbiotic plasmid. *PLoS One* 10**,** e0117392.

Opperman, D.J., Murgida, D.H., Dalosto, S.D., Brondino, C.D., and Ferroni, F.M. (2019). A three-domain copper-nitrite reductase with a unique sensing loop. *IUCrJ* 6**,** 248-258.

Ott, T., Van Dongen, J.T., Günther, C., Krusell, L., Desbrosses, G., Vigeolas, H., Bock, V., Czechowski, T., Geigenberger, P., and Udvardi, M.K. (2005). Symbiotic leghemoglobins are crucial for nitrogen fixation in legume root nodules but not for general plant growth and development. *Curr Biol* 15**,** 531-535.

Ouellet, H., Ouellet, Y., Richard, C., Labarre, M., Wittenberg, B., Wittenberg, J., and Guertin, M. (2002). Truncated hemoglobin HbN protects *Mycobacterium bovis* from nitric oxide. *Proc Natl Acad Sci U S A* 99**,** 5902-5907.

Overton, T.W., Justino, M.C., Li, Y., Baptista, J.M., Melo, A.M., Cole, J.A., and Saraiva, L.M. (2008). Widespread distribution in pathogenic bacteria of di-iron proteins that repair oxidative and nitrosative damage to iron-sulfur centers. *J Bacteriol* 190**,** 2004-2013.

Parrilli, E., Giuliani, M., Giordano, D., Russo, R., Marino, G., Verde, C., and Tutino, M.L. (2010). The role of a 2-on-2 haemoglobin in oxidative and nitrosative stress resistance of Antarctic *Pseudoalteromonas haloplanktis* TAC125. *Biochimie* 92**,** 1003-1009.

Patel, B.A., Moreau, M., Widom, J., Chen, H., Yin, L., Hua, Y., and Crane, B.R. (2009). Endogenous nitric oxide regulates the recovery of the radiation-resistant bacterium *Deinococcus radiodurans* from exposure to UV light. *Proc Natl Acad Sci U S A* 106**,** 18183-18188.

Pathania, R., Navani, N.K., Gardner, A.M., Gardner, P.R., and Dikshit, K.L. (2002). Nitric oxide scavenging and detoxification by the *Mycobacterium tuberculosis* haemoglobin, HbN in *Escherichia coli*. *Mol Microbiol* 45**,** 1303-1314.

Pauleta, S.R., Carepo, M.S.P., and Moura, I. (2019). Source and reduction of nitrous oxide. *Coord Chem Rev* 387**,** 436-449.

Pauleta, S.R., Carreira, C., and Moura, I. (2017). CHAPTER 7: Insights into nitrous oxide reductase, in *Metalloenzymes in Denitrification: Applications and Environmental Impacts* (Moura, I., Moura, J.J., Pauleta, S.R., Maia, L.B., eds.) The Royal Society of Chemistry, 141-169.

Perutz, M.F., Rossmann, M.G., Cullis, A.F., Muirhead, H., Will, G., and North, A.C. (1960). Structure of haemoglobin: a three-dimensional Fourier synthesis at 5.5-A. resolution, obtained by X-ray analysis. *Nature* 185**,** 416-422.

Pessi, G., Ahrens, C.H., Rehrauer, H., Lindemann, A., Hauser, F., Fischer, H.M., and Hennecke, H. (2007). Genome-wide transcript analysis of *Bradyrhizobium japonicum* bacteroids in soybean root nodules. *Mol Plant Microbe Interact* 20**,** 1353-1363.

Peters, J.W., Boyd, E.S., Hamilton, T.L., and Rubio, L.M. (2011). Biochemistry of Mo-nitrogenase, in *Nitrogen cycling in bacteria: molecular analysis* (Moir, J.W.B., ed.) Caister Academic Press, UK, 59-100.

Pfaffl, M.W. (2001). A new mathematical model for relative quantification in real-time RT-PCR. *Nucleic Acids Res* 29**,** e45.

Pilegaard, K. (2013). Processes regulating nitric oxide emissions from soils. *Philos Trans R Soc, B: Biol Sci* 368**,** 20130126.

Pinchbeck, B.J., Soriano-Laguna, M.J., Sullivan, M.J., Luque-Almagro, V.M., Rowley, G., Ferguson, S.J., Roldán, M.D., Richardson, D.J., and Gates, A.J. (2019). A dual functional redox enzyme maturation protein for respiratory and assimilatory nitrate reductases in bacteria. *Mol Microbiol* 111**,** 1592-1603.

Pisliakov, A.V., Hino, T., Shiro, Y., and Sugita, Y. (2012). Molecular dynamics simulations reveal proton transfer pathways in cytochrome *c*-dependent nitric oxide reductase. *PLoS Comput Biol* 8**,** e1002674.

Pittman, M.S., Elvers, K.T., Lee, L., Jones, M.A., Poole, R.K., Park, S.F., and Kelly, D.J. (2007). Growth of *Campylobacter jejuni* on nitrate and nitrite: electron transport to NapA and NrfA via NrfH and distinct roles for NrfA and the globin Cgb in protection against nitrosative stress. *Mol Microbiol* 63**,** 575-590.

Poock, S.R., Leach, E.R., Moir, J.W., Cole, J.A., and Richardson, D.J. (2002). Respiratory detoxification of nitric oxide by the cytochrome *c* nitrite reductase of *Escherichia coli*. *J Biol Chem* 277**,** 23664-23669.

Poole, P., Ramachandran, V., and Terpolilli, J. (2018). Rhizobia: from saprophytes to endosymbionts. *Nat Rev Microbiol* 16**,** 291-303.

Poole, R.K. (2005). Nitric oxide and nitrosative stress tolerance in bacteria. *Biochem Soc Trans* 33**,** 176-180.

Potter, L., Angove, H., Richardson, D., and Cole, J. (2001). Nitrate reduction in the periplasm of gram-negative bacteria. *Adv Microb Physiol* 45**,** 51-112.

Poudel, S., Colman, D.R., Fixen, K.R., Ledbetter, R.N., Zheng, Y., Pence, N., Seefeldt, L.C., Peters, J.W., Harwood, C.S., and Boyd, E.S. (2018). Electron transfer to nitrogenase in different genomic and metabolic backgrounds. *J Bacteriol* 200, e00757-17.

Preisig, O., Zufferey, R., Thony-Meyer, L., Appleby, C.A., and Hennecke, H. (1996). A high-affinity cbb_3-type cytochrome oxidase terminates the symbiosis-specific respiratory chain of *Bradyrhizobium japonicum*. *J Bacteriol* 178**,** 1532-1538.

Prendergast-Miller, M.T., Baggs, E.M., and Johnson, D. (2011). Nitrous oxide production by the ectomycorrhizal fungi *Paxillus involutus* and *Tylospora fibrillosa*. *FEMS Microbiol Lett* 316**,** 31-35.

Price, M.S., Chao, L.Y., and Marletta, M.A. (2007). *Shewanella oneidensis* MR-1 H-NOX regulation of a histidine kinase by nitric oxide. *Biochemistry* 46**,** 13677-13683.

Regensburger, B., and Hennecke, H. (1983). RNA polymerase from *Rhizobium japonicum*. *Arch Microbiol* 135**,** 103-109.

Reyes-González, A., Talbi, C., Rodríguez, S., Rivera, P., Zamorano-Sánchez, D., and Girard, L. (2016). Expanding the regulatory network that controls nitrogen fixation in *Sinorhizobium meliloti*: elucidating the role of the two-component system hFixL-FxkR. *Microbiology* 162**,** 979-988.

Rhee, K.Y., Erdjument-Bromage, H., Tempst, P., and Nathan, C.F. (2005). S-nitroso proteome of *Mycobacterium tuberculosis*: Enzymes of intermediary metabolism and antioxidant defense. *Proc Natl Acad Sci U S A* 102**,** 467-472.

Rice, S.L., Boucher, L.E., Schlessman, J.L., Preimesberger, M.R., Bosch, J., and Lecomte, J.T. (2015). Structure of *Chlamydomonas reinhardtii* THB1, a group 1 truncated hemoglobin with a rare histidine-lysine heme ligation. *Acta Crystallogr F Struct Biol Commun* 71**,** 718-725.

Richards, M.P. (2013). Redox reactions of myoglobin. *Antioxid Redox Signal* 18**,** 2342-2351.

Richardson, A.R., Dunman, P.M., and Fang, F.C. (2006). The nitrosative stress response of *Staphylococcus aureus* is required for resistance to innate immunity. *Mol Microbiol* 61**,** 927-939.

Richardson, D.J. (2011). Redox complexes of the nitrogen cycle, in *Nitrogen cycling in bacteria: Molecular Analysis* (Moir J.W.B., ed.) Caister Academic Press, U.K.**,** 23-39.

Richardson, D.J., Van Spanning, R.J.M., and Ferguson, S.J. (2007). CHAPTER 2: The Prokaryotic nitrate reductases, in *Biology of the Nitrogen Cycle* (Ferguson, S.J., Newton, W.E., eds.) Elsevier, Amsterdam**,** 21-35.

Richardson, D.J., and Watmough, N.J. (1999). Inorganic nitrogen metabolism in bacteria. *Curr Opin Chem Biol* 3**,** 207-219.

Rigaud, J., and Puppo, A. (1975). Indole-3-acetic acid catabolism by soybean bacteroids. *J Gen Microbiol* 88**,** 223-228.

Rinaldo, S., Arcovito, A., Giardina, G., Castiglione, N., Brunori, M., and Cutruzzolà, F. (2008). New insights into the activity of *Pseudomonas aeruginosa* cd_1 nitrite reductase. *Biochem Soc Trans* 36**,** 1155-1159.

Rinaldo, S., Giardina, G., and Cutruzzolà, F. (2014). Nitrosylation of c heme in cd_1-nitrite reductase is enhanced during catalysis. *Biochem Biophys Res Commun* 451**,** 449-454.

Rinaldo, S., Giardina, G., and Cutruzzolà, F. (2017). CHAPTER 4: Nitrite reductase-cytochrome cd_1, in *Metalloenzymes in Denitrification: Applications and Environmental Impacts* (Moura, I., Moura, J.J., Pauleta, S.R., Maia, L.B., eds.) The Royal Society of Chemistry, 59-90.

Robledo, M., Jiménez-Zurdo, J.I., Velázquez, E., Trujillo, M.E., Zurdo-Pineiro, J.L., Ramírez-Bahena, M.H., Ramos, B., Díaz-Mínguez, J.M., Dazzo, F., Martínez-Molina, E., and Mateos, P.F. (2008). *Rhizobium* cellulase CelC2 is essential for primary symbiotic infection of legume host roots. *Proc Natl Acad Sci U S A* 105**,** 7064-7069.

Rodgers, K.R. (1999). Heme-based sensors in biological systems. *Curr Opin Chem Biol* 3**,** 158-167.

Rodríguez, R.L., and Tait, R.C. (1983). *Recombinant DNA Techniques: An Introduction*, Addison-Wesley, Reading, Massachusetts.

Rowley, G., Hensen, D., Felgate, H., Arkenberg, A., Appia-Ayme, C., Prior, K., Harrington, C., Field, S.J., Butt, J.N., Baggs, E., and Richardson, D.J. (2012). Resolving the contributions of the membrane-bound and periplasmic nitrate reductase systems to nitric oxide and nitrous oxide production in *Salmonella enterica* serovar Typhimurium. *Biochem J* 441**,** 755-762.

Rubio, L.M., and Ludden, P.W. (2008). Biosynthesis of the iron-molybdenum cofactor of nitrogenase. *Annu Rev Microbiol* 62**,** 93-111.

Ruiz, B., Le Scornet, A., Sauviac, L., Rémy, A., Bruand, C., and Meilhoc, E. (2019). The nitrate assimilatory pathway in *Sinorhizobium meliloti*: contribution to NO production. *Front Microbiol* 10**,** 1526.

Rutten, P.J., and Poole, P.S. (2019). Oxygen regulatory mechanisms of nitrogen fixation in rhizobia. *Adv Microb Physiol* 75**,** 325-389.

Salgo, M.G., Stone, K., Squadrito, G.L., Battista, J.R., and Pryor, W.A. (1995). Peroxynitrite causes DNA nicks in plasmid pBR322. *Biochem Biophys Res Commun* 210**,** 1025-1030.

Sambrook, J., and Russell, D. (2001). *Molecular Cloning: a Laboratory Manual*, 3rd ed., Cold Spring Harbor Laboratory, Cold Spring Harbor, New York.

Sánchez, C., Cabrera, J.J., Gates, A.J., Bedmar, E.J., Richardson, D.J., and Delgado, M.J. (2011a). Nitric oxide detoxification in the rhizobia-legume symbiosis. *Biochem Soc Trans* 39**,** 184-188.

Sánchez, C., Gates, A.J., Meakin, G.E., Uchiumi, T., Girard, L., Richardson, D.J., Bedmar, E.J., and Delgado, M.J. (2010). Production of nitric oxide and

nitrosylleghemoglobin complexes in soybean nodules in response to flooding. *Mol Plant Microbe Interact* 23**,** 702-711.

Sánchez, C., Itakura, M., Okubo, T., Matsumoto, T., Yoshikawa, H., Gotoh, A., Hidaka, M., Uchida, T., and Minamisawa, K. (2014). The nitrate-sensing NasST system regulates nitrous oxide reductase and periplasmic nitrate reductase in *Bradyrhizobium japonicum*. *Environ Microbiol* 16**,** 3263-3274.

Sánchez, C., and Minamisawa, K. (2018). Redundant roles of *Bradyrhizobium oligotrophicum* Cu-type (NirK) and *cd*$_1$-type (NirS) nitrite reductase genes under denitrifying conditions. *FEMS Microbiol Lett* 365.

Sánchez, C., Tortosa, G., Granados, A., Delgado, A., Bedmar, E.J., and Delgado, M.J. (2011b). Involvement of *Bradyrhizobium japonicum* denitrification in symbiotic nitrogen fixation by soybean plants subjected to flooding. *Soil Biol Biochem* 43**,** 212-217.

Sander, R. (1999). *Compilation of Henry's law constants for inorganic and organic species of potential importance in environmental chemistry*. Max-Planck Institute of Chemistry, Air Chemistry Department, Mainz.

Santolini, J. (2019). What does "NO-Synthase" stand for ? *Front Biosci (Landmark Ed)* 24**,** 133-171.

Schwember, A.R., Schulze, J., del Pozo, A., and Cabeza, R.A. (2019). Regulation of symbiotic nitrogen fixation in legume root nodules. *Plants (Basel)* 8**,** 333.

Scott, N.L., Xu, Y., Shen, G., Vuletich, D.A., Falzone, C.J., Li, Z., Ludwig, M., Pond, M.P., Preimesberger, M.R., Bryant, D.A., and Lecomte, J.T. (2010). Functional and structural characterization of the 2/2 hemoglobin from *Synechococcus* sp. PCC 7002. *Biochemistry* 49**,** 7000-7011.

Seefeldt, L.C., Peters, J.W., Beratan, D.N., Bothner, B., Minteer, S.D., Raugei, S., and Hoffman, B.M. (2018). Control of electron transfer in nitrogenase. *Curr Opin Chem Biol* 47**,** 54-59.

Seth, D., Hausladen, A., Wang, Y.J., and Stamler, J.S. (2012). Endogenous protein S-Nitrosylation in *E. coli*: regulation by OxyR. *Science* 336**,** 470-473.

Seth, D., Hess, D.T., Hausladen, A., Wang, L., Wang, Y.J., and Stamler, J.S. (2018). A multiplex enzymatic machinery for cellular protein S-nitrosylation. *Mol Cell* 69**,** 451-464.

Shapleigh, J.P. (2006). The denitrifying prokaryotes, in *The Prokaryotes* (Dworkin, M., Falkow, S., Rosenberg, E., Schleifer, K.H., eds.) Springer Science +Business Media. New York, 769-792

Shatalin, K., Gusarov, I., Avetissova, E., Shatalina, Y., McQuade, L.E., Lippard, S.J., and Nudler, E. (2008). *Bacillus anthracis*-derived nitric oxide is essential for pathogen virulence and survival in macrophages. *Proc Natl Acad Sci U S A* 105**,** 1009-1013.

Shepherd, M., Barynin, V., Lu, C., Bernhardt, P.V., Wu, G., Yeh, S.R., Egawa, T., Sedelnikova, S.E., Rice, D.W., Wilson, J.L., and Poole, R.K. (2010). The single-

domain globin from the pathogenic bacterium *Campylobacter jejuni*: novel $_D$-helix conformation, proximal hydrogen bonding that influences ligand binding, and peroxidase-like redox properties. *J Biol Chem* 285**,** 12747-12754.

Shimoda, Y., Shimoda-Sasakura, F., Kucho, K., Kanamori, N., Nagata, M., Suzuki, A., Abe, M., Higashi, S., and Uchiumi, T. (2009). Overexpression of class 1 plant hemoglobin genes enhances symbiotic nitrogen fixation activity between *Mesorhizobium loti* and *Lotus japonicus*. *Plant J* 57**,** 254-263.

Shiro, Y., Sugimoto, H., Tosha, T., Nagano, S., and Hino, T. (2012). Structural basis for nitrous oxide generation by bacterial nitric oxide reductases. *Philos Trans R Soc Lond B Biol Sci* 367**,** 1195-1203.

Shoun, H., and Fushinobu, S. (2017). CHAPTER 14: Denitrification in Fungi, in *Metalloenzymes in Denitrification: Applications and Environmental Impacts* (Moura, I., Moura, J.J., Pauleta, S.R., Maia, L.B., eds.) The Royal Society of Chemistry, 331-348.

Sickerman, N.S., Rettberg, L.A., Lee, C.C., Hu, Y., and Ribbe, M.W. (2017). Cluster assembly in nitrogenase. *Essays Biochem* 61**,** 271-279.

Simon, J. (2002). Enzymology and bioenergetics of respiratory nitrite ammonification. *FEMS Microbiol Rev* 26**,** 285-309.

Simon, J., and Klotz, M.G. (2013). Diversity and evolution of bioenergetic systems involved in microbial nitrogen compound transformations. *Biochim Biophys Acta* 1827**,** 114-135.

Simon, R., Priefer, U., and Pühler, A. (1983). Vector plasmids for *in vivo* and *in vitro* manipulation of gram-negative bacteria, in *Molecular genetics of the bacteria-plant interaction* (Pühler, A., ed.) Springer Verlag, Berlin Heidelberg New York, 98-106

Smagghe, B.J., Trent, J.T., 3rd, and Hargrove, M.S. (2008). NO dioxygenase activity in hemoglobins is ubiquitous *in vitro*, but limited by reduction *in vivo*. *PLoS One* 3**,** e2039.

Souza, J.M., Peluffo, G., and Radi, R. (2008). Protein tyrosine nitration--functional alteration or just a biomarker? *Free Radic Biol Med* 45**,** 357-366.

Stern, A.M., Liu, B., Bakken, L.R., Shapleigh, J.P., and Zhu, J. (2013). A novel protein protects bacterial iron-dependent metabolism from nitric oxide. *J Bacteriol* 195**,** 4702-4708.

Stern, A.M., and Zhu, J. (2014). An introduction to nitric oxide sensing and response in bacteria. *Adv Appl Microbiol* 87**,** 187-220.

Strous, M., Kuenen, J.G., and Jetten, M.S. (1999). Key physiology of anaerobic ammonium oxidation. *Appl Environ Microbiol* 65**,** 3248-3250.

Sullivan, M.J., Gates, A.J., Appia-Ayme, C., Rowley, G., and Richardson, D.J. (2013). Copper control of bacterial nitrous oxide emission and its impact on vitamin B_{12}-dependent metabolism. *Proc Natl Acad Sci U S A* 110**,** 19926-19931.

Svensson, L., Marklund, B.I., Poljakovic, M., and Persson, K. (2006). Uropathogenic *Escherichia coli* and tolerance to nitric oxide: the role of flavohemoglobin. *J Urol* 175**,** 749-753.

Takaya, N. (2002). Dissimilatory nitrate reduction metabolisms and their control in fungi. *J Biosci Bioeng* 94**,** 506-510.

Tarricone, C., Galizzi, A., Coda, A., Ascenzi, P., and Bolognesi, M. (1997). Unusual structure of the oxygen-binding site in the dimeric bacterial hemoglobin from *Vitreoscilla* sp. *Structure* 5**,** 497-507.

Terpolilli, J.J., Hood, G.A., and Poole, P.S. (2012). What determines the efficiency of N_2-fixing *Rhizobium*-legume symbioses? *Adv Microb Physiol* 60**,** 325-389.

Thomas, P.E., Ryan, D., and Levin, W. (1976). An improved staining procedure for the detection of the peroxidase activity of cytochrome P-450 on sodium dodecyl sulfate polyacrylamide gels. *Anal Biochem* 75**,** 168-176.

Thompson, J.D., Higgins, D.G., and Gibson, T.J. (1994). CLUSTAL W: improving the sensitivity of progressive multiple sequence alignment through sequence weighting, position-specific gap penalties and weight matrix choice. *Nucleic Acids Res* 22**,** 4673-4680.

Tinajero-Trejo, M., and Shepherd, M. (2013). The globins of *Campylobacter jejuni*. *Adv Microb Physiol* 63**,** 97-145.

Tinajero-Trejo, M., Vreugdenhil, A., Sedelnikova, S.E., Davidge, K.S., and Poole, R.K. (2013). Nitric oxide reactivities of the two globins of the foodborne pathogen *Campylobacter jejuni*: roles in protection from nitrosative stress and analysis of potential reductants. *Nitric Oxide* 34**,** 65-75.

Toledo, J.C., Jr., and Augusto, O. (2012). Connecting the chemical and biological properties of nitric oxide. *Chem Res Toxicol* 25**,** 975-989.

Torregrosa-Crespo, J., González-Torres, P., Bautista, V., Esclapez, J.M., Pire, C., Camacho, M., Bonete, M.J., Richardson, D.J., Watmough, N.J., and Martínez-Espinosa, R.M. (2017). Analysis of multiple haloarchaeal genomes suggests that the quinone-dependent respiratory nitric oxide reductase is an important source of nitrous oxide in hypersaline environments. *Environ Microbiol Rep* 9**,** 788-796.

Torres, M.J., Argandoña, M., Vargas, C., Bedmar, E.J., Fischer, H.M., Mesa, S., and Delgado, M.J. (2014a). The global response regulator RegR controls expression of denitrification genes in *Bradyrhizobium japonicum*. *PLoS One* 9**,** e99011.

Torres, M.J., Ávila, S., Bedmar, E.J., and Delgado, M.J. (2018). Overexpression of the periplasmic nitrate reductase supports anaerobic growth by *Ensifer meliloti*. *FEMS Microbiol Lett* 365.

Torres, M.J., Bueno, E., Jiménez-Leiva, A., Cabrera, J.J., Bedmar, E.J., Mesa, S., and Delgado, M.J. (2017). $FixK_2$ is the main transcriptional activator of *Bradyrhizobium diazoefficiens nosRZDYFLX* genes in response to low oxygen. *Front Microbiol* 8**,** 1621.

Torres, M.J., Rubia, M.I., Bedmar, E.J., and Delgado, M.J. (2011). Denitrification in *Sinorhizobium meliloti*. *Biochem Soc Trans* 39**,** 1886-1889.

Torres, M.J., Rubia, M.I., de la Peña, T.C., Pueyo, J.J., Bedmar, E.J., and Delgado, M.J. (2014b). Genetic basis for denitrification in *Ensifer meliloti*. *BMC Microbiol* 14**,** 142.

Torres, M.J., Simon, J., Rowley, G., Bedmar, E.J., Richardson, D.J., Gates, A.J., and Delgado, M.J. (2016). Nitrous oxide metabolism in nitrate-reducing bacteria: physiology and regulatory mechanisms. *Adv Microb Physiol* 68**,** 353-432.

Tortosa, G., Hidalgo, A., Salas, A., Bedmar, E.J., Mesa, S., and Delgado, M.J. (2015). Nitrate and flooding induce N_2O emissions from soybean nodules. *Symbiosis* 67**,** 125-133.

Tosha, T., and Shiro, Y. (2017). CHAPTER 6: Structure and function of nitric oxide reductases, in *Metalloenzymes in Denitrification: Applications and Environmental Impacts* (Moura, I., Moura, J.J., Pauleta, S.R., Maia, L.B., eds.) The Royal Society of Chemistry, 114-140.

Treusch, A.H., Leininger, S., Kletzin, A., Schuster, S.C., Klenk, H.P., and Schleper, C. (2005). Novel genes for nitrite reductase and Amo-related proteins indicate a role of uncultivated mesophilic crenarchaeota in nitrogen cycling. *Environ Microbiol* 7**,** 1985-1995.

Trinchant, J.C., and Rigaud, J. (1982). Nitrite and nitric oxide as inhibitors of nitrogenase from soybean bacteroids. *Appl Environ Microbiol* 44**,** 1385-1388.

Udvardi, M., and Poole, P.S. (2013). Transport and metabolism in legume-rhizobia symbioses. *Annu Rev Plant Biol* 64**,** 781-805.

van Grinsven, H.J., Rabl, A., and de Kok, T.M. (2010). Estimation of incidence and social cost of colon cancer due to nitrate in drinking water in the EU: a tentative cost-benefit assessment. *Environ Health* 9**,** 58.

van Spanning, R.J. (2011). Structure, function, regulation and evolution of the nitrite and nitrous oxide reductases: Denitrification enzymes with a beta-propeller fold, in *Nitrogen Cycling in Bacteria* (Moir, J.W.B., ed.) Caister Academic Press, U.K., 135-161.

van Spanning, R.J., Richardson, D.J., and Ferguson, S.J. (2007). CHAPTER 1: Introduction to the biochemistry and molecular biology of denitrification, in *Biology of the Nitrogen Cycle* (Bothe, H., Ferguson, S.J., Newton, W.E., eds.) Elsevier, Amsterdam, 3-20

Vargas, C., Mcewan, A.G., and Downie, J.A. (1993). Detection of *c*-type cytochromes using enhanced chemiluminescence. *Anal Biochem* 209**,** 323-326.

Vasudevan, S.G., Armarego, W.L., Shaw, D.C., Lilley, P.E., Dixon, N.E., and Poole, R.K. (1991). Isolation and nucleotide sequence of the hmp gene that encodes a haemoglobin-like protein in *Escherichia coli* K-12. *Mol Gen Genet* 226**,** 49-58.

Velasco, L., Mesa, S., Delgado, M.J., and Bedmar, E.J. (2001). Characterization of the *nirK* gene encoding the respiratory, Cu-containing nitrite reductase of *Bradyrhizobium japonicum*. *Biochim Biophys Acta* 1521**,** 130-134.

Velasco, L., Mesa, S., Xu, C.A., Delgado, M.J., and Bedmar, E.J. (2004). Molecular characterization of *nosRZDFYLX* genes coding for denitrifying nitrous oxide reductase of *Bradyrhizobium japonicum*. *Antonie Van Leeuwenhoek* 85**,** 229-235.

Vine, C.E., and Cole, J.A. (2011a). Nitrosative stress in *Escherichia coli*: reduction of nitric oxide. *Biochem Soc Trans* 39**,** 213-215.

Vine, C.E., and Cole, J.A. (2011b). Unresolved sources, sinks, and pathways for the recovery of enteric bacteria from nitrosative stress. *FEMS Microbiol Lett* 325**,** 99-107.

Vine, C.E., Purewal, S.K., and Cole, J.A. (2011). NsrR-dependent method for detecting nitric oxide accumulation in the *Escherichia coli* cytoplasm and enzymes involved in NO production. *FEMS Microbiol Lett* 325**,** 108-114.

Wainwright, L.M., Elvers, K.T., Park, S.F., and Poole, R.K. (2005). A truncated haemoglobin implicated in oxygen metabolism by the microaerophilic food-borne pathogen *Campylobacter jejuni*. *Microbiology* 151**,** 4079-4091.

Wang, J., Vine, C.E., Balasiny, B.K., Rizk, J., Bradley, C.L., Tinajero-Trejo, M., Poole, R.K., Bergaust, L.L., Bakken, L.R., and Cole, J.A. (2016). The roles of the hybrid cluster protein, Hcp and its reductase, Hcr, in high affinity nitric oxide reduction that protects anaerobic cultures of *Escherichia coli* against nitrosative stress. *Mol Microbiol* 100**,** 877-892.

Wang, W., Kinkel, T., Martens-Habbena, W., Stahl, D.A., Fang, F.C., and Hansen, E.J. (2011). The *Moraxella catarrhalis* nitric oxide reductase is essential for nitric oxide detoxification. *J Bacteriol* 193**,** 2804-2813.

Weiss, B. (2006). Evidence for mutagenesis by nitric oxide during nitrate metabolism in *Escherichia coli*. *J Bacteriol* 188**,** 829-833.

Wink, D.A., Kasprzak, K.S., Maragos, C.M., Elespuru, R.K., Misra, M., Dunams, T.M., et al. (1991). DNA deaminating ability and genotoxicity of nitric oxide and its progenitors. *Science* 254**,** 1001-1003.

Witte, C.P., and Medina-Escobar, N. (2001). In-gel detection of urease with nitroblue tetrazolium and quantification of the enzyme from different crop plants using the indophenol reaction. *Anal Biochem* 290**,** 102-107.

Wolfe, M.T., Heo, J., Garavelli, J.S., and Ludden, P.W. (2002). Hydroxylamine reductase activity of the hybrid cluster protein from *Escherichia coli*. *J Bacteriol* 184**,** 5898-5902.

Wongdee, J., Boonkerd, N., Teaumroong, N., Tittabutr, P., and Giraud, E. (2018). Regulation of nitrogen fixation in *Bradyrhizobium* sp. strain DOA9 involves two distinct NifA regulatory proteins that are functionally redundant during symbiosis but not during free-living growth. *Front Microbiol* 9**,** 1644.

Wu, G., Wainwright, L.M., and Poole, R.K. (2003). Microbial globins. *Adv Microb Physiol* 47**,** 255-310.

Wunsch, P., and Zumft, W.G. (2005). Functional domains of NosR, a novel transmembrane iron-sulfur flavoprotein necessary for nitrous oxide respiration. *J Bacteriol* 187**,** 1992-2001.

Yang, C.S., Yuk, J.M., and Jo, E.K. (2009). The role of nitric oxide in mycobacterial infections. *Immune Netw* 9**,** 46-52.

Yoshinari, T., and Knowles, R. (1976). Acetylene inhibition of nitrous oxide reduction by denitrifying bacteria. *Biochem Biophys Res Commun* 69**,** 705-710.

Young, N.D., Debelle, F., Oldroyd, G.E., Geurts, R., Cannon, S.B., Udvardi, M.K., et al. (2011). The *Medicago* genome provides insight into the evolution of rhizobial symbioses. *Nature* 480**,** 520-524.

Yukl, E.T., de Vries, S., and Moenne-Loccoz, P. (2009). The millisecond intermediate in the reaction of nitric oxide with oxymyoglobin is an iron(III)--nitrato complex, not a peroxynitrite. *J Am Chem Soc* 131**,** 7234-7235.

Zamorano-Sánchez, D., Reyes-González, A., Gómez-Hernández, N., Rivera, P., Georgellis, D., and Girard, L. (2012). FxkR provides the missing link in the *fixL-fixK* signal transduction cascade in *Rhizobium etli* CFN42. *Mol Plant Microbe Interact* 25**,** 1506-1517.

Zumft, W.G. (1997). Cell biology and molecular basis of denitrification. *Microbiol Mol Biol Rev* 61**,** 533-616.

Zumft, W.G. (2005). Biogenesis of the bacterial respiratory Cu_A, Cu-S enzyme nitrous oxide reductase. *J Mol Microbiol Biotechnol* 10**,** 154-166.

9

ANEXOS

9. ANEXOS

9.1. Abreviaturas y símbolos

A	Adenina
ABC	*ATP-binding cassette*
ADN/DNA	Ácido desoxirribonucleico
ADNc/cDNA	ADN complementario
ADP	Adenosín difosfato
AEBSF	*4-(2-aminoethyl) benzenesulfonyl fluoride hydrochloride*
Ap	Ampicilina
APS	Persulfato amónico
ARA	Actividad reductora de acetileno
ARN/RNA	Ácido ribonucleico
ARNm/mRNA	ARN mensajero
ATP	Adenosín trifosfato
b	Base nitrogenada
BNF	Fijación biológica de nitrógeno
C	Citosina/Carbono
Cm	Cloranfenicol
cPTIO	*2-4-carboxyphenyl-4,4,5,5 tetramethylimidazoline-1-oxyl-3-oxide*
CRP	*Cyclic AMP receptor protein*
C-terminal	Carboxi terminal
CV	Volumen de columna
DEPC	Dietil policarbonato
DMSO	Dimetilsulfóxido
DNRA	*Dissimilatory nitrate reduction to ammonium*
DO/OD	Densidad óptica
DTT	Ditiotreitol
EDTA	Ácido etilendiaminotetra acético
FAD	Flavín adenín dinucleótido
FC	*Fold change*
Fe	Hierro
Fe-S	Grupo hierro-azufre
Flp	Flavoproteína
FMN	Flavín mononucleótido
FN	Nitrógeno fijado
FNR	*Fumarate-nitrate reductase regulator*
For	*Forward*
G	Guanina
Gm	Gentamicina
Hb	Hemoglobina
Bjgb	Hemoglobina de dominio único de *B. diazoefficiens*
fHb	Flavohemoglobina
sdHb	Hemoglobina de dominio único
tHb	Hemoglobina truncada
HCO	Oxidasa hemo-cobre
Hcp	*Hybrid cluster protein*
IPTG	Isopropil-β-D-1-tiogalactopiranósido
K_M	Constante Michaelis-Menten
Km	Kanamicina
KNO_3	Nitrato de potasio
Lb	Leghemoglobina
LbNO	Nitrosil-leghemoglobina
MFS	*Major facilitator superfamily*
Mo-$[MGD]_2$	Mo-*bis*-molibdeptorin guanina dinucleótido
n	Número de réplicas
NAD^+/NADH	Nicotín adenín dinucleótido
$NADP^+$/NADPH	Nicotín adenín dinucleótido fosfato
Nap	Nitrato reductasa periplásmica
Nar	Nitrato reductasa de membrana
Nas	Nitrato reductasa asimilativa
NCBI	*National center for biotechnology information*

Ndfa	Nitrógeno derivado del N_2 atmosférico
NDW	Peso seco de nódulo
NDWP	Peso seco de nódulo por plantas
NFW	Peso fresco de nódulo
NifH	Fe-proteína del complejo nitrogenasa
Nir/NiR	Nitrito reductasa
NNEDA	N-(1-Naftil) etilenodiamina
NNP	Número de nódulos por planta
NnrR	*Nitrite/nitric oxide reductase regulator*
Nor	Óxido nítrico reductasa
cNor	tipo *c*
qCu_ANor	tipo qCu_A
qNor	tipo q
NOS	Óxido nítrico sintasa
Nos	Óxido nitroso reductasa
NO_x	Óxidos de nitrógeno
NR	Nitrato reductasa
NrtABC	Transportador de NO_3^- de tipo ABC
NssR	*Nitrosative stress-sensing regulator*
N-terminal	Amino terminal
ONPG	Orto-nitrofenil-β-galactósido
ORF	*Open reading frame*
P	Promotor
pb/bp	Pares de bases
PCR	Reacción en cadena de la polimerasa
PDW	Peso seco de planta
qRT-PCR	PCR cuantitativa a tiempo real
r	Resistencia
Rev	Reverso
RFU	Unidades de fluorescencia
RNS	Especies reactivas de nitrógeno
ROS	Especies reactivas de oxígeno
rpm	Revoluciones por minuto
S	Azufre
SDS	Dodecilsulfato sódico
SDS-PAGE	Electroforesis en gel de poliacrilamida-SDS
Sm	Estreptomicina
S-NO	Sulfo-nitrosotiol
SNP	Nitroprusiato sódico
Spc	Espectinomicina
T	Timina
Tc	Tetraciclina
TCS	*Two-component system*
TEMED	Tetra-metiletilendiamina
TN	Nitrógeno total
UM/MU	Unidades Millers
UV	Ultravioleta
v/v	Volumen/volumen
Vis	Visible
WT	*Wild type*
w/v	Peso/volumen
X-gal	5-bromo-4-cloro-3-indolil-β-D-galactopiranósido
::	Fusión
Δ	Delta, deleción
σ	Factor sigma

Unidades

℃	Grado centígrado
A	Amperio
Da	Dalton
g	Gramo
g	Fuerza gravitatoria
h	Hora
J	Julio
l	Litro
m	Metro
M	Molar
min	Minuto
Pa	Pascal
s	Segundo
V	Voltio

Prefijos

T	Tera
M	Mega
k	Kilo
m	Mili
µ	Micro
n	Nano
p	Pico

Moléculas

CO_2	Dióxido de carbono
CO_3^-	Carbonato
$CuSO_4$	Sulfato cúprico
$FeCl_3$	Cloruro férrico
HNO_3	Ácido nítrico
H_2O_2	Peróxido de hidrógeno
KCl	Cloruro potásico
KH_2PO_4	Fosfato monopotásico
$MgSO_4$	Sulfato magnésico
$MnCl_2$	Cloruro de magnesio
N_2	Nitrógeno molecular
NaCl	Cloruro sódico
Na_2CO_3	Carbonato sódico
$NaHCO_3$	Bicarbonato sódico
Na_2HPO_4	Fosfato disódico
NaH_2PO_4	Fosfato monosódico
Na_2MoO_4	Molibdato de sodio
$NaNO_2$	Nitrito sódico
NaOH	Hidróxido sódico
NH_2OH	Hidroxilamina
NH_3	Amoníaco
NH_4^+	Amonio
NO	Óxido nítrico
NO^-	Nitroxilo
NO^+	Nitrosonio
NO_2	Dióxido de nitrógeno
NO_2^-	Nitrito
NO_3^-	Nitrato
N_2O	Óxido nitroso
O_2	Oxígeno molecular
OH	Hidroxilo
$ONOO^-$	Peroxinitrito
RbCl	Cloruro de rubidio
$ZnSO_4$	Sulfato de cinc

9.2. Abreviaturas de especies

Azotobacter vinelandii	*A. vinelandii*
Bacillus anthracis	*B. anthracis*
Bacillus azotoformans	*B. azotoformans*
Bacillus bataviensis	*B. bataviensis*
Bacillus subtilis	*B. subtilis*
Bacillus vireti	*B. vireti*
Bradyrhizobium diazoefficiens	*B. diazoefficiens*
Campylobacter jejuni	*C. jejuni*
Ensifer meliloti	*E. meliloti*
Escherichia coli	*E. coli*
Paracoccus denitrificans	*P. denitrificans*
Pseudomonas aeruginosa	*P. aeruginosa*
Pseudomonas stutzeri	*P. stutzeri*
Rhizobium etli	*R. etli*
Rhodobacter capsulatus	*R. capsulatus*
Rhodobacter sphaeroides	*R. sphaeroides*
Salmonella enterica serovar Typhimurium	*S.* Typhimurium
Shewanella loihica	*S. loihica*
Staphylococcus aureus	*S. aureus*
Vitreoscilla stercoraria	*V. stercoraria*
Wolinella succinogenes	*W. succinogenes*

9.3. Índice de figuras

9.4. Índice de tablas